



University College London

Department of Medical Physics and Biomedical Engineering

PhD thesis

**Optimising non-small cell lung cancer
radiotherapy tumour control probability model
considering immunotherapy
and normal tissue toxicity**

Huei-Tyng Huang

supervisors: Maria A. Hawkins, John D. Fenwick, Gary J. Royle

November 2023

submitted to University College London
for the degree of Doctor of Philosophy in Medical Physics

Declaration

I, Huei-Tyng Huang confirm that the work presented in this thesis is my own. Where information has been derived from other sources, I confirm that this has been indicated in the thesis.

ID – 19007635

Signature:



Acknowledgement

'If you want to run, run a mile; if you want to experience a different life, run a marathon.'

*– Emil Zátopek, the only runner to win the 5,000 metres, 10,000 metres,
and Marathon, in the same Olympic Games*

If I would like to take a sip of research, an undergrad/master project might be enough; however, I would like to experience something different, so I went all the way through the long journey and wrote a PhD thesis. Doing a PhD is a life-changing experience that I cannot finish without enormous support. I would sincerely like to thank my supervisors, without whom this thesis would not have been completed. Firstly, to Professor Maria Hawkins, for her constant support, guidance, and clinical comments over these years. Secondly, to Dr John Fenwick, for statistics, coding, writing training, and enormous amounts of time and patience on tutoring-style supervision. Finally, to Professor Gary Royle, for funding support and trust to hand over my supervision to whom does more clinical research which fits better with my academic background.

I am extremely lucky to have so much support for my research. I would like to thank Dr Michael Nix for his kindness in sharing datasets, supporting me in reproducing his earlier work, and providing comments on my research during the first two years of my PhD study. I want to thank Dr Douglas Brand for joining my meeting in the last two years and providing valuable clinical comments and guidance towards better science research writing. Also, thanks to Professor Crispin Hiley and Dr David Cobben for brainstorming with us during the paper revision phase. Many appreciations go to my dear friends who selflessly help my research. To Hung-Ching Chang, for a series of video chats discussing coding, math, and statistics. To Yu-Ming Yang, for sharing the self-learning coding modules at the beginning of my PhD study. To Cheng-Yu Tsai, for bringing many cooperation opportunities which help polish my CV and practice my academic writing abilities.

To Kai-Cheng Chuang, Chien-Yi Liao, Chieh-Te Lin, and Fang-Yi Lin, for sharing medical physics experience and perspectives in the US and Taiwan.

I would like to thank everyone I met in London, which made my PhD life more interesting and supportive. Thanks Ying Zhang, Esther Bar, Charles-Antoine Collins Fekete, Mikael Simard, Zhuoyan Shen, Boyue Ding, for those lunch and coffee breaks at UCL. Thanks Education Division of the Taipei Representative Office in the UK, for always welcoming me as a warm home. Thanks to those lovely pupils I met at The Brilliant Club placements, for the real inspiration I could bring and the experience I would never have had in the UK communities. Thanks Nicola Vermooten and Katie Booth at AccessEd NGO, for project management and fundings negotiation mentoring. Thanks to those at the London Taiwanese Biomedical Society, for networking and spiritual boosting on research. Thanks my dear flatmates, Kaiger W. Fang and Mermaid K. Liang, for unconscious daily support. Thanks to all my close friends who play and share the difficult moments together, particularly, Toffee W. Tsou, I-Jou Teng, and Kathy W. Lin.

Special appreciation for those who are always there for me, even though the distance might take a toll on our relationships. To my parents, Inn and Kuang-Yang, who always support me through all the ups and downs, and always cheer for my success despite tiny progress. To my family members who are always proud of having me pursuing my dream thousands of miles away from home. To the lifetime friends who always have my back, although we are now on the road apart: Jyun-Jie Yang, Jen-Yu Wang, Chau-Ling Ho, Yue-Hsin Lin, and Yi-Cheng Chen.

Lastly, I would like to acknowledge the financial support for my PhD programme, including UCL Overseas Research Scholarships, the Taiwan government, and Y. L. Lin Hung-Tai Education and Culture Charity Trust. Also, thanks to those friends, seniors and trustworthy mentors who helped and guided me to this fully funded PhD position: Yu-Hsien Hung, Julie Wang, Chi-Shuo Chuang, Ya-Chin Chen, and Ya-Hsin Cheng.

Abstract

Introduction: Non-small cell lung cancer (NSCLC) radiotherapy has undergone substantial technical advances. However, issues remain unanswered, including: 1) optimum radiation dose-fractionation schedules for concurrent chemoradiotherapy (cCRT); 2) the effects of adding immune checkpoint blockade (ICB) immunotherapy above cCRT alone on overall survival (OS); 3) how radiotherapy schedules can be optimised with cCRT-ICB treatment; 4) the impact of cardiac toxicity, and how cardiac-sparing might change OS. In this thesis, I test a series of hypotheses to answer these questions.

Methods: Two meta-analytic lung radiotherapy datasets were used, containing 4866 and 2196 NSCLC patients treated via radiotherapy alone, sequential CRT (sCRT), cCRT and cCRT-ICB. Models were maximum likelihood fitted. A series of radiotherapy dose-response models were used, taken hypotheses considering the effects of chemotherapy, immunotherapy, and cardiac toxicity. Chapter 3 informed the optimised prescribed dose, dose-per-fraction, and duration for cCRT. Chapter 4 identified factors influencing outcomes with cCRT-ICB. Chapter 5 optimised radiation schedules with cCRT/sCRT-ICB. Chapter 6 modelled OS effects of cardiac-sparing with photons and protons.

Results: For cCRT, accelerated repopulation began late (day 24) and was clinically significant (1.47Gy/day). The addition of ICB to cCRT improved 2-year OS by 9.9%, with tumour PDL1 $\geq 1\%$, stage IIIB/C, and longer planned ICB duration being significant predictors of benefit. Neither dose-escalation nor de-escalation relative to 60Gy in 30 fractions influenced survival with cCRT-ICB, while dose de-escalation of 5Gy might benefit patients with heavily irradiated organs at risk. Mean heart dose cardiac-sparing improved OS, and protons offered additional benefit over photons for tumours overlapped or lay below the 7th thoracic vertebra.

Conclusion: This work furthers our understanding about mechanistic processes influencing outcomes after NSCLC radiotherapy. Findings could be translated into future clinical studies, such as hypofractionation for cCRT alone, extending ICB administration to 2 years for cCRT-ICB treatment, and cardiac-sparing using photons or protons.

Impact statement

Through data collation, analysis and modelling, this hypothesis-forming research addresses the following issues regarding radiotherapy of inoperable locally-advanced non-small cell lung cancer (LA-NSCLC):

1. Inconsistent outcomes between concurrent chemoradiotherapy (cCRT) studies.
2. Interactions between radiotherapy and the chemotherapy and immunotherapy elements of combined treatments.
3. Quantitative overall survival (OS) benefits for cCRT-immune checkpoint blockade (ICB) treatment, identifying factors which might help patient selection for such tri-modality treatment.
4. Optimisation of prescribed radiation dose, dose-per-fraction, and treatment duration for cCRT and cCRT-ICB.
5. OS improvement via photon- and proton- based cardiac-sparing of cCRT and immuno-cCRT treatments.

This work has produced hypotheses that can be tested in the clinic, specifically –

1. Indications in data fits of delayed but heavily accelerated tumour repopulation for cCRT suggest that the radiotherapy element of this treatment may benefit from being given in short hypofractionated courses, within normal tissue toxicity constraints.
2. Patients with PDL1 $\geq 1\%$ or IIIB/C tumours should be treated with the addition of ICB above cCRT. The improved modelled outcomes with 2-year vs 1-year ICB duration might inform a future trial in this space.
3. For cCRT-ICB, modest dose de-escalation of around 5Gy (with prescribed radiotherapy schedule of 55Gy) from standard 60Gy in 2Gy-per-fraction

may be beneficial for patients with heavily irradiated organs at risk, as modelled reductions in OS are minimal.

4. Very large gains in 2-year OS are predicted for proton-based cardiac-sparing of patients with tumours overlapping or lying below the 7th thoracic vertebra, for both cCRT and cCRT-ICB treatments.

These findings should be tested in the clinic and can provide practical impacts on future inoperable LA-NSCLC treatments. This research brings impacts to peer researchers, the radiotherapy community, clinical workers, patients and their families, hospitals, clinical research organisations, ICB drug manufacturers, and the healthcare insurance system.

For **peer researchers and the radiotherapy community**, this thesis –

1. Generalises radiotherapy dose-response models to consider the chemotherapy and immunotherapy elements of combined treatments.
2. Achieves consistent model fits to datasets that include radiotherapy and cCRT schedules for reported outcomes are at first sight inconsistent.
3. Provides a methodology for quantify OS benefits across single-arm cCRT-ICB studies.
4. Develops a method for including the possible impact of cardiac-sparing within the radiotherapy dose-response model, by transferring ‘reported relative hazards for death related to cardiac irradiation’ over to ‘relative hazards for survival-limiting toxicities’, which is a term included in the radiotherapy dose-response models.

For **clinical workers** (i.e. physicians, medical physicists, and dosimetrists), and **patients and their families**, this thesis –

1. Provides evidence-based suggestions for the selection of radiotherapy, chemotherapy, and immunotherapy protocols in the clinic, informing the

choice of prescribed dose, dose-per-fraction and treatment duration for cCRT and cCRT-ICB, even with cardiac-sparing.

2. Helps select patients for expensive cCRT-ICB and proton treatment.

For **hospitals, clinical research organisations, ICB drug manufacturers, and the healthcare insurance systems**, this thesis –

1. Helps design of future clinical trials and modify clinical protocols.
2. Quantifies possible survival benefits versus expenses and investments (e.g. protons vs photons; ICB duration).

Work from thesis

*Published/submitted papers:

- H. Huang et al. Dose-response analysis describes particularly rapid repopulation of non-small cell lung cancer during concurrent chemoradiotherapy
(results from Chapter 3)
Cancers 2022, 14(19), 4869
<https://doi.org/10.3390/cancers14194869>
- H. Huang et al. Immuno-chemoradiation for non-small cell lung cancer: a meta-analysis of factors influencing survival benefit in combination trials
(results from Chapter 4)
Int. J. Radiat. Oncol. Biol. Phys. (under review when thesis submitted)

*Conference presentation and published abstracts:

- H. Huang et al. Tumour repopulation varies between sequential vs concurrent chemoradiation in lung cancer
(preliminary results from Chapter 3)
ESTRO 2021, Madrid, Spain – Oral Presentation (Virtual), Physics Track
Radiother. Oncol. 2021, 161:S413-414
[https://doi.org/10.1016/S0167-8140\(21\)06953-X](https://doi.org/10.1016/S0167-8140(21)06953-X)
- H. Huang et al. Locally advanced non-small cell lung cancer radiotherapy outcomes modelling: effects of immune checkpoint blockades
(preliminary results from Chapter 4)
CRUK RadNet PhD/Postdoc Symposium 2022, London, UK – Poster

- H. Huang et al. Modelling survival outcomes of immune checkpoint inhibitors on locally advanced non-small cell lung cancer following concurrent chemoradiotherapy
(preliminary results from Chapter 5)
ASTRO 2022, San Antonio, USA – Poster, Clinical Track
Int. J. Radiat. Oncol. Biol. Phys. 2022, 114(3): e375
<https://doi.org/10.1016/j.ijrobp.2022.07.1513>
- H. Huang et al. The addition of immunotherapy to lung cancer chemoradiotherapy: factors associated with survival
(preliminary results from Chapter 4)
ESTRO 2023, Vienna, Austria – Mini-oral Presentation, Clinical Track
Radiother. Oncol. 2023, 182:S373-375
[https://doi.org/10.1016/S0167-8140\(23\)08391-3](https://doi.org/10.1016/S0167-8140(23)08391-3)

Inclusion of published works in doctoral thesis

UCL Research Paper Declaration Form: referencing the doctoral candidate's own published work(s) – Chapter 3

Please use this form to declare if parts of your thesis are already available in another format, e.g. if data, text, or figures:

- have been uploaded to a preprint server;
- are in submission to a peer-reviewed publication;
- have been published in a peer-reviewed publication, e.g. journal, textbook.

This form should be completed as many times as necessary. For instance, if you have seven thesis chapters, two of which containing material that has already been published, you would complete this form twice.

| | |
|---|------------|
| 1. For a research manuscript that has already been published (if not yet published, please skip to section 2): | |
| a) Where was the work published? (e.g. journal name) | Cancers |
| b) Who published the work? (e.g. Elsevier/Oxford University Press): | MDPI |
| c) When was the work published? | 05/10/2022 |
| d) Was the work subject to academic peer review? | Yes |
| e) Have you retained the copyright for the work? | Yes |
| [If no, please seek permission from the relevant publisher and check the box next to the below statement]: | |
| <input type="checkbox"/> <i>I acknowledge permission of the publisher named under 1b to include in this thesis portions of the publication named as included in 1a.</i> | |
| 2. For a research manuscript prepared for publication but that has not yet been published (if already published, please skip to section 3): | |

| | | | |
|--|----------------------------------|--|------------|
| a) Has the manuscript been uploaded to a preprint server? (e.g. medRxiv): | Please select. | If yes, which server? Click or tap here to enter text. | |
| b) Where is the work intended to be published? (e.g. names of journals that you are planning to submit to) | Click or tap here to enter text. | | |
| c) List the manuscript's authors in the intended authorship order: | Click or tap here to enter text. | | |
| d) Stage of publication | Please select. | | |
| 3. For multi-authored work, please give a statement of contribution covering all authors (if single-author, please skip to section 4): | | | |
| <p>Conceptualisation, Maria A. Hawkins (MAH) Huei-Tyng Huang (HTH), John D. Fenwick (JDF); methodology, HTH, Michael G. Nix (MGN), and MAH; software, HTH, MGN, and JDF.; validation, HTH, and JDF; formal analysis, HTH, MAH, JF; investigation, HTH, MGN, Douglas H. Brand (DHB), David Cobben (DC), Crispin T. Hiley (CTH), JDF and MAH; data curation, HTH and MGN; writing—original draft preparation, HTH.; writing—review and editing, HTH, MGN, DHB, DC, JDF and MAH; visualisation, HTH; supervision, JDF and MAH. All authors have read and agreed to the published version of the manuscript.</p> | | | |
| 4. In which chapter(s) of your thesis can this material be found? | | | |
| Chapter 3 | | | |
| 5. e-Signatures confirming that the information above is accurate (this form should be co-signed by the supervisor/ senior author unless this is not appropriate, e.g. if the paper was a single-author work): | | | |
| Candidate: | Huei-Tyng Huang | Date: | 30/06/2023 |
| Supervisor/ Senior Author (where appropriate): | Maria A. Hawkins | Date: | 08/07/2023 |

UCL Research Paper Declaration Form: referencing the doctoral candidate's own published work(s) – Chapter 4

Please use this form to declare if parts of your thesis are already available in another format, e.g. if data, text, or figures:

- have been uploaded to a preprint server;
- are in submission to a peer-reviewed publication;
- have been published in a peer-reviewed publication, e.g. journal, textbook.

This form should be completed as many times as necessary. For instance, if you have seven thesis chapters, two of which containing material that has already been published, you would complete this form twice.

| | | |
|--|--|--|
| 1. For a research manuscript that has already been published (if not yet published, please skip to section 2): | | |
| f) Where was the work published? (e.g. journal name) | | |
| g) Who published the work? (e.g. Elsevier/Oxford University Press): | Click or tap here to enter text. | |
| h) When was the work published? | Click or tap to enter a date. | |
| i) Was the work subject to academic peer review? | Yes | |
| j) Have you retained the copyright for the work? | Yes | |
| [If no, please seek permission from the relevant publisher and check the box next to the below statement]: | | |
| <input type="checkbox"/> | <i>I acknowledge permission of the publisher named under 1b to include in this thesis portions of the publication named as included in 1a.</i> | |
| 2. For a research manuscript prepared for publication but that has not yet been published (if already published, please skip to section 3): | | |
| e) Has the manuscript been uploaded to a preprint server? (e.g. medRxiv): | No | If yes, which server? Click or tap here to enter text. |
| f) Where is the work intended to be published? (e.g. names of | International Journal of Radiation Oncology Biology Physics | |

| | | | |
|---|------------------|--|------------|
| journals that you are planning to submit to) | | | |
| g) List the manuscript's authors in the intended authorship order: | | Huei-Tyng Huang, Douglas H. Brand, John D. Fenwick, Maria A. Hawkins | |
| h) Stage of publication | | Submitted | |
| 3. For multi-authored work, please give a statement of contribution covering all authors (if single-author, please skip to section 4): | | | |
| Conceptualisation, MAH; methodology, HTH and JDF, MAH; software, HTH, DB; validation, HTH, and JDF; formal analysis, HTH, MAH, JF, DB; investigation, HTH, DHB, JDF and MAH; data curation, HTH, DHB, MAH and JDF.; writing—review and editing, HTH, DHB, JDF and MAH; visualisation, HTH; supervision, JDF and MAH. All authors have read and agreed to the submitted version of the manuscript. | | | |
| 4. In which chapter(s) of your thesis can this material be found? | | | |
| Chapter 4 | | | |
| 5. e-Signatures confirming that the information above is accurate (this form should be co-signed by the supervisor/ senior author unless this is not appropriate, e.g. if the paper was a single-author work): | | | |
| Candidate: | Huei-Tyng Huang | Date: | 30/06/2023 |
| Supervisor/ Senior Author (where appropriate): | Maria A. Hawkins | Date: | 08/07/2023 |

Contents

| | |
|---|----|
| Declaration..... | 1 |
| Acknowledgement..... | 2 |
| Abstract..... | 4 |
| Impact statement..... | 6 |
| Work from thesis..... | 9 |
| Inclusion of published works in doctoral thesis..... | 11 |
| Contents..... | 15 |
| List of Figures..... | 21 |
| List of Tables..... | 23 |
| Abbreviations..... | 25 |
| Chapter 1. Introduction..... | 29 |
| 1.0 Chapter overview..... | 29 |
| 1.1 Non-small cell lung cancer | 29 |
| 1.1.1 NSCLC staging | 31 |
| 1.1.2 NSCLC treatment: surgery, chemotherapy, and targeted therapy..... | 34 |
| 1.2 Radiotherapy for NSCLC | 37 |
| 1.2.1 Current radiotherapy treatment..... | 37 |
| 1.2.2 Acceleration and dose-escalation of LA-NSCLC..... | 41 |
| 1.2.3 Tri-modality treatment with immunotherapy | 44 |
| 1.3 Normal tissue toxicity of radiotherapy | 46 |

| | |
|---|----|
| 1.3.1 Normal tissue toxicity of NSCLC radiotherapy | 48 |
| 1.3.2 OARs in NSCLC radiotherapy: oesophagus, spinal cord, and lung | 51 |
| 1.3.3 OARs in NSCLC radiotherapy: heart | 53 |
| 1.4 Outstanding issues for LA-NSCLC radiotherapy at the start of the PhD, September 2019 | 56 |
| 1.4.1 Objectives of my PhD | 57 |
| Chapter 2. Methodology | 59 |
| 2.0 Chapter overview | 59 |
| 2.1 Clinical data..... | 59 |
| 2.1.1 CRT outcomes dataset | 59 |
| 2.1.2 cCRT-ICB outcomes dataset | 62 |
| 2.1.3 Clatterbridge and Oxford dosimetric indices | 63 |
| 2.2 Radiotherapy dose-response models | 64 |
| 2.2.1 Basic radiation biology principles..... | 65 |
| 2.2.2 Models toward clinical usages | 69 |
| 2.3 Regression models..... | 73 |
| 2.3.1 Logistic and probit regression | 74 |
| 2.3.2 Proportional hazards (Cox) time-to-event analysis..... | 76 |
| 2.4 Curve fitting optimisation methodology | 79 |
| 2.4.1 Maximum likelihood estimation | 79 |
| 2.4.2 Optimisation details..... | 81 |

| | |
|--|-----|
| 2.5 Study structure | 90 |
| Chapter 3. Investigating stage and treatment specific effects on LA-NSCLC survival following chemoradiotherapy | 91 |
| 3.0 Chapter overview | 91 |
| 3.1 Development of LA-NSCLC chemoradiotherapy | 91 |
| 3.2 Materials and methods | 95 |
| 3.2.1 Experimental design | 95 |
| 3.2.2 Retrospective data collection | 96 |
| 3.2.3 Chemo-radiotherapy outcome models | 98 |
| 3.2.4 Statistical analysis | 102 |
| 3.2.5 Supplementary dataset as validation | 103 |
| 3.3 Results | 104 |
| 3.3.1 Data description | 104 |
| 3.3.2 Models fitting | 106 |
| 3.3.3 Detailed modelling analysis | 112 |
| 3.3.4 Chemoradiotherapy dose-response | 118 |
| 3.4 Discussion | 122 |
| 3.4.1 Rapid tumour repopulation rate for cCRT | 122 |
| 3.4.2 Apparent stage-split values of tumour α/β | 124 |
| 3.4.3 Stage-specific survival-limiting toxicity | 128 |
| 3.4.4 Dose-response, statistical uncertainties and validation | 129 |
| 3.4.5 Limitation | 131 |

| | |
|--|-----|
| 3.5 Conclusion..... | 133 |
| Chapter 4. LA-NSCLC immuno-chemo-radiotherapy: effects of immune checkpoint blockade and factors affecting survival | 134 |
| 4.0 Chapter overview | 134 |
| 4.1 Clinical advances of LA-NSCLC treatments..... | 134 |
| 4.2 Materials and dataset processing..... | 138 |
| 4.2.1 Retrospective data | 138 |
| 4.2.2 OS standardisation..... | 139 |
| 4.2.3 Effective patient numbers of 2-year OS..... | 142 |
| 4.3 Models and statistical methods | 143 |
| 4.3.1 Meta-regression of OS in cCRT-ICB cohorts | 143 |
| 4.3.2 Estimation of the overall OS gain from ICB..... | 144 |
| 4.3.3 Associations between OS gains from ICB and factors | 145 |
| 4.3.4 Statistical analysis | 146 |
| 4.4 Results | 147 |
| 4.4.1 Data and OS standardisation | 147 |
| 4.4.2 Meta-regression analysis of OS in cCRT-ICB cohorts..... | 154 |
| 4.4.3 Associations between ICB OS gains and factors | 159 |
| 4.5 Discussion | 169 |
| 4.5.1 Data and modelling processing | 169 |
| 4.5.2 Factors affecting cCRT-ICB outcomes..... | 170 |
| 4.5.3 Statistical robustness | 174 |

| | |
|--|-----|
| 4.5.4 Limitation..... | 175 |
| 4.6 Conclusion | 176 |
| Chapter 5. Survival following immuno-chemo-radiotherapy of LA-NSCLC: exploration of variation with dose and treatment duration across an extended range..... | 177 |
| 5.0 Chapter overview | 177 |
| 5.1 Computational modelling of immunotherapy effects on radiation therapy | 177 |
| 5.2 Materials and methodology | 180 |
| 5.2.1 Retrospective data..... | 180 |
| 5.2.2 Dose-response models | 180 |
| 5.2.3 Statistical analysis..... | 182 |
| 5.3 Results..... | 183 |
| 5.3.1 Modelling fits of ICB effects | 183 |
| 5.3.2 Overall survival prediction with different radiation fractionation schedules, chemotherapy schedules and ICB | 185 |
| 5.3.3 For which radiotherapy doses and durations are the modelled OS rates most likely to be reliable? | 189 |
| 5.4 Discussion | 191 |
| 5.4.1 Chemo-radiotherapy schedules with the addition of ICB | 191 |
| 5.4.2 Modelling methodology..... | 192 |
| 5.5 Conclusion | 194 |
| Chapter 6. Cardiac-sparing optimisation for LA-NSCLC radiotherapy..... | 195 |

| | |
|---|-----|
| 6.0 Chapter overview | 195 |
| 6.1 Cardiac toxicity in LA-NSCLC | 195 |
| 6.2 Tabulation of cardiac dosimetry and hazard, and modelling the effect on OS..... | 198 |
| 6.2.1 Dosimetric indices..... | 198 |
| 6.2.2 Cardiac-sparing estimation and survival modelling..... | 200 |
| 6.3 Results | 204 |
| 6.4 Discussion | 209 |
| 6.5 Conclusion..... | 215 |
| Chapter 7. Conclusion | 216 |
| 7.0 Chapter overview | 216 |
| 7.1 Summary of findings..... | 216 |
| 7.2 Future directions..... | 220 |
| Chapter 8. Appendices..... | 221 |
| Chapter 9. Bibliography | 224 |

List of Figures

| | |
|--|-----|
| Figure 1.1 Dose-response curves visualise TCP, NTCP, and therapeutic window. | 46 |
| Figure 1.2 Reported associations between doses to heart substructures and OS... | 54 |
| Figure 2.1 Cell survival curves based on different SF curvatures..... | 65 |
| Figure 2.2 Radiation cell survival curves..... | 67 |
| Figure 2.3 Visualising maximum likelihood estimation using one-dimensional numerical data as an example..... | 79 |
| Figure 2.4 Graphical structure overviewing the modelling optimisation concept. | 88 |
| Figure 2.5 Graphical overview of study structure in the following chapters of my thesis..... | 89 |
| Figure 3.1 Sectional study flow chart..... | 94 |
| Figure 3.2 Two-year OS distribution versus prescribed radiation dose, dose-per-fraction, and overall radiation treatment time in 51 collected clinical trial cohorts..... | 104 |
| Figure 3.3 Models fitting abilities visualisation via calibration plots..... | 107 |
| Figure 3.4 Patient-weighted linear regression comparing 2-year OS, total dose, and radiotherapy duration versus dose-per-fraction, in More IIIA (IIIB/IIIA patient ratio >1) cohorts and More IIIB (IIIB/IIIA patient ratio <1) cohorts..... | 112 |
| Figure 3.5 Correlation matrix of the best model (Model 5)..... | 113 |
| Figure 3.6 LA-NSCLC dose-response prediction curves..... | 118 |
| Figure 4.1 Flow chart of this chapter..... | 135 |
| Figure 4.2 Univariable regression of 2-year OS in cCRT-ICB cohorts against selected patient and treatment factors..... | 155 |
| Figure 4.3 Gains in 2-year OS due to ICB plotted for the cCRT-ICB cohorts against selected factors..... | 164 |
| Figure 4.4 Survival levels for patients with PDL1 expression < or $\geq 1\%$ treated with cCRT \pm durvalumab..... | 170 |

| | |
|--|-----|
| Figure 5.1 Predicted 2-year OS rates for cCRT-ICB and cCRT alone, plotted for three radiation fractionation schemes..... | 184 |
| Figure 5.2 Predicted 2-year OS for sCRT-ICB and sCRT alone, delivered using three fractionation schemes..... | 186 |
| Figure 5.3 Scatter plots describing radiotherapy schedules in the datasets..... | 188 |
| Figure 6.1. Modelled two-year OS rates for cCRT alone for all patients, treated with standard photon, optimised photon cardiac-sparing and proton..... | 203 |
| Figure 6.2. Modelled two-year OS rates for cCRT-ICB treatment for all patients | 203 |
| Figure 6.3. Modelled two-year OS rates for cCRT alone for patients with T7 tumours..... | 204 |
| Figure 6.4. Modelled two-year OS rates for cCRT-ICB treatment for patients with T7 tumours..... | 204 |
| Figure 6.5. Modelled two-year OS rates for cCRT alone for patients with non-T7 tumours..... | 205 |
| Figure 6.6. Modelled two-year OS rates for cCRT-ICB treatment for patients with non-T7 tumours..... | 205 |
| Figure 6.7. Modelled two-year OS rates for all patients with 95% CIs accounting for uncertainty on HR alone..... | 209 |

List of Tables

| | |
|--|---------|
| Table 1.1. Clinical TNM cancer classification system for NSCLC published by Union for International Cancer Control (UICC)..... | 31 |
| Table 1.2. Clinical staging of NSCLC..... | 32 |
| Table 1.3. Overview of NSCLC radiotherapy..... | 38 |
| Table 1.4. Dose constraints of OARs for conventionally fractionated LA-NSCLC cCRT..... | 39 |
| Table 1.5 Definition of radiation toxicity scoring system..... | 49 |
| Table 2.1 Key summary of CRT dataset..... | 60 |
| Table 3.1 Patient characteristics..... | 95 |
| Table 3.2 Models comparison..... | 106 |
| Table 3.3 Models description..... | 108 |
| Table 3.4 Collinearity and overdispersion tests..... | 115 |
| Table 3.5 Calibrated AIC and likelihood-ratio test through incorporating ODF... | 115 |
| Table 3.6 The fit of Model 5 compared to models where parameters are individualised according to treatment rather than the stage, or vice-versa..... | 116 |
| Table 3.7 The Model 5 fit compared to models in which treatment- or stage-specific parameters are set to common values..... | 117 |
| Table 3.8 Key results of Model 5 prediction after 1000 times bootstrapping..... | 119 |
| Table 3.9 Best modelling prediction versus <i>PACIFIC</i> clinical trial..... | 120 |
| Table 4.1 Data characteristics of compiled datasets..... | 139 |
| Table 4.2 Patient, radiotherapy and ICB data characteristics for the cCRT-ICB cohorts..... | 146 |
| Table 4.3 Follow-up, 2-year survival, and effective patient numbers N_{eff} in the cCRT-ICB cohorts..... | 149 |
| Table 4.4 Univariable meta-regression of 2-year OS against patient and treatment factors f | 153 |

| | |
|---|-----|
| Table 4.5 Fitted parameter values in the underlying and extended CRT models.. | 158 |
| Table 4.6. Analysis of associations between patient or treatment factors f and changes in 2-year OS due to adding ICB to cCRT..... | 160 |
| Table 5.1 Outcome modelling results..... | 182 |
| Table 5.2 Best 2-year OS rates for different radiation dose-fractionation schedules, in treatments giving cCRT alone or cCRT-ICB..... | 184 |
| Table 5.3 Best 2-year OS rates for different radiation dose-fractionation schedules, in treatments giving sCRT alone or sCRT-ICB..... | 186 |
| Table 6.1 Summary of retrospective dosimetric studies used in Chapter 6..... | 197 |
| Table 6.2 Mean heart dose (MHD) indices recorded in both studies..... | 198 |
| Table 6.3 Averaged MHD values for standard and optimised photons and protons, in all patients and in T7 and non-T7 patient subgroups..... | 201 |
| Table 6.4 Modelled 2-year OS with MHD sparing considering schedules given in RTOG-1308 study: 70Gy in standard 2Gy-per-fraction..... | 211 |
| Appendix 1. Detail of CRT dataset..... | 219 |
| Appendix 2. Detail of cCRT-ICB dataset..... | 221 |

Abbreviations

| Abbreviation | Original terminology |
|------------------|--|
| AAPM | American Association of Physicists in Medicine |
| AIC | Akaike Information Criteria |
| AJCC | American Joint Committee on Cancer |
| ALK | anaplastic lymphoma kinase |
| BED | biologically effective dose |
| cCRT | concurrent chemoradiotherapy |
| CHART | Continuous, hyperfractionated, accelerated radiotherapy |
| CI | confidence intervals |
| COPD | chronic obstructive pulmonary disease |
| CPS | combined positive score |
| CRT | chemoradiotherapy |
| CT | computer tomography |
| CTCAE | Common Terminology Criteria for Adverse Effects |
| CTLA-4 | cytotoxic T lymphocyte-associated antigen 4 |
| CTV | clinical target volume |
| CV | cross-validation |
| d.f. | degrees of freedom |
| D _{LCO} | diffusing capacity for carbon oxide |
| ECOG | Eastern Cooperative Oncology Group |
| EGFR | epidermal growth factor receptor |
| EORTC | European Organisation for Research and Treatment of Cancer |
| EQD2 | equivalent dose in 2Gy-per-fraction |
| EUD | equivalent uniform dose |

| | |
|-------------------|--|
| FDG | fluorodeoxyglucose |
| FEV _{1s} | forced expiratory volume in one second |
| GTV | gross tumour volume |
| Gy | Gray |
| HR | hazard ratio |
| IASLC | International Association for the Study of Lung Cancer |
| ICB | immune checkpoint blockade |
| IDEAL-CRT | Isotoxic dose-escalated concurrent chemoradiotherapy trial |
| IGRT | image-guided radiotherapy |
| IMPT | intensity-modulated proton therapy |
| IMRT | intensity-modified radiotherapy |
| IQR | interquartile range |
| ITV | initial target volume |
| IV | independent variable |
| KM | Kaplan-Meier |
| LA-NSCLC | locally-advanced non-small cell lung cancer |
| LC | local control |
| LCC | large cell carcinoma |
| LET | linear energy transfer |
| LL | log-likelihood |
| LQ | linear-quadratic |
| LRT | likelihood ratio test |
| MHD | mean heart dose |
| ML | maximum likelihood |
| MLD | mean lung dose |
| MRI | magnetic resonance imaging |
| MV | multivariable |

| | |
|---------|--|
| NCCN | National Comprehensive Cancer Network |
| NSCLC | non-small cell lung cancer |
| NTCP | normal tissue complication probability |
| OARs | organs at risk |
| ODF | overdispersion factor |
| OS | overall survival |
| PD1 | programmed cell death 1 |
| PDL1 | programmed death-ligand 1 |
| PET | positron emission tomography |
| PFS | progression-free survival |
| PS | performance status |
| PTV | planning tumour volume |
| QUANTEC | Quantitative Analyses of Normal Tissue Effects in the Clinic |
| RBE | relative biological effectiveness |
| RIHD | radiation-induced heart disease |
| RP | radiation pneumonitis |
| RT | radiotherapy |
| RTOG | Radiation Therapy Oncology Group |
| SABR | stereotactic ablative radiotherapy |
| SBRT | stereotactic body radiotherapy |
| SCC | squamous cell carcinoma |
| SCLC | small cell lung cancer |
| sCRT | sequential chemoradiotherapy |
| SF | survival fraction |
| SLT | survival-limiting toxicity |
| SS | sum-of-squares |
| SUV | standard uptake values |

| | |
|------|--|
| T7 | the 7 th thoracic vertebra |
| TCP | tumour control probability |
| TPS | tumour proportion score |
| UICC | Union for International Cancer Control |
| UK | United Kingdom |
| UV | univariable |
| VATS | video-assisted thoracoscopic surgery |
| VEGF | vascular endothelial growth factor |
| VIF | variance inflation factor |
| VMAT | volumetric modulated arc therapy |
| WHO | World Health Organization |

Chapter 1. Introduction

1.0 Chapter overview

This chapter –

- Introduces non-small cell lung cancer.
- Introduces the radiotherapy treatment of non-small cell lung cancer, including dose-escalation studies, the combined treatment with chemotherapy and immunotherapy, and radiation toxicity.
- Outlines the gaps in what is known and objectives of this thesis.

1.1 Non-small cell lung cancer

Tumours are clusters of cells with abnormal proliferation, and clinically, they could be categorised as benign or malignant tumours based on diagnostic evidence. Cancer biologists Hanahan et al.¹ first proposed the ideas of ‘cancer hallmarks’ in 2000, indicating that all cancers share six common characteristics: sustaining proliferative signalling; evading growth suppressors; resisting cell death; enabling replicative immortality; inducing angiogenesis; and activating invasion and metastasis. The hallmarks were updated in 2011², with four new features related to the tumour microenvironment and detailed discussions about cell-cell interactions, including genome instability and mutation; tumour-promoting inflammation; deregulating cellular energetics; and evading immune destruction. Recently, with more understanding of cancer biology, the hallmarks were updated again in 2022³, with four new molecular features: unlocking phenotypic plasticity; non-mutational epigenetic reprogramming; senescent cells; and polymorphic microbiomes. Such complexity leads to diverse responses to cancer therapy, but improved

understanding with detailed mechanisms certainly sheds light on developing new cancer treatment paradigms.

Although the cancer mortality rate has been falling since 1991, each year in the United States, about 4.5 per 1000 people are still newly diagnosed with cancers, even taking away the lives of more than 150 people per 100,000 population every year⁴. Lung cancer leads the incidence and mortality rate⁵, comprising 20.1% of cancer-related mortality and 12% of new cancer cases in Europe in 2018⁶, causing more deaths than breast, prostate, colorectal, and brain cancers combined⁴. In the United Kingdom (UK), lung cancer leads the cancer-related deaths with nearly 35,000 dying each year, which accounts for around 1/5 of all UK cancer deaths and 13% of all new UK cancer cases⁷. Even though cancer treatment has improved in the past 30 years, the 5-year overall survival (OS) rate is still less than 25% for lung cancer patients, especially those with distant lesions (4.7%)⁸. According to World Health Organization (WHO), lung cancer takes 1.8 million deaths in 2020 globally⁹. In the UK, lung cancer accounts for 34,771 deaths between 2017 to 2019, which is 21% of all cancer deaths¹⁰.

Lung cancer has two main subtypes – small cell lung cancer (SCLC) and non-small cell lung cancer (NSCLC), with incidence rates of about 10-20% and 80-90%, respectively¹¹. NSCLC could further be specified into subtypes based on tumour histology, where three subtypes accounting for more than 80% of NSCLC – adenocarcinoma, squamous cell carcinoma (SCC), and large cell carcinoma (LCC). Adenocarcinoma is the most commonly seen histological subtype, which accounts for around 40% of cases, and has a higher possibility of being diagnosed before migrating into other organs due to its slow-growing abilities¹².

1.1.1 NSCLC staging

The Union for International Cancer Control (UICC) developed a cancer classification system called TNM, representing tumour size and extent of the main or primary tumour (T, Tumour), the number of lymph nodes that show signs of having cancerous cells (N, Number) and whether the cancer cells have spread to other body parts (M, Metastasis)¹¹ (Table 1.1).

Table 1.1. Clinical TNM cancer classification system for NSCLC published by the International Association for the Study of Lung Cancer (IASLC). (adapted from *Goldstraw et al., 2016*¹³)

| Stage | Description |
|---------------------------|--|
| Primary Tumour (T) | |
| Tx | Primary tumour cannot be assessed, or tumour proven by the presence of malignant cells in sputum or bronchial washings but not visualised by imaging or bronchoscopy |
| T0 | No evidence of primary tumour |
| Tis | Carcinoma <i>in situ</i> |
| T1 | <p>Tumour 3cm or less in greatest dimension, surrounded by lung or visceral pleura, without bronchoscopy evidence of invasion more proximal than the lobar bronchus. There are subtypes of T1:</p> <ul style="list-style-type: none"> - T1a (mi): minimally invasive - T1a: tumour ≤ 1cm in greatest dimension - T1b: tumour > 1cm but ≤ 2cm in greatest dimension - T1c: tumour > 2cm but < 3cm in greatest dimension |
| T2 | <p>Tumour more than 3cm but not more than 5cm; or tumour with any of the following features:</p> <ul style="list-style-type: none"> -Involves the main bronchus only (without carina) -Invades visceral pleura <p>-Associated with atelectasis or obstructive pneumonitis that extends to the hilar region of either part or the entire lung</p> <p>There are subtypes of T2:</p> <ul style="list-style-type: none"> - T2a: tumour > 3cm but ≤ 4cm in greatest dimension - T2b: tumour > 4cm but ≤ 5cm in greatest dimension |

| | |
|---------------------------------|---|
| T3 | Tumour more than 5cm but not more than 7cm in greatest dimension or tumour directly invades any of the following: parietal pleura, chest wall (including superior sulcus tumours), phrenic nerve, parietal pericardium; or separate nodule(s) in the same lobe as primary tumour |
| T4 | Tumour more than 7cm or of any size that invades any of the following: diaphragm, mediastinum, heart, great vessels, trachea, recurrent laryngeal nerve, oesophagus, vertebral body, carina; separate tumour nodule(s) in a different ipsilateral lobe to that of the primary |
| Regional Lymph Nodes (N) | |
| Nx | Regional lymph nodes cannot be assessed |
| N0 | No regional lymph node metastasis |
| N1 | Metastasis in ipsilateral peribronchial and/or ipsilateral hilar lymph nodes and intrapulmonary nodes, including involvement by direct extension |
| N2 | Metastasis in ipsilateral mediastinal and/or subcarinal lymph node(s) |
| N3 | Metastasis in contralateral mediastinal, contralateral hilar, ipsilateral or contralateral scalene, or supraclavicular lymph node(s) |
| Distant Metastasis (M) | |
| M0 | No distant metastasis |
| M1 | Distant metastasis. There are subtypes of M1: <ul style="list-style-type: none"> - M1a: separate tumour nodules in a contralateral lobe, tumour with pleural or pericardial nodules or malignant pleural or pericardial effusion - pleural (pericardial) effusion should be tested through multiple microscopic examinations, if the fluid are negative for tumour, nonbloody and not an exudate, it should be excluded as a staging descriptor. - M1b: single extrathoracic metastasis, including involvement of a single distant (non) regional lymph node - M1c: multiple extrathoracic metastases in one or more organs |

Building on the TNM classification, the American Joint Committee on Cancer (AJCC) has defined a clinical cancer staging system. This system has slowly changed over time, with the advances in diagnosis and treatment improvement. In the past decade, it was updated in 2010 and 2017. Staging definitions in the newest version (*'The Eighth Edition AJCC Cancer Staging Manual'*¹⁴) are summarised in Table 1.2.

Table 1.2. Clinical staging of NSCLC. (adapted from *AJCC guideline*¹⁴)

| AJCC stage | TNM standard | Stage description |
|------------------------|---|---|
| Occult (hidden) | Tx, N0, M0 | The primary tumour cannot be assessed, or cancer cells are seen in lung fluids (e.g. sputum sample), but the cancer is not found with other tests, so its location cannot be determined. |
| 0 | Tis, N0, M0 | The tumour is found only in the top layers of cells lining the air passages. |
| IA | T1mi, N0, M0 T1, N0, M0 | The cancer is a minimally invasive carcinoma, or the tumour is no longer than 3cm. |
| IB | T2a, N0, M0 | The tumour has one/more following features: - Larger than 3cm but less than 4cm across - Grown into the main bronchus, but with more than 2cm from the carina + less than 4cm across - Grown into the visceral pleura + less than 4cm across |
| IIA | T2b, N0, M0 | The tumour has one/more following features: - Larger than 4cm but less than 5cm across - Grown into the main bronchus, but with more than 2cm from the carina + less than 5cm across - Grown into the visceral pleura + less than 5cm across |
| IIB | T1, N1, M0 T2, N1, M0 T3, N0, M0 | The tumour has one/more following features: - Any above description in IA/IB/IIA + cancer has spread to the ipsilateral hilar lymph nodes (where the bronchus enters the lung) - Larger than 5cm but less than 7cm across - Grown into the chest wall, parietal pleura, phrenic nerve, or parietal pericardium - Have two or more separate nodules in the same lobe |
| IIIA | T1, N2, M0 T2, N2, M0 T3, N1, M0 T4, N0/N1, M0 | The tumour has one/more following features: - Any above description in IA/IB/IIA + cancer has spread to the ipsilateral lymph nodes around the carina or mediastinum - Any above description in T3 IIB (T3, N0, M0) + cancer has spread to the ipsilateral hilar lymph nodes - Larger than 7cm across |

| | | |
|-------------|--|---|
| | | <ul style="list-style-type: none"> - Grown into the mediastinum, heart, trachea, oesophagus, diaphragm, backbone, carina, or the large vessels near the heart (e.g. aorta) - Have two or more separate nodules in the different lobes |
| IIIB | T1, N3, M0 T2, N3, M0 T3, N2, M0 T4, N2, M0 | The tumour has one/more following features: <ul style="list-style-type: none"> - Any above description in IA/IB/IIA + cancer has spread to lymph nodes in any undescribed parts of the body - Any above description in T3 IIB (T3, N0, M0) or T4 IIIA (T4, N0/N1, M0) + cancer has spread to the ipsilateral lymph nodes around the carina or mediastinum |
| IIIC | T3, N3, M0 T4, N3, M0 | The tumour has one/more following features: <ul style="list-style-type: none"> - Any above description in T3 IIB (T3, N0, M0) or T4 IIIA (T4, N0/N1, M0) + cancer has spread to lymph nodes in any undescribed parts of the body |
| IV | Any T, N, M1 | Cancer can be any size or even without growing into the lymph node, but has one or more following features: <ul style="list-style-type: none"> - Cancer has spread to the other lung - Cancer has pleural (fluid around the lung) / pericardial (fluid around the heart) effusion - Cancer has spread to organs outside of the lung |

In this thesis, stage III patients are described as having locally advanced NSCLC (LA-NSCLC).

1.1.2 NSCLC treatment: surgery, chemotherapy, and targeted therapy

According to National Comprehensive Cancer Network (NCCN) guidelines for NSCLC (version 2, 2023)¹⁵, a series of investigations are recommended before deciding how to treat. These investigations include chest and abdomen computer tomography (CT), fluorodeoxyglucose (FDG) positron emission tomography

(PET)/CT, bronchoscopy, and functional tests. Cardiopulmonary exercise functional tests aim at identifying respiratory risk factors – forced expiratory volume in one second (FEV_{1s}) and diffusing capacity for carbon oxide (D_{LCO}). They were evaluated for NSCLC treatment selection together with other risk factors, such as age, sex, performance status (PS), and risks-weighted comorbidity score (e.g. heart disease, stroke or ischemia history)^{16–18}.

Surgery treats stage I, II or III NSCLC patients with resectable tumours^{12,18}. For stage I and II NSCLC, stereotactic body radiotherapy (SBRT), sometimes known as stereotactic ablative radiotherapy (SABR), has similar treatment efficacy to surgery. Different extents of lung removal are described using the terminologies: wedge resection (removing a small part of a lobe), segmentectomy (removing a large part of a lobe), lobectomy (removing an entire lobe), sleeve lobectomy (removing an entire lobe and part of the bronchus) and pneumonectomy (removing one side of the whole lung)¹⁹. Recently, video-assisted thoracoscopic surgery (VATS) has been used, with only a tiny incision by inserting thorascope^{12,19,20}. Following surgery, chemotherapy is commonly used as an adjuvant for stage IIA, IIB and IIIA NSCLC to reduce the possibility of cancer relapse.

Chemotherapy uses chemical toxicity to kill tumours. It is the standard choice for stage IV NSCLC. The treatment efficacy is influenced by histology, age, comorbidity risks and PS. In particular, side effects are severe for patients with poor PS (PS \geq 2), for whom chemotherapy is not used^{21,22}. For patients without distant metastasis (i.e. not stage IV), chemotherapy is usually given together with surgery or radiotherapy.

Precision medicine used targeted molecular markers to achieve tumour-killing, can be given either as a monotherapy or as an adjuvant with chemotherapy, and has been shown to improve OS and progression-free survival (PFS) versus chemotherapy alone. Targeted therapy has achieved useful tumour control including treatments targeting the following markers: epidermal growth factor

receptor (EGFR); vascular endothelial growth factor (VEGF); and anaplastic lymphoma kinase (ALK). For example, Osimertinib targeting EGFR has been recommended as an adjuvant for completely resected EGFR mutation-positive NSCLC patients¹⁵.

An anti-cancer immune response begins once dendritic cells recognise dying tumour debris as tumour antigens, followed by antigen transportation/presentation to lymph nodes via dendritic cells, which activate cytotoxic T cells with tumour-killing abilities. Anti-cancer immunity requires clear signal recognition from the receptors linking the tumour and immune cells. Tumours could inhibit and even shoot down anti-cancer immunity by disguising themselves from the immune system. With dysfunctional tumour antigen recognition, cancer stops the activation of cytotoxic T cells and facilitates regulatory T cells, which hold the tumour-promoting abilities²³⁻²⁵.

Bioreceptors responsible for anti-cancer immunity are called immune checkpoints, where cancer cells paralyse the tumour-killing functions by blocking either side of a checkpoint. Drugs have been developed to stop blocking of immune checkpoints, allowing anti-cancer immunity to work. Two checkpoints have been particular interest – cytotoxic T lymphocyte-associated antigen 4 (CTLA-4) and programmed cell death 1 (PD1, T cell side) / programmed death-ligand 1 (PDL1, tumour surface side)^{23,26}. Specifically, anti-PD1 and anti-PDL1 drugs have performed well in trials for multiple cancer sides, and shown the potential to be the frontline monotherapy or combined with chemotherapy, radiotherapy or targeted therapy for NSCLC²⁷⁻³⁰.

1.2 Radiotherapy for NSCLC

Ionising radiation beams comprising megavoltage photons or high energy protons can be used in NSCLC treatment. Over 60% of NSCLC patients receive radiotherapy at least once during treatment³¹.

1.2.1 Current radiotherapy treatment

Radiotherapy is vital in clinical NSCLC care, either curatively or palliatively. SBRT is the standard choice for early-stage patients unfit for surgery³². The recommended radiation dose fractionation for SBRT include: 54Gy in 3 fractions over 5 to 8 days, 55Gy in 5 fractions over 10 to 14 days, 60Gy in 5 fractions over 10 to 14 days, or 60Gy in 8 fractions over 10 to 20 days³³. However, such schedules come with about 15% lymph node failures and 20% chances of distant recurrence^{34,35}. When primary lesions are close to surrounded organs at risk (OARs), within 2cm in all directions of any mediastinal structure, standard SBRT with three fractions might lead to severe toxicity due to unavoidable OAR exposure^{36,37}. Moderately hypofractionated SBRT giving 60Gy in 15 fractions can achieve good results for ultracentral lesions, with constraints of not exceeding >150% prescribed dose within the planning tumour volume (PTV) and maximum dose limit of 80 to 90Gy tumour equivalent dose in 2Gy/fraction (EQD2) to OARs such as oesophagus³⁸. Inoperable patients with the nodal negative primary tumour within 5cm can also be treated by SBRT – delivering 100Gy EQD2 with an inter-fraction intervals between 40 hours to four days³³.

Unresectable LA-NSCLC patients with good PS are usually treated using concurrent chemoradiotherapy (cCRT). Standardly, radiation schedules delivering 60 to 66Gy in 1.8 to 2Gy/fraction in 6 to 6 ½ weeks (40 to 45 treatment days) or 55Gy in four weeks with mild hypofractionation are used together with 2-4

platinum-based chemotherapy cycles^{18,31,39}. Clinical trials comparing the 5-year OS of surgical resection and radiotherapy after induction chemotherapy or cCRT have shown that surgery is redundant and does not improve OS⁴⁰⁻⁴². However, surgery before radiotherapy or cCRT can reduce the risks of local recurrence if patients are diagnosed with multi-nodules or lesions described as extracapsular tumours¹⁹.

Clinically, around 20% of LA-NSCLC patients are at high risk of comorbidity if treated using standard cCRT, including those with poor PS (PS ≥ 2). These patients can alternatively be treated using sequential CRT (sCRT) or radiotherapy alone with the same prescribed dose and treatment duration as cCRT. An acceleration with more than one fraction per treatment day has also been suggested³⁴.

Different radiotherapy schedules are used for palliative treatments. For patients with good PS, 36 to 39Gy in 12 fractions, 30Gy in 10 fractions, or 20Gy in 5 fractions are given. For those with poor PS, 17Gy in 2 fractions and a single fraction of 10Gy are also used³³.

Table 1.3. Overview of NSCLC radiotherapy.

| Lesions description | Radiotherapy guideline summary |
|--|---|
| <i>Curative purpose</i> | |
| early stages, localised disease | <ul style="list-style-type: none"> • Inoperable: SBRT, 54Gy in 3 fractions, 55Gy in 5 fractions, or 60Gy in 5 or 8 fractions • Operable: surgery preferred, while SBRT can provide similar treatment outcomes |
| early stages, ultracentral tumours (<2cm to critical mediastinal structure) | <ul style="list-style-type: none"> • 60Gy SBRT using in 15 fractions |
| locally advanced tumours (unresectable IIB. stage III) | <ul style="list-style-type: none"> • The cCRT: 60-66Gy in 2Gy/fraction or 55Gy in four weeks + 2-4 chemotherapy cycles • The sCRT with the same prescribed dose and treatment duration as cCRT • Radiotherapy alone of 55Gy in four weeks or 54Gy in 36 fractions over 12 consecutive days |
| <i>Radiotherapy as palliative or supportive treatments</i> | |
| locally advanced tumours (unresectable IIB. stage III) | <ul style="list-style-type: none"> • Radiotherapy in different dose schedules according to PS |
| stage IV with brain metastasis | <ul style="list-style-type: none"> • Radiotherapy + surgery recommended |
| post operation radiotherapy | <ul style="list-style-type: none"> • For patients with multi-nodal lesions or extracapsular tumours, post-operation radiotherapy recommended reducing risks of local recurrence |

Regarding treatment planning, the structure contouring and expansions between gross tumour volume (GTV), clinical target volume (CTV), PTV, or OARs slightly vary depending on the protocols used by different medical centres. Also, dose constraints for normal tissues and dose coverage on tumours might vary between centres. Table 1.4. summarises the normal tissue dose constraints recommended for conventionally fractionated LA-NSCLC cCRT in the NCCN guidelines⁴³. In particular, the guideline recommended median dose of $\leq 69\text{Gy}$ for brachial plexus, while several studies set the maximum dose constraints for 60 or 66Gy⁴⁴, therefore, I did not list it in the table.

Table 1.4. Dose constraints of OARs for conventionally fractionated LA-NSCLC cCRT.

$V_{X\text{Gy}}$ denotes the dose constraints delivered to how many % of the volume receiving XGy.

| OARs structure | Dose constraint in 30 to 35 fractions, given in 1.8 to 2Gy-per-fraction |
|---|---|
| <i>standard radiation fractionation given as cCRT</i> | |
| Spinal cord | Maximum $\leq 50\text{Gy}$ |
| Lung | $V_{20\text{Gy}} \leq 35\% - 40\%$ Mean dose $\leq 20\text{Gy}$ |
| Heart | $V_{50\text{Gy}} \leq 25\%$ Mean dose $\leq 20\text{Gy}$ |
| Oesophagus | Mean dose $\leq 34\text{Gy}$ Maximum dose $\leq 105\%$ of prescribed dose $V_{60\text{Gy}} \leq 17\%$ Contralateral sparing is desirable |

In the past two decades, technological advances including intensity-modified radiotherapy (IMRT), volumetric modulated arc therapy (VMAT), and image-guided radiotherapy (IGRT) have improved radiation dose distributions, better avoiding normal tissue irradiation while maintaining tumour dose coverage. Ongoing LA-NSCLC trials may provide data guiding the optimisation of schedules used to deliver these improved dose distributions³⁴. Stratified patient selection or personalised radiotherapy may be possible in the future.

Additionally, replacing standard radiation source photons with protons might play an important role in treatment optimisation, as protons release large amounts of energy at specific depths below the body surface (i.e. Bragg Peak). This feature provides potential benefits including reducing OAR toxicities, and more safely delivering high and escalated radiation doses to tumours close to critical organs. In terms of LA-NSCLC, multiple studies have shown that proton therapy significantly improves the dose to the lungs, spinal cord, heart, oesophagus, and incidences of grade ≥ 3 radiation-induced toxicities (pneumonitis, oesophagitis) compared to photon therapy when giving the same prescribed dose^{45,46}. Most published LA-NSCLC radiotherapy data to date has been for photon beam treatment. The only randomised trial comparing cCRT with proton versus photon showed dose-volume indices improvement only for heart ($p=0.002$) but not for lung ($p=0.818$) and oesophagus ($p=0.717$); additionally, the primary endpoint of that study (grade ≥ 3 pneumonitis) was similar across arms, with a rate of 6.5% for photon and 10.5% for proton⁴⁷. More studies are needed to investigate whether proton therapy can change the landscape of LA-NSCLC treatment in the future.

1.2.2 Acceleration and dose-escalation of LA-NSCLC

A radiation schedule of 60Gy in 30 fractions in 40 days has been considered the standard treatment of LA-NSCLC by Radiation Therapy Oncology Group

(RTOG) for 40 years⁴⁸. In the UK, 55Gy in four weeks or 64 to 66Gy in 6 ½ weeks is generally used instead. Even though standard treatment has evolved from radiotherapy alone to sCRT with induction chemotherapy through to cCRT, researchers are still interested in optimising the radiation dose-response.

Accelerated radiotherapy schedules designed to limit tumour proliferation have been tested to determine whether they achieve increased survival rates. Continuous, hyperfractionated, accelerated radiotherapy (*CHART*) using 54Gy in 36 fractions within 12 consecutive days showed mild toxicity with 99% of patients completing treatments. However, even though this modified strategy slightly improved the 2-year OS (29% vs 20%, $p=0.004$), around 50% of patients had tumour recurrence eventually^{49,50}.

Radiotherapy dose-escalation has been tested extensively. In principle, escalation can improve tumour control while normal tissue doses can be limited using modern technology. Early-stage dose-escalation clinical trials have shown in limited patient cohorts that escalation can be safe and effective in improving OS⁵¹⁻⁵³. Still, effects remain controversial since the only randomised phase III clinical trial (*RTOG-0617*) published in 2015 reported that 2-year OS dropped by 29% using 74Gy cCRT, compared to standard 60Gy ($p=0.004$)⁵⁴. There was higher toxicity incidence for the high-dose arm, and inferior quality of life three months after the treatment⁵⁵.

Alternatively, personalised dose-escalation modifying tumour prescribed doses to limit OAR irradiation has been proposed as a possible approach for LA-NSCLC cCRT optimisation⁵⁰. The unrandomised phase II trial *IDEAL-CRT* (isotoxic dose-escalated concurrent chemoradiotherapy trial) applied personalised dose-escalation through evaluating patient-by-patient oesophagus tolerance. It delivered 63-71Gy in 30 fractions over five weeks (N=36; 2.1 to 2.37 Gy/fraction), or 63-73Gy in 30 fractions over six weeks (N=82; 2.1 to 2.43 Gy/fraction), showing promising toxicity with acceptable rates of severe pneumonitis and early

oesophagitis (\geq grade 3: 3.4% for five-week, 5.9% for six-week, N=118)⁵⁶. The median OS was better for the six-week arm (41.2 vs 22.1 months, $p=0.04$). Additionally, in the six-week arm, median OS of 41.2 months and PFS of 21.1 months were much better than 74Gy arm of *RTOG-0617* (median OS: 20.3 months, median PFS: 9.8 months)⁵⁷. These results suggest that the choice of prescribed dose and radiotherapy duration might influence outcomes from dose-escalation.

Other dose-escalation methods are under investigation, such as boosting the dose in regions with high PET-FDG standard uptake values (SUV) ($>50\%$ of maximum SUV), and modifying the prescribed dose after 45Gy radiation delivery – an amount that should be enough to shrink tumour significantly⁵⁸. In addition, the randomised phase II PET-boost trial (NCT01024829) escalated dose to the entire primary tumour or high pre-treatment FDG-uptake tumour subvolumes with ≥ 72 Gy in 24 fractions. It showed elevated toxicity, with 41% and 25% of patients experiencing acute and late \geq grade 3 toxicity respectively (N=107)⁵⁹. This perhaps suggests that either lower dose boost levels should be used, potentially reducing efficacy, or that levels currently used should be delivered to smaller boost volumes.

Biologically effective dose (BED) and EQD2 measures allow comparisons of results from trials that have used different radiation fractionation schedules. Using these metrics, review studies and meta-analyses found a dose-response gradient for OS, corresponding to 0.4% to 0.7% OS increase in survival per one Gy increase in BED, with an associated 0.5% increase in acute oesophagitis^{58,60}. Furthermore, modelling studies suggest that each 1% of dose-escalation might increase tumour local control (LC) by 1-2%. Additionally, escalation without protracting treatment duration might achieve better results than adding additional fractions^{61,62}. Furthermore, review data suggest that sCRT might achieve as good OS and LC as cCRT given a well-designed dose-escalation strategy⁶⁰.

In summary, despite the results from *RTOG-0617*, systemic reviews and meta-analyses suggest that OS gains may still be achievable from radiation dose-escalation. However, when considering escalation studies, it is important to –

- 1) Further analyse the effects of dose, dose-per-fraction and treatment duration on outcomes.
- 2) Achieve a deeper understanding of the influence of normal tissue toxicity on OS.
- 3) Determine whether adjuvant drugs can also improve tumour control, potentially improving OS while contributing less to toxicity than dose-escalation.

1.2.3 Tri-modality treatment with immunotherapy

Cancer immunotherapy, especially immune checkpoint blockade (ICB), has been widely investigated in the past decade⁶³. Cancers can evade immune control, and one of the most common ways to shut down anti-cancer immunity is disguising themselves from immune checkpoint recognition, where immune systems are supposed to recognise them and activate a series of cell-killing reactions. ICB targets specific receptors on tumour sides or the T cells, providing chances of activating pre-existing immunity to an anti-cancer status⁶⁴.

Clinical trials have tested the efficacy of anti-PD1 and anti-PDL1 ICB treatments of NSCLC. Both drugs have shown benefit, but the studies have had heterogeneous designs, and so patient selection criteria have yet to be determined, especially whether tumour PDL1 presentation might affect the treatment outcomes⁶⁵. Other drugs (e.g. anti-CTLA4) have also been investigated. However, published studies of radiotherapy together with ICB for NSCLC have only used anti-PD1/PDL1 drugs.

Methods of quantifying PDL1 vary as different scoring systems count the tumour tissue sections using different methodologies. The most frequently used method is called tumour proportion score (TPS), where values represent the PDL1 presented on the tumour; in contrast, combined positive score (CPS) reports PDL1 presentation by counting those markers on both the tumour and surrounding immune cells. Additionally, there are considerable variances in the PDL1 cut-off standard for ICB approvals, ranging from 1% to 50%^{28,30,65,66}. Furthermore, inconsistent clinical outcomes have been reported – higher PDL1 expression sometimes was associated with better OS^{28–30}; and sometimes with worse OS^{30,65}. A recent analysis found that tumour PDL1% expression in biopsy samples had limited association with NSCLC treatment outcomes; however, the double markers of ‘PDL1%’ plus ‘CD8+ T cell density’ may help identify patients who benefit more from anti-PDL1 ICB monotherapy⁶⁷.

Durvalumab (MEDI 4736) is an engineered ICB antibody that stops tumour PDL1 from binding to PD1, and activates cytotoxic T cells in tumour recognition and upcoming tumour elimination⁶⁸. A pre-clinical study has shown synergetic effects together with irradiation⁶⁹, and early-phase clinical trials have demonstrated good anti-tumour action on late-stage NSCLC⁷⁰.

In *PACIFIC* (NCT02125461), a phase III, randomised, double-blind, placebo-controlled, multi-centre, international trial of MEDI 4736 (durvalumab) given adjuvantly followed definitive cCRT for LA-NSCLC patients, OS was notably and significantly improved versus standard cCRT (p=0.003) with 2-year OS rates of 66% versus 56%^{71,72}. Furthermore, toxicity was not increased. This has changed the practice with many patients now receiving ICB consolidation following cCRT.

The *PACIFIC* trial randomised patients who had not progressed after cCRT into the durvalumab and placebo groups using around a 2:1 (473:326) ratio after cCRT. 10 mg/kg durvalumab was given intravenously every two weeks, up to 12 months, starting from 1-42 days after last irradiation. In addition, cCRT

prescription includes more than two cycles of platinum-based chemotherapy plus 54-66Gy radiotherapy with radiation dose constraint for lung parenchyma V_{20} (lung parenchyma volume receiving 20Gy or more) $<35\%$ ⁷¹. The primary endpoint was OS, and there was a significant difference ($p=0.003$) between durvalumab and placebo groups, where OS was 83.1% vs 75.3% at 12 months and 66.3% vs 55.6% at 24 months, respectively. Besides, long-term radiation toxicity with grade 3/4 severe side effects was similar between groups, 30.5% for durvalumab and 26.1% for placebo^{71,72}.

Following the success of *PACIFIC*, further studies are now investigating such tri-modality treatments with different protocols – such as starting ICB concurrently with cCRT, replacing cCRT with sCRT, or allowing diverse patient eligibilities regardless of cCRT progression^{73–76}.

1.3 Normal tissue toxicity of radiotherapy

Oncology research aims at balancing benefits between maximising tumour control and minimising normal tissue toxicity, to achieve the best care for cancer patients. Therefore, it is crucial to investigate radiation toxicity.

Radiotherapy technology has progressed rapidly in the last 30 years, improving the accuracy of tumour targeting and decreasing the chances of radiation toxicity in normal tissues. Ideally, radiation would kill 100% of the tumour without damaging any normal tissue. However, in practice, tumours usually lie close to normal tissues, and many late toxicities appear long after radiotherapy as a result of normal tissue irradiation.

To achieve the best treatment efficacy, it is needed to identify and design radiation schedules that maximise tumour-killing and minimise toxicity. Treatment schedules can be evaluated via dose-response curves in terms of tumour control

probability (TCP) and normal tissue complication probability (NTCP) (Figure 1.1). The x-axis refers to the radiation dose and can be presented in terms of different metrics accounting for fractionation effects (e.g. EQD2, BED). In contrast, the y-axis describes the rates of tumour control or normal tissue complication. The region between two curves is called the ‘therapeutic window’, and is a dose range in which useful rates of tumour control are achieved while limiting toxicity of normal tissues. Clinically, the wider the window, the better is the treatment. Precise radiation delivery techniques have widened therapeutic windows by limiting doses to normal tissues while maintaining tumour dose coverage^{77,78}.

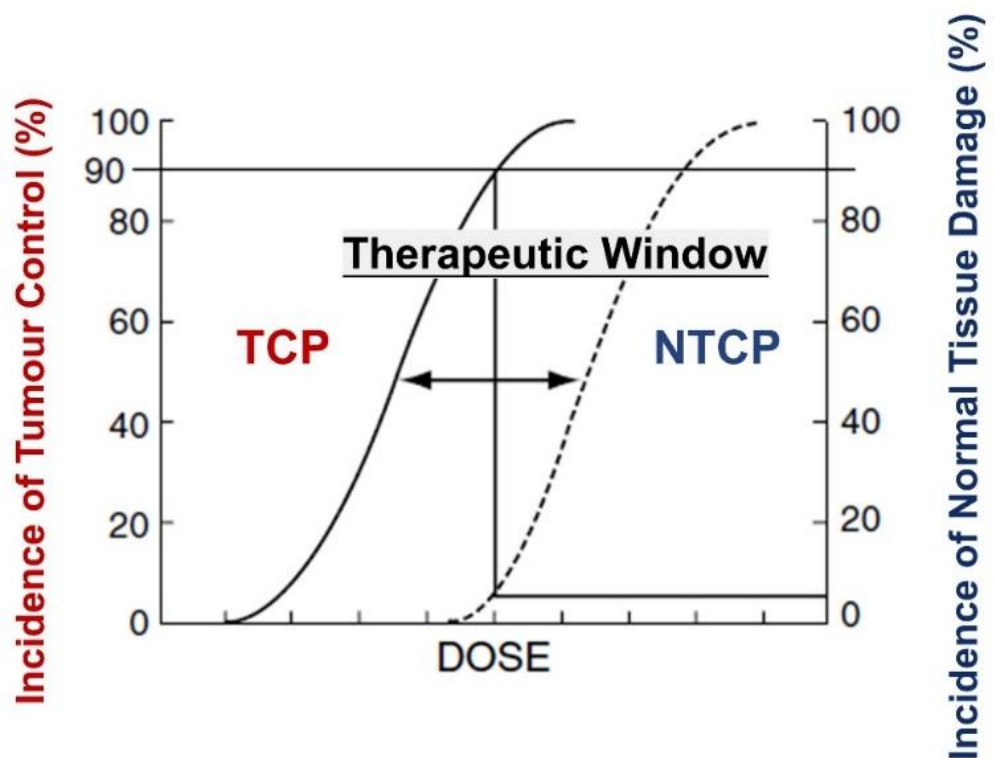


Figure 1.1 Dose-response curves visualise TCP, NTCP, and therapeutic window. (adapted from *Basic radiation oncology*⁷⁸)

1.3.1 Normal tissue toxicity of NSCLC radiotherapy

Radiation toxicity is a critical issue for NSCLC as there are several OARs, including the heart, lung, oesophagus, and spinal cord. With the technological advances from conformal, IMRT, to VMAT, the toxicity has been well-reduced. However, challenges remain towards optimising dose-per-fraction, treatment duration, and combined chemotherapy/immunotherapy.

A study analysed the NSCLC outcomes with a large dataset treated before 2003. It compared cohorts receiving surgery with and without radiotherapy, showing that radiotherapy provided increased mortality from heart disease (hazard ratio HR: 1.30; 95% confidence intervals CI: 1.04, 1.61; $p=0.019$; $N=6148$, around 1:1 patient split)⁷⁹. Such outcomes were supported by another study with 98 NSCLC patients treated between 1994 and 2004. The results indicated that radiotherapy greater than 54Gy was associated with higher death rates for patients with left-sided tumours ($p<0.05$). Even though these patients were mainly treated with cobalt-60 instead of modern radiotherapy, such findings suggested that radiation-induced heart disease (RIHD) might be a concern for NSCLC radiotherapy⁸⁰. Besides, an epidemiology study containing more than 30000 NSCLC patients treated between 1991 to 2002 showed an increased risk of cardiac dysfunction given radiotherapy or chemoradiotherapy (CRT), with the HR of 1.54 (95% CI: 1.29, 1.83) and 2.36 (95% CI: 1.91, 2.92) respectively⁸¹.

In the IMRT era, dose-escalation with precise radiation delivery techniques has been widely tested for optimising LA-NSCLC radiotherapy. In the long-term follow-up of *RTOG-0617*, there was greater grade ≥ 3 dysphagia (12.1% vs 3.2%, $p=0.0005$) and oesophagitis (17.4% vs 5.0%, $p < 0.0001$) in the high-dose 74Gy arm compared to standard 60Gy arm⁵⁷. There is a limitation on interpreting the toxicity results of *RTOG-0617*, as the study suggested the heart dose contouring guideline but did not require strict compliance. The key findings showed that heart volume receiving ≥ 5 Gy (V_5) was significantly associated with the OS (HR: 1.008,

95% CI: 1.002, 1.013)⁵⁷. In 2021, secondary analyses of 488 patients with accurate voxel-wise dose mapping information showed that heart region dose to the base of the heart was significant against OS ($p < 0.001$) and should be more critical than standard dose-volume information such as V_5 ⁸².

Additionally, LA-NSCLC dose-escalation studies based on dose constraints of specific OARs have been tested, such as *IDEAL-CRT*, through patient-by-patient oesophagus toxicity evaluation^{56,83}. Toxicity in *IDEAL-CRT* is acceptable, with 37% of grade ≥ 3 and 8% of grade ≥ 4 early or late radiation complications. Besides, either heart or lung volume receiving ≥ 20 Gy (V_{20}), 40Gy (V_{40}), and 60Gy (V_{60}) did not affect the OS, whereas the OS showed a negative association against heart volumes receiving radiation doses from 63 to 69Gy⁵⁶.

Giving chemotherapy together with radiotherapy exacerbates treatment toxicity, in particular for cCRT. Patient characteristics such as PS and functional indices like FEV_{1s} and D_{LCO} have been associated with OS levels following cCRT for LA-NSCLC⁸⁴⁻⁸⁷. Regarding radiotherapy indices, mean heart dose (MHD) and mean lung dose (MLD) are most frequently used in evaluating NSCLC radiotherapy plans because RIHD and pneumonitis have been found to be associated with OS, and pneumonitis is a common toxicity of LA-NSCLC radiotherapy^{88,89}.

Loap et al.⁹⁰ proposed a new toxicity evaluation concept by plotting a dose-toxicity correlation network. This framework speculates that substructure doses might impact long-term toxicity more than current understanding, especially in OARs with motion issues during the treatment, such as heart and lung. Further studies might help identify critical substructures for toxicity sparing and elucidate unconfirmed causal relationships between toxicity and death.

The radiotherapy toxicity of NSCLC has yet to be fully understood. At least, there is a consensus that toxicity scoring systems should be used to reflect the

potential harm of the treatment. Multiple scoring systems have been used to grade radiation toxicity. The most commonly used system includes the Common Terminology Criteria for Adverse Effects (CTCAE)⁹¹, Radiation Therapy Oncology Group, and European Organisation for Research and Treatment of Cancer (RTOG/EORTC) standard⁹². Despite the detailed definition slightly differing, all systems categorise the toxicity in five grade levels, starting with the mildest grade 1 to the deadly grade 5. In most cases, patients with grade 1 or 2 toxicity may need intervention to alleviate the unwellness. Those with grade ≥ 3 toxicity require medical intervention and may consider stopping or modifying the radiation delivery. Symptoms related to NSCLC radiation toxicity have been reported, including oesophagitis, dysphagia, fatigue, upper gastrointestinal haemorrhage, coughing, and vomiting^{57,59}. However, most toxicity cases were usually mild (grade ≤ 2) when they were not related to lung or heart⁵⁹; therefore, the definition of toxicity scoring systems for general disorders, lung, and heart are summarised in Table 1.5.

Table 1.5 Definition of radiation toxicity scoring system. CTCAE version 5.0 for general disorders is listed; RTOG/EORTC standard toxicity for heart and lung are reported.

| Grade | CTCAE 5.0 (for general disorders) | RTOG/EORTC | |
|-------|--|--|--|
| | | Lung | Heart |
| 1 | Asymptomatic or mild symptoms; observations only; intervention not indicated | Mild dry cough or dyspnoea or exertion | Asymptomatic but ECG changes or pericardial abnormalities w/o other issues |
| 2 | Minimal, local or non-invasive intervention indicated; limiting instrumental ADL | Persistent cough requires narcotic or dyspnoea with minimal effort but not at rest | Symptomatic with ECG changes and radiological findings of congestive heart failure or pericardial disease w/o treatment required |
| 3 | Severe or medically significant but not immediately life-threatening; | Severe cough unresponsive to narcotic or dyspnoea at rest or evidence of acute | Congestive heart failure, angina pectoris, or pericardial disease requires therapy |

| | | | |
|---|--|---|--|
| | hospitalisation indicated; limiting self-care ADL | pneumonitis may require intermittent oxygen or steroids | |
| 4 | Life-threatening consequences; urgent intervention indicated | Severe respiratory insufficiency requires continuous oxygen or assisted ventilation | Same symptoms as grade 3 but not responsive to nonsurgical therapy |
| 5 | Death | Death | Death |

Table abbreviation: ECG for electrocardiogram, w/o for without, ADL for activities of daily living

1.3.2 OARs in NSCLC radiotherapy: oesophagus, spinal cord, and lung

OARs with dose constraints for conventionally fractionated LA-NSCLC cCRT are listed in Table 1.4, including the oesophagus, spinal cord, lung, brachial plexus, and heart. This section will introduce the OARs that have been understood more with limited updates in recent years.

Oesophagitis is the most seen oesophageal toxicity. Early oesophagitis starts with oesophageal inflammation and potential haemorrhage, whereas it can typically be resolved within two to three weeks after completion of radiotherapy⁹³. In a review study, the occurrence rate of grade ≥ 3 acute oesophagitis was less than $<5\%$ for LA-NSCLC studies with radiotherapy duration of >35 days regardless of dose-escalation, reflecting the compensatory mucosal proliferation⁶¹. Late oesophagitis usually becomes fibrosis, happening months or years after the end of radiotherapy. It is not a serious concern as multiple escalation trials show low rates of late oesophagitis, with $<2\%$ and 0% of grade 3 and 4 events, respectively⁶¹.

Radiation myelopathy is often discussed as spinal cord toxicity. In LA-NSCLC, the current cord dose constraints of 50Gy should be plausible, and studies that limit the constraints using <43 Gy showed no grade ≥ 3 toxicity given cCRT⁶¹. 45 to 50Gy delivered in 1.8 to 2.0Gy-per-day is the most held limit, as no

myelopathies have been reported at this dose level without a pre-existing history of extenuating circumstances such as progressive nerve deficit⁹⁴.

Lung toxicity happens as the radiation passes through lung volumes in treating NSCLC. The most commonly seen events include unrepairable lung fibrosis and radiation pneumonitis (RP). Either lung fibrosis or RP starts with inflammation after radiation exposure. They can be best diagnosed through imaging such as CT or magnetic resonance imaging (MRI), with radiopaque features reflecting the alveolar damage and interstitial infiltrates. Clinical pictures of pneumonia usually appear earlier, starting around 6 to 12 weeks after irradiation⁹⁵; fibrosis typically develops 6 to 24 months after irradiation⁹⁶. Fibrosis and RP are not histopathologically independent, and both start from damaging the lung's most radiosensitive alveolar-capillary complex. The accumulation and infiltration of inflammatory cells, fibroblasts, and extracellular matrix proteins such as collagen characterises the pathological presentation. Specifically, fibrosis often comes with some scars, which might indicate lung dysfunction; while RP often comes with the alveolar histoarchitecture destruction around pulmonary interstitium^{95,96}.

Associations have been reported between radiation-induced lung injury following radiotherapy of NSCLC, and patient characteristics such as age (>65 years old), pre-existing lung diseases, and receiving CRT instead of radiotherapy alone⁹⁷. Specifically, chronic obstructive pulmonary disease (COPD) patients with pre-existing lung function issues had higher lung toxicity after lung cancer radiotherapy ($p=0.026$)⁹⁸. Various dosimetric indices have been reported to be related to lung toxicity. For example⁹⁷, one study reported that MLD was strongly correlated with RP; whereas other studies found that lung V_{20} and V_{30} were the only significant parameters in predicting RP. Relatedly, about 15% of grade ≥ 2 RP and fibrosis rates are seen in escalation studies and are associated with MLD⁶¹. In addition, the branchial plexus has also been investigated, with a limited rate of severe toxicity – grade ≥ 3 branchial stenoses only occurred in <5% of patients in

dose-escalation studies up to 84Gy of prescribed dose⁶¹. All in all, there is a consensus that greater irradiation of lung and higher MLD results in more severe lung toxicity. There is, though, still room to fine-tune the dosimetric constraints to account for pre-existing diseases, tumour locations, and breathing during the treatment which are thought affect complication probabilities.

1.3.3 OARs in NSCLC radiotherapy: heart

Compared to the OARs mentioned in the previous section, cardiac toxicity is much more complicated, with less clinical consensus to date. In particular, several issues are still pending to be sorted, including:

- 1) The relationships between cardiac events and absolute survival rate.
- 2) The relationships between heart irradiation, RIHD and OS, and whether doses to particular sub-volumes may be more predictive than measures of whole heart irradiation.
- 3) The precise mechanisms of radiation damage resulting in cardiac toxicity, dysfunction and death.

Historically, pre-clinical *in-vivo* studies revealed that radiotherapy might cause cardiac infarction and congestion dysfunction resulting in heart failure⁸¹. However, most animal studies give radiation in few fractions with higher dose-per-fraction, which only loosely reflect clinical treatment with standard fractionation schedules. Besides, most guidelines about heart constraints come from the Quantitative Analyses of Normal Tissue Effects in the Clinic (QUANTEC) study, which mainly focused on cardiac toxicity dose-responses following radiotherapy of oesophageal cancer and lymphoma⁹⁹. QUANTEC suggested that MHD should be kept below 15Gy, and heart V₃₀ should be kept below 46%; however, there were no lung cancer patients in this study, and MHDs were often roughly estimated^{99,100}.

As the heart is located in the centre of the chest, it is challenging to limit cardiac irradiation without compromising tumour control for lung cancer. RIHD following radiation for lung cancer is usually seen within 90 days of completion of the treatment¹⁰⁰. Mechanistically, cardiac irradiation induces acute inflammation, often presenting as acute pericarditis. Such microvascular damage can lead to fibrosis of the myocardium, affecting heart distensibility and elasticity. These changes can lead to further complications, such as arrhythmias, late pericarditis, pericardial effusion, and myocardial infarction¹⁰¹.

Cardiac toxicity has been raised as a serious issue since increased heart doses may explain the lower OS seen in the 74Gy dose-escalation arm of *RTOG-0617*⁵⁴. Specifically, in post hoc analyses of *RTOG-0617*, heart volumes receiving more than 5Gy (V_5) and 30Gy (V_{30}) were negatively associated with survival^{102,103}. However, in a 2021 review Banfill et al. found that while pre-existing cardiac disease was repeatedly reported to be negatively associated with OS following NSCLC, dose volume indices were inconsistently associated with OS¹⁰⁰. For example, heart V_5 was associated with OS in *RTOG-0617* but not in *ESPAUE*, a phase III trial comparing surgery versus radiotherapy given in 45Gy over 30 fractions for operable LA-NSCLC¹⁰⁴.

Thus there is no consensus yet regarding which critical cardiac substructures might affect NSCLC treatment outcomes, as analyses of different patient cohorts have produced inconsistent results (Figure 1.2)¹⁰⁰. The heart therefore continues to be a single OAR in lung cancer radiotherapy, and current protocols for limiting MHD and dose to the whole heart or pericardium are still recommended. More studies are needed to guide the identification of particular critical substructures.

Additionally, the mechanism of how heart irradiation affects OS is not well understood. Recorded rates of death due to heart failure are too small to account for the reported variations in OS with heart dose, suggesting that either cardiac-related deaths are under-reported or that mechanisms other than cardiac toxicity

are responsible for the link between cardiac doses and OS, for example, depletion of immune cells passing through the heart¹⁰⁵.

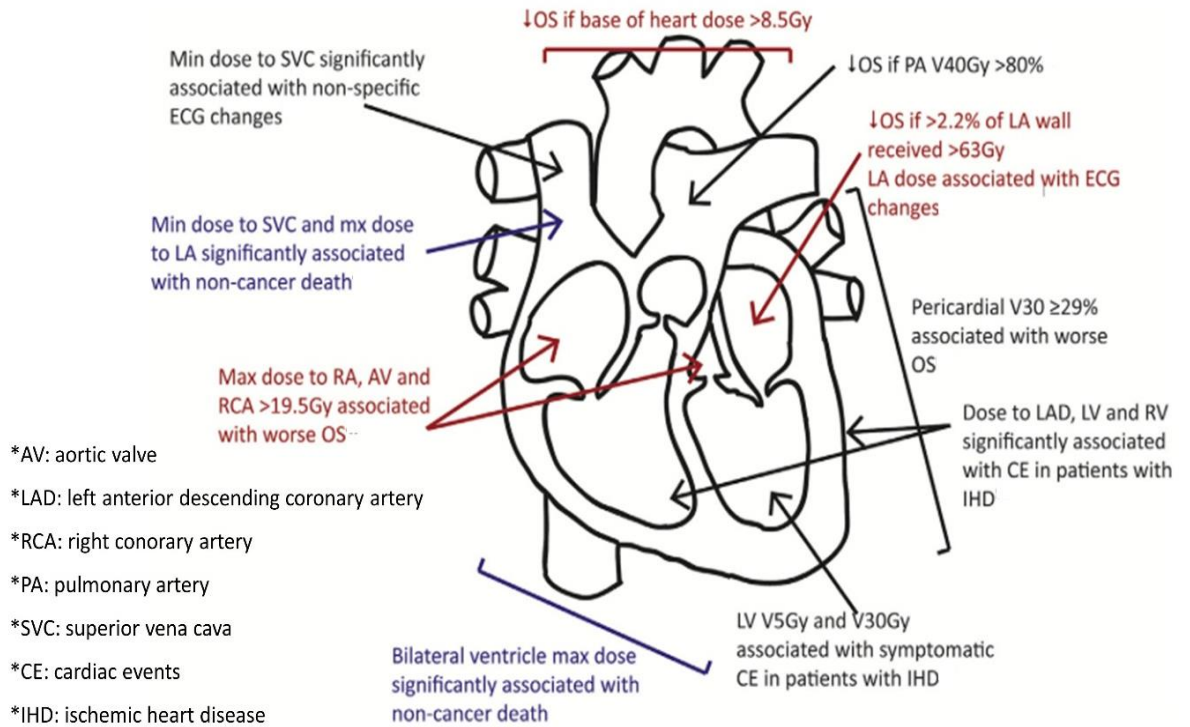


Figure 1.2 Reported associations between doses to heart substructures and OS. (adapted from *Banfill et al., 2021*¹⁰⁰)

1.4 Outstanding issues for LA-NSCLC radiotherapy at the start of the PhD, September 2019

The many developments in technology and scheduling of radiotherapy, chemotherapy and immunotherapy of LA-NSCLC over the last 20 years have raised a series of issues which have yet to be fully addressed, in particular –

1. OS remains poor even using cCRT. Also, dose-escalation studies have reported inconsistent results without clear evidence-based explanations (e.g. *RTOG-0617* vs *IDEAL-CRT*).
2. There is little consensus on tumour fractionation dependence. In the UK, due to busy queues in radiotherapy centres, the clinical treatment prefers hypofractionation in 55Gy over standard 2Gy-per-fraction in 60Gy. Studies have suggested the usage of SBRT for early-stage NSCLC, whereas the benefits of hypofractionation for LA-NSCLC remain limited known although *SOCCAR* study had shown the feasibility of delivering sCRT/cCRT in 55Gy over 20 fractions⁸⁴.
3. Interactions between the different elements of combined treatments (radiotherapy, chemotherapy, immunotherapy) and their relative timings are not fully understood.
4. *PACIFIC* has established cCRT-ICB as a new standard of care for LA-NSCLC. However, there are no quantitative models describing the survival levels expected for cCRT-ICB treatment and their dependence on dose-per-fraction, treatment duration, ICB scheduling, etc.
5. Designs of cCRT-ICB trials have been heterogeneous. There is no consensus on patient selection, and the roles of patient, tumour, radiotherapy, and immunity characteristics remain unclear.

6. Studies report the heart as an important OAR for LA-NSCLC, perhaps explaining the lack of OS advantage seen in *RTOG-0617*. However, analyses and modelling studies have yet to be carried out to delineate possible survival levels achieved by dose-escalated radiotherapy with cardiac-sparing.

1.4.1 Objectives of my PhD

This research aims to improve outcomes achieved by cCRT and cCRT-ICB treatments of LA-NSCLC. In the following chapters, I will build dose-response models that describe a range of factors potentially affecting survival, and fitted them to datasets that describe OS levels achieved by many different radiotherapy, cCRT, and cCRT-ICB treatments. Using the fitted models, I will explore how the therapeutic window can be widened by modifying factors such as the relative timings and durations of radiation, chemotherapy, and immunotherapy; total radiation dose and fractionation; and patient selection. The work is described in the following chapters –

| Chapter 3: Investigating stage and treatment specific effects on LA-NSCLC survival following chemoradiotherapy

To improve the description of the LA-NSCLC cCRT survival data, and better inform the choice of dose, dose-per-fraction and treatment duration for cCRT schedules by further generalisations of radiotherapy TCP/NTCP models. (reflecting outstanding issues 1, 2, and 3)

| Chapter 4: LA-NSCLC immuno-chemo-radiotherapy: effects of immune checkpoint blockades and factors affecting survival

To identify potential patient and treatment characteristics and biomarkers associated with LA-NSCLC survival benefit in cCRT-ICB by delineating the ICB contribution across cCRT-ICB studies. (reflecting outstanding issues 3, 4, and 5)

| Chapter 5: Survival following immuno-chemo-radiotherapy of LA-NSCLC: exploration of variation with dose and treatment duration across an extended range

To provide LA-NSCLC radiation schedules optimisation considering adding ICB as adjuvants on cCRT. (reflecting outstanding issues 4)

| Chapter 6: Cardiac-sparing optimisation for LA-NSCLC radiotherapy

To optimise LA-NSCLC radiation schedules considering optimised photon and proton cardiac toxicity sparing. (reflecting outstanding issue 6)

Chapter 2. Methodology

2.0 Chapter overview

This chapter –

- Describes the datasets used in the thesis.
- Describes the standard radiotherapy dose-response models.
- Introduces the statistical methods used in model fitting and testing.

2.1 Clinical data

Clinical survival and dosimetry can be analysed to identify and quantify relationships between radiotherapy (RT) and outcomes. For the work presented in this thesis, I used two retrospective non-small cell lung cancer (NSCLC) datasets to achieve the objectives stated in Chapter 1: firstly, the chemoradiotherapy (CRT) dataset; and secondly, a dataset describing the results obtained using the concurrent CRT with immune checkpoint blockade (cCRT-ICB). There are additional datasets that I used for cardiac dosimetric indices, which will be introduced in Section 2.1.3.

2.1.1 CRT outcomes dataset

The retrospective NSCLC CRT dataset has 4866 patients across 51 cohorts in 33 published studies. This dataset will mainly be used in Chapter 3, in which I investigate the variation of survival with the different total radiation doses, doses-per-fraction, treatment durations, and scheduling of chemotherapy tested in the various studies contributing to the dataset. Chapter 3 aims at improving the description of NSCLC CRT survival data. Thus, this dataset will help inform the

choice of radiation dose, fractionations and treatment duration by further generalisations of standard tumour control probability (TCP) and normal tissue complication probability (NTCP) models. This dataset will also be used in other chapters, as it provides survival data for CRT alone, which can be used as a baseline to investigate tri-modality treatments with CRT-ICB combination.

The CRT dataset was initially collated by Michael G. Nix et al.³⁹ (Department of Medical Physics and Engineering, Leeds Teaching Hospitals NHS Foundation Trust), with an agreement of data access and extending the dataset for the work in this thesis. He utilised a large cohort of published studies to predict chemotherapy and toxicity effects in NSCLC RT dose-response models. In Nix' work, clinical trials published between 1995-2016 were collected using the term "NSCLC Radiotherapy Dose-Escalation" in academic search engines, including *PubMed*, *ScienceDirect*, and *Google Scholar*. Treatments were categorised into RT, sequential CRT (sCRT) and cCRT groups. Trial arms with fewer than 20 patients and profoundly hypofractionated schedules (≥ 4 Gy-per-fraction) were excluded. Publications with absent/ambiguous descriptions of either dose, fraction, RT delivery days, chemotherapy prescriptions, patient staging, or 2-year overall survival (OS) were also excluded. North American studies without lung tissue heterogeneity correction were recalibrated, raising the prescribed dose and dose-per-fraction by 5% as per the American Association of Physicists in Medicine (AAPM) recommendations¹⁰⁶. The same 5% dose correction was also applied to the *RTOG-0617* cohort to calibrate the reported 95% planning tumour volume (PTV) dose¹⁰⁷.

In this thesis, the CRT dataset is initially used to investigate inconsistent outcomes seen in recent dose-escalation trials and synthesise them into a coherent model (Chapter 3 objective). My focus will be on LA-NSCLC treated with relatively conventional fractionation and quite modern irradiation techniques (3D-conformal, and intensity-modulated radiotherapy). Therefore, I removed studies

meeting the following criteria: conventional 2D planning technique, $\geq 60\%$ stage I/II patients, profound hypofractionation of $>3.0\text{Gy}$ -per-fraction, and studies published before 2000 considering general treatment advancement in the past decades.

After data processing, the median published year of the CRT dataset was 2008 after weighting patient numbers of each cohort, with an interquartile range (IQR) of 2005 to 2012. Key features are summarised in Table 2.1. The patient staging system followed the American Joint Committee of Cancer (AJCC) staging version 4-7. This is the major limitation of this dataset, as without the constituent components of staging, I was unable to harmonise scores to newest AJCC criteria. I did not add any modern studies published after 2016 in the CRT dataset, as the *PACIFIC* study giving cCRT-ICB has significantly improved the OS and changed the standard-of-care. Regarding prescribed dose, 19 cohorts received $\leq 66\text{Gy}$ given as RT alone (4 cohorts), or as part of sCRT (9 cohorts), or cCRT (6 cohorts). Escalated doses of $>66\text{Gy}$ were given to 32 cohorts, 6 treated using RT alone, 17 using sCRT, and 9 using cCRT. Detail of the whole dataset are listed in Appendix 1.

Table 2.1 Key summary of CRT dataset. Mean values of each feature are reported after weighting the patient numbers in each cohort.

| | RT (10 cohorts) | sCRT (26 cohorts) | cCRT (15 cohorts) | Total (51 cohorts) |
|------------------------|----------------------------|------------------------------|------------------------------|-------------------------------|
| Patient numbers | | | | |
| Stage I/II | 188 | 212 | 62 | 462 (9.5%) |
| Stage IIIA | 514 | 732 | 1020 | 2266 (46.6%) |
| Stage IIIB | 490 | 848 | 800 | 2138 (43.9%) |

| | | | | |
|---|------------------|------------------|------------------|------------------|
| RT dose (Gy) (range) | 71 (58 – 81) | 70 (55 – 95) | 69 (55 – 78) | 70 (55 – 95) |
| BED (Gy)[†] (range) | 85 (70 – 97) | 84 (66 – 114) | 83 (66 – 94) | 84 (66 – 114) |
| RT fractions (range) | 36 (20 – 58) | 33 (20 – 43) | 36 (20 – 58) | 35 (20 – 58) |
| RT days (range) | 35 (17 – 46) | 42 (16 – 60) | 43 (28 – 52) | 41 (16 – 60) |
| 2-year OS (range) | 36% (21 – 56) | 37% (18 – 59) | 49% (32 – 68) | 41% (18 – 68) |

[†] BED was a rough estimation for clinical comparison. It was calculated by taking prescribed RT dose, assuming all dose ranges given in 2Gy-per-fraction, with a radiosensitivity value α/β of 10.

Table abbreviation: RT for radiotherapy, sCRT for sequential chemoradiotherapy, cCRT for concurrent chemoradiotherapy, BED for biological effective dose, OS for overall survival

2.1.2 cCRT-ICB outcomes dataset

The retrospective cCRT-ICB dataset has 2196 NSCLC patients from 10 cohorts in 8 studies. This dataset will be used in Chapters 4 to 6, investigating relationships between survival and patient and treatment characteristics for ICB combined with standard cCRT.

This dataset was established by searching *PubMed* and *ScienceDirect*; the last search was done on July 25th, 2022. Three keywords, ‘NSCLC’, ‘Radiotherapy’, and ‘Immunotherapy’, were used, collecting cohorts with reported 2-year OS. Exclusion criteria include: studies using non-ICB immunotherapy agents, studies with stage IV patients, palliative studies, non-photon radiation, and systemic treatment with targeted drugs beyond cCRT-ICB. Radiation dose, dose-per-fraction, treatment duration, tumour staging, ICB drug, drug time, and ICB

schedules starting concurrently with or sequentially after cCRT was reported. Detail can be seen in Appendix 2.

2.1.3 Clatterbridge and Oxford dosimetric indices

These two small, published datasets provide information about cardiac dosimetry and the extent to which heart irradiation can be reduced using optimised volumetric arc therapy (VMAT) treatments and proton radiotherapy. Chapter 6 will utilise this information to investigate the survival level that might possibly be achieved using cardiac-sparing photon and proton radiotherapy.

The Clatterbridge dataset contained 20 locally-advanced NSCLC patients who were treated using standard cCRT at Liverpool Clatterbridge Cancer Centre between 2016 and 2017¹⁰⁸. The dataset was initially used in a study re-optimising the cardiac dose distribution with optimised treatment planning. Patients were given in 2Gy-per-fraction, with a median prescribed dose of 68.8Gy (range: 63.0, 73.0Gy). Tumour contours were drawn on average intensity projections of 4D computed tomography images. Heart contours were defined followed the *SCOPE-1* and *IDEAL-CRT* guidelines. Treatment planning was carried out using VMAT. Baseline and reoptimised heart dose volume measures were listed.

The Oxford dataset contained a further 20 locally-advanced NSCLC patients whose treatment was planned using VMAT and intensity-modulated proton therapy (IMPT)¹⁰⁹. The dataset was originally used for identifying patient subgroups who would benefit from proton therapy compared to photon therapy. Results indicated that patients with pre-existing cardiac diseases or tumours with anatomical locations inferior to the T7 vertebra are likely to benefit more from protons than photons. For photons, the prescribed dose was 70Gy in 35 fractions, and for protons the same effective prescribed dose was explored after allowing for a relative biological effectiveness (RBE; for protons, RBE is defined as the ratio

of absorbed dose of a reference beam of photons to the absorbed dose of protons) of 1.1. Heart delineation and dose constraints used for treatment planning followed *RTOG-1106* and *RTOG-1308* respectively⁴⁵.

2.2 Radiotherapy dose-response models

Radiotherapy depends on radiation physics interactions resulting in downstream biological effects that achieve tumour killing. There are three typical types of radiation physics interaction that lead to energy being transferred from the photons to electrons¹¹⁰: 1) photoelectric effect (most relevant at kilovolt energies), when a photon interacts with an inner-shell electron of the target atom and transfers all energy to the emitted electron; 2) Compton scattering (most relevant at typical megavolt energies for treatment), when a photon interacts with the outer-shell electron at the target atom then transfers part of its energy to the scattered electron, producing another energy-reduced scattered photon; and 3) pair production, when a photon interacts with the strong electromagnetic field and transfers all its energy to generate an electron-positron pair. Each effect has distinct energy deposition characteristics. The energised electrons deposit their energy in small steps, mostly involving electromagnetic interactions with atomic electrons, but occasionally involving electromagnetic interactions with nuclei. The former lead to lots of small energy losses, resulting in chemical bond changes and biological effects; while the latter changes the direction of electron plus generating Bremsstrahlung radiation with characteristic X-rays. The photon energy and the atomic number of the chosen target atom would decide the relative contribution of photon-matter interactions. However, although physical interactions are well understood, the complex biological responses require dose-response models.

2.2.1 Basic radiation biology principles^{78,111}

Radiation biology refers to the knowledge of how ionising radiation affects cells and bodies. The energy absorbed per unit mass defines ‘the absorbed dose’. It is expressed in the units of Gray (Gy), where 1Gy = 1 absorbed Joule (J) per kilogram (kg).

Radiation biology principles were established from simple living systems, such as *in-vitro* culture systems. Such systems measure the biological impacts on the cellular level, investigating the cell survival fraction (SF) by counting the colonies generated by seeded cells in irradiated cell cultivation plates. Historically, various ‘target theories’ were used to describe the shapes of survival curves which describe the variations of SF with radiation dose (Fig. 2.1). Exponential cell death (Equation 2.2.1) is described as ‘single-target’ ‘single-hit’ SF for the neutron or alpha particles with more linear SF. Photons have a lower linear energy transfer (LET; defined as energy release per unit length), and this leads to ‘shoulder’ in the dose-response curve. The dose below shoulder shows limited effects on cell-killing. The ‘multiple-targets’ ‘single-hit’ models with Equation 2.2.2 (zero initial slopes) or Equation 2.2.3 (non-zero initial slope) have been used to describe these curves, showing dependence on cell types. Regarding the parameters, D_0 describes the dose leading to a cell survival fraction of 37%, D_q describes the shoulder of photon dose-response curve, $1/D_1$ the slope of the initial region, $1/D_0$ the slope of the terminal part, N_0 the initial cell numbers, $N(D)$ for the survived cell numbers given radiation dose D , and n the number of targets in a cell that have to be hit for the cells to die.

$$SF = \exp^{-D/D_0} = \frac{N(D)}{N_0} \quad \text{--- Equation 2.2.1}$$

$$SF = 1 - [1 - \exp^{-D/D_0}]^n \quad \text{--- Equation 2.2.2}$$

$$SF = \exp^{-D/D_1} \times [1 - (1 - \exp^{-D/D_0})^n] \quad \text{--- Equation 2.2.3}$$

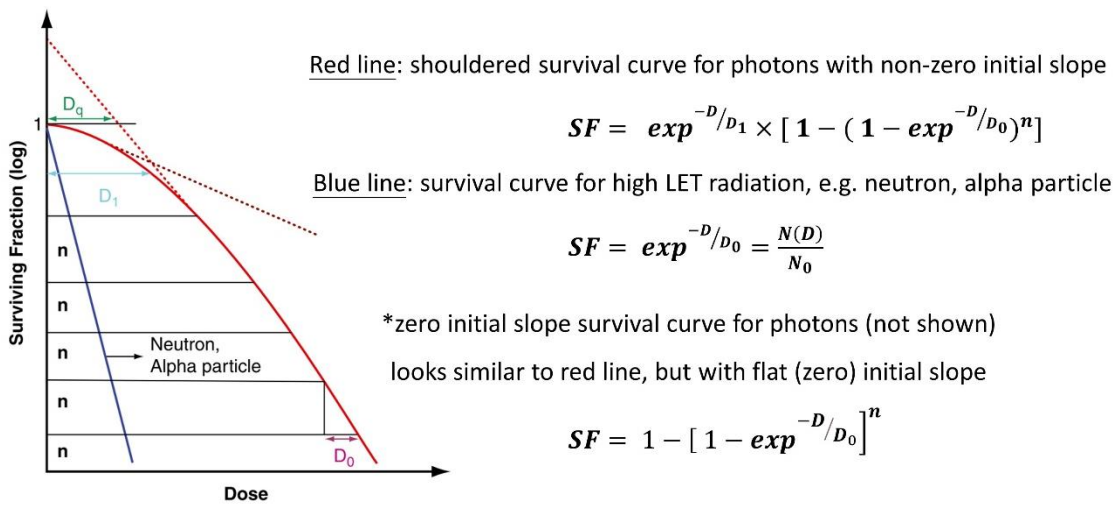


Figure 2.1 Cell survival curves based on different SF curvatures. The solid red line represents the non-zero initial slope curve for photons, while the blue line is for neutron and alpha particles (adapted from *Basic radiation oncology*⁷⁸)

For the photon beam, another theory assumes SF curves contain two components – a linear component (termed alpha) where cell-killing is proportional to dose, and a quadratic component (termed beta) where cell-killing is proportional to the square of a given dose. Therefore, the cell survival given a single radiation fraction can be described as the linear-quadratic (LQ) model using

$$S_{LQ}(d) = \exp(-\alpha d - \beta d^2) \quad \text{--- Equation 2.2.4}$$

where d stands for dose-per-fraction, α for the initial linear slope, and β for the curvature slope. Specifically, there is no D_0 for the LQ model, as the non-linear SF features do not allow the fixed D_0 value under different radiation doses. Relatedly, such non-linear features change SF due to the amounts of radiation delivered. It is why LQ describes survival using d (dose-per-fraction) instead of D (total radiation dose) when it comes to multi-fractionation treatments. Several assumptions are used to simplify the descriptions of multi-fraction treatment, including complete recovery after each fraction, no tumour repopulation, and no cell assortment

changes. The LQ model is more commonly used than target theories as the LQ model fits the *in-vitro* cell survival data better than target theories. Therefore, according to the LQ model, the overall cell survival following multiple radiotherapy fractions is

$$S_{LQ}(D) = \prod_i^n S_{LQ}(d_i) = \prod_i^n \exp(-\alpha d_i - \beta d_i^2) = \exp\left(\sum_{i=1}^n -\alpha d_i \left(1 + \frac{d_i}{\alpha/\beta}\right)\right)$$

--- Equation 2.2.5

where d_i is the dose-per-fraction for the i^{th} fraction. Together, Equation 2.2.5 can be simplified as

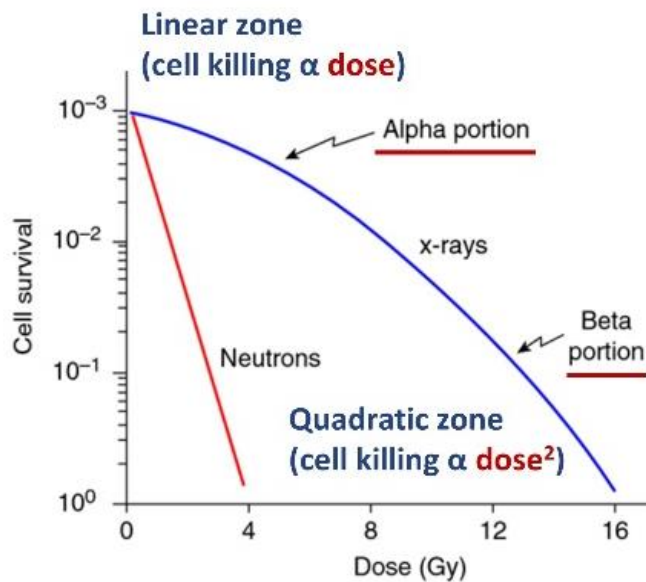
$$S_{LQ}(D) = (S_{LQ}(d))^n = \exp^{-\alpha D \left(1 + \frac{d}{\alpha/\beta}\right)} \quad \text{--- Equation 2.2.6}$$

where α/β ratio describes the radiosensitivity against dose-per-fraction d .

Regarding the practical usage of the LQ photon radiotherapy survival theory, normal tissues can be categorised as early or late responding based on their α/β ratio. Early responding tissues in which acute complications arise generally have higher α/β ratios, around 10Gy, correspondingly straighter cell survival curves. In contrast, late complications arise in late responding tissues, which typically have α/β ratios of around 3Gy, corresponding to greater curvature¹¹². Several tumours such as head and neck squamous cell carcinoma have α/β ratios similar to early responding tissues; while other tumours such as prostate cancer and melanoma have α/β ratios similar to late responding tissues.

| Survival curves using different radiation sources

- Linear-Quadratic theory



| Survival curves using different cells

- Early responding tissues
- Late responding tissues

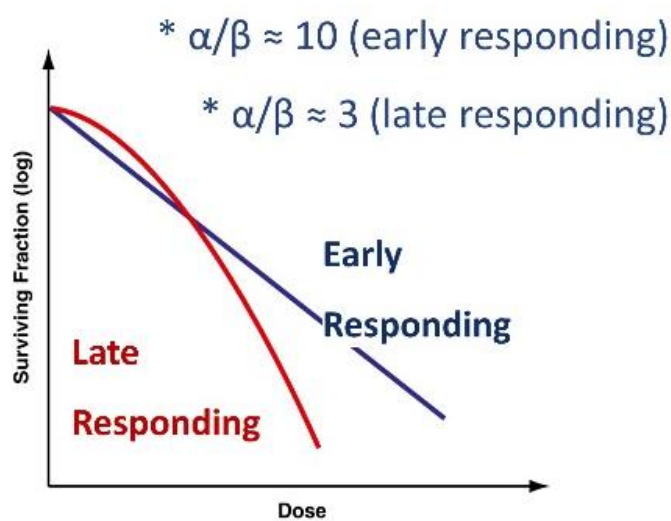


Figure 2.2 Radiation cell survival curves. Both plots illustrate the relationships between radiation dose and cell survival. On the top, the neutron provides a straight line (i.e. the α/β ratio is very high); however, the x-ray has a two-portion curve – α portion where the cell dies stably with the risen dose; β portion where the cell dies dramatically with the increasing dose. The bottom plot indicates two different dose-responses for tissues/tumours – ‘early responding tissue’ dies stably with the risen dose; ‘late responding tissue’ shows the steeper survival response changes with rising doses. (adapted from *Basic radiation oncology*⁷⁸ and *Radiation biology for medical physicists*¹¹¹)

2.2.2 Models toward clinical usages^{78,111,113,114}

The basic LQ theory was established via *in-vitro* studies in 1960s. However, developing models which allow the likelihoods of tumour control and normal tissue complication to be predicted in the clinic requires results for individual cells to be extended to describe the dose-response of whole tumour or normal tissues. Here, I will introduce the TCP and NTCP models, which follow different probability distribution estimation.

Poisson distribution estimation

In statistics, Poisson distribution is a probability distribution that describes the number of events within a specific time interval. It assumes – data are counts of events, events are independent, and the probability of event does not change during the time interval. The Poisson distribution probability function can be written as

$$Poisson(X = k | \lambda) = \frac{\lambda^k \times exp^{-\lambda}}{k!} \quad \text{--- Equation 2.2.7}$$

where X is the observed numbers of occurrence, and λ is the expected mean number of occurrences. The occurrences might, for example, be cells surviving irradiation, making X the actual number in any one tumour, and lambda the mean number

survives. Thus, if the mean number of tumour cells surviving a treatment is λ , the probability that none survive and therefore the tumour is killed is $\exp^{-\lambda}$. Giving radiotherapy over multiple fractions n , cell SF according to the LQ model is an $\exp^{-n(\alpha d + \beta d^2)}$. Consequently, if there are initially N_0 cells in the tumour, the expected numbers surviving irradiation is $\lambda = N_0 \times \exp^{-n(\alpha d + \beta d^2)}$. Thus, the probability none survive in the tumour is

$$TCP = P_{LQ}(X = 0 | D) = \exp^{-N_0 \times S_{LQ}(D)} = \exp^{-N_0 \times \exp(\alpha D \left(1 + \frac{d}{\alpha/\beta}\right))}$$

--- Equation 2.2.8

where D is the total dose, equals to $n \times d$, and α and β for radiosensitivity.

These assumptions have been applied to clinical data studies. This TCP model based on the Poisson distribution describes a sigmoidal dose-response, this being the same general shape seen clinically too. However, when the radiosensitivity parameters in the equation are given values typical of those measured *in-vitro*, the resulting dose-response slopes described by the model are usually some way steeper than those seen clinically, most likely because the model to this point does not include the effect of patient-to-patient variability in radiosensitivity^{115,116}.

Normal distribution estimation

Consequently, the LQ Poisson model has been modified to account for the patient-to-patient tumour heterogeneity. It assumes that tumour radiosensitivity heterogeneity can be presented using the normal distribution function $f(\alpha)$ with mean radiosensitivity value α_0 and standard deviation σ ^{117,118}. Therefore, with initial numbers of tumour clonogens N_0 , the TCP model can be written as

$$TCP = \int_0^{\infty} \mathbf{f}(\alpha) \times \exp\left[-N_0 \times \exp^{-\alpha D \left(1 + \frac{d}{\alpha/\beta}\right)}\right] d\alpha ;$$

$$\text{where } f(\alpha) = \frac{1}{\sqrt{2\pi}\sigma} \exp^{-\frac{1}{2}\left(\frac{\alpha-\alpha_0}{\sigma}\right)^2} \text{ --- Equation 2.2.9}$$

Subsequently, if I neglect the effects of β and solve the above integral, the above equation can be approximated as a cumulative function, written as^{117,119}

$$TCP = \Phi\left(\frac{\alpha_0 D - \ln N_0 - \Gamma}{\sigma D}\right) \rightarrow \Phi\left(\frac{D - \frac{\ln N_0 + \Gamma}{\alpha_0}}{\frac{\sigma}{\alpha_0} D}\right) \equiv \Phi\left(\frac{D - D_{50}}{m \times D}\right) \text{ --- Equation 2.2.10}$$

where the Euler-Mascheroni constant Γ is 0.5771, D_{50} identifies the dose needed to achieve a 50% likelihood of tumour control, m inversely relates to the gradient at the steepest point as it appears at the denominator of the cumulative normal distribution function Φ . To sum up, when taking the heterogeneous radiosensitivity into account, the TCP model takes the form of the integrated normal function of equation (Equation 2.2.10), which is often approximated to

$$TCP = \Phi\left(\frac{D - D_{50}}{m \times D_{50}}\right) \text{ --- Equation 2.2.11}$$

in essence the same form proposed empirically for normal tissue complications by Lyman in 1980s. The equations up to 2.2.11 describe the effects of a single dose-level D . In this thesis, I will explore outcomes from LA-NSCLC radiotherapy, in which tumours receive fairly uniform doses, so Equation 2.2.11 will be the general form used to describe tumour control in the following chapters.

Nonetheless, normal tissues and sometimes tumours do not receive uniform doses, so variety of approaches have been suggested to convert the dose distribution within volumes of tumours into a single equivalent uniform dose (EUD). EUD describes the summation of each uniform radiation dose (D_i) to all small volume voxels (V_i) comprising organs/tumours of interest (Equation 2.2.12). Subsequently, EUD can be used as the D to describe the effects of tumour heterogeneity with normal distribution assumption (Equation 2.2.13).

$$EUD = \left(\sum_i V_i D_i^{\frac{1}{V}} \right)^V \quad \text{--- Equation 2.2.12}$$

$$TCP_{EUD}(D) = \frac{1}{\sqrt{2\pi}} \int_{-\infty}^t \exp\left(\frac{-x^2}{2}\right) dx, \text{ where } t = \frac{D - D_{50}}{m \times D_{50}} \quad \text{--- Equation 2.2.13}$$

The non-uniformity can be handled using such approaches, but in this work it is not an issue as LA-NSCLC radiotherapy uses relatively uniform dose. In addition, NTCP can also be estimated as an analogy of TCP based on the heterogeneous features of normal tissues, which has been widely accepted and used^{120,121}. Therefore, Equation 2.2.11 will be the general form for both TCP and NTCP in this thesis.

In practical usage, the prescribed dose D is often replaced with either the biologically effective dose (BED), or the equivalent dose in 2Gy-per-fraction ($EQD2$). When BED or $EQD2$ is used in the equations, the D_{50} value in the formulae is understood as representing either BED_{50} or $EQD2_{50}$, the BED or $EQD2$ needed for 50% tumour control or normal tissue complication. BED is calculated from D and the dose-per-fraction d , with the radiosensitivity α/β :

$$BED = n \times d \times \frac{1+d}{\alpha/\beta} \quad \text{--- Equation 2.2.14}$$

Equivalent dose for dose-fractionation comparisons

BED and $EQD2$ are usually used for comparing dose-fractionation. Standard form of BED is written as Equation 2.2.14, and for some fast-repopulating cancers (e.g. lung, head and neck cancer¹¹²), BED has been tweaked by considering the tumour repopulation effects. It is written as

$$BED = n \times d \times \frac{1+d}{\alpha/\beta} - K \times (T - T_k) \quad \text{--- Equation 2.2.15}$$

where K is the rate of tumour repopulation (Gy/days), T the total radiation treatment duration (days) and T_k the kick-off day of tumour repopulation. $EQD2$

comes from the LQ theory, given the referenced dose-per-fraction of 2Gy. It provides a comparison for clinically familiar fractionation, also, allows for comparing radiosensitivity (α/β).

$$S_{LQ}(D) = \exp^{-\alpha D(1+\frac{d}{\alpha/\beta})} = \exp^{-\alpha D_{ref}(1+\frac{d_{ref}}{\alpha/\beta})} = S_{LQ}(D_{ref}); D = n \times d$$

$$\text{when } D_{ref} = D; d_{ref} = 2Gy \rightarrow EQD2 = \frac{n \times d(1+\frac{d}{\alpha/\beta})}{1+\frac{2}{\alpha/\beta}} \quad \text{--- Equation 2.2.16}$$

In my works, I use the tweaked version of TCP by applying *EQD2* (Equation 2.2.17), which allows comparing dose-per-fraction variations with standard 2Gy-per-fraction delivery. I also use this equation to describe the NTCP of survival-limiting toxicities.

$$TCP/NTCP = \Phi\left(\frac{EQD2 - EQD2_{,50}}{m \times EQD2_{,50}}\right) \quad \text{--- Equation 2.2.17}$$

2.3 Regression models

Regression helps identify the relationships between treatment outcomes and variables of interest. Different types of regression describe the associations between the independent variables (factors) and dependent variables (outcomes) under specific conditions. The simplest form of regression is linear regression, which can be written as

$$y_i = \beta_0 + \beta_1 x_1 + \dots + \beta_n x_n + \varepsilon_i \quad \text{--- Equation 2.3.1}$$

where y_i is the dependent variable, β_0 is the intercept, β_i is the regression coefficient for independent variable x_i , and ε_i is the random error term, capturing impacts from other factors influencing the dependent variable y_i . In practical usage, a fitted regression coefficient represents the expected change in the dependent variable

(the change that would be seen on average if the experiment was repeated many times) given a known change in the independent variable. The error term is minimised to get the best regression coefficient. In other words, linear regression is fitted by selecting the coefficients resulting in the least summed squares of errors. As the regression is usually taken from a population sample, 95% confidence intervals (CI) are usually reported along with the best fits. It describes the uncertainty ranges for fitted values and explains the regression features. It also allows an understanding of potential values that may occur in true population¹²².

2.3.1 Logistic and probit regression^{123,124}

Logistic regression describes sigmoidal relationships between independent and dependent variables. In contrast to linear regression, logistic regression aims to fit a sigmoidal curve, and data with binary outcomes are usually used to describe the probability of being in class 1 (vs class 0) given independent variables x_1 to x_n . Therefore, by definition, the dependent variable y is usually a categorical variable, and the logistic regression provides estimated probabilities between these categorical outcomes y called ‘the odds’.

There are two types of logistic regression: binary and polytomous logistic regression. Binary regression is usually used in cancer oncology research as treatment outcomes are usually binary, such as OS and progression-free survival (PFS). The binary y follows the Bernoulli distribution, a discrete probability distribution which takes the labelled value ‘1’ as probability p and ‘0’ as the probability $q = 1 - p$. The independent variable x can be either the categorical or continuous variable.

The standard logistic sigmoidal function is defined as

$$\sigma(t) = \frac{\exp^t}{\exp^t + 1} = \frac{1}{1 + \exp^{-t}} \quad \text{--- Equation 2.3.2}$$

where t is a linear combination of the various factors. Once t is substituted into the sigmoidal line function $t = \beta_0 + \sum_{i=1}^n \beta_i x_i$ with sigma to describe the sigmoidal response between the combination of independent variables x and outcome probability p , the above equation can be written as

$$p(x) = \sigma(t) = \frac{1}{1 + \exp^{-(\beta_0 + \sum_{i=1}^n \beta_i x_i)}} \quad \text{--- Equation 2.3.3}$$

Therefore, the binary logistic regression is written as

$$y_i = \text{logit}(p) = \log\left(\frac{p_i(x)}{1-p_i(x)}\right) = \beta_0 + \beta_1 x_1 + \dots + \beta_n x_n = \beta_0 + \sum_{i=1}^n \beta_i x_i$$

--- Equation 2.3.4

where the logit (log odds) describes the ratio between the binary event probabilities p and q (i.e. $1-p$). With the logarithm ratio between binary events, the exponential term in the sigmoidal equations can be negligible, and the odds can be written as

$$\text{odds} = \frac{p(x)}{1-p(x)} = \exp^{(\beta_0 + \sum_{i=1}^n \beta_i x_i)} \quad \text{--- Equation 2.3.5}$$

where $p(x)$ is the probability of the outcome depending on the combination of predictors x , β_0 is the intercept, β_i is the regression coefficient for independent variables x_i . Relatedly, there is another sigmoidal regression called ‘probit regression’. Assuming the y_i in Equation 2.3.1 is a binary variable, the population probit model with multiple regressions x_1, x_2, \dots, x_n can be written as

$$P(y_i = 1 | x_1, x_2, \dots, x_n) = \Phi(\beta_0 + \beta_1 x_1 + \dots + \beta_n x_n + \varepsilon_i)$$

--- Equation 2.3.6

where Φ is the cumulative normal distribution function. The main difference between logistic and probit regressions lies in the fine detail in the sigmoidal curves they describe. Often, the data is not precise enough to distinguish between these shapes, therefore practically some practitioners prefer logistic regression because it uses the closed form formula of Equation 2.3.3, which is easy to

calculate. In this work, I use the probit form because it is directly mechanistically based on TCP model with a normal distribution of radiosensitivity value, and today's computational power makes it easy to calculate values from Equation 2.3.6 rather than Equation 2.3.3.

2.3.2 Proportional hazards (Cox) time-to-event analysis^{125,126}

Cox proposed the proportional hazards regression to describe time-to-event data for each individual. This regression makes two assumptions:

- 1) Survival has a fixed baseline hazard function.
- 2) There are linear relationships between the log hazard and each variable.

Censoring plays a vital role in oncology studies, as many patients might die, be withdrawn or not completely followed-up before the end of the study (i.e. right censoring). Censored data points are used in model calculations until the censoring timepoint, which keeps the study power as much as possible without simply deleting the data from patients that did not complete the study. Patients who die or withdraw before the end of the study are unlikely to be a random sample, and therefore excluding them would potentially bias results. Analysing data including results for censored patients limits this bias and makes the best use of the available data. Studies with high levels of censoring have less robustness when interpreting the results. In particular, censoring is expected to be 'non-informative', where patients who dropped out of the study due to reasons unrelated to treatment. In contrast, 'informative' censoring where patients were lost in follow-up due to reasons related to the study might bias the results. For example, patients in the control arm of cancer treatment study might be too sick to follow-up. Therefore, it should always be noted that censoring reasons are potentially different between study arms and limit the model robustness in studies using data from multi-sources.

The proportional hazards regression describes the time-to-event outcomes (e.g. survival) against one or more variables, also known as Cox regression. The subjects are assumed to share a common event distribution against time from study enrolment. The coefficient in the regression refers to hazard, and the regression typically assumes the fixed ratio of event rates over time (i.e. hazard ratio, HR). In terms of the application in survival analysis, the data points follow the exponential distribution. Therefore, the hazard rate h at time t is defined as:

$$h(t) = \lambda_0(t) \times \exp(\beta_1 x_1 + \dots + \beta_n x_n) = \lambda_0(t) \times \exp(\beta_i x_i)$$

--- Equation 2.3.7

where λ_0 is the baseline hazard, β_i is the regression coefficient for independent variables x_i . Therefore, the survival at specific time t with patient number N_0 at starting point and patient number N at time t can be written as:

$$\text{survival} \left(\frac{N}{N_0} \right): \frac{dN}{dt} = -h(t) \times N_0 \rightarrow \frac{dN}{N_0} = -h(t) \times dt$$

$$\rightarrow \frac{N}{N_0} = -\exp \int h(t) dt \quad \text{--- Equation 2.3.8}$$

where the cumulative hazard is represented by the integral of the constant hazard rate $h(t)=\lambda$ over time. Finally, the HR between two factors (x_i, x_j) can be written as:

$$\text{hazard ratio (HR)} = \frac{h_i(t)}{h_j(t)} = \frac{\lambda_0(t) \times \exp(\beta_i x_i)}{\lambda_0(t) \times \exp(\beta_j x_j)} = \exp \left(\sum_i \beta_i x_i \right);$$

for a single β_1 and dichotomous x ($x_i = 1, x_j = 0$), $HR = \exp(\beta_1)$

--- Equation 2.3.9

where HR quantifies how much the survival might change given a unit change of the independent variable. The HR represents the continuous risk over the whole study period, given the censoring consideration based on the Cox regression. For a dichotomous variable, the definition of β is very natural, with $HR = \exp(\beta_1)$

giving the HR with/without the variable. For a continuous variable, β and HR are defined per unit change in x . Thus, the answer each HR depends on the units of measuring x . For example, if age was the factor, β would be 12 times greater if I measured it in years than in months, and 365 times greater than if it was measured in days.

The null hypothesis of the Cox regression assumes that the independent variable has no relationship with the survival outcome. Therefore, HR can be used to calibrate the OS to evaluate the optimised OS given specific conditions. By definition, OS can be represented using N and N_0 , the patient numbers at different time points. Therefore, if the HR acts as a constant factor affecting the OS, the new OS can be calculated by processing the old OS with exponential HR.

$$OS = \frac{N}{N_0} = \exp\left(-\int h(t) dt\right) \rightarrow OS_{new} = \exp\left(-HR \times \int h(t) dt\right)$$

$$\rightarrow OS_{new} = OS_{old}^{HR} \quad \text{--- Equation 2.3.10}$$

This idea will be used later in Chapter 6 when I identify the HR of mean heart dose against OS, aiming to model the OS given different cardiac-sparing conditions.

2.4 Curve fitting optimisation methodology

This thesis aims to optimise the radiotherapy dose-response models in describing clinical data. As the dose-response models predict binary categorical outcomes, likelihood estimation is used across all chapters. The use of maximum likelihood fitting is therefore of interest.

2.4.1 Maximum likelihood estimation

Parameters of probability distribution functions given some observed data can be estimated using maximum likelihood (ML) techniques¹²⁷. This approach has been broadly used in clinical analysis, particularly in medical physics research, such as TCP and NTCP dose-response models¹²⁸. It hypothesises that the data distribution features are the combination of probabilities, so ML aims to find the likelihood with highest occurrence rate by calculating the probability density function¹²⁹. The likelihood equations can be written as Equation 2.4.1, where f is the function with corresponding variables x_1, \dots, x_n whose distribution depends on θ . Consequently, the corresponding likelihood form function could be written as L .

$$f_{\theta}(x_1, \dots, x_n) = L(\theta|x_1, \dots, x_n) \quad \text{--- Equation 2.4.1}$$

Equation 2.4.2 represents the form that can be used to maximise the specific likelihood, where $arg\ max$ stands for ‘arguments of the maxima’, indicating the specific points where corresponding likelihood functions $\widehat{\theta}_{ML}$ are maximised. The normal distribution is the most used distribution in ML, so the modified form with normal distribution assumption is written as Equation 2.4.3. Subsequently, Equation 2.4.4 describes ML estimators with likelihood L , where μ and σ^2 indicates mean and variance individually.

$$\widehat{\theta}_{ML} = arg_{\theta} \max \{L(\theta|x)\} \quad \text{--- Equation 2.4.2}$$

$$f(x) = f(x|\mu, \sigma) = \frac{1}{\sqrt{2\pi}\sigma} \exp\left(-\frac{(x-\mu)^2}{2\sigma^2}\right) \quad \text{--- Equation 2.4.3}$$

$$L(\mu, \theta) = \prod_{j=1}^n \frac{1}{\sqrt{2\pi}\sigma} \exp\left(-\frac{(x_j-\mu)^2}{2\sigma^2}\right) \quad \text{--- Equation 2.4.4}$$

This thesis applies ML fitting through an open-accessed *bbmle* package using *R* programming language¹³⁰. ML is usually followed by the likelihood ratio test (LRT) with corresponding chi-square distribution, testing the overall performance between two fitted models^{127,131}. The null hypothesis is that there is no difference between the likelihood of the models, where $\alpha=0.05$ is used as the criteria to test the null hypothesis. The ML possesses several advantages, such as consistency (e.g. the estimated parameters tend to approach the actual values as the sample size increases) and efficiency (e.g. the estimated parameters have the least variability among all unbiased estimators). Figure 2.3 visualises the ML concepts.

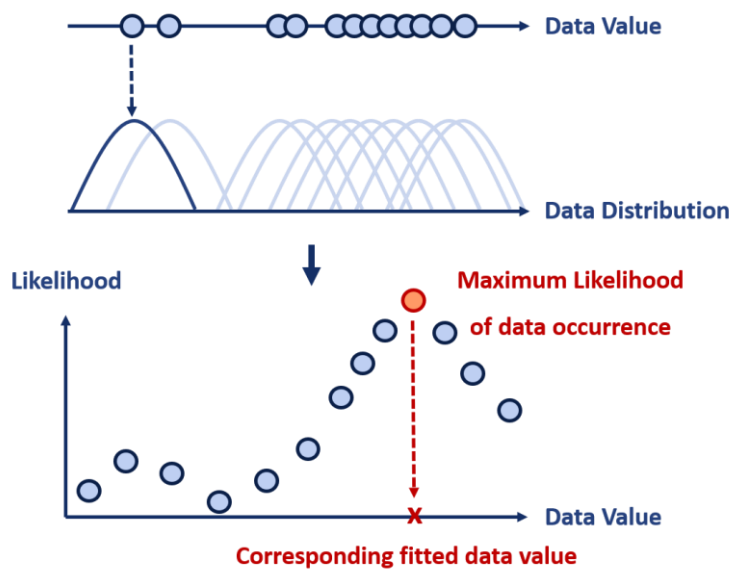


Figure 2.3 Visualising maximum likelihood estimation using one-dimensional numerical data as an example. Binary categorical data is also available when the data is binary distributed, and ML allows finding the best fits between 1 and 0.

2.4.2 Optimisation details

Missing data

If missing data is in the original dataset, the researcher could choose either ‘complete case analysis’ by excluding samples with any missing data, or doing the ‘data imputation’ to allow more samples to be tested in the models. Several data imputation methods exist, including mean, mode, regression and multiple imputation^{132,133}. Mean imputation replaces missing values with the mean of the non-missing values. Mode imputation replaces the missing values with the most frequently occurred value. Regression imputation estimates the missing values based on the regression relationships between the factors in the dataset. Multiple imputation creates several plausible sets of imputed values to account for the uncertainty in the imputation process. These imputed sets can be generated through either mean, mode, or regression imputation. Finally, by pooling the repeated datasets and calculating the missing data's mean value, variance and CI, multiple imputation provides much better accuracy than single imputation method. In this thesis, I will use complete case analysis to exclude data cohorts which do not fit the selection criteria as it provides more robust modelling outcomes. In chapter 4, I further correct the effective patient number for each cohort given various censoring issues. I try to limit the bias as much as possible, and the data are randomly (non-informatively) censored, which does not bias the results.

Covariance, correlation, collinearity, confounder, covariates

These terminologies have different definitions, but all might affect the model's robustness. Therefore, it is important to define these terms before doing the model optimisation. Covariance measures the degree to which two variables tend to deviate from their means in similar ways; in other words, the joint variability of two variables. Covariance can be written as

$$\mathbf{covariance} (X, Y) = E[(X - E[X])(Y - E[Y])] \quad \text{--- Equation 2.4.5}$$

where E represents the expected value of the corresponding variable (i.e. the mean of X , Y for $E[X]$, $E[Y]$). Whereas covariance depends on the widths of the distributions of the two data factors being considered, the correlation coefficient is a normalised measure that more intuitively describes the relationships between the two variables. It can be defined as

$$\mathbf{correlation} (r_{X,Y}) = \frac{\mathbf{covariance} (X,Y)}{\sigma_X \sigma_Y} \quad \text{--- Equation 2.4.6}$$

where σ is the standard deviation for variables X and Y . The correlation coefficient (r) ranges from -1 to 1, describing the negative/positive relationships with different correlation strengths. Regarding the strength, the absolute r values ($|r|$) can be classified into very weak, weak, moderate, strong, and very strong with standards below/above 0.20, 0.40, 0.60, 0.80¹³⁴. As the routine correlation hypothesises the linear relationships between variables (Pearson's correlation), splitting the individual variable contribution out within the complicated model might be difficult when there is a strong correlation between independent variables. For example, in a multivariate model, it might be challenging to decide which of two heavily correlated variables is most associated with the dependent variable and should be retained in the model. It could be that both are causally related to the dependent variable, but due to the correlative structure of the data, whether that is the case or whether just one of the variables is associated with the dependent variable remain unknown.

Collinearity refers to a situation when two or more independent variables in a regression model are highly correlated with each other. The effects of such collinearities can be examined through the correlation matrix, checking which correlated variables could possibly be removed. It can also be quantified through the variance inflation factor (VIF):

$$\mathbf{VIF}_i = \frac{1}{1-R_i^2} = \frac{1}{\mathbf{Tolerance\ of\ each\ parameter}} \quad \text{--- Equation 2.4.7}$$

$$R_i^2 = 1 - \frac{\text{residual SS}}{\text{total SS}} = 1 - \frac{\sum(y_i - y_{\text{fitted}})^2}{\sum(y_i - y_{\text{mean}})^2} = 1 - \frac{\text{Log-Likelihood}(\text{proposed model})}{\text{Log-Likelihood}(\text{saturated model})}$$

--- Equation 2.4.8

where R_i^2 expresses what fraction of the variability of the dependent variable y_i can be explained by the proposed model. At the same time, tolerance represents the regressing effects of all independent variables against every other independent variable. There is no standard cut-off for VIF, while the consensus implies that the $VIF > 10$ shows the model has a collinearity problem. The small tolerance or large VIF generally indicates strong collinearity, which might destabilise variable selections and model interpretation¹³⁵.

Confounder refers to dependent variables which can affect the relationships between the independent and other dependent variables, while these variables do not exist within the causal relationships between them. The confounder can misguide the explanations between independent and dependent variables, whereas no statistical algorithm can directly identify them due to the complexity of real-world scenarios, as there might be many interconnected relationships among variables. Strategies such as randomisation, restriction (e.g. control the age within the testing between smoking and lung cancer), and matching (e.g. select data with equal distribution of possible confounders for independent and dependent variables) can be applied¹³⁶.

Covariate refers to the naturally existing variables that might affect the dependent but not the independent variables. Covariate is essentially a potential confounder. Whether covariate becomes a confounder depends on whether it is correlated with another factor that in turn is associated with the dependent variable. In other words, covariate is not a problem if: 1) it is not correlated with any factors being explored; or 2) it is not correlated with any of the factors explored that are associated with the dependent variable. It is worth considering and discussing the covariates when addressing the analyses. A commonly used method of dealing with

covariates require executing two analyses with and without covariates, thus allowing understanding impacts of covariates against the outcomes.

In this thesis, I will plot correlation matrices and apply VIF to limit the number of variables, particularly in Chapter 3, aiming to extend the radiation models by taking multiple hypotheses into account with additional parameters.

Variable selection

It is essential to select variables which should be accounted for in the optimisation models. In terms of practical variable selection in clinical research, it is necessary to consider the clinical perspectives of including/excluding specific factors before applying standard variable selection methods. In other words, biologically implausible variables should be removed initially, as they might affect the interpretation of models. Critical steps of variable selection start from univariable (UV) analyses, followed by multiple methods to select variables incorporated in the multivariable (MV) analyses. Specifically, UV analyses with a p-value ≤ 0.2 are usually used as the threshold instead of a p-value of 0.05 when selecting factors in the MV models, as there might be some confounding effects which could lead to over/under-estimating the impacts of specific factors¹²². Backward elimination starts with the global model, removing the most insignificant independent variable (IV) until no IV with a p-value higher than the threshold is left. Forward selection is entirely different, beginning with the most significant factor in UV analysis, and then adding the IV by its significance order until there is no IV with a low p-value lying within the threshold. Stepwise selection combines forward and backward methods, deciding the selected variables by comparing a series of p-values with different variables combination¹³⁷. I will use the stepwise selection in Chapter 4 when identifying factors that might affect the OS of cCRT-ICB. However, it should be noted that the stepwise variable selection often artificially inflates the precise estimates as it assumes a single fit of the model to the data, overfitting the data well in-sample, but do poorly out-of-

sample. I will only use stepwise selection when selecting and pooling factors from UV to MV models. In terms of model selection given different numbers of parameters and degrees of freedom, I will use penalised likelihood as discussed in the below section.

Models testing with underfitting, overfitting and validation

Underfitting means that the model is too simple to capture variance in the independent variable, while overfitting implies that the model is too complicated to fit the training data a bit too accurately. The ideal likelihood model must find the best likelihood values without getting involved with either underfitting or overfitting. The deviance statistics testing the proposed model versus the saturated model are used to evaluate the underfitting, and overdispersion statistics and cross-validation (CV) address the overfitting. Specifically, overfitting might be of more concern. In this thesis, I aim to add new parameters that have not been investigated before in the radiotherapy dose-response models, which might result in overfitting with unnecessarily model complexity. Therefore, I explain how to test the model performance before introducing the methods that examine overfitting.

The modelling performance of the ML estimation can be checked using the LRT. The LRT is used to diagnose the significance of a set of independent variables in the regression. If the likelihood difference between ‘pre-testing probability without specific parameters’ and ‘post-testing probability with specific parameters’ lies above 95% of the chi-square distribution given corresponding degrees of freedom (d.f.), it suggests that these specific parameters should be included to improve data description ability. In addition, Akaike Information Criteria (AIC) can be used along with the LRT, and AIC values can be more straightforward in describing the modelling performance than the LRT¹³⁸. The AIC assesses model quality and aids in model selection for analysing capture-recapture data. It emphasises model parsimony, meaning that when comparing an approximating

model to the actual model, the one with the lowest AIC should be chosen. Hence, the AIC measures the information lost using the following equation:

$$AIC = 2k - 2 \times \ln(L) \quad \text{--- Equation 2.4.9}$$

where k is the estimated variable numbers in a model, and L is the maximum value of the likelihood function for that corresponding model¹³⁹. Specifically, the model with the lowest AIC is theoretically the model expected to best describe future data. Furthermore, the AIC can be used to compare un-nested model, whereas the LRT can only distinguish between same models with or without certain factors included.

AIC estimates how well a model is likely to fit future data; and trades off the goodness of the fit to the current data ($-2\ln L$) against model parsimony ($2k$). When increasing modelling complexity with a new parameter returns a tiny improvement (AIC change <2 , less than penalisation of 2) in model performance, it hints that the model might be overfitting, as the AIC improvement seems to be coming from the noise instead of the real data description effects^{139,140}. In these circumstances, the AIC itself actually goes up, (i.e. gets worse), and the model is viewed as being definitely less good than the one without the extra variable. There is a bit of a debate about just how much AIC should fall when adding a new variable for it to be worthwhile. For example, if $-2\ln L$ falls by 2.3, then the AIC will fall by only 0.3 and it is arguable that whether the extra variable is all that useful. But strictly, the model with the better AIC (even if only by a very small amount) is viewed as the better model. Consequently, post-hoc checking and validation testing are needed to enhance the study robustness.

Overdispersion is when the random variability in observed data is greater than expected given theoretical probability functions, such as binomial distribution. In other words, there is more variation than expected because of, for example, patient numbers. This variability may arise from factors not accounted for modelling, such as subtle centre-to-centre protocol differences. Overdispersion is checked using

the overdispersion factor (ODF), calibrating the AIC to get the accurate ranges of CI and validate the model selection. ODF can only determine the overdispersion once getting a model including all the factors of relevance. In other words, if the model has not included several factors, that itself might cause the overdispersion. In the chapter 3, I will try AIC to get the supposedly best model, then check for overdispersion, and ODF might cause me to choose a simpler model with fewer factors. ODF starts from the sum-of-squares (SS) residuals calculation,

$$SS = \sum_i \frac{(Observed_i - Modelled_i)^2}{[Modelled_i \times (1 - Modelled_i)] / (Patient\ number_i)} \quad \text{--- Equation 2.4.10}$$

where observed/modelled values and patient numbers refer to cohort i in the dataset. Subsequently, ODF can be obtained by dividing SS with d.f. in fitting. The practical application relies on the calibrated AIC (AIC'), allowing model reselection and broader profile-likelihood CI estimation^{138,141}.

$$ODF = \frac{SS}{d.f.} \quad ; \quad AIC' = 2k - \frac{2 \times \ln(Likelihood)}{ODF} \quad \text{--- Equation 2.4.11}$$

Model validation can be done using external validation or internal validation. The external validation uses an external dataset to compare the model fitting results performed using the model training dataset. CV is a standard internal validation method in data modelling research, which allows for preventing overfitting. There is no exception in medical physics, where holdout CV, leave-one-out CV, or k-fold CV are commonly seen in published works¹²⁸. The CV starts with separating the whole dataset into training and testing data subsets (commonly by a 90:10 or 80:20 split). Secondly, models are fitted to training subsets, and tested using testing subsets. Thirdly, rotating the folds are required in CV. In each iteration of CV, a different fold is held out as the validation dataset, while the other folds are used for training. This ensures that each data point in a dataset is used both in model training and validation. Finally, the difference between each training and testing dataset is calculated and retained for model selection, as the model might perform excellently in specific folds of datasets but not all datasets.

The difference between CV types lies in how they split the data; holdout CV randomly holds some data as testing and leaves others as training. In contrast, leave-one-out CV chooses one data point for testing each time; and k-fold CV breaks the dataset into k subsets, then each time selects one subset for testing and groups the others together for training. The model with the lowest CV values should have the best performance in describing future data. With CV techniques, it is possible to minimise noise impacts in specific cohorts¹⁴². In this thesis, I will use 10-fold CV and ODF to examine the overfitting issues.

Confidence intervals

CI describes how precisely values of model parameters have been identified in the fitting process. Three types of CI are commonly used – asymptotic CI, profile-likelihood CI, and bootstrapped CI.

Asymptotic CI is the standard and easiest method, used in most cases. It estimates the CI from the local curvature of the likelihood function and the asymptotic distribution of this function according to the central limit theory. The profile-likelihood CI estimates the CI based on the same asymptotic distribution of the likelihood function, but now explicitly evaluating changes in the function with changing parameter values rather than estimating the changes from the function curvature. Profile-likelihood CI is usually more accurate than the asymptotic CI, as less assumptions are made in the calculation^{143,144}. The bootstrapped CI is estimated entirely numerically by resampling data with replacements. Repeatedly bootstrapped resamples of the original datasets are created, and by fitting each, distributions of fitted parameter values are generated. From these distributions, the CI can be identified directly as the ranges of parameter values obtained for some percentage of bootstraps, 95% for example in the case of a 95% CI. The standard is to use at least 1000 bootstrapped resamples¹⁴⁵. In this thesis, I will use profile-likelihood and bootstrapped CIs to report the uncertainties.

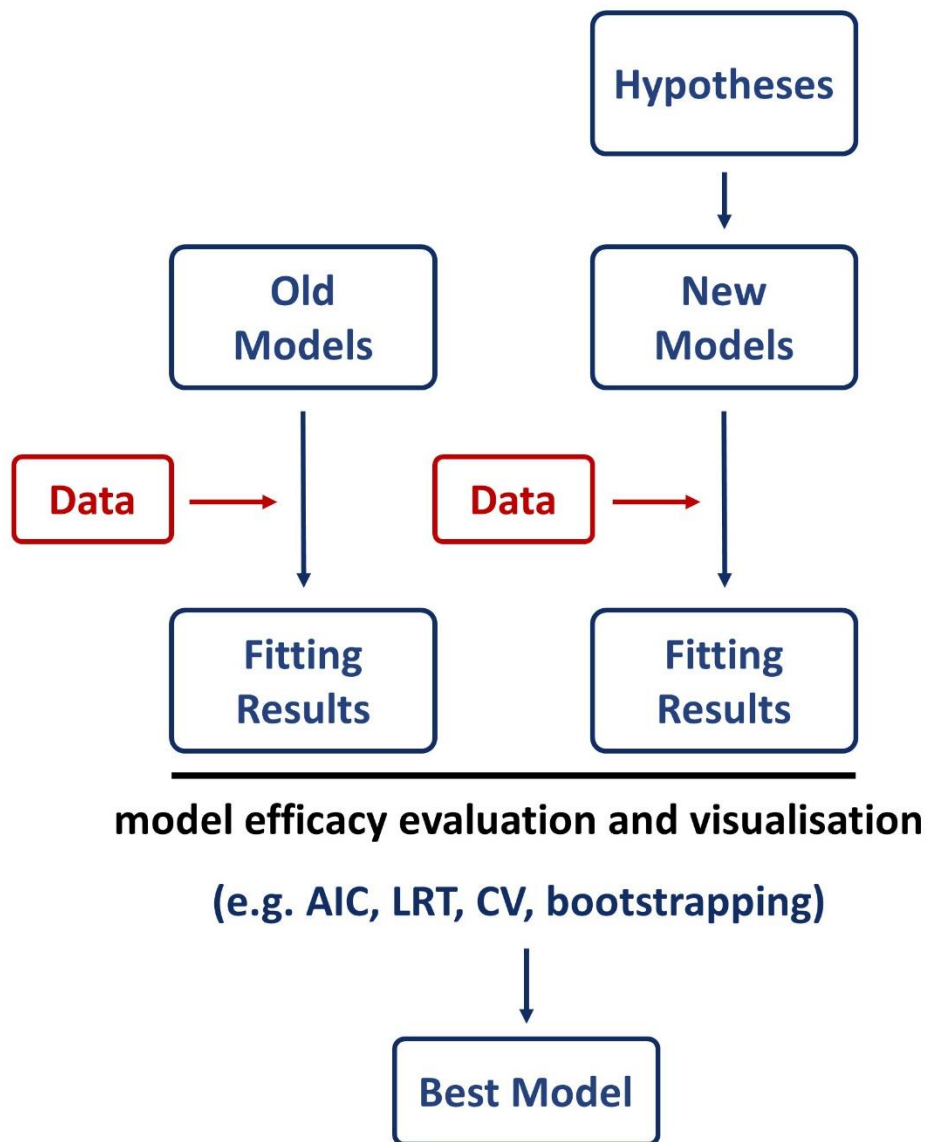


Figure 2.4 Graphical structure overviewing the modelling optimisation concept. This figure outlines how I use data to examine specific hypotheses for optimising dose-response models.

2.5 Study structure

This research aims to optimise radiotherapy dose-response models to describe clinical outcomes more accurately, with specific aims of 1) explaining the underlying features behind clinical outcomes, 2) predicting how outcomes might change with treatment modification, and 3) informing factors which might affect the outcomes.

There are a series of sections for the rest of the thesis. In Chapter 3, I will take Nix' earlier model³⁹, and explore new hypotheses by adding additional parameters describing extra patient factors. In Chapters 4, I will use the extended model to describe the OS expected for the CRT components of CRT-ICB treatments, allowing the OS gains obtained by adding ICB to be estimated, and the associations between these gains and treatment and patient factors to be explored. In Chapters 5 and 6, I will use the model fits created in Chapter 3 and the extended model with ICB effects (CRT-ICB model) to explore how OS might change given dose-escalation of the radiotherapy components of treatments, and with cardiac-sparing techniques. A graphical overview of the project is shown in Fig. 2.5.

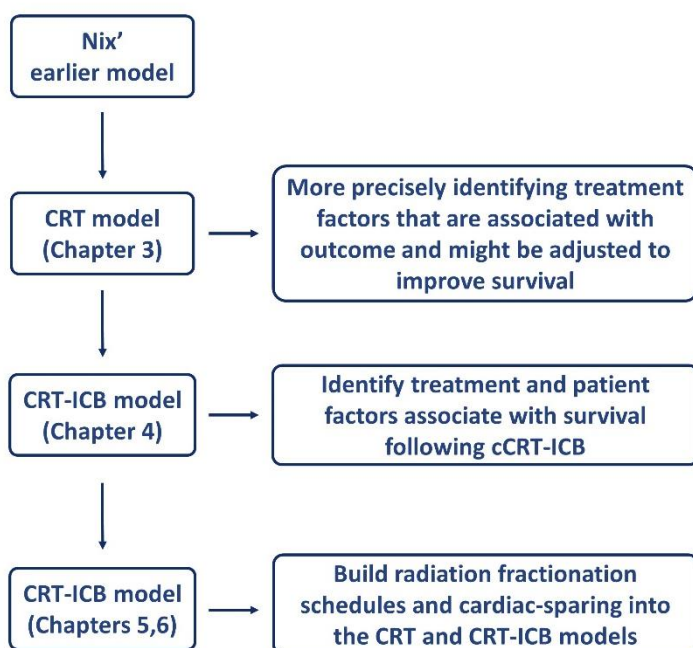


Figure 2.5 Graphical overview of study structure in the following chapters of my thesis.

Chapter 3. Investigating stage and treatment specific effects on LA-NSCLC survival following chemoradiotherapy

3.0 Chapter overview

This chapter –

- Investigates stage-/treatment- specific effects following concurrent chemoradiotherapy (cCRT).
- Highlights cCRT-repopulation, stage- α/β , and stage-toxicity.
- Stratifies overall survival for patients with stage-/treatment- features are predicted following the advanced modelling.

*This chapter has been revised and published in *Cancers 2022, 14, 4869*.

The published manuscript can be found via

<https://doi.org/10.3390/cancers14194869>

3.1 Development of LA-NSCLC chemoradiotherapy

Lung cancer is one of the most death-causing diseases globally, accounting for 20% of cancer-related death in Europe in 2018⁶. Also, more than three-fourths of patients can only be diagnosed when cancer becomes regionally or distantly metastatic⁸, making it more life-threatening than other cancers diagnosed earlier. Non-small cell lung cancer (NSCLC) accounts for more than 80% of lung cancer¹¹, and more than 60% of NSCLC patients would receive radiotherapy (RT) within any phase of their treatment³¹. For early-stage NSCLC, stereotactic body

radiotherapy (SBRT) with a high dose per fraction has been considered a clinical frontline treatment, especially for patients who cannot undergo surgery^{34,146}. In terms of locally-advanced NSCLC (LA-NSCLC), the best chance of survival is offered by concurrent chemo-RT (cCRT), given as 60 to 66Gy in daily 2Gy fractions with 2 to 4 chemotherapy cycle, so cCRT has become the clinical standard care for inoperable cases^{18,31}. However, many patients are insufficiently fit for cCRT and instead receive RT alone or sequential chemo-RT (sCRT).

It remains challenging to identify optimal RT schedules for LA-NSCLC. Compared to conventional fractionation, a 12-day accelerated hyper-fractionated course of RT alone achieved improved 2-year overall survival (OS) (29% vs 20%, $p = 0.004$) but tumours nevertheless recurred in 47% of patients receiving the accelerated treatment⁴⁹. Meta-analyses found that survival was improved by combined chemo-RT, and that cCRT achieved an absolute survival benefit of roughly 5% compared to sCRT^{147,148}. Data from some early-phase clinical trials of radiation dose-escalation showed improved OS⁵² and acceptable toxicity⁵³, and a meta-analysis showed survival gains for escalation of RT alone and sCRT¹⁴⁹. For cCRT, however, a survival gain was not seen and the *RTOG-0617* phase III trial reported a median survival of 20.3 months for 74Gy in 2Gy fractions compared to 28.7 months for the baseline 60Gy treatment, a survival reduction of 8.4 months in the high-dose arm ($p = 0.004$)⁵⁴. These findings are not coherently explained by standard *in-silico* models, and improved models are needed to guide the optimisation of radiation treatments.

Radiotherapy models have been widely used for decades, such as tumour control probability (TCP) models based on the linear-quadratic cell survival fraction theory¹¹³, and normal tissue complication probability (NTCP) models established on heterogeneous tumour sub-volume hypotheses proposed by Lyman, Kutcher and Burman^{78,111}. In 2011, Partridge et al.⁶² improved TCP prediction for NSCLC in two years through applying standardised tumour equivalent doses in

2Gy-per-fraction (EQD₂), which incorporated the different dose-per-fraction and treatment duration between trials. Also, they corrected tumour EQD₂ by adding repopulation weighting λ and repopulation onset day T_k , which successfully fit the data with diverged ranges of treatment days⁶². In this research, the model results suggested the survival gain with increasing EQD₂ using data from 24 published trials. Nix et al.³⁹ recently updated the model by considering chemotherapy effects, improving OS prediction accuracy through combining TCP and NTCP. Even so, the radiosensitivity parameter α/β was fixed as 3 for normal tissues, and low tumour α/β of 4.0 occurred in the best fitting revealing the potentially different properties versus routinely used tumour α/β of 10³⁹. In terms of the modelling outcomes, the OS rates first rose with increasing EQD₂ before falling again. In a plot of survival levels calculated from the model for cCRT treatments given in increasing numbers of 2Gy fractions over 40 days, survival for stage IIIA patients started to fall as doses increased beyond 68Gy. This was a lower turnover point than for RT alone or sCRT, for which modelled survival continued to rise through to 80Gy. Consequently, additional add-ons are required to consolidate the radiosensitivity findings and examine the details.

Aside from radiosensitivity issues, there are still some incomprehensible clinical observations. Firstly, the International Staging Project collecting lung cancer database by the International Association for the Study of Lung Cancer (IASLC) showed OS difference between IIIA (N=3200) and IIIB (N=2140) NSCLC, reporting 2-year OS as 55% versus 44% and 5-year OS was 36% versus 26%^{13,150}. However, there is only a tiny difference between IIIA and IIIB clinical staging definitions. Patients with more regional lymph node metastasis would be defined as IIIB with similar primary tumour sizes and no distant metastasis^{11,14}. Also, both stage IIIA and IIIB are classified as LA-NSCLC, which follows the same treatment protocols in clinic^{18,151}. Consequently, there might be some

intrinsic tumour heterogeneities between IIIA and IIIB, possibly affecting cCRT efficacy and leading to the OS difference.

Secondly, although the enhanced tumour EQD₂ could partially quantify how cCRT benefits patients via radio-sensitisation parameter incorporated in the published models³⁹, reasons why OS did not enhance as theoretically believed in accelerated trials have yet to be explained. De Ruyscher et al.¹⁵² speculated that cCRT might sufficiently suppress tumour repopulation and neutralise the effect of avoiding repopulation through accelerating radiation fractionation since both OS and toxicity remained similar in stage III NSCLC using either conventional fractionation or accelerated planning. Thirdly, recent *PACIFIC* clinical trials showed notable OS improvement in cohort administering immunotherapy after cCRT versus standard cCRT on LA-NSCLC^{71,72}. Still, detailed interaction between immunotherapy, chemotherapy and RT have not been clearly understood.

Together, a thorough investigation of cCRT is necessary to optimise LA-NSCLC treatments. We develop advanced treatment outcome models by modifying parameters based on three hypotheses to shed light on better cCRT dose-response schedules. First, we explore whether tumour accelerated repopulation varies with treatment-type (cCRT vs RT/sCRT) in accordance with a recent proposal that cCRT might suppress re-population, negating the effect of treatment acceleration¹⁵². Second, we investigate the origin of the low radiosensitivity (α/β ratio), studying whether it is driven by a particular disease stage or treatment-type. And finally, we allow the survival-limiting term to vary with stage, since larger volumes of normal tissues are irradiated to high dose-levels during treatment of higher stage disease. By building a dose-response model for chemo-RT, we also aim to create a platform for future work characterising the additional effects on survival of combined immuno-chemo-RT treatments.

3.2 Materials and methods

3.2.1 Experimental design

This study looks over possible factors, including ‘tumour repopulation onset time difference’ between treatments (RT alone/sCRT/cCRT), tumour α/β by stages, and stage-specific toxicity. Firstly, we fit the retrospective data using standard TCP model⁶² (Model 1), then fit it again using the chemo-radiation model published by Nix et al.³⁹ (Model 2). Regarding the new models we develop, we first split repopulation-related parameters λ and T_k by treatments (Model 3). Secondly, we split tumour α/β by stages, testing whether low α/β found under the chemo-radiation model still appears across stages (Model 4). Finally, we fit NTCP by stages to examine the possible normal tissue toxicity difference as a surrogate trial to support stage-individualised tumour α/β (Model 5). The graphical study flow chart was presented in Fig. 3.1.

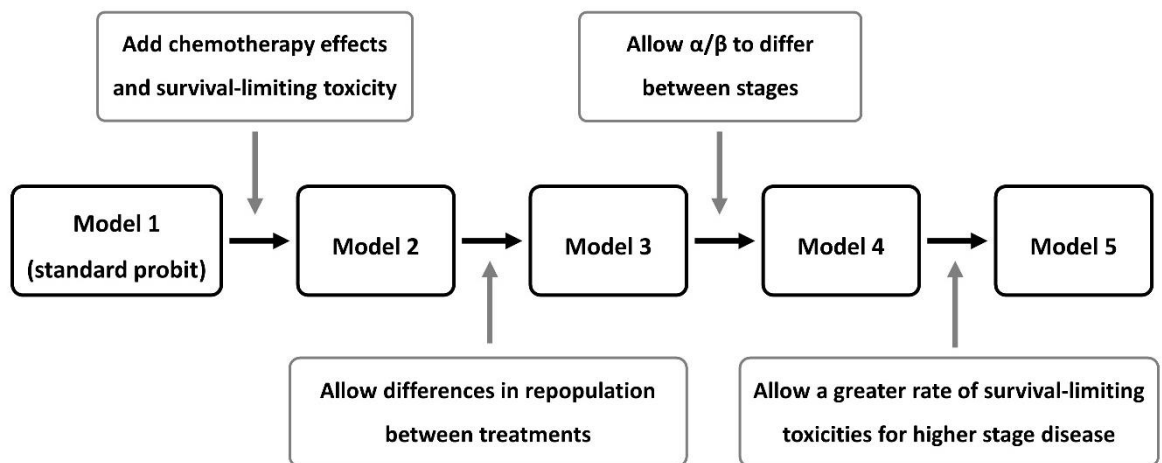


Figure 3.1 Sectional study flow chart. The flow chart outlines the research structure in this chapter also lists the main hypotheses and modulated parameters in each model.

The study aimed to improve treatment OS prediction using modified radiotherapy dose-response models and explain unclarified clinical observations based on proper modelling hypotheses. Dose-response curves were plotted, then compared to the clinical outcomes after modelling works.

3.2.2 Retrospective data collection

Modelling data were collated through *PubMed*, *Google Scholar*, and *ScienceDirect*. The medical subject keyword ‘NSCLC radiotherapy dose-escalation’ were used in searches. Either institutional trials or multi-centred trials were included only if 2-year OS was reported, but the limitation was set to remove the trial with palliative purpose, less than 20 patients in any cohorts, >60% of stage I/II patients, and schedules >3.0Gy dose-per-fraction. Also, as a study investigating tumour repopulation onset day, trials published before 2000 were excluded to avoid non-3D conformal radiotherapy without robust computed treatment planning or some conventionally 2D-planned trials taking days of treatment interruption between fractionations^{153,154}. 5% data pre-processing were raised on doses and doses-per-fraction for cohorts without lung tissue heterogeneity correction in North America¹⁰⁶ and *RTOG-0617*⁵⁴ prescribed using 95% planning target volume¹⁰⁷. All in all, as an extended modelling research, the dataset was originally derived from Nix et al.³⁹. Data re-searching and sorting criteria have been updated as mentioned. The data contained 4866 patients in 51 cohorts between 2000-2016. Data characteristics were summarised in Table 3.1.

Table 3.1 Patient characteristics. Results are expressed as either total values or mean values with the range.

| 4866 non-small cell lung cancer (NSCLC) patients in 51 cohorts | | | |
|---|---|---|--------------|
| Radiotherapy (RT) alone | Sequential Radiotherapy (sCRT) | Concurrent Radiotherapy (cCRT) | Total |

| | 10 cohorts | 26 cohorts | 15 cohorts | 51 cohorts |
|--|----------------|----------------|----------------|----------------|
| Patient Numbers | | | | |
| Stage I | 116 | 127 | 3 | 246 (5.1%) |
| Stage II | 72 | 85 | 59 | 216 (4.4%) |
| Stage IIIA | 514 | 732 | 1020 | 2266 (46.6%) |
| Stage IIIB | 490 | 848 | 800 | 2138 (43.9%) |
| Total | 1192 | 1792 | 1883 | 4866 |
| Histology* (%): squamous cell carcinoma/adenocarcinoma/other NSCLC | | | | |
| | 49.4/24.2/26.4 | 42.5/32.8/24.7 | 32.8/31.0/30.8 | 42.6/29.6/27.8 |
| RT technique (# of cohorts): rectangular field RT/conformal RT/IMRT | | | | |
| | 2/7/1 | 3/22/1 | 0/11/4 | 5/40/6 |
| IIIB Patient Numbers / IIIA Patient Numbers in each cohort | | | | |
| | 0.92 | 1.22 | 0.83 | 1.05 |
| | (0 – 1.92) | (0 – 2.89) | (0.16 – 1.72) | (0 – 2.89) |
| Dose** (Gy) | | | | |
| | 71 | 70 | 69 | 70 |
| | (58 – 81) | (55 – 95) | (55 – 78) | (55 – 95) |
| Radiotherapy Fractions | | | | |
| | 36 | 33 | 36 | 35 |
| | (20 – 58) | (20 – 43) | (20 – 58) | (20 – 58) |
| Dose / Fraction (Gy) | | | | |
| | 2 | 2 | 2 | 2 |
| | (1.3 – 3.0) | (1.7 – 2.8) | (1.3 – 2.8) | (1.3 – 3.0) |
| Overall Radiation Treatment Time (Days) | | | | |
| | 35 | 42 | 43 | 41 |
| | (17 - 46) | (16 - 60) | (28 - 52) | (16 - 60) |
| Biological Effective Dose, BED (Gy)[†] | | | | |
| | 43 | 40 | 43 | 42 |
| | (24 – 70) | (24 – 52) | (24 – 70) | (24 – 70) |
| 2-year Overall Survival (%) | | | | |
| | 36 | 37 | 49 | 41 |
| | (21 – 56) | (18 – 59) | (32 – 68) | (18 – 68) |

* Histology data was only available for 39/51 cohorts (9 RT alone, 16 sCRT, 14 cCRT).

** 5% Dose escalation has been processed for trials without lung heterogeneity correction and those reported with 95% planning tumour volume doses in *RTOG-0617*.

† BED was a rough estimation for clinical comparison. It was calculated by taking prescribed RT dose, assuming all dose ranges given in 2Gy-per-fraction, with a radiosensitivity value α/β of 10.

3.2.3 Chemo-radiotherapy outcome models

All models in this research aimed to optimise 2-year OS fitting through applying different parameters. We named the five models from the simplest to the most complicated as Model 1 to 5 sequentially (Figure 3.1). More stratification of parameters or treatment effects were incorporated in the advanced models.

Model 1: Standard TCP model

In the basic model, $EQD_{2,tum}$ was initially calculated using standard biological effective dose (BED), where tumour radiosensitivity parameter α/β , through prescribed radiation dose (D) and dose-per-fraction (d) were used. Later, accounting tumour repopulation effects through weighting repopulation rate (λ), overall radiotherapy treatment time ($ORTT$), and repopulation onset day (T_k).

$$EQD_{2,tum} = D \times \left(\frac{1 + \frac{d}{\alpha/\beta}}{1 + \frac{2}{\alpha/\beta}} \right) - \lambda \times \text{Max}[ORTT - T_k, 0]$$

--- Equation 3.1

As the basic standard model has not taken NTCP into account, modelled TCP results equal to the modelled results of OS, where sigmoidal TCP was calculated via cumulative normal distribution function (Φ):

$$OS = TCP = \sum_i \left\{ f_i \Phi \left[\frac{EQD_{2,tum} - EQD_{2,tum50}(S_i)}{m \times EQD_{2,tum50}(S_i)} \right] \right\} \times 100\%$$

--- Equation 3.2

where f_i represented the fraction of *stage i* (S_i) (stage I, II, IIIA, or IIIB) patients in each cohort, m symbolised the dose-response gradient, while $EQD_{2,tum50}(S_i)$ indicated the required prescribed dose for achieving 50% of tumour control in each stage.

Model 2: Basic chemo-radiation model

The standard TCP model has been extended via adding chemotherapy parameters and incorporating normal tissue toxicity³⁹. An updated generalised function can be written as Equation 3.3.

$$OS = TCP \times [OS_{Max}^{Treatment}] \times (1 - NTCP) \times (1 - R \times Year Calibration)$$

--- Equation 3.3

where OS_{Max}^{RT} was fixed at 85% for RT-only cohorts since 15% post-treatment distant failure was reported for patients who did not receive chemotherapy^{39,155}, while OS_{Max}^{CRT} was fitted together for both sCRT and cCRT cohorts with minimum boundary of 85% – assuming incorporating chemotherapy could benefit patients at least as good as singly treated using RT alone. Besides, R represented overall clinical treatment improvement unrelated to treatment schedules, as treatment planning techniques improved from 2000 to 2016. *Year Calibration* reflected how many years each study published before the most recent one in 2016.

In detail, $EQD_{2,tum}$ was slightly modified by adding a chemo-radiosensitisation parameter RS^{cCRT} for cohorts treated with cCRT. RS^{cCRT} was counted before incorporating tumour repopulation calibration, fixing at 1 for RT alone/sCRT but allowed to be fitted >1 for cCRT. Toxicity effects were modelled through $EQD_{2,NT}$ and sigmoidal NTCP as

$$EQD_{2,NT} = \frac{BED}{1+\frac{2}{3}} = D \times \left(\frac{1+\frac{d}{3}}{1+\frac{2}{3}} \right)$$

--- Equation 3.4

$$NTCP = \Phi \left[\frac{EQD_{2,NT} - EQD_{2,NT50}}{m_{NT} \times EQD_{2,NT50}} \right] \quad \text{--- Equation 3.5}$$

where $\alpha/\beta_{normal\ tissue}$ was fixed at 3^{39} . As model was fitted using OS data without detailed toxicity information, NTCP factor was referred as the survival-limiting toxicity. $EQD_{2,NT50}$ linked to the prescribed dose resulting in 50% of death-causing side effects, while m_{NT} symbolised the dose-toxicity response gradient.

Model 3: Splitting tumour repopulation by treatments

To specifically investigate the tumour repopulation effects, repopulation related parameters λ and T_k were modified as treatment-specific parameters, testing the possibly existing difference between cCRT versus radiotherapy alone or sCRT. Namely, λ and T_k in Equation 3.1 were fitted differently for cCRT vs RT/sCRT. Consequently, Equation 3.1 was replaced using Equation 3.6:

$$EQD_{2,tum} = D \times \left(\frac{1 + \frac{d}{\alpha/\beta}}{1 + \frac{2}{\alpha/\beta}} \right) - \lambda^{Treatment} \times \text{Max}[ORTT - T_k^{Treatment}, 0]$$

--- Equation 3.6

In brief, repopulation parameters (λ and T_k) were allowed to take different fitted values for cCRT vs RT alone/sCRT.

Model 4: Splitting tumour α/β by stages

$EQD_{2,tum}$ of each stage was more precisely calculated through splitting tumour α/β in this model. However, as there were limited stage I/II patients (<10% in total), both stages were fitted together, while stage IIIA and IIIB were fitted independently. In other words, tumour α/β was fitted differently for early stages vs stage IIIA vs stage IIIB. The extended version of $EQD_{2,tum}$ calculation using α/β (S_i) for radiosensitivity of stage i (S_i) (early-stage, IIIA, or IIIB) patients become

$$EQD_{2,tum} = D \times \left(\frac{1 + \frac{d}{\frac{\alpha}{\beta}(S_i)}}{1 + \frac{2}{\frac{\alpha}{\beta}(S_i)}} \right) - \lambda^{Treatment} \times \text{Max}[ORTT - T_k^{Treatment}, 0]$$

--- Equation 3.7

In brief, tumour α/β was allowed to take different fitted values for stage I/II vs IIIA vs IIIB.

Model 5: Splitting toxicity by stages

As normal tissues might have a higher chance to be irradiated if there are more nodal spreads planned to be treated in higher-stage patients. Here, we tried describing toxicity by stages via incorporating F_i , representing the proportion of patients with life-threatening severe toxicity. Consequently, Equation 3.5 was replaced using Equation 3.8.

$$NTCP = \sum_i \left\{ f_i \times F_i \times \Phi \left[\frac{EQD_{2,NT} - EQD_{2,NT50}}{m_{NT} \times EQD_{2,NT50}} \right] \right\} \times 100\%$$

--- Equation 3.8

In a nutshell, 2-year OS was fitted using equations described under each model, and modifications in the simpler models were always be kept in the progressively complicated models. (e.g. Equation 3.6 was kept in Model 4 and Model 5)

3.2.4 Statistical analysis

Models were fitted using the maximum likelihood estimation method through *bbmle2* package in *R* language¹³⁰, then plotting dose-response curves via *ggplot2* package¹⁵⁶. Akaike Information Criteria (AIC) estimating the relative information lost in a model was used to compare the model good-of-fit performance^{129,139}. Significances of adding parameters in updated models were tested by likelihood ratio test (LRT). A cross-validation score calculating the least sum-of-squared residuals through 10-fold cross-validation was applied to validate the AIC results¹⁴². 95% profile-likelihood confidence intervals (CI) of fitted parameters were calculated using the model judged best based on AIC, LRT, and cross-validation score¹⁵⁷. Profile-likelihood CIs were calculated based on multi-dimensional methods, where likelihood profile got by varying all parameters at the same time, and recorded the boundary values when the log-likelihood fell by $\chi^2_{(1,0.95)} = 3.84$ (chi-square distribution, with degree of freedom = 1) from the best fits. Two-sided significances were used in all comparisons.

Calibration plots comparing observed OS and modelled OS were calculated to measure the model fitting goodness. Linear regressions are plotted, where weighting number of patients in each cohort through minimising a sum-of-squares by

$$\sum_i \left\{ (OS_{i,observed} - OS_{i,modelled})^2 \right. \\ \left. / \left[OS_{i,modelled} \times \left(\frac{1 - OS_{i,modelled}}{\text{Patient number in each cohort}} \right) \right] \right\}$$

--- Equation 3.9

Additionally, gradients' significances of scatter plots were determined through F-tests after linear regression¹⁴⁵. Linear fits to cohort data in scatter plots were determined by minimising sums of squared errors weighted by patient numbers, to

provide more informative relationships between factors and outcomes. Also, as models were fitted through counting patient numbers in each cohort, weighted regression should be applied in comparing fits and predicted outcomes.

Significances of differences in treatment characteristics between sets of cohorts were assessed using the Wilcoxon rank-sum test. Visualisation matrix describing correlation properties between parameters in the most complicated model (Model 5) was plotted through *corrplot* package in *R* after variance-covariance calculation¹⁵⁸. Variance inflation factor (VIF) and overdispersion factor (ODF) were also calculated as post-hoc check-ups after modelling¹⁵⁹.

3.2.5 Supplementary dataset as validation

To validate model prediction efficacy, published 2-year OS data of *PACIFIC* clinical trial were used^{71,72}. *PACIFIC* trial aimed at investigating whether adding immunotherapy drug could improve the LA-NSCLC cCRT outcomes through durvalumab versus placebo after cCRT.

The placebo arm of the *PACIFIC* trial was used to validate our prediction. We assumed 1:1 IIIA vs IIIB patients receiving 60Gy or 70Gy *EQD_{2,tum}* to calculate the OS – where 60Gy and 70Gy stand for the median doses of low-dose groups (91.6% patients treated with 54 to 66Gy) and high-dose groups (8% patients treated with 66 to 74Gy) in *PACIFIC*.

3.3 Results

3.3.1 Data description

The dataset contains 4866 patients retrieved from 51 cohorts in 33 studies with 5.1% of stage I, 4.4% of stage II, 46.6% of stage IIIA and 43.9% of stage IIIB NSCLC respectively. Tumour histology was available in 39/51 cohorts, where 43% had squamous cell carcinoma (SCC), while 30% had adenocarcinoma and 28% with other NSCLC histologies. Most cohorts were treated with conformal techniques (40/51), 6 with IMRT and 5 with conventional rectangular fields. Among these, 10 of them were treated with RT alone. Chemotherapy and radiotherapy were given sequentially as sCRT in 26 cohorts, and 15 cohorts were treated simultaneously as cCRT (Table 3.1). In more detail, 26 cohorts receiving sCRT included 12 with neo-adjuvant and 1 with adjuvant chemotherapy, while 13 cohorts were either mixed or not clearly described.

The data only had 9.5% of early-stage patients (stage I/II), allowing deeper investigation focusing on LA-NSCLC. Slightly longer mean overall radiation treatment time were found in sCRT (42 days) and cCRT cohorts (43 days) compared to RT alone (35 days), with borderline statistical significance ($p = 0.026$ for sCRT; $p = 0.055$ for cCRT). Dispersed mean 2-year OS ranged from 18% - 68%.

Two-year OS was statistical insignificant against prescribed radiation dose ($p = 0.18$) and RT treatment duration ($p = 0.79$), while having significant relationships against dose-per-fraction ($p = 0.03$). The increase of OS with increasing prescribed dose was quite modest (shallow slope of 0.002), with a 2% increase in survival every 10Gy in dose. 0.2% increases of OS per Gy of prescribed dose is way lower than 1-3% per Gy – the normal gradients for radiation dose-survival relationship in human tumours¹⁶⁰. Dose-per-fraction seems to be a bit more effective with a 7%

OS increase for every 1 Gy-per-fraction increase between 1 to 3 Gy-per-fraction (Fig. 3.2).

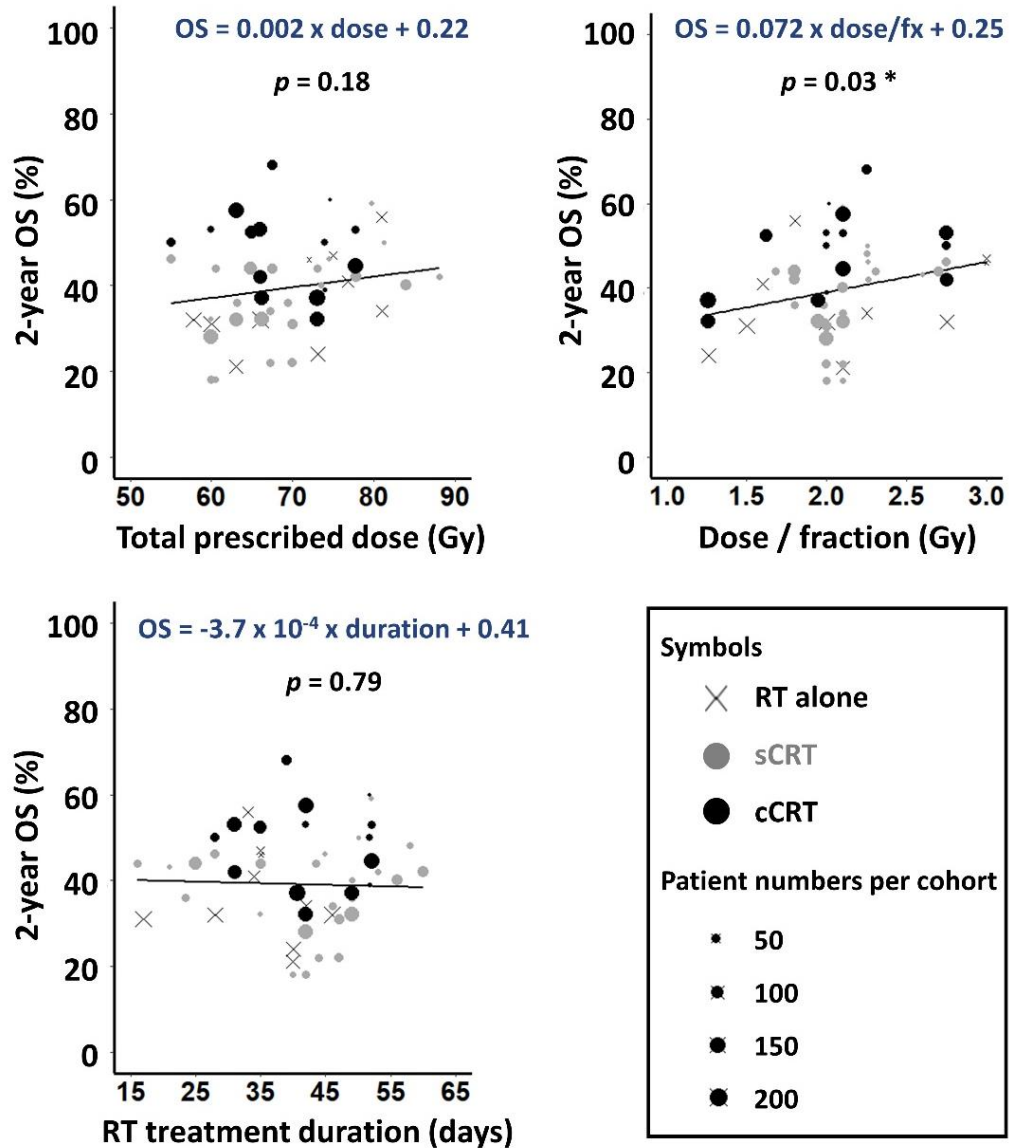


Figure 3.2 Two-year OS distribution versus prescribed radiation dose, dose-per-fraction, and overall radiation treatment time in 51 collected clinical trial cohorts. Statistical testing is shown using linear regression, where the regression was weighted by patient numbers of each cohort. Gradients with $p < 0.05$ are defined as significant (*). Larger symbols represent cohorts with more patients.

3.3.2 Models fitting

This study aimed to understand the hidden reasons behind the inconsistent radiation dose-response in the clinic. We modified the radiotherapy models based on a series of hypotheses, from dichotomising tumour repopulation weighting and onset days into cCRT versus RT or sCRT, splitting α/β by stages, to individualising stage-specific toxicity weighting (Fig. 3.1).

Fitting efficacy comparisons are listed in Table 3.2, and visualised through calibration plots comparing modelled OS and original OS as Fig. 3.3. Model 2 with chemotherapy and NTCP incorporation had significantly improved the goodness-of-fit versus the standard TCP model ($p = 6.2 \times 10^{-21}$), which matched the published findings in previous research using a similar dataset³⁹. Step-by-step modelling generalisation with different hypotheses improved fitting from Model 2 to Model 5. Model 5 (which incorporated treatment-specific repopulation, stage-specific α/β , and stage-specific toxicity) had the best modelling efficacy with the lowest AIC and cross-validation score. The fitting improvements comparing standard TCP (Model 1) and basic chemo-radiation model (Model 2) with Model 5 reached p-values of 3.6×10^{-23} and 3.4×10^{-5} , respectively (Table 3.2).

In terms of models' goodness of fit (Fig. 3.3), least-square gradients between residuals of observed OS and modelled OS came from 0.24 for Model 1, 0.65 for Model 2, 0.70 for Model 3, 0.77 for Model 4, and 0.79 for Model 5. Such outcomes were consistent with the AIC and cross-validation results, indicating that modelling accuracy increased, followed by each incremental generalisation in this series of testing.

Table 3.2 Models comparison. Model efficacies are compared using Akaike Information Criteria (AIC), likelihood ratio tests through log-likelihood and degrees of freedom in fitting (df), and 10-fold cross-validation. $p < 0.05$ is defined as significant.

| | Model 1 Standard TCP (df = 43) | Model 2 Chemo- radiation (df = 38) | Model 3 Split Repopulation (df = 36) | Model 4 Split α/β (df = 34) | Model 5 Split Toxicity (df = 30) |
|-------------------------------|---|---|---|--|---|
| Log-likelihood | -3234.3 | -3182.4 | -3178.3 | -3169.6 | -3164.7 |
| | Reference | $p = 6.2 \times 10^{-21}$ | $p = 3.7 \times 10^{-21}$ | $p = 2.2 \times 10^{-23}$ | $p = 3.6 \times 10^{-23}$ |
| Likelihood - ratio test | - | Reference | $p = 0.023$ | $p = 6.9 \times 10^{-5}$ | $p = 3.4 \times 10^{-5}$ |
| | - | - | Reference | $p = 2.2 \times 10^{-4}$ | $p = 1.5 \times 10^{-4}$ |
| | - | - | - | Reference | $p = 0.034$ |
| AIC | 6485 | 6391 | 6387 | 6373 | 6371 |
| Cross- validation score | 65.2 | 26.7 | 24.1 | 18.0 | 12.7 |

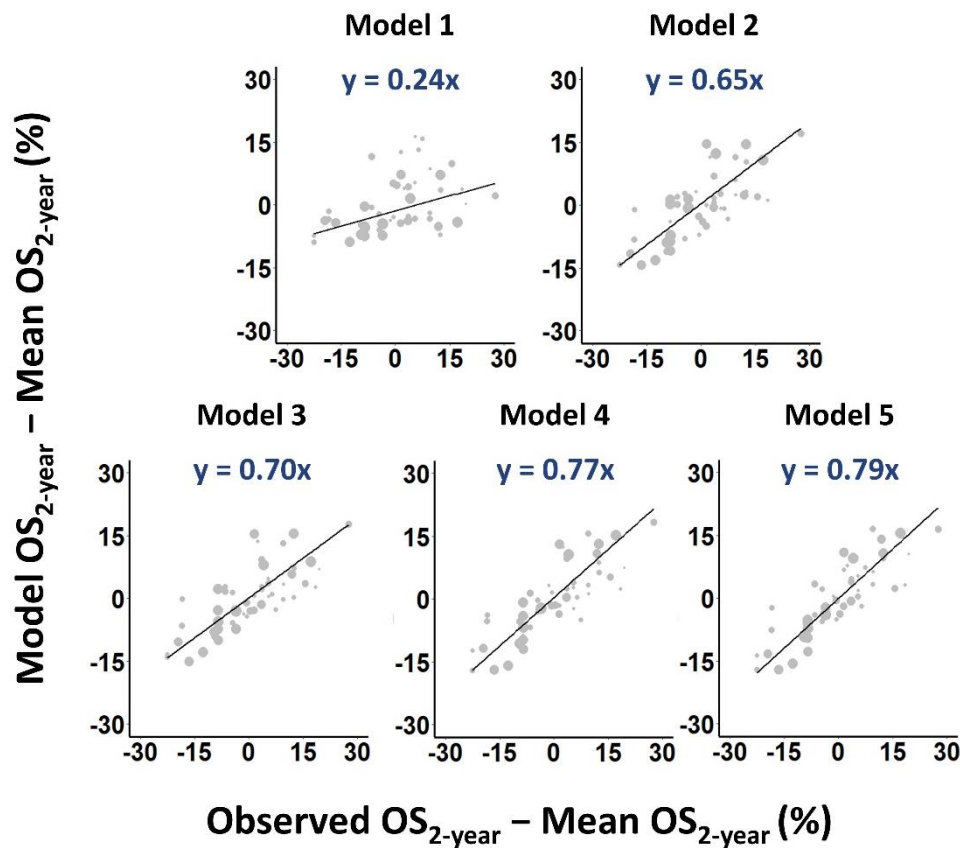


Figure 3.3 Models fitting abilities visualisation via calibration plots. The difference between predicted OS in the models and original OS are presented using calibration plots. Higher gradients and less dispersion indicate better fits. Larger symbols are used to indicate cohorts with more patients.

Modelling fits are shown in Table 3.3. Tumour repopulation took account of 0.64 and 0.32Gy EQD_{2,tum} reduction per day in Model 1 and Model 2, while its rate rose to 1.47Gy reduction per day (95% CI: 0.36, 2.57Gy) for cohorts treated with cCRT in Model 5. Besides, the kick-off timing of tumour repopulation also changed. It started on day 18 of the treatment in Model 2, where chemotherapy effects had been counted. However, it slightly deferred to day 24 of the treatment

for cCRT using Model 5. To sum up, cCRT postponed the onset timing of tumour repopulation, but with faster rates of decreasing $EQD_{2,tum}$ once it started.

The fitted α/β ratio was 4.0Gy (95% CI: 2.1, 9.2Gy) and 3.0Gy (95% CI: 1.6, 5.6Gy) for Model 1 and Model 2, respectively, which was way lower than the commonly used value of 10Gy, however, such findings of α/β align with what had been reported in the previous research³⁹. For Model 4 and 5, where stages split α/β , the fitted values of α/β were around 10Gy for early-stage (stage I/II), high with wider CIs for stage IIIA (62.8Gy for Model 4; 32.1Gy for Model 5), and extremely low for stage IIIB (0.4Gy for Model 4; 0.6Gy for Model 5).

Stage-by-stage normal tissue toxicity fitting illustrated sharper gradient of NTCP in Model 5 (0.31, 95% CI: 0.11, 1.00) compared to the Model 2 (0.60, 95% CI: 0.47, 1.00). The fitting results specify that when treating patients with 54Gy prescribed EQD_2 ($EQD_{2,NT50}$), more patients in advanced stages would have 50% chances of OS-affected side effects, where possibilities arise from 33% for stage I and II, 41% for stage IIIA, to 58% for stage IIIB.

Table 3.3 Models description. Results include degrees of freedom in fitting (df), fitted parameter values and 95% profile-likelihood CIs. Key results comparing the best model (Model 5) versus conventional models (Model 1 and 2) are summarised here. The complete table is shown on the page after the summarised table.

| Parameters | Model 1 Standard TCP (df = 43) | Model 2 Chemo-radaition (df = 38) | Model 5 Best model (df = 30) |
|-----------------------|--------------------------------------|---|---|
| α/β * (Gy) | 4.0 (2.1 - 9.2) | 3.0 (1.6 - 5.6) | S_I & S_{II} : 10.0 (0.6 - infinite) S_{IIIA} : 32.1 (9.0 - infinite) S_{IIIB} : 0.6 (-0.2 - 1.0) |
| T_k * (days) | 33 (18 - 39) | 25 (16† - 36) | RT & sCRT: 17 (16† - 32) cCRT: 24 (16† - 47) |
| λ * (Gy/day) | 0.64 (0.30 - 0.99) | 0.40 (0.23 - 0.72) | RT & sCRT: 0.30 (0.18 - 0.47) |

| | <i>cCRT</i> : 1.47 (0.36 - 2.57) | | |
|---|---|--|--|
| <i>EQD_{2,tum50}</i> (Gy) ** | <i>S_I</i> : 74 (66 - 81) | <i>S_I</i> : 48 (13 - 52) | <i>S_I</i> : 54 (49 - 58) |
| | <i>S_{II}</i> : 74 (66 - 84) | <i>S_{II}</i> : 48 (19 - 52) | <i>S_{II}</i> : 54 (49 - 58) |
| | <i>S_{III}</i> : 74 (66 - 84) | <i>S_{III}</i> : 49 (42 - 54) | <i>S_{III}</i> : 54 (49 - 58) |
| | <i>S_{IIIB}</i> : 88 (75 - 103) | <i>S_{IIIB}</i> : 61 (52 - 69) | <i>S_{IIIB}</i> : 54 (49 - 58) |
| <i>m</i> | 0.72 (0.64 - 1.00†) | 0.28 (0.19 - 0.47) | 0.15 (0.12 - 0.24) |
| <i>OS_{Max}^{cCRT}</i> (%) | - | 93 (85† - 100†) | 91 (85† - 100†) |
| <i>RS^{cCRT}</i> | - | 1.11 (1.05 - 1.22) | 1.40 (0.99 - 1.40†) |
| <i>R</i> (per year) | - | 0.016 (0.006 - 0.022) | 0.016 (0.012 - 0.026) |
| <i>EQD_{2,NT50}</i> (Gy) | - | 96 (83 - 116) | 54 (26 - 104) |
| <i>m_{NT}</i> | - | 0.60 (0.45 - 1.00†) | 0.31 (0.11 - 1.00†) |
| <i>F</i> (%) ** | - | - | <i>S_I</i> : 33 (0† - 78) |
| | - | - | <i>S_{II}</i> : 33 (0† - 86) |
| | - | - | <i>S_{III}</i> : 41 (20 - 100†) |
| | - | - | <i>S_{IIIB}</i> : 58 (35 - 100†) |

* In Model 5, a common α/β value was fitted for stage I and II cohorts, and common T_k and λ values for RT alone and sCRT treatments.

** For $EQD_{2,tum50}$ and F , fitting was constrained so that IIIB values were \geq IIIA \geq II \geq I.

† The profile-likelihood CI was truncated at a lower or upper boundary of the range explored.

Parameters: α/β (S_i) – α/β ratio for stage S_i ; T_k – repopulation kick-off time; λ – dose-per-day repopulated; $EQD_{2,tum,50}(S_i)$ – EQD₂ required to achieve 50% tumour control for stage S_i ; m – dose-response gradient; OS_{Max}^{cCRT} – maximum overall survival for chemoradiotherapy; RS^{cCRT} – radiosensitisation of dose-effects by cCRT; R – variation of 2-year OS with study publication year; $EQD_{2,NT50}$ – EQD₂ causing 50% modelled complications related to death; m_{NT} – dose-toxicity response gradient; $F(S_i)$ – toxicity weighting for stage S_i .

| Parameters | Units | Model 1 | Model 2 | Model 3 | Model 4 | Model 5 |
|---------------------------------------|--------|---|--|---|--|--|
| | | Standard TCP (df = 43) | Chemo-radiation (df = 38) | Split Repopulation (df = 36) | Split α/β by stage (df = 34) | Split Toxicity by stage (df = 30) |
| λ | Gy/day | 0.64 (0.30 - 0.99) | 0.40 (0.23 - 0.72) | <i>RT/sCRT</i> : 0.32 (0.20 - 0.49) <i>cCRT</i> : 1.00 (0.47 - 1.74) | 0.33 (0.22 - 0.60) 1.31 (0.78 - 2.43) | 0.30 (0.18 - 0.47) 1.47 (0.36 - 2.57) |
| T_k | Days | 33 (18 - 39) | 25 (16 [†] - 36) | <i>RT/sCRT</i> : 16 (16 [†] - 30) <i>cCRT</i> : 35 (16 [†] - 42) | 16 (16 [†] - 25) 38 (16 [†] - 46) | 17 (16 [†] - 32) 24 (16 [†] - 47) |
| α/β^* | Gy | 4.0 (2.1 - 9.2) | 3.0 (1.6 - 5.6) | 2.6 (1.5 - 4.5) | <i>S_I & S_{II}</i> : 10.2 (0.6 - infinite) <i>S_{III}</i> : 62.8 (17.1 - infinite) <i>S_{IV}</i> : 0.4 (-0.3 - 1.0) | 10.0 (0.6 - infinite) 32.1 (9.0 - infinite) 0.6 (-0.2 - 1.0) |
| <i>EQD_{2,um50}**</i> | Gy | <i>S_I</i> : 74 (66 - 81) <i>S_{II}</i> : 74 (66 - 84) <i>S_{III}</i> : 74 (66 - 84) <i>S_{IV}</i> : 88 (75 - 103) | 48 (13 - 52) 48 (19 - 52) 49 (42 - 54) 61 (52 - 69) | 49 (13 - 53) 49 (13 - 54) 49 (44 - 54) 58 (53 - 67) | 54 (13 - 56) 54 (19 - 57) 54 (50 - 57) 54 (50 - 57) | 54 (49 - 58) 54 (49 - 58) 54 (49 - 58) 54 (49 - 58) |
| <i>m</i> | - | 0.72 (0.64 - 1.00 [†]) | 0.28 (0.19 - 0.47) | 0.25 (0.17 - 0.43) | 0.16 (0.13 - 0.26) | 0.15 (0.12 - 0.24) |
| <i>OS^{CRT}_{Max}</i> | % | - | 93 (85 [†] - 100 [†]) | 91 (85 [†] - 100 [†]) | 85 (85 [†] - 98) | 91 (85 [†] - 100 [†]) |
| <i>RS^{CRT}</i> | - | - | 1.11 (1.05 - 1.22) | 1.10 (0.99 - 1.40 [†]) | 1.10 (0.99 - 1.40 [†]) | 1.40 (0.99 - 1.40 [†]) |
| <i>EQD_{2,NT50}</i> | Gy | - | 96 (83 - 116) | 96 (85 - 114) | 96 (85 - 111) | 54 (26 - 104) |
| <i>m_{NT}</i> | - | - | 0.60 (0.45 - 1.00 [†]) | 0.60 (0.45 - 1.00 [†]) | 0.60 (0.42 - 1.00 [†]) | 0.31 (0.11 - 1.00 [†]) |
| <i>R</i> | /year | - | 0.016 (0.006 - 0.022) | 0.016 (0.008 - 0.023) | 0.015 (0.009 - 0.022) | 0.016 (0.012 - 0.026) |
| <i>F**</i> | % | - | - | - | - | <i>S_I</i> : 0.33 (0 [†] - 0.78) <i>S_{II}</i> : 0.33 (0 [†] - 0.86) <i>S_{III}</i> : 0.41 (0.20 - 1 [†]) <i>S_{IV}</i> : 0.58 (0.35 - 1 [†]) |

3.3.3 Detailed modelling analysis

To discover data-driven reasons behind stage-specific fitting, we split the dataset into the ‘More IIIA’ patient group versus the ‘More IIIB’ patient group based on IIIB/IIIA patient ratio in each cohort. By so doing, we analysed whether more IIIB/IIIA patients affect the relationship between dose-per-fraction versus OS, prescribed dose, and overall radiation treatment time. Besides, in order to increase modelling robustness, correlation plots of the best model (Model 5), VIF for collinearity, and ODF-calibrated AIC accounting over-dispersion were plotted or calculated. Furthermore, fitting using other possibly existing hypotheses were also tested (e.g. whether the stage-specific difference in tumour repopulation exists), trying to justify the hypotheses selection in this research. Finally, 1000 times bootstrapping were applied to test the modelling robustness and investigate the statistical uncertainties.

In Fig. 3.4, OS rose more with dose-per-fraction in the ‘More IIIB’ group ($p = 0.002$) when the data were split into the ‘More IIIA’ patient group versus the ‘More IIIB’ patient group based on IIIB/IIIA patient ratio in each cohort. In more detail, the prescribed dose fell more with increasing dose-per-fraction for ‘More IIIA’ than ‘More IIIB’, by about 10Gy in total as schedules change from 1.5 to 3.0 Gy-per-fraction. It partially explained why OS rose less with dose-per-fraction for ‘More IIIA’ than ‘More IIIB’. Also, dose reduction for ‘More IIIA’ should be balanced by 9 days decrease of treatment duration as dose-per-fraction change over 1.5 to 3.0 Gy-per-fraction, while there was 3 days increase for ‘More IIIB’.

In Fig 3.4, the regression was calculated using patient numbers as weighting in each sub-dataset. Each sub-dataset contains 27 and 22 cohorts (2354 and 2384 patients) respectively for ‘More IIIA’ and ‘More IIIB’ cohorts. Two cohorts (128 patients) with equal numbers of IIIA/IIIB were excluded. Together, such exploratory analyses investigating underlying data characteristics back up the findings of apparent α/β changes in the advanced models.

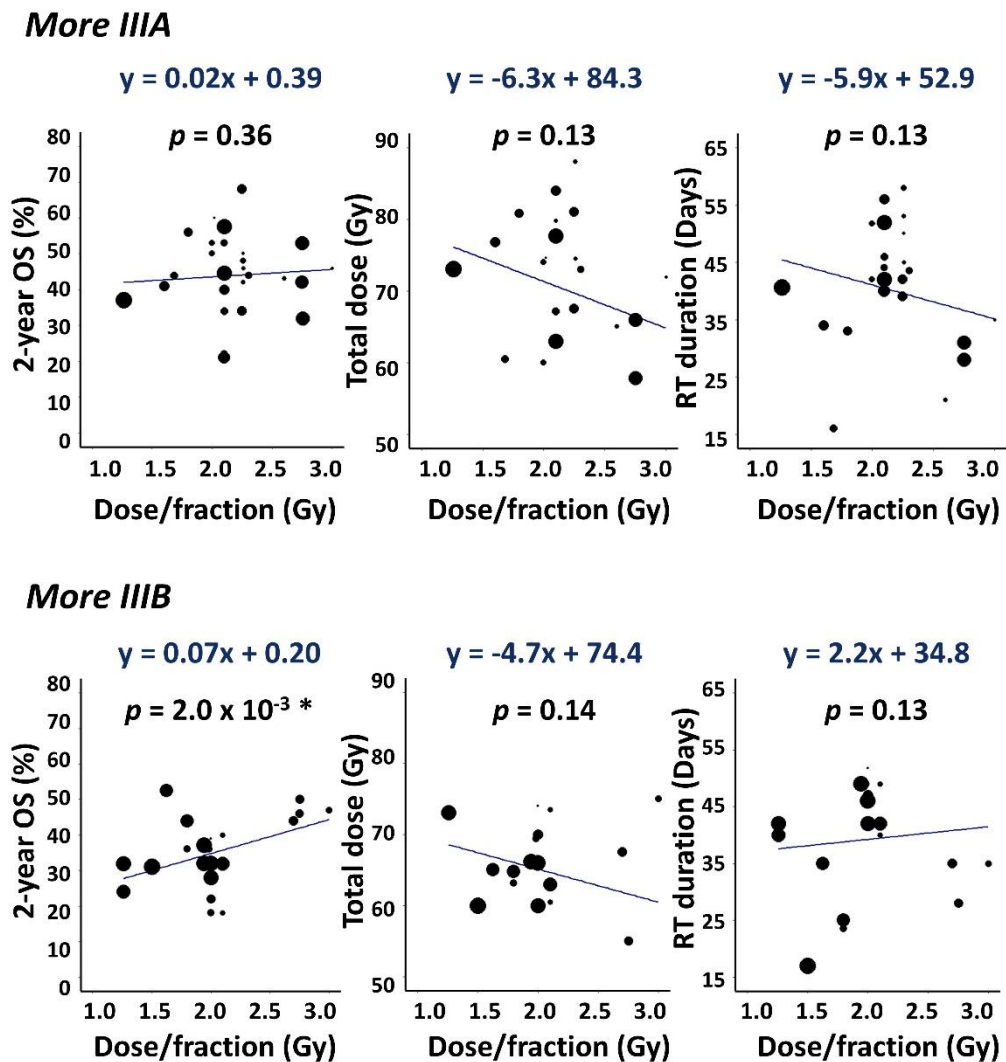


Figure 3.4 Patient-weighted linear regression comparing 2-year OS, total dose, and radiotherapy duration versus dose-per-fraction, in More IIIA (IIIB/IIIA patient ratio >1) cohorts and More IIIB (IIIB/IIIA patient ratio <1) cohorts. $p < 0.05$ is defined as significant (*)

After variance-covariance calculation, the correlation matrix was plotted to examine the dependency of newly added parameters in the best model (Fig. 3.5). $EQD_{2,tum50}(S_{IIB})$, was strongly negatively correlated with the repopulation rate for RT alone and sCRT ($|r| \leq 0.7$), which was the only strong correlation between parameters. In general, there was only mild ($0.3 \leq |r| < 0.7$) or even no correlation regarding novel features – the high repopulation rate for cCRT, low α/β for stage IIIB, and stage-specific toxicity. Despite these moderate parameter correlations, the 95% CI of the low α/β value for IIIB disease (-0.2, 1.0Gy) excluded the conventional α/β value of 10Gy by a large margin. However, the 95% CI on the repopulation rate for cCRT (0.36, 2.57 Gy/day) did include the 0.6-0.7 Gy/day repopulation rates, which often used in schedule effect calculations of NSCLC⁶².

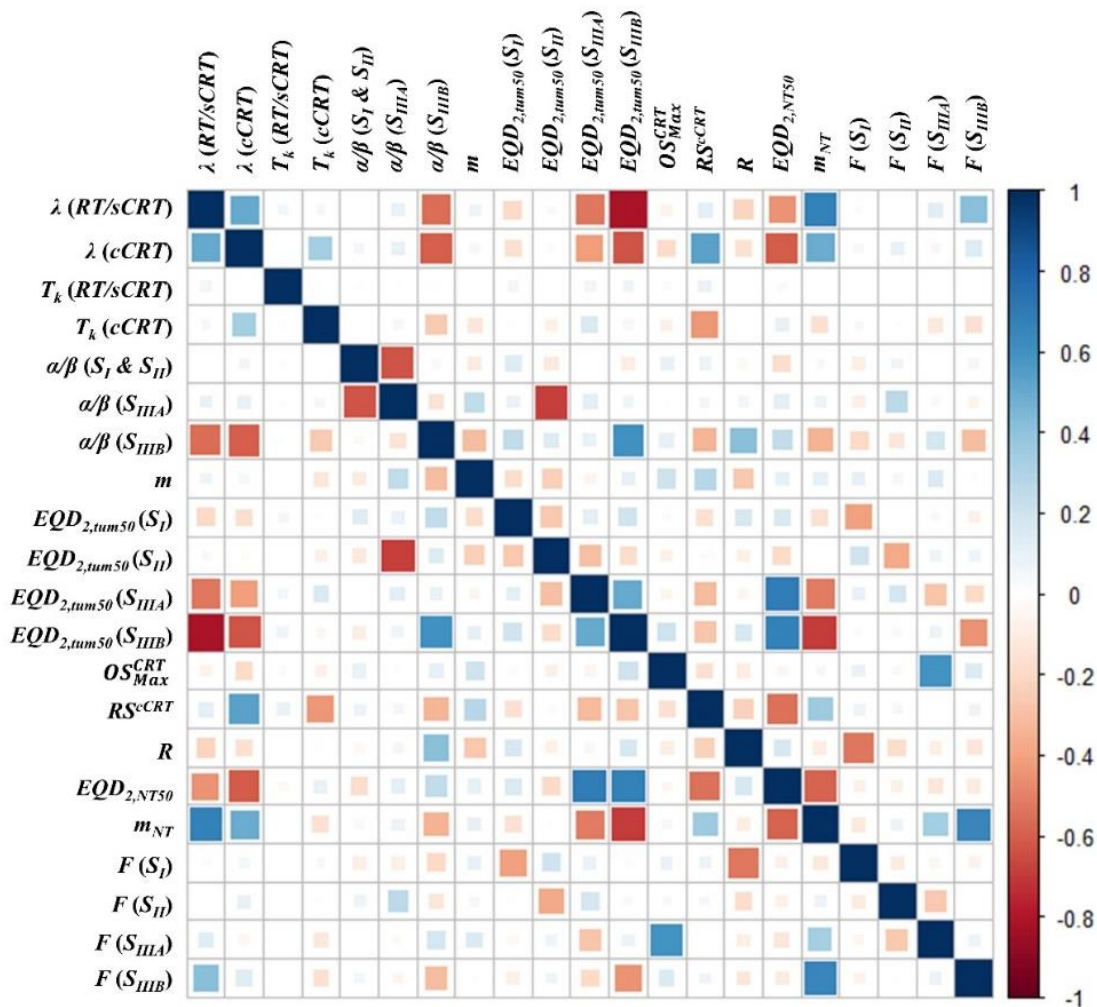


Figure 3.5 Correlation matrix of the best model (Model 5). Correlation values are visualised as blue to red from 1 to -1, where larger squares in colours reflect larger absolute values of the correlation, indicating the stronger relationship between parameters either positively or negatively. Legends correspond to parameters in Model 5.

With existed collinearity and overdispersion, either the chemo-radiation model published previously (Model 2) or the advanced model developed in this research cannot perfectly describe the data (Model 5). According to Table 3.4, Model 5 had VIF >10, which indicated possible collinearity issue. Additionally, sum-of-squares residual values of both models lie above the chi-square distribution given corresponding degrees of freedom in fitting, indicating the possibly existed overdispersion phenomenon. The underlying collinearity and overdispersion might resulted from centre-to-centre differences in patient and treatment factors that are not accounted for in the modelling, generally because data for them is unavailable. Consequently, calibrated AIC using the overdispersion factor of the best model was calculated, and a new likelihood-ratio test was executed using calibrated values (Table 3.5).

Factoring overdispersion into the analysis presented here leads to Model 4 having a marginally better AIC than Model 5 and thus being marginally preferred if overdispersion is accounted for. As can be seen, even allowing for overdispersion the analysis continues to point to a low α/β ratio for stage IIIB NSCLC but a significantly higher α/β ratio for stage IIIA, and to the repopulation rate during cCRT being significantly faster than during sCRT or RT alone. To sum up, such post-hoc correction did not change the results, and reasonable extents of collinearity and overdispersion did not cause problems in this research.

Table 3.4 Collinearity and overdispersion tests. Collinearity was tested using VIF. Overdispersion monitors whether the sum-of-squares residual values lies in the proper chi-square distribution corresponding to degrees of fitting in each model (i.e. whether residual errors are greater than expected binomial errors). Model 2 (chemo-radiation model) and Model 5 (best model) were compared.

| | Model 2 Chemo-radiation (df = 38) | Model 5 Split Toxicity (df = 30) |
|---|--|---|
| VIF | 6.76 | 16.52 |
| Boundary of χ^2 distribution with corresponding df | 53.4 | 43.8 |
| Sum-of-squares values | 107.5 | 81.3 |
| Overdispersion factor (ODF) | 2.83 | 2.71 |

Table 3.5 Calibrated AIC and likelihood-ratio test through incorporating ODF. ODF of 2.7 was used as it was the ODF from the best model. Calibrated AIC was calculated through $2 * parameters + (-2 * log-likelihood) / ODF$.

| | Model 1 Standard TCP (df = 43) | Model 2 Chemo-radiation (df = 38) | Model 3 Split Repopulation (df = 36) | Model 4 Split α/β (df = 34) | Model 5 Split Toxicity (df = 30) |
|---------------------------|---|--|---|--|---|
| Log-likelihood | -3234.3 | -3182.4 | -3178.3 | -3169.6 | -3164.7 |
| (-2*log-likelihood) / ODF | 2395.8 | 2357.3 | 2354.3 | 2347.9 | 2344.2 |
| Calibrated AIC | 2412 | 2383 | 2384 | 2382 | 2386 |

| | | | | | |
|---------------------------|-----------|---------------------------|---------------------------|---------------------------|---------------------------|
| | Reference | $p = 3.0 \times 10^{-15}$ | $p = 3.4 \times 10^{-15}$ | $p = 1.3 \times 10^{-16}$ | $p = 4.1 \times 10^{-16}$ |
| New likelihood-ratio test | - | Reference | $p = 0.059$ | $p = 0.001$ | $p = 0.001$ |
| | - | - | Reference | $p = 0.002$ | $p = 4.6 \times 10^{-4}$ |
| | - | - | - | Reference | $p = 0.103$ |

Alternative models were tested and summarised in Table 3.6 and Table 3.7. The results showed that either tumour repopulation was fitted stage-specific rather than treatment-specific, tumour α/β was treatment-specific rather than stage-specific, or toxicity weighting (F) was treatment-specific rather than stage-specific, the model can't perform as well as Model 5. Similarly, using Model 5 with common values for tumour repopulation, α/β , or stage-specific toxicity cannot be as good as Model 5.

Table 3.6 The fit of Model 5 compared to models where parameters are individualised according to treatment rather than the stage, or vice-versa.

Although the AIC score of Model 5-3 is marginally better than that of Model 5, the fitted values of $F_{cCRT} = 0.41$ and $F_{RT\&sCRT} = 0.38$ in the fit of Model 5-3 are similar, and the AIC of Model 4 (the variant of Model 5 in which these parameters have a common value; AIC: 6373, Table 3.2) is worse than that of Model 5.

| | Model 5 (df = 30) | Model 5-1 (df = 31) | Model 5-2 (df = 28) | Model 5-3 (df = 32) | Model 5-4 (df = 28) |
|-----------------------|------------------------------|--------------------------------|--------------------------------|--------------------------------|--------------------------------|
| Log-likelihood | -3164.7 | -3166.7 | -3166.9 | -3166.1 | -3163.3 |
| AIC | 6371 | 6373 | 6380 | 6370 | 6373 |

Model 5-1: α/β individualised by treatment (cCRT vs others) rather than stage.

Model 5-2: λ and T_k individualised by stage (early, IIIA, IIIB) rather than treatment.

Model 5-3: toxicity (F) individually weighted by treatment (cCRT vs others) rather than stage.
 Model 5-4: λ and T_k individualised by RT, sCRT, cCRT rather than cCRT vs others.
 df: degrees of freedom in fitting

Table 3.7 The Model 5 fit compared to models in which treatment- or stage-specific parameters are set to common values.

| | Model 5 (df = 30) | Model 5 with common α/β for all stages (df = 32) | Model 5 with common toxicity for all stages (df = 34) | Model 5 with common repopulation for all treatments (df = 32) |
|-----------------------|------------------------------|---|--|--|
| Log-likelihood | -3164.7 | -3171.9 | -3169.9 | -3167.8 |
| AIC | 6371 | 6382 | 6374 | 6374 |

df: degrees of freedom in fitting

3.3.4 Chemoradiotherapy dose-response

To describe the clinical implication and modelling changes, routinely used 2 Gy-per-fraction schedules between 60Gy in 5 weeks 5 days to 74Gy in 7 weeks 2 days were plotted as Fig. 3.6 after fitting, explicitly focusing on stage IIIA and IIIB. Model 5 showed positively steeper dose-response curves than the other two models for RT and sCRT, the predicted OS rise with increasing dose by around 1% per Gy, higher than 0.2% per Gy of observed OS gain plotted in Fig. 3.2. It indicated that RT alone or sCRT could still benefits patient effectively with radiation dose-escalation, while cCRT might not. Relatedly, predicted OS fell with increasing dose for cCRT using Model 5 – a different trend versus the other two models when dose-escalated. Longer treatment duration over escalated doses with standard fractionation linked to the higher value of repopulation rate in cCRT (Table 3.3), thus resulting in OS decreases using a high dose. Dose-escalation appeared to incur

more toxicity to patients in cCRT, resulting in OS decreases when treating between 64 to 74Gy for both stages. The modelling results revealed the potential hazard of dose-escalation with cCRT, especially for stage IIIB.

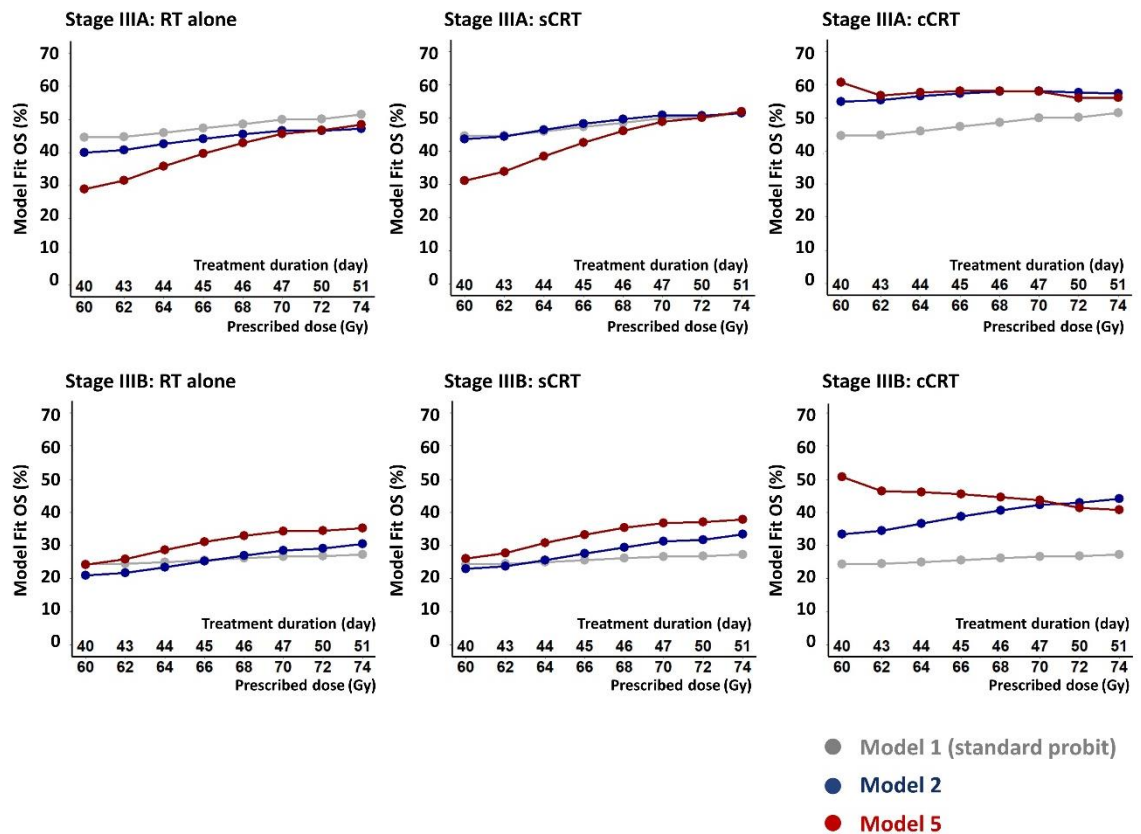


Figure 3.6 LA-NSCLC dose-response prediction curves. 2-year OS predictions are plotted based on Model 1, 2 and 5, where the x-axis is set as treatment duration and prescribed dose given in standard 2 Gy-per-fraction.

Uncertainties of dose-responses were assessed by 1000 times resampling bootstraps, refitting Model 5 to recalculate the expected change in survival with dose. For cCRT, average increases in modelled survival were 0% (95% CI: -32, 24%) for IIIA and -6% (-38, 16%) for IIIB, compared to increases of 23% (-18,

49%) for IIIA and 16% (-23, 39%) for IIIB when using sCRT. In 86% and 96% of the bootstrapped resamples, increases in survival for both stages were less for cCRT than for sCRT by $\geq 10\%$ and $\geq 0\%$ respectively, with similar results for stage IIIB.

Table 3.8 Key results of Model 5 prediction after 1000 times bootstrapping.

(A) ‘OS (74Gy) - OS (60Gy)’ using RT/sCRT/cCRT

| Stage IIIA | RT | sCRT | cCRT |
|---|--------------------|--------------------|--------------------|
| Mean values with 95% CI after bootstrapping | 21% (-18%, 46%) | 23% (-18%, 49%) | 0% (-32%, 24%) |
| Stage IIIB | RT | sCRT | cCRT |
| Mean values with 95% CI after bootstrapping | 15% (-22%, 37%) | 16% (-23%, 39%) | -6% (-38%, 16%) |

(B) Percentages of the bootstraps that the increase in survival between 60 and 74Gy seen for sCRT more than 0%/5%/10%/15% greater than the increase seen for cCRT

| sCRT – cCRT (74Gy – 60Gy) | >15% | >10% | >5% | >0% |
|------------------------------|------|------|-----|-----|
| Stage IIIA | 78% | 86% | 92% | 96% |
| Stage IIIB | 74% | 86% | 91% | 96% |

External validation through placebo group of *PACIFIC*^{71,72} trial was executed, comparing the prediction of the best model (Model 5) to the placebo group of

PACIFIC results, where patients were treated using standard cCRT between 54 to 74Gy. The prediction results with a 2-year OS of 56.1% through fits acquired in Model 5 showed the goodness of prediction using external validation. Also, it is worthy of mentioning that such prediction can't well-described the OS of another *PACIFIC* trial arm when immunotherapy drug durvalumab was given after the cCRT.

Table 3.9 Best modelling prediction versus *PACIFIC* clinical trial.

| | 2-year OS | IIIA patients | IIIB patients |
|--|---------------------------------|------------------------------------|---------------|
| Placebo group of <i>PACIFIC</i> trial | 55.6% (95% CI: 48.9%, 61.8%) | 125 | 107 |
| durvalumab group of <i>PACIFIC</i> trial | 66.3% (95% CI: 61.7%, 70.4%) | 252 | 212 |
| Modelling OS using 92% 60 Gy vs 8% 70Gy as weights* | | | |
| Model 5 | 56.1% | Assuming 1:1 stage-mix patients ** | |

* Placebo group cCRT radiation schedules in *PACIFIC* trial:

- 91.6% patients received 54 - 66Gy, and 8% patients received 66 - 74Gy
- 0.4% received personalized dose-adjustment, which were excluded in our comparison

**Placebo group cCRT in *PACIFIC* trial contained 53%:45%:2% of patients with

IIIA/IIIB/other stages, so we assumed 1:1:0 in terms of IIIA/IIIB/others

3.4 Discussion

This research aims to discover hidden reasons for inconsistent LA-NSCLC treatment outcomes and narrow down the gaps between the clinical facts and radiotherapy models by providing better dose-response prediction. We have shown that incorporating fundamental personalised radiobiological related factors such as tumour repopulation, tumour radiosensitivity (α/β), and stage-specific treatment toxicity can improve 2-year OS model prediction in LA-NSCLC treated with radical radiotherapy. Multiple statistical comparisons justify that Model 5 is the best fitting model.

The model fits in this research indicate the different tumour responses for cCRT – the tumour repopulation onset was delayed by 7 days compared to RT alone or sCRT. However, the delayed repopulation become 4.9 times faster (dose lost per day: 1.47 Gy/day for cCRT; 0.30 Gy/day for RT/sCRT) once the effects kick-off. Besides, stage-specific fitting indicated the extremely low tumour α/β for stage IIIB, and survival-related toxicity rose with the disease stage progress.

3.4.1 Rapid tumour repopulation rate for cCRT

The model highlights a potential effect of concurrent chemotherapy related to tumour response to radiotherapy: treatment-specific repopulation depends on the timing of chemotherapy relative to radiotherapy. Rapid tumour repopulation under cCRT might due to paradoxical effects of chemotherapy which can kill majority of cancer cells but facilitate the growing of cancer stem cells¹⁶¹. The days to repopulation kick-off appears to be delayed when cCRT is delivered (24 days, 95% CI: 16, 47) vs RT/sCRT (17 days, 95% CI: 16, 32), and the loss of Gy/day can be as high as 1.47Gy (95% CI: 0.36, 2.57) in cohorts receiving cCRT versus only 0.30 Gy (95% CI: 0.18, 0.47) in RT/sCRT. We also tried separating RT, sCRT and cCRT

on repopulation but with worse AIC and similar values between RT and sCRT, so repopulation parameters were fitted together for RT/sCRT. The 95% CI of fitted repopulation rate for cCRT include the normally used values of around 0.6 to 0.7 Gy/day in NSCLC⁶². These findings are supported by a study which hypothesised that cCRT had suppressed accelerated-repopulating tumour clonogens sufficiently with chemotherapy, neutralising the effect of radiation acceleration, as no benefit was seen in the reported prospective trial with dose-escalated and accelerated cCRT in lung cancer¹⁵².

T_k of laryngeal cancer has been reported in ranges of 21 to 36 days¹⁶². Trials for stage III head and neck cancer have suggested radiation acceleration cannot fully compensate for the missing doses of chemotherapy¹⁶³ – the effects of one-week radiotherapy acceleration are approximately equal to a cycle of chemotherapy when given concurrently¹⁶⁴. A single-institution analysis of 956 patients has revealed that dose-escalation only benefits LA-NSCLC when cCRT can be done within 49 days¹⁶⁵. Additionally, the accelerated repopulation is not only consistent with what has been seen in *RTOG-0617*, but it could also explain the failure to increase OS in that trial, since repopulation might have neutralised the dose-escalation effects in the final days of 7.5 weeks schedules⁵⁴. Our results concur with these findings, suggesting that limiting the duration of cCRT is particularly important whether using dose-escalation or not, as treatment protraction might lead to stronger tumour repopulation and treatment failure.

Histological subtypes might possibly lead to such split in tumour repopulation, as the dataset had fewer SCC patients for cCRT compared to RT/sCRT. However, an additional trial splitting repopulation by tumour histology did not describe the data as well as treatment-dependent repopulation split. Further studies with more complete histology data are needed to investigate the effects of histological subtypes on tumour repopulation.

Although the fitted repopulation rate was 1.47Gy EQD₂-per-day for cCRT, this can be countered by giving only an extra 1.05 Gy-per-day of physical dose in 2Gy fractions, due to the radiosensitising property of cCRT which is accounted for in Models 2 to 5 by scaling cCRT radiation doses by the RS^{cCRT} factor. This 1.05 Gy-per-day figure is, however, still substantially greater than conventional estimates of 0.6 to 0.7Gy lost per day to repopulation, and the associated modelled reduction in survival is high, governed either by the 1.05 Gy-per-day figure considered in relation to the radiosensitised (steepened) dose-response curve for cCRT, or equivalently by the 1.47 Gy-per-day figure in relation to the dose-response curve for sCRT. The high fitted rate of loss of cell-killing effect due to repopulation, together with increased modelled survival-limiting toxicity at higher doses, lies behind the reduction in OS calculated from the fit of Model 5 for cCRT schedules delivering greater numbers of 2Gy fractions over longer schedules.

3.4.2 Apparent stage-split values of tumour α/β

Model performance improved when α/β took high values for stages I-II and IIIA disease but a low value for IIIB. There is a clear α/β difference between stage IIIA (32.1Gy, 95% CI: 9.0Gy, infinite) and IIIB (0.6Gy, 95% CI: -0.2, 1.0Gy).

There might be some intrinsic tumour heterogeneities between IIIA and IIIB, so separating tumour radiosensitivity parameter (α/β) by stages was tested, examining whether the modelling low α/β ³⁹ is true across the board. NSCLC exhibits strong α/β heterogeneity both *in-vitro* and clinical, ranging from 2.8 to 20Gy and beyond¹⁶⁶. Besides, a genome-based model for adjusting radiotherapy dose (GARD) revealed the genomic impacts on radiotherapy in lung cancer, indicating heterogeneities between stages might exist as the tumour progresses¹⁶⁷. Regarding LA-NSCLC radiotherapy, Sun et al.¹⁶⁸ reported that miRNA signature

could be the factor to predict treatment outcomes, also, as the marker to select patients for dose-escalation.

For early-stage NSCLC, low α/β of 3.9Gy and 2.8Gy were reported through data mixing conventional fractionation and hypo-fractionated cohorts^{169,170}. However, our findings add little information since we intentionally excluded cohorts with many stages I/II patients, and the fitted α/β ratio for these patients had a broad 95% CI covering all values above 0.6Gy – the extremely low fitted value for stage IIIB. In terms of LA-NSCLC, to our knowledge, we are the first group to investigate the α/β specifically¹⁷¹. The discrepancy between stage IIIA and IIIB might be specific on NSCLC since a recent study splitting patients by risks using prostate cancer showed similar tumour α/β in each risk group¹⁷².

Our modelled α/β suggests different fractionation usages for LA-NSCLC – the current fractionation is probably right for stage IIIA, but fewer fractionations should be better for stage IIIB. To interpret the results mathematically, $EQD_{2,tum}$ can approximately be calculated through the fitted α/β while not considering repopulation effects. *Equation 3.1* could be simplified then roughly written as $EQD_{2,tum} (S_{IIIA}) \approx D$ when the α/β is exceptionally high, and $EQD_{2,tum} (S_{IIIB}) \approx D*(d/2)$ when the α/β becomes extremely small. Collectively, $EQD_{2,tum} \approx (1-f)*D + f *D*(d/2)$ where f is the fraction of IIIB and $(1-f)$ is the fraction of IIIA.

Data features underlying this α/β stage-split are shown in Figure 3.4 which plots 2-year OS, prescribed dose and RT duration against dose-per-fraction. The data are plotted separately for 27 ‘More IIIA’ and 22 ‘More IIIB’ cohorts in which IIIA/IIIB ratios of patients were respectively greater or less than 1, the remaining two cohorts having an equal balance. Survival increased notably and significantly with dose-per-fraction in ‘More IIIB’ but not ‘More IIIA’ cohorts, suggesting a lower α/β value (greater dependence of radiation cell-killing on dose-per-fraction) for IIIB disease. Based on regression in Fig. 3.4, there was 9.5Gy prescribed doses

reduction for ‘More IIIA’ but just 7.1Gy reduction for ‘More IIIB’ if we increase dose-per-fraction from 1.5 to 3.0Gy.

In terms of clinical medical physics perspectives, stage IIIA radiotherapy features may lead to higher α/β for stage IIIA as α/β obtained from survival analyses based on prescribed doses will be artificially increased if treatment failures occur in untargeted regions that receive doses (and doses-per-fraction) below the prescribed level. There are more nodal spreads in stage IIIB than IIIA; however, as more mediastinum is purposefully irradiated when treating stage IIIB, more lymph nodes lie outside the target region in IIIA patients. Consequently, such failures of receiving doses lower than prescribed might raise the α/β for stage IIIA.

Tumour histology seems unlikely to account for the α/β difference as percentages of subtypes were similar in ‘More IIIA’ and ‘More IIIB’ cohorts (SCC : adenocarcinoma : others = 42% : 30% : 28% for ‘More IIIA’; 46% : 28% : 26% for ‘More IIIB’). A tested model splitting α/β by histology described the data less well than stage-dependent α/β . We also refitted the data using Model 5 in which stage III patients belonging to the ‘More IIIA’ and ‘More IIIB’ cohorts were assigned separate α/β values. Fitted α/β ratios obtained were 12.7Gy (95% CI: 8.4, 24.8Gy) for the 2050 stage III patients (64% IIIA) in the ‘More IIIA’ cohorts, and 1.2Gy (95% CI: -0.5, 4.7Gy) for the 2256 stage III patients (60% IIIB) in the ‘More IIIB’ cohorts. These values differ significantly but less sharply than original results in Model 5, and are arguably linked more directly to the underlying data since most cohorts included both IIIA and IIIB patients. Additionally, it should be noted that there might be some stage migration effects given the dataset containing studies published between 2000 to 2016. For example, some IIIA patients staged before introducing the fluorodeoxyglucose (FDG) – positron emission tomography (PET) staging might be staged as IIIB subsequently.

There is no direct evidence backing up the causes and effects of α/β differences between stage IIIA and IIIB, as low α/β of early stages^{169,170} or all stages³⁹ has been reported. It might link to tumour-specific biomarkers or genomic divergence, which have not been accounted for in this research since stage IIIA and IIIB are always following the same treatment guidelines^{18,150}. Single nucleotide polymorphism and miRNA differences have been successfully proved to dichotomise stage III patients into radiosensitive/radioresistant and treatment effective/ineffective cohorts, but no detailed description splitting stage IIIA and IIIB have been reported^{173,174}. Furthermore, over-expression and under-expression of miRNA lead to radiosensitive or radioresistant changes depending on DNA damages^{175,176}. A study showed that ‘miR-200c’ changed radiation cytotoxic effects using cell-cultured experiments with three different NSCLC cell lines and *in-vivo* models, where α/β rose from about 5 to nearly infinite if ‘miR-200c’ was stably overexpressing¹⁷⁶. Given that ‘miR-200c’ inhibits tumour invasion and metastasis in clinical¹⁷⁷, stage IIIA could possibly express more ‘miR-200c’ and higher α/β . Alternatively, a cell-cultured NSCLC study showed that ‘miR-328-p inhibition’ transfected cells would have α/β of about 0.35, whereas ‘miR-328-p mimic’ transfected cells have α/β of nearly infinite with straight dose-survival line¹⁷⁵. Given that ‘miR-328-p’ is under-expressed in stage IIIB, it might indirectly support our findings – a higher α/β for stage IIIA.

If α/β is truly low for NSCLC, at least for stage IIIB, then hypofractionated treatments delivering larger doses-per-fraction should perform as well as or better than conventionally fractionated treatments, particularly given that they can be delivered straightforwardly in shorter overall times. Towards future immune combination, moderate hypofractionation with fewer fractions delivering through higher doses-per-fraction appear to be more effective, including evidence of reduced lymphopenia¹⁷⁸.

3.4.3 Stage-specific survival-limiting toxicity

Regarding the NSCLC toxicity, our results suggest that individualising toxicity by stages improved the fitting, with a higher possibility of survival-limiting toxicity might occur in higher stages. This is anticipated since high grade complications, or reduced treatment effectiveness would be expected more often in higher stage patients with larger irradiated normal tissue volumes.

There is no consensus on choosing suitable variables for NTCP models; no fitted area under the receiver operating characteristic curve could reach more than 0.65 among published models¹⁷⁹. By splitting the toxicity by stages through $F(S_i)$, the results partly support the tumour α/β difference between stages and provide straight understandings of dose- side effects responses towards the clinical usage.

A study mentioned that 65% of LA-NSCLC death in 2 years resulted from respiratory or cardiac issues, and the 95% CIs of 2-year OS lie between 40% - 60%, supporting our fitting in both IIIA and IIIB¹⁸⁰. In addition, dose issues have been discussed with specific organ constraints to prevent severe toxicity – maximum <76 Gy for oesophagus, maximum <80 Gy for central bronchi, and mean dose <20 Gy for heart¹⁸¹. Together, the literature shows a similar tendency to our fitting that more OS-related toxicity may occur when doses are high enough, mainly affecting stage IIIB as larger volumes of normal tissues might be irradiated during the treatment.

It might be argued that OS differences could be related to toxicities, whereas in *RTOG-0617* study, there were no significant differences in grade ≥ 3 toxicities between standard dose arm and the dose-escalated arm⁵⁴. Relatedly, in the other dose-escalation study *IDEAL-CRT*, only 9.5% (8/84) patients were reported with grade ≥ 3 oesophagitis or pneumonitis⁸³.

3.4.4 Dose-response, statistical uncertainties and validation

This study aimed to coherently account for the effects on survival of factors including disease stage, prescribed dose, dose-per-fraction, RT duration, use and timing of chemotherapy, and possible survival-limiting toxicities. Using AIC and cross-validation techniques we chose the model that best balanced parsimony with quality of fit to the large dataset. Nevertheless, this model included 21 fitted parameters some of which were correlated, broadening 95% CI on fitted values. We therefore checked the robustness of our main findings.

As plotted in Fig. 3.6, dose-response prediction looks quite different between Model 1 2, and 5, illustrating more careful prescribed dose decisions should be considered, especially for IIIB cCRT. Survival-limiting toxicities at high dose-levels, together with rapid tumour repopulation, result in falling of modelled cCRT OS by 4% and 10% absolute respectively for stage IIIA and IIIB patients as prescribed dose increased from 60 to 74Gy given in 40 and 51 days.

Uncertainties on these figures were assessed by creating 1000 bootstrap datasets in which cohorts were sampled from the original set with replacement, refitting Model 5 to each bootstrap and using each model fit to recalculate the expected change in survival with increased dose. Average reductions in modelled survival and 95% ranges were 0% (-24, 32%) for IIIA and 6% (-16, 38%) for IIIB patients treated using cCRT, compared to increases of 23% (-18, 49%) and 16% (-23, 39%) for sCRT. In 96% of the bootstrap resamples, changes in survival with dose were lower (less of an increase/more of a reduction) for cCRT than for sCRT treatment. In 93% of bootstraps the fitted repopulation rate was faster for cCRT. Results for RT alone were similar to those for sCRT. In summary, the model fit to the original dataset indicated a survival reduction with increased dose given in 2Gy fractions, as did average results from model fits to the bootstraps. In most bootstraps the fall in survival was greater for cCRT than for sCRT, and the fitted rate of repopulation was faster for cCRT. Thus, it can robustly be concluded that

dose-escalation with treatment protraction is a poorer option for cCRT than for sCRT or RT alone.

The dose-response changes between models might be explainable by changes of slopes – m and m_{NT} . m decreases from 0.72 in Model 1 to 0.15 in Model 5 indicate the steepness changes in tumour control response. Both values are still acceptable for NSCLC if one transforms published Poisson distribution-based TCP normalised slope γ_{50} (0.57 - 2.00)^{160,182} into m (0.20 - 0.70) in normally distributed models using the converting function¹⁸³. Moreover, m_{NT} of 0.60 in Model 2 and 0.31 in Model 5 stand in the reasonable ranges as an overall NTCP slope, since research focused on side effects found the highly varied m_{NT} corresponding to specific organs, including 0.22 for lung¹²⁰, 0.67 for heart¹²⁰, and 0.11 to 0.35 for oesophagus¹⁸⁴.

In terms of correlation, all new features (Fig. 3.5) are independent; consequently, there should not be any artefacts regarding the findings. Mild collinearity and over-dispersion are acceptable (Table 3.4) as the corrected AIC through ODF did not change the modelling contents from Model 1 to 5. Also, datasets compiled from multiple sources, even for the best-performing model the scale of differences between the model fits and observed OS rates was higher than expected on the basis of binomial statistical uncertainties alone^{138,141,159}. Overdispersion is often ignored but can be worked into the modelling process by dividing goodness-of-fit measures by an overdispersion factor. The effect is to reduce the measures to levels expected from binomial statistics, widen CI on fitted parameters, and potentially cause simpler models to be preferred over more complex ones, since in the AIC the penalty term for increased numbers of model factors remains unchanged whereas the goodness-of-fit factor is weighted down. Factoring overdispersion into the analysis presented here leads to Model 4 having a marginally better AIC than Model 5 and thus being marginally preferred if overdispersion is accounted for. Even allowing for overdispersion, the analysis

continues to point to a low α/β ratio for stage IIIB NSCLC but a significantly higher α/β ratio for stage IIIA, and to the repopulation rate during cCRT being significantly faster than during sCRT or RT alone.

Even though the modelling data include recent dose-escalation trials *IDEAL-CRT*⁸³ and *RTOG-0617*⁵⁴, the external validation through the newest trial could enhance the model robustness. *PACIFIC* trial was selected since the patients were all treated using standard fractionation cCRT, and mainly composed by stage III NSCLC^{71,72}. Model 5 can be appropriately validated by assuming a 1:1 stage-mixed patient proportion, with a prediction value of 56.1% (Table 3.9), closely matching the placebo group results of 55.6% in *PACIFIC*. Intriguingly, 56.1% is still 10% away from successfully fitting improved OS given durvalumab after cCRT (66.3%), indicating the need to incorporate immune parameters in the future. This sets up the model well as a baseline for future work characterising the additional effects on survival of combined immuno-chemoradiotherapy treatments.

3.4.5 Limitation

Aside from the factors studied in this retrospective analysis, inevitable cohort-to-cohort variations in other patient- and treatment-related characteristics may not only lead to overdispersion but also potentially bias the results obtained. We lacked enough histological information and did not specifically investigate lung, heart or oesophagus toxicity but used common NTCP for all death-threatening side effects. The radiation dose to normal tissues was non clearly mentioned in most data collated for this research, so modelling estimation using prescribed dose is an approximation. In this research, toxicity was hypothesised to arise in normal tissues lying close to the tumour, and the incidence is linked to the prescribed dose. Besides, although AJCC staging was recorded from the literature, the staging

system had slight changes between 2000 to 2016, which may cause internal bias within the dataset¹⁸⁵.

In this research, the hypotheses are very focused around radiation schedules and the radiation biology effects, while with relatively course description of chemotherapy. It is performed based on the medical physics perspective, with purposes to shed lights on understandings for radiation oncology community. In should be noted that this might cause potential limitations regarding to the chemotherapy drug features of related pharmacodynamics.

This retrospective study is essentially hypothesis-forming, so more research is required to elucidate precisely how high α/β ($S_{III A}$) and how low α/β ($S_{III B}$) are, repopulation status under different schedules, and the toxicity difference between stages. Additionally, EQD₂ analyses are based on prescribed doses, which may be slightly different if organ tolerance and toxicity are evaluated through actual tissue absorbed doses. Lastly, the *PACIFIC* validation was done using published OS and summarised data tables⁷², so better validation might be achieved if more information is accessible.

3.5 Conclusion

Improved prediction of NSCLC 2-year OS can be achieved by incorporating tumour stages and treatment toxicity as radiobiological parameters. 2-year OS was described best by a model fit in which tumour accelerated repopulation progressed at 1.47Gy EQD₂-per-day for cCRT compared to 0.30Gy per day for sCRT and RT alone. These rates suggest that cCRT treatments should be given in the shortest times in which prescribed doses can be tolerated, but that treatment acceleration offers less advantage for RT alone or sCRT. Hypofractionation provides one way of accelerating cCRT, and the low overall fitted α/β ratio of 3.0Gy suggests this approach should be efficacious as well as practical provided normal tissue EQD₂s are not increased in the process. It should, though, be noted that when split by cohort-type, α/β was low only for cohorts with more IIIB than IIIA patients.

We have reached the limit of developing these models, and further research is required to improve prediction models, and efforts to incorporate patient and tumour specific characteristics of biology and imaging should be considered in the future. With these advanced models which incorporate the factors affecting dose-responses of chemoradiotherapy, it provides us with good position to extend such research into characterising immuno-chemoradiotherapy combinations.

Chapter 4. LA-NSCLC immuno-chemo- radiotherapy: effects of immune checkpoint blockade and factors affecting survival

4.0 Chapter overview

This chapter –

- Quantifies the net contribution of immunotherapy on locally-advanced non-small cell lung cancer following concurrent chemoradiotherapy (cCRT), using models extended from Chapter 3.
- Investigates the relationships between factors and immunotherapy induced survival contribution following cCRT.
- Identifies whether patient/tumour/treatment factors have potential trends of affecting the survival outcomes of tri-modality treatment using immunotherapy plus cCRT.

*This chapter has been tailored and submitted to *Int J Rad Onc Biol Phys* at the time of thesis submission.

4.1 Clinical advances of LA-NSCLC treatments

Lung cancer accounts for one in five cancer-related deaths globally⁸. More than 80% of cases are non-small cell lung cancer (NSCLC)¹¹ and at diagnosis around 35% of NSCLC cases are locally-advanced (LA-NSCLC)⁶⁰. Patients with inoperable LA-NSCLC and good performance status (PS) receive combined

chemoradiotherapy (CRT). Standardly, radiotherapy (RT) doses of 60-66 Gy in 2Gy fractions are delivered over 6-6.5 weeks concurrently with platinum-based chemotherapy¹⁴⁹. However, 5-year overall survival (OS) following concurrent CRT (cCRT) alone remains below 40% for stage III NSCLC¹³.

Modified radiation schedules for LA-NSCLC have been evaluated in many trials. Radiotherapy dose-escalation is potentially harmful as randomised phase III trial *RTOG-0617* showed the worse median OS using 74Gy cCRT than the standard 60Gy cCRT, with a hazard ratio (HR) of 1.38 (95% CI: 1.09, 1.76, p=0.004)⁵⁴. To date, the greatest improvement has been achieved by following cCRT with immune checkpoint blockade (ICB). ICB agents act at the interface between T-cells, tumour cells and their microenvironment, blocking signals that inhibit T-cell activation or the tumoricidal effects of activated T-cells. The most prominent results come from a randomised phase III trial *PACIFIC*, when cCRT was followed by durvalumab (MEDI 4736, anti-PD-L1 drug). The 2-year OS increased from 56% for cCRT alone to 66% for the cCRT-ICB treatment, with HR of 0.68 (95% CI: 0.53, 0.87, p=0.003)^{71,72}. This finding changed the standard-of-care for inoperable LA-NSCLC, and subsequently results have been published for other cCRT-ICB studies which have tested a range of CRT and ICB schedules^{75,76}. Given the heterogeneous nature of these trials an analysis of outcomes may help identify patient and treatment related factors associated with survival following cCRT-ICB. Presently, for locally advanced disease there are no biomarkers to aid patient selection, while for metastatic lung cancer PDL1 is the only approved biomarker to aid treatment decisions aside from genomic factors.

There is limited knowledge about modelling ICB, not to mention the models combining ICB with radiotherapy¹⁸⁶. In contrast, RT outcomes can be analysed through tumour control probability (TCP) and normal tissue complication probability (NTCP). Recently, TCP and NTCP elements have been combined in a single survival dose-response model that could describe survival rates which

initially rise with increasing radiation dose before falling at higher dose-levels (Chapter 3)^{39,187}. The combined model was fitted to a dataset detailing 2-year OS rates achieved by RT and CRT treatments of LA-NSCLC, and included terms that accounted for the effects of RT dose, dose-per-fraction and duration, NSCLC stage and delivery of chemotherapy sequentially (sCRT) or concurrently with RT. Here, this model is extended to describe the effects of ICB treatment, and used to analyse levels of survival seen in the cCRT-ICB studies and associations with patient characteristics, tumour pathology data, and CRT and ICB factors.

This chapter was designed to respond to two unanswered questions as the success of cCRT-ICB combination in *PACIFIC*^{71,72} has triggered clinical interest and changed standard-of-care cCRT protocols for inoperable LA-NSCLC:

- 1) Does meta-analysis across heterogenous published studies of cCRT-ICB support the OS gain seen with ICB addition in the *PACIFIC* study?
- 2) Which patient/tumour/CRT/ICB factors would possibly affect the efficacy of ICB contribution on treatment outcomes?

We collated data published for cCRT-ICB trials and investigated associations between reported OS levels and patient, tumour, CRT and ICB factors. We also investigated associations between changes in OS due to ICB agents and the factors. Because most cCRT-ICB studies were single-arm, the OS changes were estimated by fitting the extended survival model to data from studies of RT alone, CRT and cCRT-ICB. We assumed that patients in single-arm studies would have the same treatment response as in the randomised studies. The simplest form of extended model included a term describing an overall change in survival with ICB (referring as ‘OS gain’), and the significance of this term was tested. Then ‘OS gain’ was replaced by an indicator function, informing its relationships between factors. Thus, we aimed to delineate the ICB contribution to survival across studies and identify potential biomarkers associated with survival benefit (Fig. 4.1).

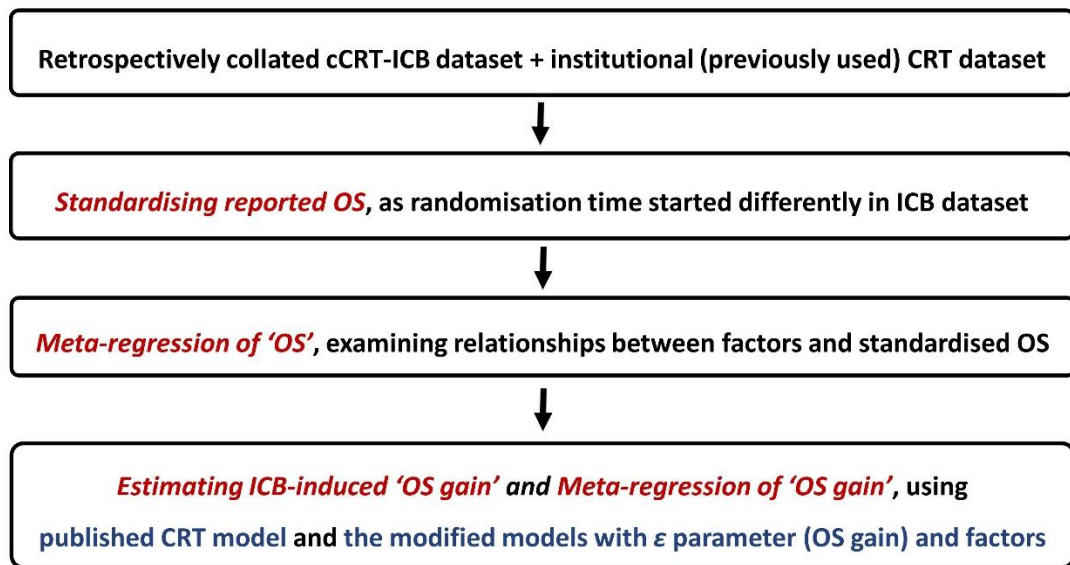


Figure 4.1 Flow chart of this chapter. This figure highlights the modelling structure in this chapter.

4.2 Materials and dataset processing

4.2.1 Retrospective data

Two datasets were compiled from published results, ‘cCRT-ICB’ for studies of cCRT combined with ICB, and ‘CRT’ for studies of RT, sCRT, or cCRT alone. The cCRT-ICB dataset was collated from searches of *PubMed* and *ScienceDirect* databases, using the keywords ‘NSCLC’, ‘Radiotherapy’, and ‘Immunotherapy’. The last search being made on 25th July 2022. From these studies data were extracted for: American Joint Committee of Cancer (AJCC) tumour staging (version 7 to 8), median age, gender proportion, histology (squamous cell carcinoma, SCC or non-SCC), PDL1 immunohistochemistry (proportion of patients with PDL1>1%), Eastern Cooperative Oncology Group (ECOG) PS, ICB drug agents (Pembrolizumab, Atezolizumab, Durvalumab, Nivolumab, Sugemalimab), ICB drug type (anti-PD1 vs anti-PDL1), ICB timing (start during vs after cCRT), planned ICB treatment duration and the length of intervals between ICB drug administration, prescribed radiation dose, dose-per-fraction, and radiotherapy duration. Studies were excluded if they used profound hypofractionation (radiation dose-per-fraction > 3.0Gy), delivered non-photon RT, included patients with stage IV disease, added targeted drugs or did not report 2-year OS.

The CRT dataset has been used in Chapter 3. It provided LA-NSCLC survival following RT alone, sCRT or cCRT. It consisted of 51 cohorts comprising 4866 patients treated in 33 studies published between 2000 and 2016. For each cohort, 2-year OS, median age, sex, cancer stage-mix (AJCC versions 4-7), ECOG PS, histology (proportion of patients with SCC), use and scheduling of chemotherapy, and prescribed RT dose, dose-per-fraction and duration were tabulated.

4.2.2 OS standardisation

2-year OS was analysed. Recruitment time-points varied between studies, either pre-cCRT or post-cCRT on confirmation of no progression. This potentially introduced a small degree of bias into some 2-year survival rates, including immortal time bias, which we took steps to eliminate.

Recruitment time-points varied between studies, either pre-cCRT or post-cCRT on confirmation of no progression. This potentially introduces bias in to 2-year survival rates which we have attempted to reduce by applying correction factors close to one, standardising survival relative to the start of cCRT. Specifically, for studies that recruited post-cCRT and reported survival relative to the recruitment time-point we multiplied reported 2-year OS rates by three correction factors, thus –

$$OS_{2yr,standardised} = OS_{2yr,reported} \times F_1 \times F_2 \times F_3 \quad \text{--- Equation 4.1}$$

where $F_1 = OS_T$, the OS at the recruitment date (T after CRT began) relative to OS at the start of CRT;

$F_2 = \left(\frac{OS_{2yr}}{OS_{2yr+T}} \right)$, the 2-year OS after the start of CRT relative to OS at 2 years + T ;

$F_3 = 1 - OS_T + PFS_T$, progression-free survival at T being denoted by PFS_T .

For cohorts that recruited post-cCRT, $OS_{2yr,reported}$ is essentially (OS_{2yr+T}/OS_T) . Since the purpose of the correction process is to obtain estimates of OS_{2yr} , multiplication by F_1 and F_2 alone might seem sufficient, the third factor F_3 appearing unnecessary. However, studies that recruited after cCRT excluded patients who were still alive at the recruitment date but had progressed since the start of CRT. These patients would have been included in cohorts recruited pre-cCRT and would likely have died by 2 years after cCRT. Thus, their exclusion from

post-cCRT cohorts artificially increased 2-year survival levels in those cohorts compared to levels in cohorts recruited pre-cCRT. This form of ‘immortal time bias’ is corrected for by F_3 , which reduces the standardised OS by a factor of 1 minus the fraction of patients who had progressed but were alive at T , this fraction equalling the difference between overall and progression-free survival (PFS) levels at T .

In principle F_1 , F_2 and F_3 all vary with T which is cohort-specific. However, for all relevant T , OS_T and thus F_1 took values of 1.00 in the only Kaplan-Meier (KM) curve of survival relative to the start of CRT published for a cCRT-ICB cohort. Where possible, values of the second factor were obtained directly from KM curves published for cohorts for which survival was being standardised. For some cohorts, KM curves were not available and values of the second factor were set to averages of values obtained from KM curves published for the other cCRT-ICB cohorts. The third factor was set to 0.98, reflecting OS and PFS rates at 10 weeks after the start of 60Gy cCRT in the *RTOG-0617* study⁵⁷.

Key data characteristics combining both datasets after OS standardisation are summarised in Table 4.1.

Table 4.1 Data characteristics of compiled datasets. Characteristics are listed by treatment-type (RT alone/sCRT, cCRT, or cCRT-ICB). Results are expressed as either total values or mean values with the range.

| | RT alone/sCRT | cCRT | cCRT-ICB | Total |
|---|-----------------|-----------------|-----------------|-----------------|
| Cohorts | 36 | 15 | 10 | 61 |
| Patient # | | | | |
| Stage I/II | 400 | 62 | 16 | 478 (6.8%) |
| Stage IIIA | 1246 | 1020 | 1104 | 3370 (47.7%) |
| Stage IIIB/C | 1338 | 800 | 1076 | 3214 (45.5%) |
| Total | 2984 (42.3%) | 1882 (26.6%) | 2196 (31.1%) | 7062 (100%) |
| Prescribed dose (Gy): mean (range) | | | | |
| | 70 (55 – 95) | 69 (55 – 78) | 60 (60 – 70) | 69 (55 – 95) |
| RT fractions (#): mean (range) | | | | |
| | 34 (20 – 58) | 36 (20 – 58) | 33 (30 – 35) | 34 (20 – 58) |
| Dose-per-fraction (Gy): mean (range) | | | | |
| | 2.1 (1.3 – 3.0) | 2.0 (1.3 – 2.8) | 2.0 (2.0 – 2.0) | 2.1 (1.3 – 3.0) |
| RT duration (days): mean (range) | | | | |
| | 40 (16 – 60) | 43 (28 – 52) | 43 (40 – 47) | 41 (16 – 60) |
| OS _{2-year} (%): mean (range) ⁺ | | | | |
| | 37 (18 – 59) | 49 (32 – 68) | 66 (59 – 80) | 43 (18 – 80) |

⁺OS_{2-year} was standardised for cCRT-ICB cohorts.

4.2.3 Effective patient numbers of 2-year OS

Data have been analysed using a maximum-likelihood technique, assuming the survival rate observed for each cohort i was distributed binomially according to N_i , the number of patients treated. In practice, however, the length of follow-up varied from cohort-to-cohort, and censoring due to short follow-up effectively reduced the number of patients contributing to survival estimates. To account for this, we replaced N_i for each cohort with an effective patient number, $N_{eff,i}$, calculated from the 95% confidence interval width (CI_i) on the cohort's 2-year OS via

$$CI_i = 3.92 \sigma_i = 3.92 \times (OS_{2yr,i}(1 - OS_{2yr,i})/N_{eff,i})^{1/2} \text{ --- Equation 4.2}$$

that is, interpreting the CI width as ± 1.96 times σ_i , the one standard deviation uncertainty on survival given $N_{eff,i}$ patients. When median follow-up was longer than 2-years, $N_{eff,i}$ values were similar to N_i .

Where possible, CIs on 2-year OS were taken directly from study publications. For some cohorts, CIs were not published and were instead determined by scanning the cohorts' KM curves into the *IPDfromKM* package¹⁸⁸. For a few cohorts neither CIs nor KM curves were published, and CI widths were instead estimated from widths published for other cohorts with similar stage-mixes and median follow-up times, scaled by $(N_{other}/N)^{1/2}$ where N and N_{other} are the numbers of patients in the cohort of interest and the other cohort.

4.3 Models and statistical methods

4.3.1 Meta-regression of OS in cCRT-ICB cohorts

The cCRT-ICB trials tested different treatment schedules and ICB agents in heterogeneous patient populations. We therefore used a chi-square test and associated I^2 values to assess whether differences in survival between cohorts exceeded levels expected given the cohort variances σ^2 alone, as underlying uncertainty (e.g. ICB pharmacokinetics) might affect the outcomes. Subsequently, we further analysed the OS data using a DerSimonian-Laird random effects model^{189–191}. The binomial variance σ^2 and I^2 for cohort i is written as

$$\sigma_i^2 = \frac{OS_i \times (1-OS_i)}{N_{eff,i}} \quad \text{--- Equation 4.3}$$

$$I^2 = \frac{[\sum_{i=1}^n (OS_{observed,i} - OS_{modelled,i})^2 / \sigma_i^2] - (n-1)}{\sum_{i=1}^n (OS_{observed,i} - OS_{modelled,i})^2 / \sigma_i^2} = \frac{\text{sum of squares} - (n-1)}{\text{sum of squares}}$$

--- Equation 4.4

where the I^2 values describe the fraction of the difference between the model and observation explained by the binomial σ^2 . Values of weighted-mean survival $\overline{OS}_{2yr,cCRT-ICB}$ and additional random variance Δ^2 were obtained by minimising the log-likelihood (LL) term

$$-2\ln L = \sum_{i=1}^{n_{ICB \text{ cohorts}}} \frac{(\overline{OS}_{2yr,cCRT-ICB} - OS_{2yr,i})^2}{\sigma_i^2 + \Delta^2} + \ln(\sigma_i^2 + \Delta^2) \quad \text{--- Equation 4.5}$$

where $n_{ICB \text{ cohorts}}$ denotes the number of cCRT-ICB cohorts. The significance of Δ^2 was derived from the change in LL between the best fit for the factor with the factor gradient and Δ^2 both freely fit, and the best fit with the gradient freely fit but the Δ^2 set to zero.

Incorporating binomial and random variances allows testing OS with underlying uncertainty, as standard linear regression only tests uncertainty from

the spread of the data points (i.e. binomial uncertainty). With random variance, we could down-weight the variance of fits in smaller cohorts while still accounting for the between-cohort variation.

Associations between levels of 2-year OS in the cCRT-ICB cohort and patient and treatment related factors f were investigated univariably by replacing $\overline{OS}_{cCRT-ICB}$ in Equation 4.5 with $(A_{ICB} \times f_i + C_{ICB})$ in which A_{ICB} and C_{ICB} are fitted regression parameters and value f_i is the value of f for the i th cohort. The significance of the regression term A_{ICB} and the ongoing significance of Δ^2 were determined using the likelihood-ratio test. Associations were visualised by plotting the survival levels observed for each cohort against factor values, with the fitted regression lines added.

Factors with fitted A_{ICB} coefficients having p-values <0.2 in univariable analyses were entered into a multiple regression analysis, and the multivariable model with the best Akaike information criterion (AIC) score was identified using bidirectional stepwise parameter selection.

4.3.2 Estimation of the overall OS gain from ICB

Most cCRT-ICB studies were single arm. Therefore gains in OS achieved by adding ICB to treatments were evaluated by simultaneously fitting data from studies of RT alone, CRT and cCRT-ICB, using the extended CRT Model (Model 5 in Chapter 3)¹⁸⁷. The extended CRT Model include terms describing the ICB gains in OS (ϵ) and their associations with different factors.

$$OS_{2yr,CRT-ICB} = OS_{2yr,CRT Model}(D, d, T, chemo, stage-mix) + \epsilon \times I$$

--- Equation 4.6

where D , d , T denote total RT dose, dose-per-fraction, and duration; $chemo$ describes whether chemotherapy was given sequentially, concurrently or not at all;

stage-mix is the stage composition of a cohort, and further details of the CRT model have been described in Chapter 3 (Model 5, Chapter 3)¹⁸⁷. The indicator function *I* took values of 0 for RT and CRT treatments and 1 for cCRT-ICB treatments. The model was fitted to the CRT and cCRT-ICB datasets, minimising the LL term

$$-2\ln L = -2 \left\{ \sum_{i=1}^{n_{coh}} N_{eff,i} \times \left[OS_{2yr,obs,i} \times \ln OS_{2yr,CRT-ICB Model,i} + (1 - OS_{2yr,obs,i}) \times \ln(1 - OS_{2yr,CRT-ICB Model,i}) \right] \right\}$$

--- Equation 4.7

where n_{coh} is the total number of cohorts fitted and $OS_{2yr,obs,i}$ is the observed survival for cohort i . Comparing to Chapter 3, we did a fine tuning on ‘study time calibration parameter’ R as newest study has now published in 2022 instead of 2016 in the cCRT-ICB dataset. Besides, we replaced the patient numbers N using effective patient numbers (N_{eff}) at 2-year for cCRT-ICB cohorts.

4.3.3 Associations between OS gains from ICB and factors

Associations between changes in OS due to ICB drug administration and patient and treatment related factors f were investigated by fitting the model

$$OS_{2yr,CRT-ICB} = OS_{2yr,CRT Model} (D, d, T, chemo, stage-mix) + A \times f + C + (A_{ICB gain} \times f + C_{ICB gain}) \times I \text{ --- Equation 4.8}$$

in which I was again set to a value of 1 for cCRT-ICB and 0 otherwise; $(A \times f + C)$ describes the association between factor f and survival following RT or CRT; and $(A_{ICB gain} \times f + C_{ICB gain})$ describes the association between f and OS changes.

For factors such as D , d and T which are already included in the CRT survival model, the CRT-ICB model is simplified to

$$OS_{2yr, CRT-ICB} = OS_{2yr, CRT Model}(D, d, T, chemo, staging) + (A_{ICB gain} \times f + C_{ICB gain}) \times I$$

--- Equation 4.9

This simpler model was also used for ICB-specific factors such as drug-type and ICB start time, which are unrelated to outcomes of RT alone or CRT.

Associations between survival gains and factors were visualised by plotting gains in 2-year OS for each cohort against factor values and adding fitted ($A_{ICB gain} \times f + C_{ICB gain}$) lines. The survival gains were calculated as the 2-year OS observed for a cohort minus the OS predicted by the model fit for the cohort's CRT treatment alone (i.e. the modelled survival for each patient cohort in the absence of ICB administration). Factors whose fitted A or $A_{ICB gain}$ coefficients had p-values <0.2 in univariable analyses were entered into a multiple regression analysis.

4.3.4 Statistical analysis

RStudio software (version 2022.02.3) was used for analyses. Model fitting and meta-regression were performed using maximum likelihood estimation through the *bbmle* package¹³⁰, comparing fits using likelihood-ratio testing and the AIC. The multi-dimensional profile-likelihood technique was used to estimate 95% CIs on fitted parameter values¹⁵⁷. Bidirectional stepwise parameter selection for multivariable analyses was executed using the *MASS* package¹³⁷. Meta-regression results were plotted using the *ggplot2*¹⁵⁶. Reported significance levels were two-sided.

4.4 Results

4.4.1 Data and OS standardisation

The cCRT-ICB dataset is detailed in Table 4.2 and 4.3. It comprises 2196 NSCLC patients (99% stage III) belonging to 10 cohorts treated with cCRT-ICB in eight studies published between 2018 and 2022^{72,192–198}. Median follow-up times for these cohorts had an average length of 21.0 months weighted by patient number, and a range of 13.7 to 32.6 months. The total effective patient number N_{eff} at the 2-year time-point was 1668. As the median follow-up was less than the 24-month endpoint timepoint, so we calibrate the patient number as described in the methodology section. It would not be a serious issue as *PACIFIC* trial also had a short median follow-up of 14.5 month when it was firstly published in 2017⁷¹.

The mean 2-year OS level reported for the cohorts was 64.8%, weighted by patient number. ICB administration began during cCRT in four cohorts and after completion of cCRT in six. Survival was reported relative to the recruitment time-point, which in these latter six cohorts followed completion of cCRT. In two of these cohorts, patients were recruited on average 21 and 28 days after cCRT completion. In the other four, recruitment was assumed to be on average 28 days after cCRT, this time-point lying within all the ranges of recruitment times published for cohorts in which ICB began following cCRT. After correcting back to the start of cCRT, standardised 2-year OS levels across all cohorts had a weighted mean of 65.5% and a range of 59.0% to 80.0%.

Table 4.2 Patient, radiotherapy and ICB data characteristics for the cCRT-ICB cohorts. Average values are weighted by patient numbers per cohort.

| Cohort | 1 | 2 | 3 | 4 | 5 | 6 | 7 | 8 | 9 | 10 | Total or average |
|------------------|--------------------------|---|-----------|-----------------------------|----------------------------|--|------------|----------------------------|-----------------------------|---------------------------------------|------------------|
| Author | Durm <i>et al</i> (2020) | ↔ Lin <i>et al</i> (2020) ^a | | Antonia <i>et al</i> (2018) | Peters <i>et al</i> (2021) | ↔ Reck <i>et al</i> (2022) ^{a,b} | | Bryant <i>et al</i> (2022) | Landman <i>et al</i> (2021) | Zhou <i>et al</i> (2022) ^c | - |
| Study name | LUN-14-179 | DETERRED | | PACIFIC | NICOLAS | KEYNOTE-799 | | Institutional series | Institutional series | GEMSTONE-301 | - |
| Patient # | | | | | | | | | | | |
| Stage I/II | 0 (0%) | 1 (10%) | 5 (17%) | 8 (2%) | 0 (0%) | 0 (0%) | 0 (0%) | 0 (0%) | 0 (0%) | 2 (1%) | 16 (1%) |
| IIIA | 55 (60%) | 2 (20%) | 12 (40%) | 252 (53%) | 28 (36%) | 41 (37%) | 39 (38%) | 574 (57%) | 27 (69%) | 74 (29%) | 1104 (50%) |
| IIIB/C | 37 (40%) | 7 (70%) | 13 (43%) | 212 (45%) | 50 (64%) | 71 (63%) | 63 (62%) | 432 (43%) | 12 (31%) | 179 (70%) | 1076 (49%) |
| Total | 92 (100%) | 10 (100%) | 30 (100%) | 472 (100%) | 78 (100%) | 112 (100%) | 102 (100%) | 1006 (100%) | 39 (100%) | 255 (100%) | 2196 (100%) |

RTDose^d (Gy) (range). All treatments given in 2Gy fractions, 5 days-per-week.

| | | | | | | | | | | |
|--------------|----------|----------|----------|-------------------|-----|-----|-----|------|-----|------|
| 60 | 66 | 66 | 60 | 66 | 60 | 60 | 60 | 69.9 | 60 | 60.5 |
| (59.4, 66.6) | (60, 66) | (60, 66) | (54, 66) | (- ^e) | (-) | (-) | (-) | (-) | (-) | (-) |

Patient-related factors

Median age (years)

| | | | | | | | | | | |
|----|----|----|----|----|----|----|----|------|----|------|
| 66 | 66 | 68 | 64 | 62 | 66 | 64 | 69 | 66.5 | 61 | 66.2 |
|----|----|----|----|----|----|----|----|------|----|------|

Eligibility criteria

| | | | | | | | | | | |
|----------------------|----------------------|-------------------|-------------------|-------------------|-------------------|-------------------|-------------------|----------------------|----------------------|---|
| cCRT, no progression | cCRT, no progression | Standard for cCRT | cCRT, no progression | cCRT, no progression | - |
|----------------------|----------------------|-------------------|-------------------|-------------------|-------------------|-------------------|-------------------|----------------------|----------------------|---|

Male/female (% of patients)

| | | | | | | | | | | |
|-----------|-----------|-----------|-----------|-----------|-----------|-----------|----------|-----------|----------|-----------|
| 64.0/36.0 | 90.0/10.0 | 60.0/40.0 | 70.2/29.8 | 67.1/32.9 | 67.9/32.1 | 60.8/39.2 | 95.0/5.0 | 64.0/36.0 | 93.0/7.0 | 83.1/16.9 |
|-----------|-----------|-----------|-----------|-----------|-----------|-----------|----------|-----------|----------|-----------|

Histology SCC/other (% of patients)

| | | | | | | | | | | | |
|--|-----------|-----------|-----------|-----------|-----------|-----------|-----------|-----------|-----------|-----------|-------------------|
| | 45.0/55.0 | 70.0/30.0 | 23.0/77.0 | 47.1/52.9 | 35.4/64.6 | 65.2/34.8 | 0.0/100.0 | 48.2/51.8 | 28.2/71.8 | 70.0/30.0 | 47.9/52.1 |
| Tumour PDL1 immunohistochemistry $\geq 1\%$ ^f (% of patients) | 79.2 | 44.0 | 44.0 | 67.2 | - | 75.0 | 58.8 | - | 62.1 | 58.5 | 65.2 ^g |
| Performance status ≥ 1 (% of patients) | - | - | - | 50.8 | 53.2 | 54.5 | 44.1 | - | 77.0 | 69.0 | 56.1 ^g |

ICB-related factors

ICB drug type: anti- (drug name)

| | | | | | | | | | | |
|------------------------|------------------------|------------------------|----------------------|--------------------|------------------------|------------------------|----------------------|----------------------|-----------------------|---|
| PD1(Pembr olizumab) | PDL1(Atez olizumab) | PDL1(Atez olizumab) | PDL1(Durv alumab) | PD1(Nivolu mab) | PD1(Pembr olizumab) | PD1(Pembr olizumab) | PDL1(Durv alumab) | PDL1(Durv alumab) | PDL1(Suge malimab) | - |
|------------------------|------------------------|------------------------|----------------------|--------------------|------------------------|------------------------|----------------------|----------------------|-----------------------|---|

ICB timing, begun concurrently with or sequentially after cCRT

| | | | | | | | | | | |
|------------|------------|------------|------------|------------|------------|------------|------------|------------|------------|---|
| Sequential | Sequential | Concurrent | Sequential | Concurrent | Concurrent | Concurrent | Sequential | Sequential | Sequential | - |
|------------|------------|------------|------------|------------|------------|------------|------------|------------|------------|---|

Intervals between ICB drug administration (weeks)

| | | | | | | | | | | |
|---|---|---|---|-----|---|---|---|---|---|-----|
| 3 | 3 | 3 | 2 | 3-4 | 3 | 3 | 2 | 2 | 3 | 2.3 |
|---|---|---|---|-----|---|---|---|---|---|-----|

Planned ICB duration (months)

12 12 12 12 12 12 12 12 12 24 13.4

^a The DETERRED and KEYNOTE-799 studies each included two separate cohorts treated with cCRT-ICB.

^b 2-year OS was reported in Reck *et al* (2022) while other KEYNOTE-799 data was taken from Jabbour *et al* (2021).

^c Aside from 86 patients in Cohort 10 treated with sCRT-ICB all the other 2110 patients (96%) in the cCRT-ICB dataset (96%) received cCRT-ICB.

^d Tabulated doses are medians, except for Cohort 9 for which the mean dose was reported.

^e In individual cohort columns, data items not available from study publications are indicated by '-'.

^f Tumor PDL1 immunohistochemistry was not available for every patient in every cohort. The figures shown here therefore represent numbers of patients with PDL1 $\geq 1\%$ as percentages of those for whom data was available.

^g These values are averages over the sets of cohorts for which data was reported.

Table 4.3 Follow-up, 2-year survival, and effective patient numbers N_{eff} in the cCRT-ICB cohorts.

| Cohort | 1 | 2 | 3 | 4 | 5 | 6 | 7 | 8 | 9 | 10 | Total or average* |
|--------|---|---|---|---|---|---|---|---|---|----|-------------------|
|--------|---|---|---|---|---|---|---|---|---|----|-------------------|

| | | | | | | | | | | | |
|---|--------------------------|-----------------------|------------------|-------------------------|------------------|------------------|------------------|-----------------------------|--------------------------|-------------------------|------|
| | 63.9 | 59.0 | 80.0 | 69.2 | 63.7 | 64.3 | 71.2 | 61.6 | 67.7 | 79.6 | 65.5 |
| N_{eff} at 2 years** | 83 | 6 | 24 | 425 | 77 | 88 | 73 | 791 | 31 | 70 | 1668 |
| Time of recruitment/enrolment ('Time 0' from which published OS was recorded) | | | | | | | | | | | |
| | 28-56 days after cCRT | 21 days after cCRT | Start of cCRT | 1-42 days after cCRT | Start of cCRT | Start of cCRT | Start of cCRT | Start of ICB, after cCRT | 14-28 days after cCRT | 1-42 days after cCRT | |
| Typical time of recruitment after the start of cCRT*** | | | | | | | | | | | |
| | 28 days | 21 days | - | 28 days | - | - | - | 28 days | 21 days | 28 days | - |

* The average value of median follow-up was weighted by patient numbers in the different cohorts. Average values of reported and standardized 2-year OS were weighted by effective patient numbers.

† 95% CIs shown are either published values or were determined from published KM curves using *IPDfromKM*.

** For Cohorts 6, 7 and 9 neither the 95% CI on OS_{2yr} nor the underlying KM curve were published. For Cohorts 6 and 9 N_{eff} was therefore determined via scalings of the CI of Cohort 8 which had a similar median follow-up time. For Cohort 7 N_{eff} was similarly determined from the scaled CIs of Cohorts 3 and 10.

*** For Cohorts 2 and 9, the tabulated typical times are average times following cCRT published for these cohorts. For cohorts 1, 4, 8 and 10 the typical time is assumed to be 28 days after the end of cCRT, a figure lying within the ranges of recruitment times published for cohorts 1, 4, 9 and 10.

4.4.2 Meta-regression analysis of OS in cCRT-ICB cohorts

The variance in 2-year OS rates reported for the cCRT-ICB cohorts significantly exceeded the level due to cohort binomial statistical uncertainties σ_i^2 alone ($p < 0.001$), with the additional random effects variance Δ^2 accounting for 59.5% of the total according to the I^2 index. Correspondingly, Δ^2 was significantly different to zero in fits of Equation 4.5 to the cCRT-ICB survival data ($p < 0.001$). With random effects included in the model, the fitted weighted mean 2-year OS was 67.7% (95% CI: 64.8, 70.9%) for the cCRT-ICB cohorts.

In univariable analyses, median age, planned ICB duration and tumour PDL1 $\geq 1\%$ were significantly associated with OS (Table 4.4 and Fig. 4.2). The association between median age and survival was negative, the fitted value of A_{ICB} indicating a 1.5% absolute fall in 2-year OS per added year of age (95% CI: 0.9, 2.1%; $p < 0.001$). Longer planned ICB duration was positively associated with survival, the fit indicating an increase in 2-year OS of 13.6% absolute (95% CI: 5.3, 21.7%; $p = 0.002$) for a planned duration of two years vs one. Tumour PDL1 $\geq 1\%$ was also positively associated with survival, 2-year OS increasing by 1.6% (95% CI: 1.3, 1.9%; $p = 0.023$) for each 10% increase of patients with tumour PDL1 $\geq 1\%$. For these three factors, the added random effects variance Δ^2 contributed 13.5%, 28.6% and 34.3% respectively (according to I^2 values. Equation 4.4) to the overall variance of regression residuals and was insignificantly different to zero.

Age, ICB duration and tumour PDL1 $\geq 1\%$ were tested in a multivariable analysis of 2-year OS, together with the fractions of patients with stage IIIB/C disease and PS = 0 which also had univariable p-values < 0.20 . Multivariable models were fitted to survival levels in the six cohorts for which data existed for all these factors. Using stepwise factor selection, no multivariable model was found with an AIC better than that of the univariable regression of OS against intended ICB duration, which in these six cohorts had a p-value < 0.001 .

Table 4.4 Univariable meta-regression of 2-year OS against patient and treatment factors f .

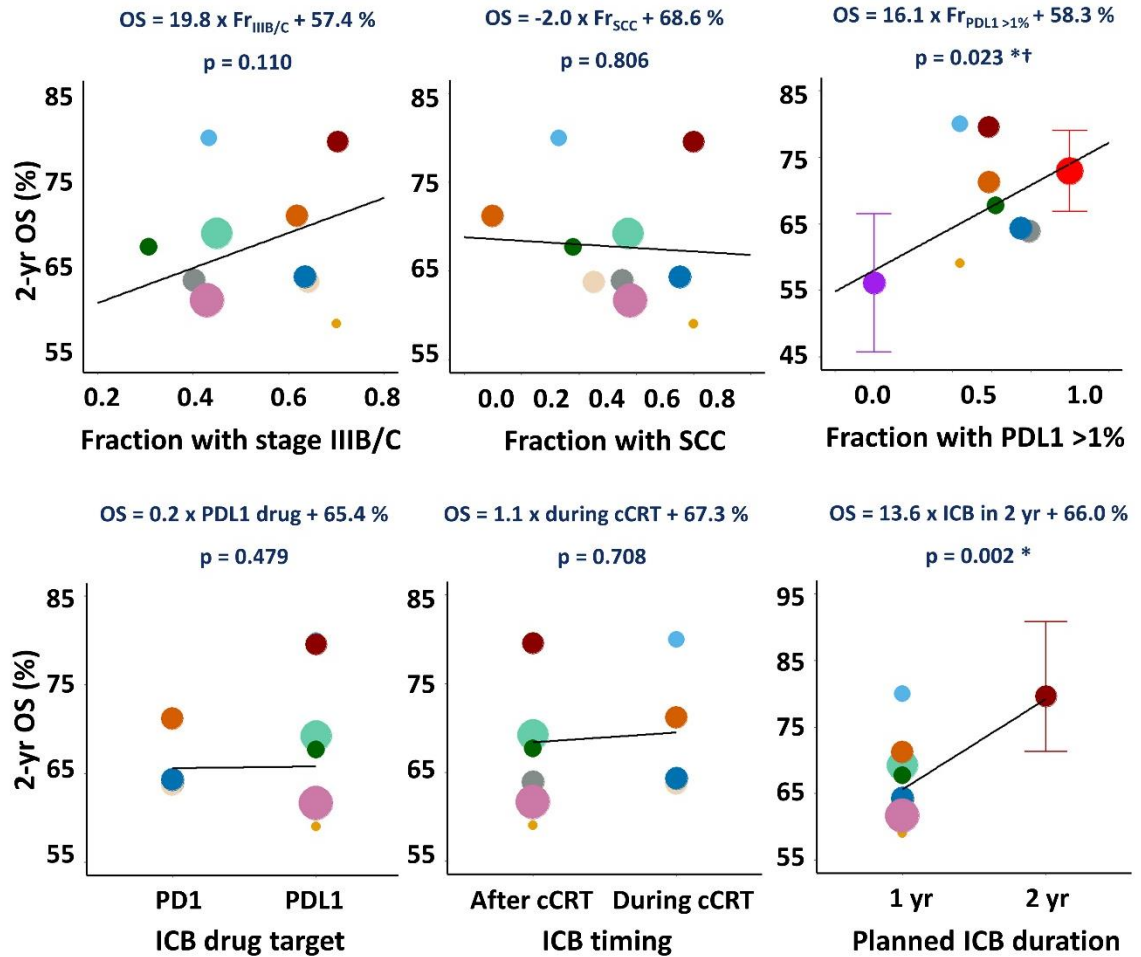
| Factors f | Regression $OS_{fit} = A_{ICB} \times f + C_{ICB}$ | A_{ICB} 95% CI | A_{ICB} significance | Δ^2 (random variance) | Δ^2 95% CI | Δ^2 significance | Cohorts fitted |
|-------------------------------|---|---------------------|---------------------------|---------------------------------|----------------------|----------------------------|-------------------|
| None | 67.7% | - | - | 0.0016 | (0.0004, 0.0051) | $p < 0.001$ | 10 |
| <i>Patient/RT factors</i> | | | | | | | |
| Median age (years) | $- 1.5\% \times f + 162.9\%$ | (-2.1, -0.9)% | $p < 0.001$ | 0.0000 | (0.0000, 0.0057) | $p = 1.000$ | 10 |
| Fraction with PDL1 $\geq 1\%$ | $+ 16.1\% \times f + 58.3\%$ | (+13.2, +19.2)% | $p = 0.023$ | 0.0001 | (0.0000, 0.0055) | $p = 0.590$ | 9* |
| Fraction with stage IIIB/C | $+ 19.8\% \times f + 57.4\%$ | (-5.1, +41.6)% | $p = 0.110$ | 0.0009 | (0.0000, 0.0039) | $p = 0.126$ | 10 |
| Fraction with PS = 0 | $- 23.6\% \times f + 80.4\%$ | (-53.1, +5.9)% | $p = 0.119$ | 0.0000 | (0.0000, 0.0040) | $p = 1.000$ | 6* |
| Fraction with SCC | $- 2.0\% \times f + 68.6\%$ | (-17.8, +13.5)% | $p = 0.806$ | 0.0016 | (0.0004, 0.0054) | $p = 0.021$ | 10 |
| RT duration (days) | $+ 0.2\% \times f + 60.0\%$ | (-1.1, +1.5)% | $p = 0.777$ | 0.0016 | (0.0003, 0.0054) | $p = 0.024$ | 10 |
| RT dose (Gy) | $+ 0.1\% \times f + 59.7\%$ | (-0.9, +1.1)% | $p = 0.806$ | 0.0016 | (0.0004, 0.0054) | $p = 0.024$ | 10 |

| <i>ICB factors</i> | | | | | | | |
|-----------------------------------|----------------------------|----------------|-----------|--------|------------------|-----------|----|
| Planned ICB duration [†] | + 13.6% × <i>f</i> + 66.0% | (+5.3, +21.7)% | p = 0.002 | 0.0006 | (0.0000, 0.0025) | p = 0.287 | 10 |
| ICB drug type [†] | + 0.2% × <i>f</i> + 65.4% | (-5.5, +6.0)% | p = 0.479 | 0.0013 | (0.0002, 0.0053) | p = 0.039 | 10 |
| ICB timing [†] | + 1.1% × <i>f</i> + 67.3% | (-5.2, +7.3)% | p = 0.708 | 0.0016 | (0.0003, 0.0054) | p = 0.028 | 10 |

* PS and PDL1 factor data were not reported for every cCRT-ICB cohort. Regressions of OS against these factors were therefore carried out for the six and eight cohorts respectively for which data was available. For *PACIFIC* survival data was available separately for patients with PDL1 < and ≥1%, bringing the number of cohorts fitted for this factor to 9.

[†] For these categorical variables *f* was set to 1 versus 0 for a planned ICB duration of two versus one years, for anti-PDL1 versus anti-PD1 drug-type, and for ICB began concurrently with versus after cCRT.

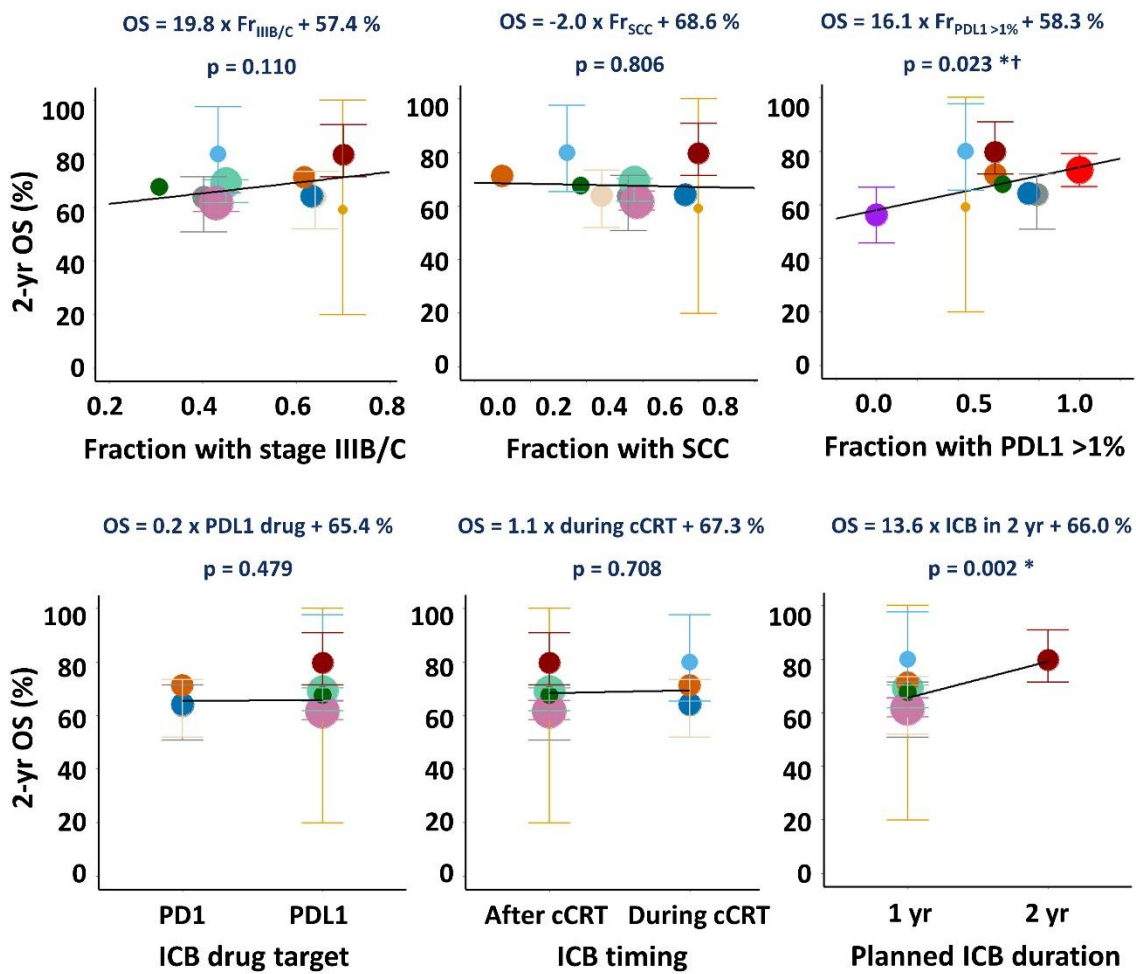
(A)



| Cohort | N_{eff} | Cohort | N_{eff} |
|--------|-----------|--------|-----------|
| 1 | 83 | 6 | 88 |
| 2 | 6 | 7 | 73 |
| 3 | 24 | 8 | 791 |
| 4 | 425 | 9 | 31 |
| 5 | 77 | 10 | 70 |

[†] The fraction of patients with PDL1 $\geq 1\%$ could only be regressed against OS for eight cohorts for which PDL1 data was published. For *PACIFIC*, however, survival data was available separately for patients with or without PDL1 $\geq 1\%$ (purple and red dots), bringing the number of cohorts up to nine.

(B)



| Cohort | N _{eff} | Cohort | N _{eff} |
|--------|------------------|--------|------------------|
| 1 | 83 | 6 | 88 |
| 2 | 6 | 7 | 73 |
| 3 | 24 | 8 | 791 |
| 4 | 425 | 9 | 31 |
| 5 | 77 | 10 | 70 |

† The fraction of patients with PDL1 ≥1% could only be regressed against OS gain for eight cohorts for which PDL1 data was published. However, for *PACIFIC* survival data was available separately for patients with or without PDL1 >1% (purple and red dots), bringing the number of cohorts up to nine.

Figure 4.2 Univariable regression of 2-year OS in cCRT-ICB cohorts against selected patient and treatment factors. A single 95% CI on OS is shown for key cohorts (A); all 95% CIs are shown in (B). Significant associations are asterisked.

4.4.3 Associations between ICB OS gains and factors

The fitted value of the gain in OS across the cCRT-ICB cohorts was 9.9% (95% CI: 7.6, 12.2%). It indicated that the net contribution brought by ICB was significant against OS of cCRT alone ($p=0.018$). Modelled fits with OS gain parameter ϵ , values of parameters were listed in Table 4.5.

Table 4.6 (A) and Figure 4.3 describe associations between estimated ICB gains in 2-year OS and treatment and patient factors considered one at a time. The fraction of patients with $PDL1 \geq 1\%$, the fraction with stage IIIB/C disease and the planned ICB duration were all significantly positively associated with estimated OS gains. Each 10% increase in the fraction of patients with $PDL1 \geq 1\%$ corresponded to a 2.4% absolute increase in 2-year OS gain (95% CI: 0.5, 4.4%; $p=0.034$), and each 10% increase in the fraction of stage IIIB/C patients corresponded to a 3.2% increase in OS gain (95% CI: 0.6, 5.7%; $p=0.021$). A planned ICB duration of two years vs one year corresponded to a 14.8% increase in 2-year OS gain (95% CI: 4.2, 23.5%; $p=0.008$). Age was significantly negatively associated with OS gain. No other factors investigated, including RT dose and start timing of ICB during vs after cCRT, were associated with estimated OS gains.

Survival trends in cohorts treated using RT or CRT alone are summarised in Table 4.6 (B). Greater median age was significantly negatively associated with 2-year OS in these cohorts, as it was with the OS gains from adding ICB to cCRT in cCRT-ICB cohorts. The fraction of patients with $PDL1 \geq 1\%$ was also significantly negatively associated with survival in RT and CRT cohorts, 2-year OS falling by 1.1% for each 10% increase in patients with $PDL1 \geq 1\%$ (95% CI: 0.4, 2.8%, p

=0.012). The scale of this trend was less than that of the significant positive association between the PDL1 factor and the ICB survival gain in cCRT-ICB treatments, and therefore OS following cCRT-ICB was significantly positively associated with patient PDL1 status (Table 4.5).

In a multivariable analysis of all factors with univariable p-values <0.20, the best model of OS according to the AIC was built from the fraction of patients with PDL1 $\geq 1\%$ and planned ICB duration (Table 4.6 (C)). The directions of associations between these factors and estimated OS gains from ICB were positive in the multivariable model, as they had been in the factor-by-factor analysis of Table 4.6 (A).

Table 4.5 Fitted parameter values in the underlying and extended CRT models.

| Parameters | CRT model fitted to published CRT dataset (Chapter 3) | CRT model fitted to both datasets | CRT model with ϵ term fitted to both datasets |
|---------------------------|---|-----------------------------------|--|
| λ_{cCRT} (Gy/day) | 1.47 | 1.07 | 1.06 |
| $T_{k, cCRT}$ (days) | 24 | 39 | 19 |
| α/β (Gy) | S _{early} : 10.0 | S _{early} : 10.0 | S _{early} : 10.0 |
| | S _{III A} : 32.1 | S _{III A} : 32.3 | S _{III A} : 32.0 |
| | S _{III B/C} : 0.6 | S _{III B/C} : 0.4 | S _{III B/C} : 0.7 |
| $EQD_{2,tum50}$ (Gy) | 54 | 55 | 55 |
| m | 0.15 | 0.14 | 0.15 |
| $OS_{max,CRT}$ (%) | 91 | 92 | 93 |
| RS^{cCRT} | 1.40 | 1.07 | 1.40 |
| $EQD_{2,SLT50}$ (Gy) * | 54 | 64 | 61 |
| m_{SLT} * | 0.31 | 0.16 | 0.18 |
| R (per year) | 0.016 | 0.016 | 0.013 |

| | | | |
|------------------------------|----------------------------|----------------------------|----------------------------|
| | S_{early} : 0.33 | S_{early} : 0.20 | S_{early} : 0.28 |
| $F_{SLT}^{*\dagger}$ | S_{IIIA} : 0.41 | S_{IIIA} : 0.39 | S_{IIIA} : 0.43 |
| | $S_{\text{IIIB/C}}$: 0.58 | $S_{\text{IIIB/C}}$: 0.48 | $S_{\text{IIIB/C}}$: 0.52 |
| ε | - | - | 0.099 |
| AIC | - | 8537.2 | 8533.5 |
| Likelihood ratio test | - | reference | p = 0.018 |

* In Chapter 4, I renamed normal tissue complication probability (NTCP) term used in Chapter 3 with survival-limiting toxicity (SLT) term following the publication of Chapter 3.

† Fitted values of F_{SLT} were constrained so that $F_{SLT, \text{IIIB/C}} \geq F_{SLT, \text{IIIA}} \geq F_{SLT, \text{early stage}}$.

Nomenclature: λ_{cCRT} , dose-per-day repopulated during cCRT; $T_{k, cCRT}$, repopulation kick-off time during cCRT; α/β , tumour fractionation dependence; $EQD_{2, \text{tum}50}$, EQD_2 required to achieve 50% tumour control; m , tumour dose-response relative gradient; $OS_{\text{max}, cCRT}$, maximum overall survival for chemoradiotherapy; RS^{cCRT} , radiosensitisation of dose-effects by cCRT; $EQD_{2, SLT50}$, EQD_2 causing a 50% modelled survival-limiting toxicity rate; m_{SLT} , survival-limiting toxicity response relative gradient; R , variation of 2-year OS with study publication year; F_{SLT, S_i} , survival-limiting toxicity weighting for stage S_i ; ε , the gain in 2-year OS that results from adding ICB to cCRT.

Table 4.6. Analysis of associations between patient or treatment factors f and changes in 2-year OS due to adding ICB to cCRT. (A) & (B) Univariable analysis details, showing fitted values of (A) terms added to the underlying CRT survival model to describe differences in survival following cCRT-ICB compared to cCRT alone, and (B) further terms added to describe associations between survival following RT or CRT alone and factors not included in the underlying CRT model. (C) The multivariable model with the lowest AIC score built from $A_{ICBgain}$ and A terms for factors with p-values <0.20 on univariable analysis; the model was fitted to the 50 RT, CRT or cCRT-ICB cohorts for which data was available for all these factors.

(A)

| Univariable analysis of factors f | $OS_{gain} = A_{ICB\ gain} \times f + C_{ICB\ gain}$ | 95% CI on $A_{ICB\ gain}$ | Statistical significance | Cohorts fitted ^a |
|--|--|---------------------------|--------------------------|-----------------------------|
| Overall OS_{gain} | 9.9% | - | p = 0.018 ^b | 61 |
| <i>Patient/RT factors^c</i> | | | | |
| Median age (years) ^d | - 0.66% $\times f$ + 50.0% | (-1.08, -0.29)% | p = 0.012 | 50 |
| Fraction with PDL1 $\geq 1\%$ ^d | + 24.4% $\times f$ + 3.2% | (+4.6, +43.7)% | p = 0.034 | 60 |
| Fraction with stage IIIB/C | + 32.0% $\times f$ - 6.0% | (+6.0, +56.6)% | p = 0.021 | 61 |

| | | | | |
|-----------------------------------|------------------------------|--------------------|-------------|----|
| Fraction with PS=0 ^d | $- 19.1\% \times f + 16.5\%$ | $(-26.2, +12.2)\%$ | $p = 0.439$ | 35 |
| Fraction with SCC ^d | $- 11.6\% \times f + 14.9\%$ | $(-34.6, +11.3)\%$ | $p = 0.210$ | 49 |
| RT duration (days) | $+ 0.13\% \times f + 5.1\%$ | $(-0.51, +1.33)\%$ | $p = 0.776$ | 61 |
| RT dose (Gy) | $+ 0.16\% \times f + 0.3\%$ | $(-0.60, +0.88)\%$ | $p = 0.614$ | 61 |
| <i>ICB factors^c</i> | | | | |
| Planned ICB duration ^e | $+ 14.8\% \times f + 9.0\%$ | $(+4.2, +23.5)\%$ | $p = 0.008$ | 61 |
| ICB drug type ^e | $+ 0.94\% \times f + 8.7\%$ | $(-4.92, +6.61)\%$ | $p = 0.777$ | 61 |
| ICB timing ^e | $+ 3.3\% \times f + 7.9\%$ | $(-3.2, +7.8)\%$ | $p = 0.348$ | 61 |

(B)

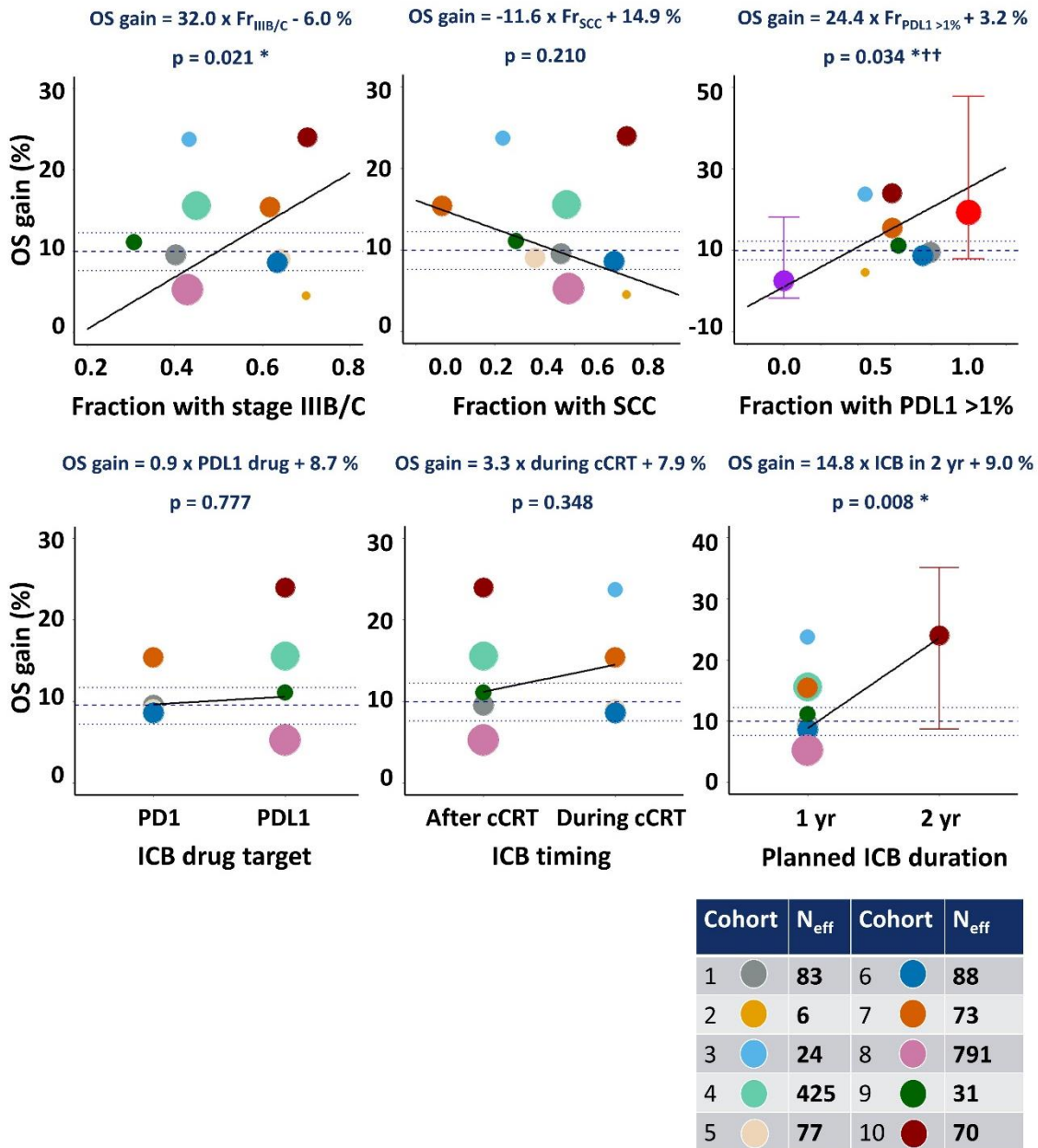
| Univariable analysis of factors f | $OS_{fit} = A \times f + C$ | 95% CI on A | Statistical significance | Cohorts fitted [†] |
|---|------------------------------|-----------------|--------------------------|-----------------------------|
| Median age (years) | $- 0.82\% \times f + 56.5\%$ | (-1.13, -0.20)% | $p = 0.017$ | 50 |
| Fraction with PDL1 $\geq 1\%$ | $-11.1\% \times f + 7.5\%$ | (-27.7, -3.8)% | $p = 0.012$ | 60 |
| Fraction with PS=0 | $- 6.0\% \times f + 11.7\%$ | (-8.9, +3.0)% | $p = 0.163$ | 35 |
| Fraction with SCC | $+ 2.6\% \times f - 0.7\%$ | (-8.2, +13.6)% | $p = 0.247$ | 49 |

(C)

| Multivariable analysis of 50 cohorts | | | | | |
|---|------------------------|---------------------------|------------|---------------|--------|
| <i>Best model according to AIC</i> | Fitted $A_{ICB\ gain}$ | 95% CI on $A_{ICB\ gain}$ | Fitted A | 95% CI on A | AIC |
| Fraction with PDL1 $\geq 1\%$ | $+ 13.5\%^f$ | (+2.0, +25.1)% | - | - | 6240.8 |
| & | | | | | |
| Planned ICB duration (years) | $+ 11.9\%$ per year | (+0.8, +21.3)% | - | - | |

- ^a The cohorts fitted are generally those for which data about the factor being tested were available. However, PDL1 data was only available for two of the cohorts treated using CRT alone. Consequently, for this factor the whole model was fitted to all cohorts (except two cCRT-ICB cohorts for which PDL1 data was unavailable), but the $(A \times F + C)$ term was fitted only to the arm of PACIFIC receiving CRT alone, split into two sub-cohorts with PDL1 < or ≥ 1 .
- ^b The significance of the overall OS_{gain} was tested for a constant gain across all cCRT-ICB cohorts versus no gain.
- ^c The significance levels reported for associations between OS_{gain} or OS and factors are for fitted versus zero gradients.
- ^d For factors not included in the underlying CRT survival model and which do not describe ICB treatment regimens (eg age but not immune drug type or RT dose) the additional terms listed in Table 4.6(B) also formed part of the model fit and contributed to total OS rates calculated for CRT and cCRT-ICB treatments (equation 4.8).
- ^e For these categorical variables, f was set to 1 versus 0 for a planned ICB duration of two versus one years, for anti-PDL1 versus anti-PD1 drug type, and for ICB began concurrently with versus after cCRT.
- ^f Absolute percentage change in OS gain as the fraction of patients changes from zero to one (i.e. from 0 to 100%)

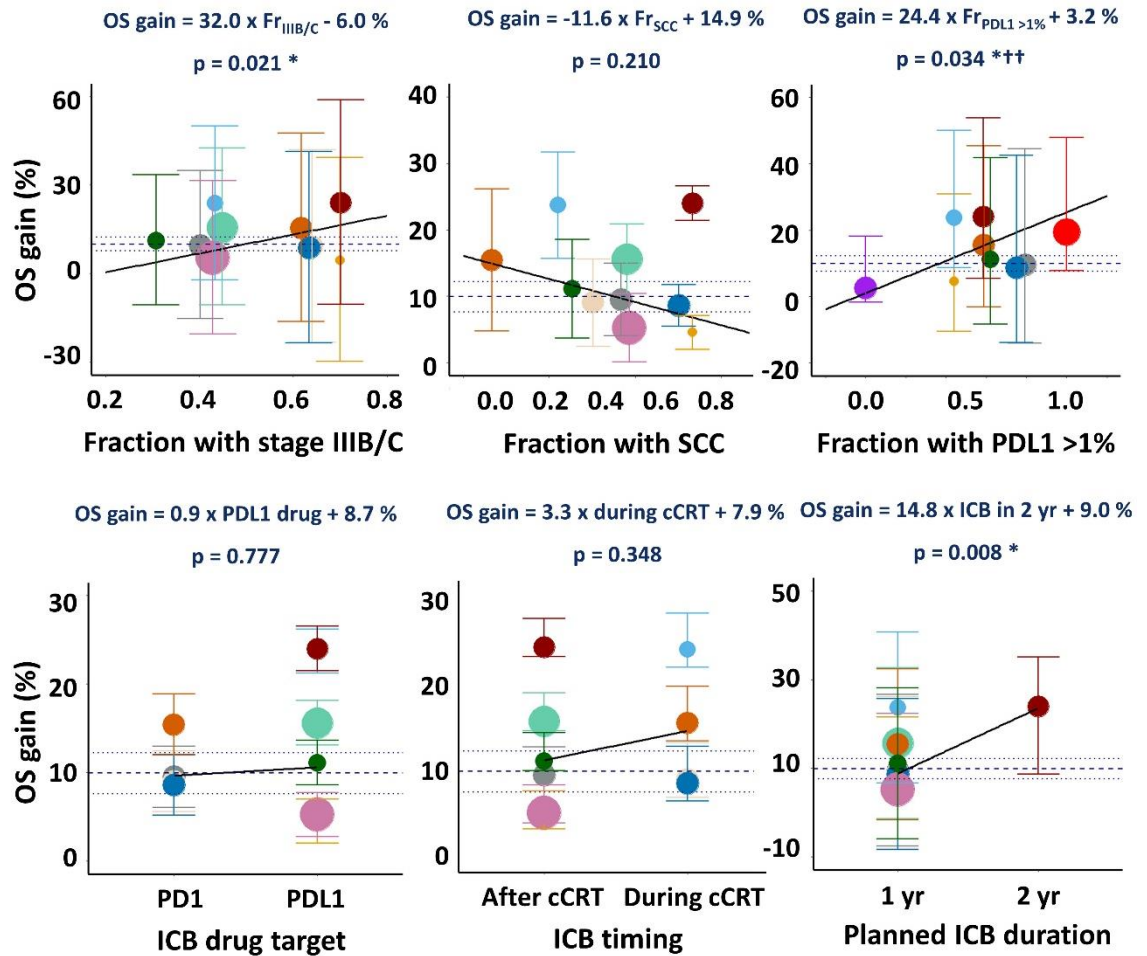
(A)



† The CI on the OS gain for a cohort c and factor f was obtained by first reparametrising the OS gain term of the model fit as $A_{ICB \text{ gain}} \times (f - f_c) + C_{ICB \text{ gain}}$, where f_c is the value of f for cohort c , and then using the profile-likelihood method to obtain the CI on $C_{ICB \text{ gain}}$ which corresponds to the OS gain for cohort c .

†† The fraction of patients with PDL1 $\geq 1\%$ could only be regressed against OS gain for eight cohorts for which PDL1 data was published. For *PACIFIC*, however, survival data was available separately for patients with or without PDL1 $>1\%$ (purple and red dots), bringing the number of cohorts up to nine.

(B)



| Cohort | N_{eff} | Cohort | N_{eff} |
|--------|-----------|--------|-----------|
| 1 | 83 | 6 | 88 |
| 2 | 6 | 7 | 73 |
| 3 | 24 | 8 | 791 |
| 4 | 425 | 9 | 31 |
| 5 | 77 | 10 | 70 |

† The CI on the OS gain for a cohort c and factor f was obtained by first reparameterizing the OS gain term of the model fit as $A_{ICB \text{ gain}} \times (f - f_c) + C_{ICB \text{ gain}}$, where f_c is the value of f for cohort c , and then using the profile-likelihood method to obtain the CI on $C_{ICB \text{ gain}}$ which corresponds to the OS gain for cohort c .

†† The fraction of patients with $PDL1 \geq 1\%$ could only be regressed against OS gain for eight cohorts for which PDL1 data was published. However, for *PACIFIC* survival data was available separately for patients with or without $PDL1 > 1\%$ (purple and red dots), bringing the number of cohorts up to nine.

Figure 4.3 Gains in 2-year OS due to ICB plotted for the cCRT-ICB cohorts against selected factors. The OS gains are differences between each cohort's observed OS and the model-predicted OS for the cCRT component of treatment. 95% CIs on OS gains are shown for key cohorts in (A) and for all cohorts in (B). Solid, dashed and dotted lines respectively show fitted linear regression terms, the fitted overall OS gain and its 95% CI. Significant associations are asterisked.

4.5 Discussion

We aimed to answer two questions about the cCRT-ICB regimen for inoperable LA-NSCLC treatment:

- 1) Does ICB's contribution across multiple studies support the results seen in the *PACIFIC* study?
- 2) Which patient/tumour/CRT/ICB factors might affect the cCRT-ICB outcomes?

We have investigated associations between 2-year OS and factors in datasets collated from results published for cCRT-ICB, RT and CRT treatments of LA-NSCLC. We also assessed associations between these factors and gains in OS due to the ICB components of the cCRT-ICB treatments. To our knowledge, this is the first systematic analysis of factors associated with survival following immuno-cCRT for NSCLC.

4.5.1 Data and modelling processing

Since many of the published studies were single arm, associations between OS gain and patient and treatment factors were determined by jointly fitting a model to OS rates reported for both cCRT-ICB treatments and RT/CRT alone, the model including terms describing the gain in OS due to immune treatment and its possible variation with different factors. This approach provided a practical way of distinguishing the effects of the immune treatments tested in trials of cCRT-ICB from the effects of different CRT schedules and cohort-to-cohort differences in patient factors. Compared to direct fitting of OS gains observed in phase 3 trials of cCRT-ICB vs cCRT, the method will introduce some bias due to differences between cohorts not being fully accounted for by patient and treatment data included in the analysis. To date, however, results have only been published for

one phase 3 trial of cCRT-ICB, *PACIFIC*. Changes in the NSCLC staging system over time will also have introduced some inconsistencies into cohort stage-mixes, AJCC versions 4-7 having been used for the CRT cohorts and versions 7-8 for the cCRT-ICB cohorts. We sought to limit these inconsistencies by categorising patients into broad stage bands, grouping stage IIIC patients with stage IIIB, and not splitting down stages I or II into sub-stages.

CRT Model was designed to model the outcomes after the starting of cCRT¹⁸⁷, so delayed randomisation in the cCRT-ICB regimen should be corrected. The Kolmogorov-Smirnov test was applied for each OS estimation to ensure no discrepancy between read-in KM curves and extracted KM curves¹⁸⁸. In terms of patient eligibility, selecting patients without post-cCRT progression might bias the treatment outcomes, while no difference was found between these subgroups, either using reported OS (p=0.628) or standardised OS (p=0.570). The length of intervals between ICB drug administration has been recorded, while given the discrepancies of ICB half-life, and pharmaco-kinetics of each drug, no factors related to ICB delivery intervals or ICB dose intensity were tested.

4.5.2 Factors affecting cCRT-ICB outcomes

After accounting for the stage-mixes of the patient cohorts and the cCRT regimens used to treat them, the fitted gain in 2-year OS achieved across the whole dataset by adding ICB to cCRT was 9.9%, in good agreement with the 10.7% OS gain reported for the cCRT-plus-durvalumab arm of *PACIFIC* relative to the cCRT-alone arm⁷². We also tried splitting the OS gain by ICB timing, where 12.0% (95% CI: 6.1%, 17.5%) for concurrent and 8.8% (95% CI: 6.3%, 11.2%) for sequential showed no statistical difference (p=0.237), in line with the findings that ICB timing was not a significant factor against OS gain (p=0.348, Table 4.6 (A)). Tumour PDL1 $\geq 1\%$, clinical stage IIIB/C and 2-year planned ICB duration were

significantly and positively associated with greater OS gains from ICB, whereas greater age was significantly negatively associated with OS gain.

The positive association between 2-year planned ICB duration and 2-year OS gain was dependent on a single 2-year duration cohort¹⁹⁷ and should be interpreted with caution unless confirmed in further studies since scheduling of immunotherapy is an evolving field. Intriguingly, OS rates reported for the ten cohorts comprising the cCRT-ICB dataset fell by a median of 16.3% (range 0.0, 33.8%) between 1 and 2 years, but in the cohort receiving ICB for two years the fall was only 5.8%. This was the second lowest fall in survival during the second year recorded for any of the cohorts and contributed to the high 2-year OS seen for the cohort. A similar effect has been seen in *CheckMate 153*, a study of 1 year vs continuous ICB monotherapy (nivolumab) for previously treated advanced or metastatic NSCLC. In that study, continuous ICB resulted in a lower risk of death (HR 0.62; 95% CI: 0.42, 0.92), with a divergence in progression-free survival occurring after treatment discontinuation in the 1-year arm¹⁹⁹.

The positive association between the fraction of patients with PDL1 $\geq 1\%$ and OS gain ($p=0.034$) is consistent with the rationale for designing immune drugs that block PDL1 and its receptor PD1, and with results from sub-group analyses of *PACIFIC* in which a significant improvement in progression-free survival was seen for PDL1 $\geq 1\%$ patients receiving durvalumab, but not for patients with PDL1 $< 1\%$ ²⁰⁰. While the fraction of patients with PDL1 $\geq 1\%$ was significantly positively associated both with OS gain and with 2-year OS itself following cCRT-ICB, the association with OS was less steep than the association with OS gain, implying that the greater survival gains achieved for patients with PDL1 $\geq 1\%$ by adding immune treatment to CRT were partly offset by lower baseline survival levels for these patients when treated using CRT alone. In *PACIFIC* patients receiving cCRT alone, 2-year OS was indeed lower for those with PDL1 $\geq 1\%$ than for others, 53.7% vs 66.4% (Figure 4.4), consistent with findings for several cancers that

PDL1 overexpression is associated with poorer prognosis²⁰¹. This data lies behind the significant negative association between PDL1 $\geq 1\%$ and OS following CRT alone seen in our analysis.

(A) *PACIFIC* 2-year OS data from Paz-Ares et al.

| | Fraction of PDL1 <1% | | Fraction of PDL1 >1% | |
|--------------------|-------------------------|-----------------|-------------------------|---|
| With Durvalumab | 56.1% (45.0%, 65.8%) | HR ₃ | 72.9% (66.2%, 78.4%) | Reported HR ₁ : 1.14 (0.71, 1.84) Reported HR ₂ : 0.59 (0.41, 0.83) Estimated HR ₃ : 0.51 (0.35, 0.73) |
| Without Durvalumab | 66.4% (52.4%, 77.1%) | HR ₄ | 53.7% (42.6%, 63.5%) | Estimated HR ₄ : 1.32 (0.82, 2.14) |

(B) 2-year OS rates calculated from the CRT-ICB model fit

| | Fraction of PDL1 <1% | Fraction of PDL1 >1% |
|--------------------|-------------------------|-------------------------|
| With Durvalumab | 59.2% (45.6%, 79.8%) | 71.2% (57.6%, 91.8%) |
| Without Durvalumab | 65.8% (52.2%, 86.4%) | 53.4% (39.7%, 73.9%) |

* ‘Reported HR’ values shown for panel A were taken directly from Paz-Ares *et al.* (2020), ‘Estimated HR’ values were obtained by reading Kaplan-Meier curves from the same publication into the *IPDfromKM* package.

Figure 4.4 Survival levels for patients with PDL1 expression < or $\geq 1\%$ treated with cCRT \pm durvalumab. (A) Observed 2-year OS levels and hazard ratios (HR*) in data reported by Paz-Ares *et al.* (2020) for *PACIFIC*²⁰⁰. (B) 2-year OS levels predicted by our fitted model for cohorts with a 50:50% split of stage IIIA versus IIIB/C patients, similar to the stage-mix in *PACIFIC*.

The association between ICB effectiveness and the fraction of patients with different tumour staging is a novel finding, as the OS shows no difference ($p=0.110$) while the gain in OS achieved by adding ICB ($p=0.021$) is significant for stage IIIB/C cancer. A plausible explanation is that immuno-CRT provides a more effective treatment of micro-metastatic disease than does CRT alone, the OS gain from ICB consequently increasing with the extent of the disease.

The negative associations between median age and both 2-year OS ($p < 0.001$) and OS gain ($p = 0.012$) are consistent with findings that age is an adverse prognostic factor for lung cancer treated using RT, chemotherapy, cCRT, immunotherapy or immuno-RT^{202–204}, and with the greater competing risks of death in older patients.

It has been suggested that better outcomes might be achieved by starting immune treatments concurrently with cCRT, potentially increasing the extent to which T-cells activated by antigens released from radiation-damaged tumour cells can kill further tumour cells^{205,206}. Presently, though, there is no consensus on the scheduling of ICB relative to RT, and both adjuvant and concurrent/adjuvant ICB treatments are being investigated in ongoing trials^{193,194}. Despite analysing data for 322 patients belonging to four cohorts in which ICB began concurrently with cCRT, and for 1874 patients belonging to six cohorts in which ICB began after cCRT, we did not find a significant difference between OS gains in the two sets of cohorts. Neither were survival gains associated with the choice of anti-PD1 or anti-PDL1 immune drug. The latter finding is perhaps unsurprising since anti-PD1 and anti-PDL1 drugs respectively bind to PDL1 on tumour cells and its receptor PD1 on immune cells, both targeting the same immune checkpoint.

PS and SCC histology do not affect treatment outcomes. Most cCRT-ICB patients had PS=0 or 1, while PS should be ≥ 2 to correlate with heart base radiation toxicity and related survival²⁰⁷. No consensus has been reached on whether SCC adds prognostic information independently on NSCLC^{208,209}. The HR between SCC (0.72; 95% CI: 0.52, 0.99) and non-SCC subgroup (0.61; 95% CI: 0.44, 0.86) was similar in *PACIFIC*; recent meta-analyses showed that ICB can provide benefits for LA-NSCLC regardless of histology²¹⁰.

The ICB gains were not significantly associated with RT doses or durations. Thus, in this dataset there was no indication of an interaction between immune and RT treatments that might cause ICB survival gains to be higher or lower at

escalated radiation dose levels. However, while median doses in the cCRT-ICB cohorts ranged from 60 to 70Gy, cohorts receiving median doses above 66Gy comprised only 39 patients (2%), limiting the power to detect such an interaction. Additionally, fits of the CRT survival model suggested that OS following CRT alone can be improved by using shorter, more intense, RT schedules¹⁸⁷, and therefore that survival following cCRT-ICB treatments might be further improved by using such intensified RT schedules if they are tolerable in the immuno-cCRT setting.

4.5.3 Statistical robustness

PACIFIC outcomes were recorded through original literature published by Antonia et al.⁷² as it is the prominent report which has been widely discussed. Recently published 5-year follow-up with the updated 2-year OS of 66.3% (95% CI: 61.8%, 70.4%)²¹¹ was nearly the same as the reported OS in the selected publication (66.3%; 95% CI: 61.7%, 70.4%).

OS and OS gain were estimated using the single time point due to limited availability of the continuous survival curves from the literature. However, direct regression of survival against factors was seen to be more informative than relative measures such as hazard ratio, which assumes the risk rate ratio was proportional to factors²¹². With fixed time point analyses, the absolute risk with greater interest than the relative risk against factors could be calculated²¹³.

It is arguable that the cohort-by-cohort OS gain differs between the factors with and without common effects (whether there is $A \times f + C$ before $A_{gain} \times f + C_{gain}$). This cohort-by-cohort study was based on aggregated data, and its statistical power would have been greater if individual patient-by-patient data had been analysed. Nevertheless, by collating data from multiple clinical series we have been able to assess OS variations across wider ranges of treatment factors than

would have been possible using patient-by-patient data from a single trial. The immuno-chemoradiotherapy landscape is becoming more complex, with ongoing studies evaluating the addition of other immune agents and combinations to standard cCRT-ICB²⁰⁴. Analyses of results collated from multiple studies will therefore have ongoing utility.

4.5.4 Limitation

Although meta-regression analyses identify the impacts of factors against ICB-induced OS gain, the modelled OS gain is still hypothetically generalised. There were only ten cCRT-ICB cohorts, so the multivariable results might not be that conclusive. Most studies were designed following the encouraging results of the *PACIFIC* trial, so treatment schedules were similar.

Some factors have limited variance in this retrospective study. PDL1% was not an evaluable marker in the CRT era, so there was no information in the CRT dataset. Consequently, we added the placebo cohort from the *PACIFIC* study in common effects analyses ($A \times f + C$)²⁰⁰, as we were unaware of any other PDL1 information for cCRT alone. Besides, all cCRT-ICB cohorts received standard radiation fractionation in 2Gy-per-fraction, and all ICB drugs targeted PD1/PDL1. In addition, biological factors such as lymphocyte counts, neutrophil counts, and neutrophil-lymphocyte ratio have been reported to have possible impacts on cCRT-ICB^{214,215}, but they were not usually reported in studies with 2-year outcomes. Greater availability of individual patient level data, and detailed collection and reporting of clinical parameters in current trials, will increase the precision of such analyses aiming to identify tumour-specific biomarkers and treatment strategies that maximise individual patient benefit.

4.6 Conclusion

The estimated gain in OS from ICB was significantly positively associated with the fraction of patients with tumour PDL1 $\geq 1\%$, the fraction with stage IIIB/C disease and the planned duration of ICB. The fitted increase in OS gain achieved by giving ICB for two years rather than one was considerable but had a wide 95% CI and was driven by data from a single study of 2-year ICB duration. Further investigation into ICB duration may be warranted, though, given some similar data in the advanced disease setting (*CheckMate 153*). The OS gain from ICB was significantly negatively associated with patient age but was not associated with radiation prescribed dose, radiation duration or whether immune treatment began concurrently with CRT. In summary, this analysis suggests that survival following cCRT-ICB may be further increased by prolonging administration of ICB beyond one year, and that gains in survival due to ICB are greater in younger patients and those with tumour PDL1 $\geq 1\%$ or more advanced disease.

Chapter 5. Survival following immuno-chemo-radiotherapy of LA-NSCLC: exploration of variation with dose and treatment duration across an extended range

5.0 Chapter overview

This chapter –

- Predicts overall survival (OS) for chemoradiotherapy and immuno-chemo-radiotherapy treatments of locally-advanced non-small cell lung cancer.
- Explores the OS within and beyond the ranges of radiation dose and fractionations found in the datasets fitted. Bootstrapped confidence intervals were used to judge the precision of the predictions, since the uncertainties outside the range of fitted values may be large.

5.1 Computational modelling of immunotherapy effects on radiation therapy

Immune checkpoint blockade (ICB) has contributed to significantly improved overall survival (OS) for locally-advanced non-small cell lung cancer (LA-NSCLC)^{71,72}. However, questions remain unanswered across different perspectives, such as the interaction with chemotherapy/radiotherapy and best ICB delivery

schedules. Computational modelling allows the investigation of schedules and treatment responses for the ICB-radiotherapy combination.

In Chapter 4, I empirically analysed the effects of ICB on chemoradiotherapy outcomes. In this chapter, I extend the simple modelling that I used in that analysis, to predict outcomes across ranges of doses, doses-per-fractions, and treatment duration.

Several mechanistic bottom-up models have been devised to describe the dynamics of the interactions between the anti-tumour immune system, tumour microenvironment and compartmental drug distribution of ICB monotherapy¹⁸⁶. Serre et al.²¹⁶ first proposed the concepts of modelling ICB-radiotherapy. They simplified the complicated anti-tumour dynamics into three compartments – tumour, doomed tumour, and lymphocytes. The model used equations describing radiation cancer-killing, ICB-induced primary (tumour-killing) immune response, ICB-induced secondary (memory) immune response, and radiation-induced secondary immune response. This model accounted for those doomed tumours that had become antigen debris and been recognised by the immune system. Although it was just a conceptual model focusing on tumour size changes, it established some fundamentals of mathematical modelling of ICB-radiotherapy.

Relatedly but based on different perspectives, Kosinsky et al.²¹⁷ added the radiation effects on standard pharmaco-kinetic models. Radiation-induced cell death was described as liberating tumour antigen which systemically circulate, contributing to ICB anti-tumour response. Recently, Gonzalez-Crespo et al.²⁰⁶ chose standard linear-quadratic (LQ) radiation survival equations as the base to incorporate ICB effects, in particular, modelling the biological delay between radiation cell-killing, antigen activation of immune cells, and further tumour cell killing by the activated immune cells. The model suggested that the effectiveness of combined treatment may be reduced if the administration of ICB is delayed beyond two days post-start of radiotherapy. However, these models were all fitted

using animal data, representing the conditions some way from the clinic. None of them had modelled clinical treatment outcomes using either OS or progression-free survival (PFS), leaving a large gap between the pre-clinical models and their implication in clinics.

Regarding data-driven top-down models, a few studies have developed the simpler mathematical descriptions of the pharmaco-kinetics of ICB monotherapy and checked them against pre-clinical and clinical outcomes from treatments using single anti-PD-1 drug, pembrolizumab^{218–220}. These models varied between studies, so further validation is needed before interpreting them confidently.

When I started this research, there were no clinical data-driven models for ICB-radiotherapy, and only a limited number of pre-clinical mechanistic models had been published. The randomised phase III *PACIFIC* study has shown a significant and substantial improvement in survival for LA-NSCLC following concurrent chemoradiotherapy (cCRT)-ICB versus cCRT alone^{72,221}. Such outcomes suggest there may be underlying ‘head room’ to optimise radiation dose fractionation, such as radiation dose de-escalation. Therefore, I aimed to model how LA-NSCLC OS might change as radiotherapy dose, fractionations, and duration are varied by extending the largely empirical models I have previously developed¹⁸⁷.

In this chapter, I build a hypothesis-generating model to –

- 1) Predict the OS of cCRT-ICB given ranges of radiation dose, fractions, treatment durations.
- 2) Predict the OS of sequential chemoradiotherapy (sCRT)-ICB, which has not broadly been tested in the clinic.

In Chapter 4, I analysed the ICB effect empirically as an additional percentage change in OS. That worked fine when analysing observations across the dataset studied. However, the approach might ultimately prove problematic when

exploring a wide range of dose fractionations because logically, if the radiation dose is sufficiently escalated it alone could kill off all tumours entirely, reducing the OS gain from ICB to nothing. Therefore, in this chapter I reframe the model, hypothesising that the ICB gain can be quantified as an effective increase in radiation dose (unit: Gy) rather than a % increase in OS. This approach is described further in the methods.

The benefits of cCRT-ICB over cCRT alone are potentially derived from ICB's effects on both metastases⁷² and primary tumours²²². In the modelling of this chapter, I focused on the tumour effects for reasons discussed below. In Chapter 4, I found no evidence of interactions between radiotherapy and immune effects (i.e. 'OS gain' did not depend on the radiation dose or duration). Therefore, in this chapter, I assumed that ICB makes a purely additive contribution to cCRT tumour control.

5.2 Materials and methodology

5.2.1 Retrospective data

This study used two independent datasets with published clinical trials – cCRT-ICB and CRT datasets. Both datasets were introduced and used in previous chapters. The fitted datasets were the same as in Chapter 4.

5.2.2 Dose-response models

Outcome models were fitted using 2-year OS as the endpoint analysed. The two datasets were fitted together. The ICB contribution to OS gain was quantified as a fixed increase in the equivalent dose per-2-Gy fraction (EQD2) on tumour control in the CRT-ICB model.

CRT model (Model 5, Chapter 3)¹⁸⁷

The baseline CRT model was clearly described in Chapter 3. Equations 5.1 to 5.4 are the same as in the earlier work and included for completeness. Normal tissue complication (NTCP) has been renamed as survival-limiting toxicity (SLT) following the publication of Chapter 3.

$$TCP_{S_i} = \Phi \left[\frac{EQD2_{tum} - EQD2_{tum50}(S_i)}{m \times EQD2_{tum50}(S_i)} \right] \times 100\% \quad \text{--- Equation 5.1}$$

$$SLT_{S_i} = F_{SLT,i} \times \Phi \left[\frac{EQD2_{SLT} - EQD2_{SLT50}}{m_{SLT} \times EQD2_{SLT50}} \right] \times 100\% \quad \text{--- Equation 5.2}$$

$$OS = \sum_i f_i \times TCP_{S_i} \times (1 - SLT_{S_i}) \times Max_{chemo} \times Tech_{improved} \quad \text{--- Equation 5.3}$$

$$Tech_{improved} = (1 - R \times (2022 - Study\ Published\ Year)) \quad \text{--- Equation 5.4}$$

CRT-ICB model

In this chapter, I slightly adjusted the CRT-ICB model to account for ICB by adding a dose-equivalent parameter $D_{eff,immune}$ rather than a percent increase in survival. ICB leads to the death of cells in both the primary tumour and metastases, and I chose to model its effects on primary tumour control. Consequently, $EQD2_{tum}$ was modified by adding a parameter $D_{eff,immune}$, describing the overall effects in cohorts treated with ICB as

$$EQD2_{tum} = EQD2_{tum} + D_{eff,immune} \quad \text{--- Equation 5.5}$$

Any contribution to OS provided by improved metastatic control could be quantified as a systemic effect similar to that of chemotherapy, and represented in the model by splitting the Max_{chemo} term into the current two parameters respectively describing the maximum OS rates following radiotherapy alone and cCRT that would be seen if these treatments kill all primary tumours, plus an

additional third parameter describing the same rate for cCRT-ICB. In the interests of model simplicity, I chose to include only one parameter, $D_{eff,immune}$, rather than both $D_{eff,immune}$ and $Max_{chemo-ICB}$.

Regarding LA-NSCLC, Abe et al. found out that cCRT-ICB significantly improved one-year local control compared to cCRT alone (86% vs 62%, $p=0.005$), where their patients received following-up computed tomography (CT) every 2 to 3 months for evaluating local control²²². This supported my focus of ICB's benefits on tumour control. In addition, modelling ICB as $D_{eff,immune}$ allowed clear understanding of predicting OS given various radiation fractionation schedules.

In principle, ICB could further impact OS by increasing survival-limiting toxicity rates. However, in a pooled meta-analysis, no increase in radiation-related adverse effects were seen when ICB was added within 90 days of radiotherapy²²³. Therefore, it seems reasonable to leave the toxicity term unchanged from the baseline CRT model.

After fitting the modified model, I explored how predicted OS would vary with different radiation doses, fractionations, treatment durations and chemotherapy schedules (cCRT vs sCRT). Clinical studies of radiotherapy for LA-NSCLC have often explored schedules based on standard fractionation, 2Gy-per-fraction, five days a week. Additionally, schedules delivering 30 fractions in six weeks and 20 fractions in four weeks are also of interest (see Chapters 2 and 3). Consequently, these are the schedules studied in this chapter.

5.2.3 Statistical analysis

RStudio (version 2022.02.3) was used, with *bbmle* package¹³⁰ for maximum likelihood fitting and *ggplot2* package¹⁵⁶ for visualisation of dose-response curves. Uncertainties of fitted parameters were estimated using multi-dimensional profile-

likelihood 95% confidence intervals (CI)¹⁵⁷. Two-sided significance was reported for a likelihood ratio test comparing the efficacies of two models.

Stratified blocked bootstrapping (1000x) was used to robustly estimate the uncertainties on predicted 2-year OS levels predicted by the model fit, across ranges of radiation dose, treatment durations and fractions. In this approach, the cCRT-ICB and CRT datasets were bootstrapped independently, resampling the cohorts comprising each dataset with replacement. Pairs of the resampled cCRT-ICB and CRT datasets were combined to form bootstrapped datasets and the model was repeatedly refitted to 1000 of these bootstrapped datasets. For all the doses, doses-per-fraction and treatment durations of interest, I then determined 95% CIs on OS as ranges between the 2.5% and 97.5% percentiles of the bootstrapped OS distribution.

5.3 Results

5.3.1 Modelling fits of ICB effects

As expected from clinical results and the analysis of Chapter 4, the improved outcomes achieved by cCRT-ICB caused the CRT model to be outperformed by the CRT-ICB model, which included an additional effective dose contributed by the ICB treatment ($p=0.006$). The overall effects of ICB accounted for 13.5Gy (parameter $D_{eff,immune}$, 95% CI: 0.3, infinite) of EQD2 dose on tumour control (Table 5.1).

I further tried splitting the $D_{eff,immune}$ factor to have different values for cohorts starting ICB concurrently with vs sequentially after cCRT, but without achieving a significant improvement in the model fit ($p=0.708$). Consequently, the model used to predict the OS values plotted in the rest of the chapter included a single common value of $D_{eff,immune}$.

Table 5.1 Outcome modelling results. Fits of CRT and CRT-ICB models, including degrees of freedom (df) in fitting, fitted parameters (with 95% profile-likelihood CIs), log-likelihood values, AIC and likelihood ratio test.

| Parameters | CRT model (df = 42) | CRT-ICB model (df = 41) |
|-----------------------------------|--|--|
| λ (Gy/day) | <i>RT & sCRT</i> : 0.29 (0.22, 0.43) <i>cCRT</i> : 1.07 (0.70, 2.41) | <i>RT & sCRT</i> : 0.31 (0.22, 0.44) <i>cCRT</i> : 1.06 (0.74, 2.19) |
| T_k (days) | <i>RT & sCRT</i> : 17 (16 [†] , 27) <i>cCRT</i> : 39 (22, 43) | <i>RT & sCRT</i> : 17 (16 [†] , 25) <i>cCRT</i> : 19 (16 [†] , 40) |
| α/β (Gy) | <i>S_{III}</i> : 10.0 (1.2, infinite) <i>S_{III A}</i> : 32.3 (14.1, infinite) <i>S_{III B/C}</i> : 0.4 (0.0, 0.8) | <i>S_{III}</i> : 10.1 (1.5, infinite) <i>S_{III A}</i> : 39.0 (16.6, infinite) <i>S_{III B/C}</i> : 0.6 (-0.1, 1.0) |
| $EQD2_{tum50}$ (Gy) ^{††} | <i>S_{III}</i> : 55 (48, 58) <i>S_{III A}</i> : 55 (49, 58) <i>S_{III B/C}</i> : 55 (49, 58) | <i>S_{III}</i> : 55 (47, 58) <i>S_{III A}</i> : 55 (47, 58) <i>S_{III B/C}</i> : 55 (47, 58) |
| m | 0.14 (0.09, 0.22) | 0.15 (0.13, 0.25) |
| Max_{chemo} (%) | 92 (85 [†] , 100 [†]) | 93 (85 [†] , 100 [†]) |
| RS^{cCRT} | 1.07 (1.03, 1.34) | 1.40 (1.03, 1.40 [†]) |
| $EQD2_{SLT50}$ (Gy) | 64 (50, 105) | 61 (52, 112) |
| m_{SLT} | 0.16 (0.11, 0.75) | 0.25 (0.18, 0.76) |
| R (per year) | 0.016 (0.012, 0.021) | 0.013 (0.008, 0.017) |
| F_{SLT} ^{††} | <i>S_{III}</i> : 0.20 (0 [†] , 0.58) <i>S_{III A}</i> : 0.39 (0.19, 0.80) <i>S_{III B/C}</i> : 0.48 (0.31, 1 [†]) | <i>S_{III}</i> : 0.27 (0.10, 0.80) <i>S_{III A}</i> : 0.45 (0.21, 1 [†]) <i>S_{III B/C}</i> : 0.55 (0.33, 1 [†]) |
| $D_{eff,immune}$ (Gy) | - | 13.5 (0.3, infinite) |
| log-likelihood | -4247.6 | -4243.8 |
| AIC score | 8537.2 | 8527.6 |

| | | |
|-----------------------|-----------|-----------|
| Likelihood ratio test | reference | p = 0.006 |
|-----------------------|-----------|-----------|

† The profile-likelihood CIs were truncated at the lower or upper boundary of the range explored.

†† Fitted values of $EQD2_{tum50}$ and F_{SLT} were constrained as stage IIIB/C values \geq IIIA \geq II/I.

Parameters: λ , dose-per-day repopulated; T_k , repopulation kick-off time; α/β , tumour fractionation dependence; $EQD2_{tum50}$, EQD2 required to achieve 50% tumour control; m , tumour dose-response gradient; Max_{chemo} , maximum overall survival for chemoradiotherapy; RS^{cCRT} , radiosensitisation of dose-effects by cCRT; $EQD2_{SLT50}$, EQD2 causing a 50% modelled survival-limiting toxicity rate; m_{SLT} , survival-limiting toxicity response gradient; R , variation of the 2-year OS with study publication year; F_{SLT} , survival-limiting toxicity weighting for stage S_i ; $D_{eff,immune}$, ICB effects on tumour control.

5.3.2 Overall survival prediction with different radiation fractionation schedules, chemotherapy schedules and ICB

Modelled 2-year OS rates for immuno-chemo-radiotherapy giving 50 to 74Gy prescribed doses are plotted in Fig. 5.1 (cCRT-ICB) and 5.2 (sCRT-ICB) for three fractionation schemes. The corresponding highest OS levels for each fractionation scheme given different doses-per-fraction are listed in Table 5.2 (cCRT-ICB) and 5.3 (sCRT-ICB).

The best modelled treatment outcomes were achieved using cCRT-ICB, reaching 71% (95% CI: 62%, 84%) and 73% (95% CI: 55%, 90%) for stage IIIA and IIIB/C, respectively. For stage IIIB/C, the four-week schedules gave the best OS. However, there was not really any significant indication that four weeks is better since the CIs of the best OS for each schedule extensively overlapped. Compared to cCRT alone, there was around a 10% increase in modelled OS for cCRT-ICB under standard 2Gy-per-fraction, consistent with the ICB-induced OS gain I quantified in Chapter 4. For standard 2Gy-per-fraction, 60Gy provided the best modelled OS for cCRT-ICB, and both escalation and de-escalation of dose from this point reduced the modelled OS.

The results for dose ranges <58Gy in 2Gy-per-fraction and six weeks and <55Gy or >65Gy for four-week schedules are greyed out. In these regions, the CIs on OS were wide as only relatively few fitted data points lay within them (see Figure 5.3 below). As dose was increased to 65Gy given in standard 2Gy fractions, modelled OS rates for cCRT alone remained steady for standard 2Gy fractionation and rose progressively for six-week schedules. However, for cCRT-ICB, 2-year OS dropped by around 0.5 to 1% for each 1Gy of prescribed dose increases beyond 60Gy, regardless of fractionation schedules.

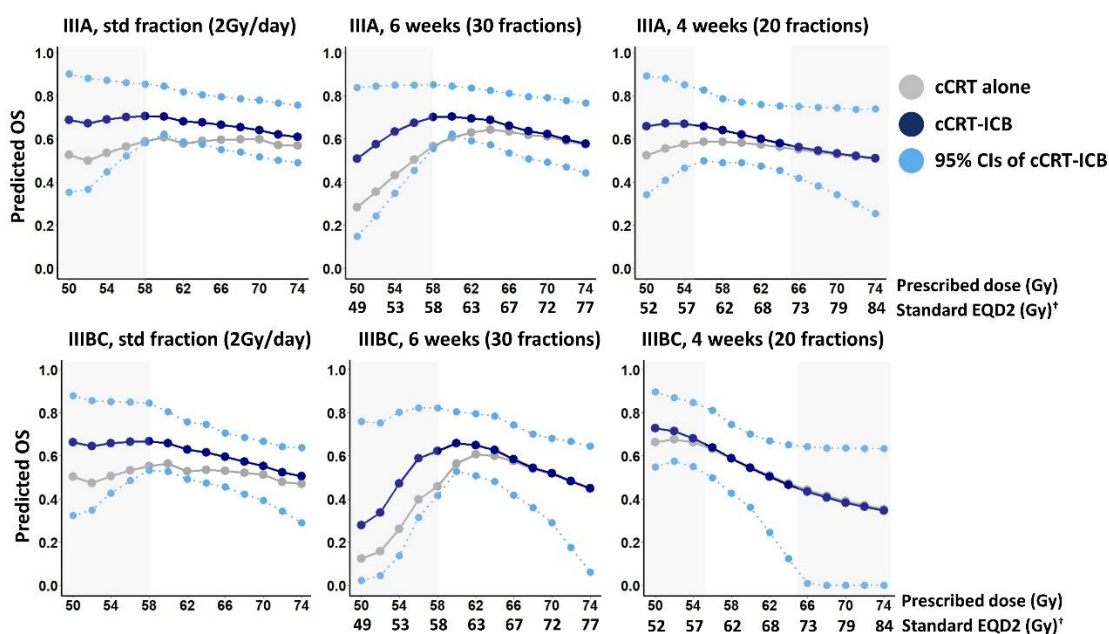


Figure 5.1 Predicted 2-year OS rates for cCRT-ICB and cCRT alone, plotted for three radiation fractionation schemes. The predicted OS with prescribed dose <58Gy and ‘<55Gy/>65Gy for four weeks’ are greyed out due to limited fitted data in these regions and corresponding higher OS uncertainty. [†]Standard EQD2 was a rough estimation for clinical comparison. It was calculated by taking prescribed dose, assuming all dose ranges given in 2Gy-per-fraction, with a radiosensitivity value α/β of 10, and no repopulation effects.

Table 5.2 Best 2-year OS rates for different radiation dose-fractionation schedules, in treatments giving cCRT alone or cCRT-ICB. Bootstrapped 95% CIs on OS are also shown.

| | cCRT alone | | | cCRT-ICB | | |
|--|----------------------|----------------------|----------------------|----------------------|----------------------|----------------------|
| | Std 2Gy/Fx | 6 weeks | 4 weeks | Std 2Gy/Fx | 6 weeks | 4 weeks |
| Stage IIIA | | | | | | |
| Prescribed dose | 60Gy | 64Gy | 58Gy | 58Gy | 60Gy | 52Gy |
| Best 2-year OS (Bootstrap 95% CIs) | 61% (46%, 80%) | 64% (52%, 78%) | 59% (37%, 78%) | 71% (62%, 84%) | 70% (62%, 84%) | 67% (41%, 88%) |
| Stage IIIB/C | | | | | | |
| Prescribed dose | 60Gy | 62Gy | 52Gy | 58Gy | 60Gy | 50Gy |
| Best 2-year OS (Bootstrap 95% CIs) | 56% (41%, 76%) | 61% (41%, 76%) | 68% (46%, 86%) | 67% (53%, 84%) | 66% (53%, 81%) | 73% (55%, 90%) |

I have also modelled 2-year OS for sCRT-ICB even though our dataset included no results for cohorts treated using sCRT-ICB. The best modelled OS levels for sCRT alone appeared above 68Gy, reaching 55 to 60% using standard 2Gy-per-fraction. This reflected the lower fitted repopulation rate for sCRT (0.31 vs 1.06 Gy/day for cCRT; Table 5.1), meaning that dose-escalation with schedule protraction was more effective for sCRT.

For sCRT-ICB, the best modelled OS rate for stage IIIA was achieved by giving 70Gy, either in 2Gy-per-fraction or over six weeks; whereas for IIIB/C, the best modelled OS rate was seen at 52Gy in four weeks. Again, however, the CIs of the best OS rates for the four-week and 2Gy-per-fraction schedules were wide and heavily overlapping. Nonetheless, the best modelled OS rates for sCRT-ICB were 59% for IIIA and 66% for IIIB/C, compared to 53% for IIIA and 60% for IIIB/C when treated using sCRT alone, suggesting that sCRT-ICB would be a useful treatment option for patients unfit for cCRT. It should be remembered, though, that

the data to which the models were fitted did not include any sCRT-ICB cohorts, and therefore the OS rates predicted for these treatments will reflect the structure of the fitted model, as well as the data fitted for sCRT alone in comparison to cCRT and cCRT-ICB.

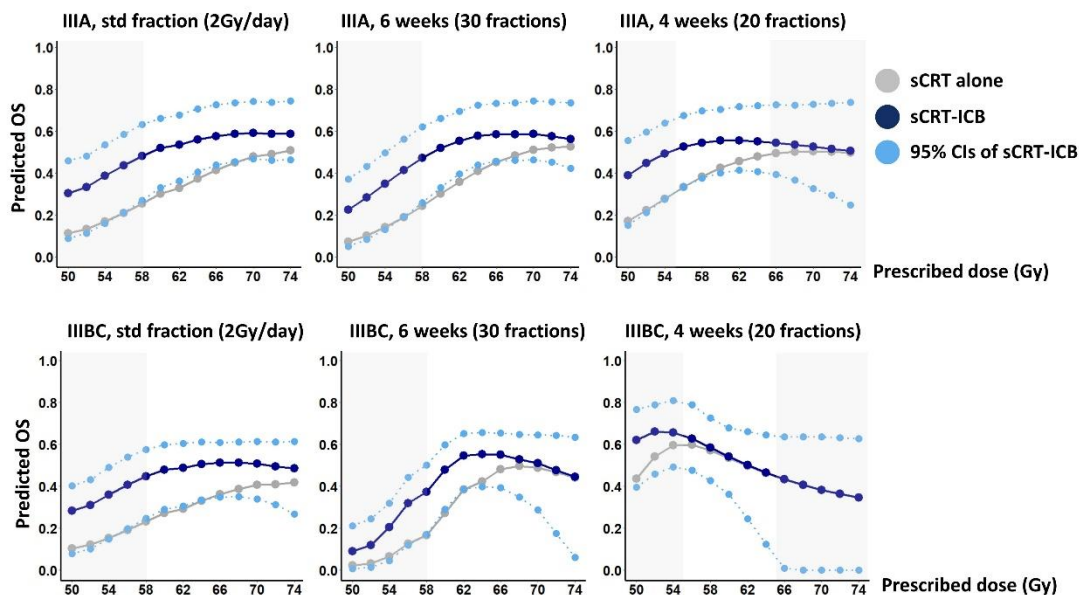


Figure 5.2 Predicted 2-year OS for sCRT-ICB and sCRT alone, delivered using three fractionation schemes.

Table 5.3 Best 2-year OS rates for different radiation dose-fractionation schedules, in treatments giving sCRT alone or sCRT-ICB. Bootstrapped 95% CIs on OS are also shown.

| | sCRT alone | | | sCRT-ICB | | |
|--|----------------------|----------------------|----------------------|----------------------|----------------------|----------------------|
| | Std 2Gy/Fx | 6 weeks | 4 weeks | Std 2Gy/Fx | 6 weeks | 4 weeks |
| Stage IIIA | | | | | | |
| Prescribed dose | 74Gy | 74Gy | 70Gy | 70Gy | 70Gy | 62Gy |
| Best 2-year OS (Bootstrap 95% CIs) | 51% (36%, 65%) | 53% (37%, 70%) | 50% (30%, 71%) | 59% (46%, 74%) | 59% (46%, 74%) | 56% (41%, 72%) |

| Stage IIIB/C | | | | | | |
|--|----------------------|----------------------|----------------------|----------------------|----------------------|----------------------|
| Prescribed dose | 74Gy | 68Gy | 56Gy | 66Gy | 64Gy | 52Gy |
| Best 2-year OS (Bootstrap 95% CIs) | 42% (23%, 55%) | 50% (32%, 61%) | 60% (41%, 74%) | 51% (35%, 61%) | 55% (40%, 66%) | 66% (46%, 79%) |

5.3.3 For which radiotherapy doses and durations are the modelled OS rates most likely to be reliable?

Fig. 5.3 (A) shows the prescribed dose and treatment duration ranges for the cohorts in the fitted CRT and cCRT-ICB datasets, with treatment type annotated. In Fig. 5.3 (B) I have plotted the doses and treatment durations for which OS rates were calculated from the fitted model, and shaded them red, blue, or green according to the fractionation schemes to which they belong. Fig 5.3 (C) merges these plots, providing an intuitive picture of how the ranges and durations of schedules for which modelled OS rates were calculated compare to the data underpinning the model used. Many cohorts were treated using standard 2Gy-per-fraction schedules, some were treated in six weeks, and a few in shorter times. For schedules delivered in six weeks or more, prescribed doses were ≥ 60 Gy; while for shorter schedules, they were between 55 and 65Gy. Thus, OS predictions for doses outside these ranges should be viewed as tentative.

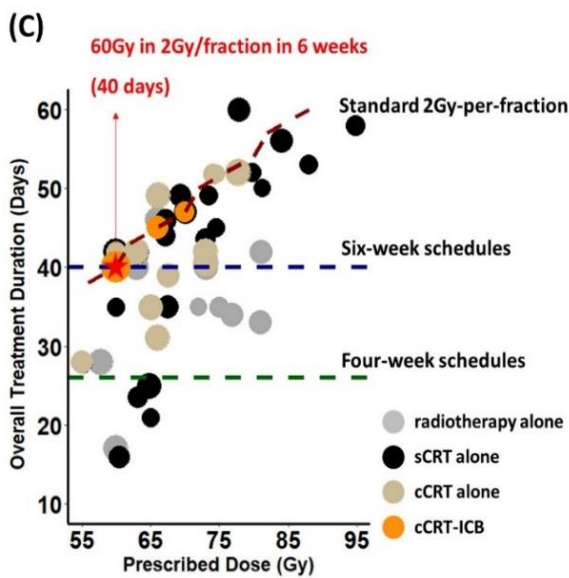
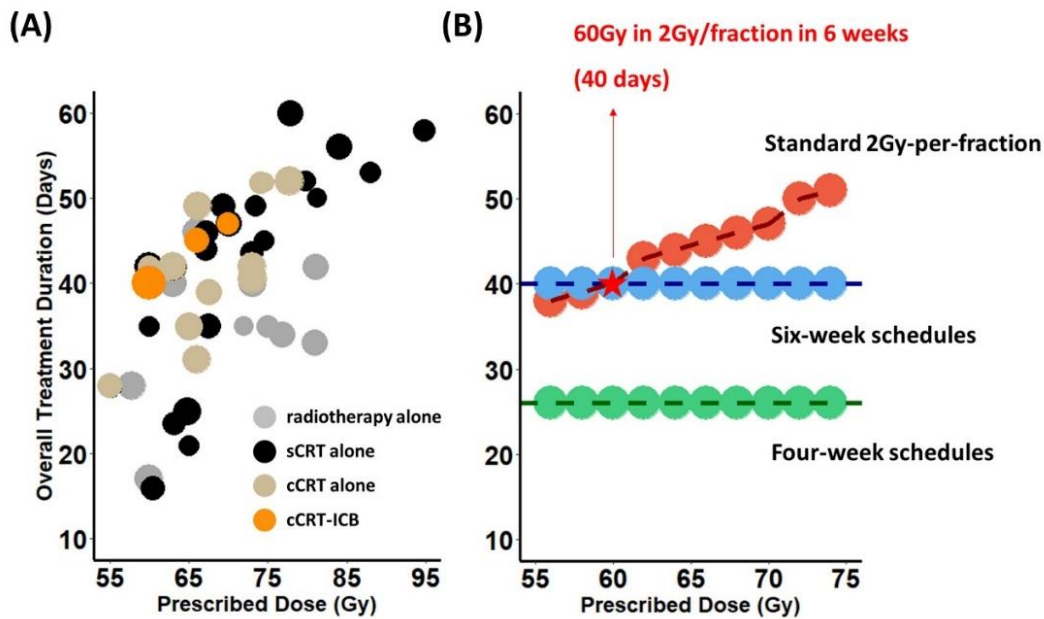


Figure 5.3 Scatter plots describing radiotherapy schedules in the datasets. (A) A scatter plot of the doses and durations of the schedules used to treat patients in the datasets; (B) A scatter plot of all the doses and durations of schedules for which the OS levels show in Figures 5.1 and 5.2 were calculated using the models; (C) A plot shows how the fitted data line up with the schedules that the predicted OS was modelled.

5.4 Discussion

The success of the cCRT-ICB combination in *PACIFIC*^{71,72} has changed the standard of care for inoperable LA-NSCLC. However, many questions remain unanswered. I aimed to answer two here –

- 1) How should radiation fractionation schedules be selected for cCRT-ICB and sCRT-ICB to achieve the best survival rates possible?
- 2) What are the best modelled OS rates achieved by cCRT-ICB and sCRT-ICB?

To my knowledge, this is the first study focusing on dose-response modelling for immuno-chemo-radiotherapy. One key finding is that the 2-year OS rate from cCRT-ICB is unlikely to be improved by escalating or de-escalating from 60Gy in 2Gy-per-fraction for which modelled OS rates were 70% and 66% for stage IIIA and IIIB/C, respectively. Another is that sCRT-ICB might be a good alternative for patients who are not fit for cCRT, achieving a best modelled OS rate of 59% for IIIA and 66% for IIIB/C.

5.4.1 Chemo-radiotherapy schedules with the addition of ICB

Modelled 2-year OS rate for cCRT rose when dose was escalated from 50 to 60Gy, given in standard 2Gy-per-fraction or six weeks, regardless of ICB. However, there was no OS gain following the radiation dose escalation of cCRT-ICB above 60Gy. Although no ICB cohorts were actually treated using 50 to 60Gy, the modelled outcomes align with results from the *RTOG-7301* study of radiotherapy alone reported in 1980s. This study compared doses of 40, 50, and 60Gy given in 2Gy-per-fraction and reported median times to treatment failure of 8, 12, and 19 months at these dose levels^{48,224}.

Since modelled OS rates for cCRT-ICB do not fall very rapidly as doses are reduced below 60Gy in 2Gy-per-fraction, treatments giving 55Gy might be useful for patients in whom critical OARs receive high radiation doses, as they would reduce toxicity with only 2% modelled reduction in OS (Fig. 5.1).

In the randomised phase III *GEMSTONE-301* study¹⁹⁷, sub-analyses of sCRT (4% patients; HR: 0.59, 95% CI: 0.39, 0.91) and cCRT (96% patients, HR: 0.66, 95% CI: 0.44, 0.99) showed positive impacts of ICB on PFS for both treatments. This partially supports the prediction of our models which show increased OS for sCRT-ICB versus sCRT alone. These considerations suggest that sCRT-ICB treatments should be trialled in UK clinics, since 55% of stage III NSCLC patients treated with curative radiation doses are given sCRT²²⁵.

5.4.2 Modelling methodology

There were some differences between fitted parameters of the CRT and CRT-ICB models. For example, tumour repopulation for cCRT starts at day 39 (95% CI: 22, 43) in the fitted CRT model but at day 19 (95% CI: 16, 40) in the CRT-ICB model. Some underlying differences between the CRT and cCRT-ICB datasets may lie behind the differences in fitted parameter values. A greater dose-response might be seen in cCRT-ICB treatment, which would favour an increased radiosensitisation parameter (RS^{cCRT}) offset by greater repopulation losses resulting from earlier start time. Over the ranges of radiotherapy doses and durations fitted, these differences in parameter values will offset each other to some degree, introducing only small net changes in modelled OS rate. They may, however, have greater effects on OS rates predicted for dose schedules lying outside the fitted dataset. Consequently, in plots of modelled OS rates, I have greyed out dose ranges in which limited data were available for fitting.

A single time point (two-year) was used as the modelled OS endpoint. Arguably, datasets with multiple time points would provide more detail regarding OS, but limited published clinical data is available.

For CRT-ICB cohorts, all fitted data correspond to prescribed doses of 60 to 70Gy, given concurrently with chemotherapy, similar to the *PACIFIC* protocols. Thus, the CIs on modelled OS rates for treatments giving ICB are quite wide at dose levels below and above the 60-70Gy range. More generally, predictions for doses <58Gy given in 2Gy-per-fraction or in six weeks, and <55Gy or >65Gy given in four weeks should be viewed more as a best guess than a reliable indicator, since the fitted datasets included no treatments giving doses in these ranges.

5.5 Conclusion

No gains were made in modelled OS rates for cCRT-ICB, by either escalating or de-escalating from the standard 60Gy in 2Gy-per-fraction treatment. Nevertheless, the reduction in modelled OS for cCRT-ICB when radiation dose was decreased from 60Gy to 55Gy, given in 2Gy-per-fraction, was only 2%, potentially making modest dose de-escalation a useful option for patients with heavily irradiated OARs.

The best modelled OS rate for sCRT-ICB is 6% higher than for sCRT alone, raising the question of whether sCRT-ICB should be used to treat the 55% of UK LA-NSCLC patients who currently receive sCRT alone. It should be noted, though, that the modelled gain from ICB is simply a reflection of the gain seen clinically for ICB combined with cCRT, together with the structure of the fitted model which does not distinguish between the effective dose contribution of ICB in sCRT and cCRT treatments. Consequently, the modelled increase in OS when ICB is added to sCRT should be viewed with some caution.

In the future, outcomes modelling of CRT-ICB treatments would benefit from the collation and analysis of data for individual patients rather than cohort averages. This would better allow modelled predictions to be used in the design of stratified or personalised treatments.

Chapter 6. Cardiac-sparing optimisation for LA-NSCLC radiotherapy

6.0 Chapter overview

This chapter –

- Is exploratory research, investigating the effects of cardiac-sparing on overall survival (OS) and survival-limiting toxicities; specifically, how modelled OS might change if the mean heart dose was varied relative to the prescribed dose.
- Compares the effects of ‘proton’ versus ‘optimised photon’ cardiac-sparing treatment, both against regular photon treatment (not optimised to spare the heart).
- Determines whether the effect of cardiac-sparing on OS varies substantially with tumour location.
- Quantifies modelled rates of 2-year OS achievable for locally-advanced non-small cell lung cancer using (immuno)-chemoradiotherapy with different cardiac-sparing techniques.

6.1 Cardiac toxicity in LA-NSCLC

Cardiac irradiation during radiotherapy for locally-advanced non-small cell lung cancers (LA-NSCLC) is an increasing concern. Both heart V_5 (volume receiving $\geq 5\text{Gy}$) and V_{30} (volume receiving $\geq 30\text{Gy}$) have been reported as independent predictors for poorer overall survival (OS) in the phase III randomised

dose-escalation study *RTOG-0617*⁵⁴. Existing dose constraints are based on the Quantitative Analyses of Normal Tissue Effects in the Clinic (QUANTEC)⁹⁹. However, those are old and easily made, and in practice, heart doses can often be reduced substantially below these levels without substantially raising doses to other structures. Additionally, new evidence has been emerging, suggesting that doses delivered to some cardiac substructures may be of particular importance¹⁰⁰.

Across studies, no consistent picture has yet emerged of which dose levels and substructures might be particularly critical. A review of thoracic radiotherapy listed studies that identified various factors associated with poor OS¹⁰⁰:

- 1) > 8.5Gy of mean heart dose (MHD),
- 2) > 19.5Gy of maximum dose to the right atrium, aortic valve, and right coronary artery,
- 3) > 2.2% of left atrium wall receiving > 63Gy,
- 4) > 80% of heart receiving dose > 40Gy ($V_{40} > 80\%$),
- 5) > 29% of the pericardial region receiving dose > 30Gy ($V_{30} > 29\%$).

Additionally, several associations between cardiac dose and cardiac events have been reported in this review. The dose to the superior vena cava has been found to be associated with the electro-cardiogram signal changes. And the dose to ventricles on both sides and the left anterior descending aorta was associated with cardiac events.

Most currently published studies with cardiac dosimetric analyses were for photon-based radiotherapy. Theoretically, proton beam therapy, given its lack of exit dose, might reduce radiation exposure to organs at risk (OARs) such as the heart⁴⁶. Planning studies have shown that protons provide good tumour coverage, together with sparing of the lung in treatment of LA-NSCLC^{226,227}. However, such advantages have not been fully seen in the clinic yet, as the only published

randomised study comparing photon (N=92) and proton (N=57) LA-NSCLC treatment reported improvements in dose-volume indices for the heart ($p=0.002$) but not for lung ($p=0.818$) or oesophagus ($p=0.717$)⁴⁷. Relatedly, rates of grade ≥ 3 radiation pneumonitis (the primary endpoint) were similar in the photon and proton arms of this study.

In previous chapters, I have analysed OS using a model that comprised terms describing tumour control and survival-limiting toxicity (SLT) rates. In this chapter, I have extended the models to estimate how OS might change if heart doses in treatment plans were reduced. Specifically, several studies have reported associations between OS and MHD, quantifying these as hazard ratios (HR) for death per 1Gy increase in MHD. I therefore hypothesised the OS did indeed depend on MHD, but that the tumour control rate depended only on tumour dose, not the heart dose. Accordingly, I developed a procedure for translating the HR for death (HR_{OS}) into a HR for SLT (HR_{SLT}), as described in detail in Section 6.2. Then working from the published literature, I estimated the reductions in average MHDs in patients that could be achieved using protons or optimised photons treatment planning. By combining these reductions with HR_{SLT} per 1Gy change in MHD, I estimated the resulting OS changes.

This modelling analysis was carried out for concurrent chemoradiotherapy (cCRT) alone and for cCRT with immune checkpoint blockade (ICB). Additionally, I investigated whether reductions in MHD varied with tumour location, and carried out further analyses to estimate any resulting dependence of OS levels in ‘proton’ and ‘optimised photon’ treatments on tumour site.

6.2 Tabulation of cardiac dosimetry and hazard, and modelling the effect on OS

6.2.1 Dosimetric indices

For photon radiotherapy, cardiac dose indices were taken from a planning study carried out at Liverpool Clatterbridge Cancer Centre between 2016 and 2017¹⁰⁸. In the study, plans were created for 20 LA-NSCLC patients, giving cCRT in 63 to 73Gy in 30 fractions. Having initially planned the patients following the standard *IDEAL-CRT* isotoxic protocol^{83,228}, the investigators studied how much heart doses could be reduced without exceeding doses to other OARs or compromising planning tumour volume (PTV) coverage.

In the Liverpool study, initial treatment planning was done using the volumetric arc therapy (VMAT) technique. Plans were reoptimised to prioritise the cardiac dose reduction. Among the 20 patients studied, 7 had ‘T7’ tumours, which overlapped or lay below the 7th thoracic vertebra (T7). These received greater cardiac doses as their superior-inferior locations overlapped the heart. The treatment reoptimisation was executed with the requirement that the following tumour coverage constraints were met: $D_{PTV-90\%} > 95\%$ of prescribed dose; $D_{PTV-98\%} > 90\%$ of prescribed dose. Thus, the study provided the cardiac dose indices for ‘standard photon’ and ‘optimised photon’ using optimised planning regulations.

For proton beam therapy, dosimetric indices were taken from a published study carried out at Oxford Cancer Centre¹⁰⁹. In twenty patients with stage III NSCLC, the study determined how much heart doses could be reduced using proton rather than photon treatments, and whether the reductions depend on tumour location. Therefore, both intensity-modulated proton therapy (IMPT) and photon VMAT plans were created for each patient. As will be seen, the MHDs of photon plans in the Oxford study were very similar to those of reoptimised photon

plans in the Liverpool study. Since the Oxford study investigated potential gains from expensive proton treatment, it would have made no sense to compare these to unoptimised photon plans. Thus, this study presumably provided cardiac dose indices for protons and optimised photons, but I only use the proton data in this chapter because the photon data was similar to that in the Liverpool study.

In the Oxford treatment plans, a prescribed dose of 70Gy was given in 35 fractions. A relative biological effectiveness (RBE) of 1.1 was used for IMPT. Planning including tumour target, OAR delineation, and dose constraints following protocol for *RTOG-1308*, the ongoing clinical study comparing proton and photon cCRT for LA-NSCLC⁴⁵. Specifically, for VMAT treatment, the internal target volume (ITV) was expanded by 8mm to form the clinical target volume (CTV); and by a further 5mm to form the PTV. For IMPT, 99% of the CTV was covered by the prescribed dose as there was no PTV for proton.

The average MHD of standard photon treatments for all patients in the Liverpool study was considered to represent the typical clinical situation. Consequently, it was used as a baseline against which MHDs tabulated for other types of treatment plan and for selected groups of patients were compared. Tables 6.1 and 6.2 summarise these MHDs for proton and optimised and standard photon plans, and for overall, T7, and non-T7 tumour groups.

Table 6.1 Summary of retrospective dosimetric studies used in Chapter 6.

Cardiac dose indices for standard and optimised photon plans were taken from the Liverpool study¹⁰⁸, while indices for proton plans were taken from the Oxford study¹⁰⁹.

| | Liverpool study | Oxford study |
|---------------|--|--|
| Study purpose | Determine cardiac-sparing achieved by reoptimising the standard photon beam cCRT | Identify sub-group for possible patient selection using IMPT |

| | | |
|-----------------------------|--|--|
| Patient and prescribed dose | <ul style="list-style-type: none"> • 20 patients, 7 had tumours covering T7 and below • 10 patients had left side primary tumour • 68.8Gy (63 – 73Gy) in 30 fractions | <ul style="list-style-type: none"> • 20 patients, 16 had tumours covering T7 and below • 10 patients had left side primary tumour • 70Gy in standard 2Gy/fraction |
| Tumour target regulations | $D_{PTV-90\%} > 95\%$ of prescribed dose $D_{PTV-98\%} > 90\%$ of prescribed dose | $D_{PTV-95\%} >$ prescribed dose for VMAT $D_{CTV-99\%} >$ prescribed dose for IMPT |
| Toxicity constraints | Follow <i>SCOPE-1, IDEAL-CRT</i> | Heart delineation follows <i>RTOG-1106</i> , while dose constraints follow <i>RTOG-1308</i> |

Table 6.2 Mean heart dose (MHD) indices recorded in both studies. MHDs were recorded for standard photon, optimised photon, and proton treatment plans, and for overall and T7 and non-T7 tumour groups.

| | Tumour locations | Std photon | Optimised photon | Proton |
|---------------------------|------------------|---------------|------------------|--------|
| Liverpool study | T7 (N=7) | 26.3Gy | 15.7Gy | - |
| | Non-T7 (N=13) | 6.2Gy | 4.5Gy | - |
| | Weighted average | 13.2Gy | 8.4Gy | - |
| Oxford study [†] | T7 (N=16) | - | 16.7Gy* | 6.5Gy |
| | Non-T7 (N=4) | - | 4.4Gy* | 1.9Gy |

[†]Weighted averages are not presented for the Oxford study, because the T7/non-T7 patient split is not representative of typical patient population.

*These values are not used subsequently because they are very similar to the ones in the Liverpool study.

6.2.2 Cardiac-sparing estimation and survival modelling

Given that ICB does not increase the risks of radiation-induced adverse effects when given together with radiotherapy²²³, I have characterised it as having no effect on the (*I-SLT*) term in OS models, the same approach taken in Chapter 5.

Transferring HR_{OS} to HR_{SLT}

The risks of cardiac exposure have been reported using HRs for death^{229,230}, which are related to OS, thus,

$$\frac{dN}{dt} = -N \times h_0(t) \rightarrow \frac{N}{N_0} = S_0 = \exp(-\int h_0(t) dt) \quad \text{--- Equation 6.1}$$

where N is patient number at time t , N_0 is patient number at time 0, $h_0(t)$ is the hazard rate for death, and S_0 is survival. If the hazard function increased by a constant factor (i.e. the HR), the survival S becomes

$$S = \exp(-HR \times \int h_0(t) dt) \equiv S = S_0^{HR} \quad \text{--- Equation 6.2}$$

Consequently, OS using the cardiac-sparing technique can be estimated via

$$OS \text{ with sparing} = (\text{Baseline OS})^{HR_{OS}} \quad \text{--- Equation 6.3}$$

However, my dose-response models assumed that OS was a combination of tumour control probability (TCP) and (I - SLT), accounting for the dose delivered to the tumour and the OARs, respectively. Therefore, mechanistically the TCP term is unaffected by any cardiac-sparing, leaving its contribution to the OS curve unchanged; whereas the (I - SLT) term is affected by the cardiac-sparing, and therefore this is the term the HR modifies. However, the HR acting on (I - SLT) is not the original HR_{OS} because that describes changes in OS rates rather than (I - SLT). Instead, it can be determined by transferring HR_{OS} to the SLT term as follows

$$(\text{Baseline OS})^{HR_{OS}} = \sum_i f_i \times TCP_{S_i} \times (1 - SLT_{S_i})^{HR_{SLT}} \quad \text{--- Equation 6.4}$$

For example, there was a 4.8Gy MHD decrease between ‘standard photon’ and ‘optimised photon’ plan¹⁰⁸. Raising HR_{OS} ($\Delta 1$ Gy), the HR_{OS} per 1Gy reduction in MHD of 0.954 (95% confidence interval, CI: 0.913, 0.993)²³⁰, to the power of 4.8, gives an HR_{OS} for this reduction in cardiac dose of 0.798²³⁰. I took the HR_{OS} ($\Delta 1$ Gy) value from an analysis published for patients treated in Oxford²³⁰. The HR_{SLT} values obtained from Equation 6.4 depend not only on HR_{OS} but also on the

patient stage split represented by f_i and splits of treatments used to treat a cohort. For consistency, I used the stage and treatment split reported for the study from which I took the HR_{OS} ($\Delta 1Gy$) value, specifically, 1:1 stage IIIA vs IIIB/C, and a 2:1:1 split of patients treated using radiotherapy alone, sequential CRT (sCRT) and cCRT.

Other studies have reported different HR_{OS} ($\Delta 1Gy$) values, either higher or lower. The effects of this source of uncertainty on the OS values that I calculated is described in the discussion section 6.4.

MHD values versus technique and tumour location

Anatomically, the heart is located at or below the T7 vertebra, and so will likely receive higher doses when T7 tumours are treated rather than tumours lying higher in the lung. This will lead to poorer OS, represented by greater HR_{OS} and HR_{SLT} . In the Liverpool study, there was a 20.1Gy difference in the averaged MHD of patients with T7 versus non-T7 tumours¹⁰⁸. In Table 6.3, I list averaged MHDs for patients receiving standard and optimised photon treatments and proton treatments, both for overall patient groups, and for patient subgroups with T7 and non-T7 tumours. The T7/non-T7 splits in MHDs were taken directly from the Liverpool and Oxford datasets. The average photon and proton MHDs of all patients were weighted based on the T7/non-T7 ratio seen in the Liverpool study (7:13). There are literatures support such ratio split as NSCLC is less likely distributed at the right middle lobe, right lower lobe, and left lower lobe^{45,231,232}.

I also tabulate the differences between these MHDs and the baseline 13.2Gy value for the overall patient group treated using the standard photons. And I list the HR_{SLT} values corresponding to these MHDs differences.

For each technique and patient group, the OS was calculated using model fitted in Chapter 5, raising the ($I-SLT$) term to the power of the HR_{SLT} value listed for that technique and patient group in Table 6.3.

Table 6.3 Averaged MHD values for standard and optimised photons and protons, in all patients and in T7 and non-T7 patient subgroups. Also shown are differences between MHDs and the baseline 13.2Gy values and the corresponding HR_{OS} and HR_{SLT} values.

| Technique | Tumour location | Ave MHD | ΔMHD (Ave MHD – 13.2Gy baseline) | HR _{OS} † (95% CI) | HR _{SLT} †† (95% CI) |
|------------------|--------------------|---------------|----------------------------------|-----------------------------|-------------------------------|
| Standard photon | T7 | 26.3Gy | +13.1Gy | 1.80 (1.10, 2.98) | 2.75 (1.30, 5.19) |
| | Non-T7 | 6.2Gy | -7Gy | 0.73 (0.56, 0.95) | 0.53 (0.18, 0.99) |
| | Weighted average | 13.2Gy | Baseline reference | 1 | 1 |
| Optimised photon | T7 | 15.7Gy | +2.5Gy | 1.12 (1.02, 1.23) | 1.34 (1.13, 1.57) |
| | Non-T7 | 4.5Gy | -8.7Gy | 0.68 (0.48, 0.94) | 0.42 (0.02, 0.97) |
| | Weighted average | 8.4Gy | -4.8Gy | 0.80 (0.67, 0.97) | 0.69 (0.41, 1.02) |
| Proton | T7 | 6.5Gy | -6.7Gy | 0.74 (0.57, 0.95) | 0.55 (0.21, 1.00) |
| | Non-T7 | 1.9Gy | -11.3Gy | 0.60 (0.39, 0.92) | 0.27 (0.00, 0.94) |
| | Weighted average** | 3.5Gy | -9.7Gy | 0.65 (0.45, 0.93) | 0.36 (0.00, 0.96) |

*Δdose changes in Gy refers to the total dose change versus standard photon delivery of 13.2Gy.

** Weighted according to the T7/non-T7 patient split seen in the Liverpool cohort.

† HR_{OS} was calculated directly. For example, the HR_{OS} of 2.5Gy refers to $1.046^{(2.5)} = 1.119$. The 95% CI was calculated by converting the CI of 1.046 (per Gy change, i.e. 1.007, 1.087) as reported.

†† HR_{SLT} was calculated using a two-step method, where they can only be estimated once HR_{OS} had been calculated. The 95% CI was calculated by converting the CIs of HR_{OS}.

6.3 Results

As in Chapter 5, modelled 2-year OS values are plotted for three types of schedules, 2Gy fractionation, 30 fractions and 20 fractions. Furthermore, results are shown for standard photon treatment, optimised photon treatment, and protons, and for whole patient groups, and T7/non-T7 subgroups. The dose ranges over which OS values are plotted are those that were not greyed out in Chapter 5, these being ranges for which data exist in the dataset to which models were fitted. All the doses for which OS levels have been plotted are physical doses, and in the model these are converted into EQD2s via the usual linear-quadratic model before being converted on into TCP and SLT effects.

Modelled predictions shown in this chapter are less tightly linked to the datasets to which the OS models were fitted than those presented earlier, because they include the effects of changes in MHDs, which have been estimated using data from an independent study²³⁰. The effects of this on uncertainties in the plotted OS rate are described in the discussion section.

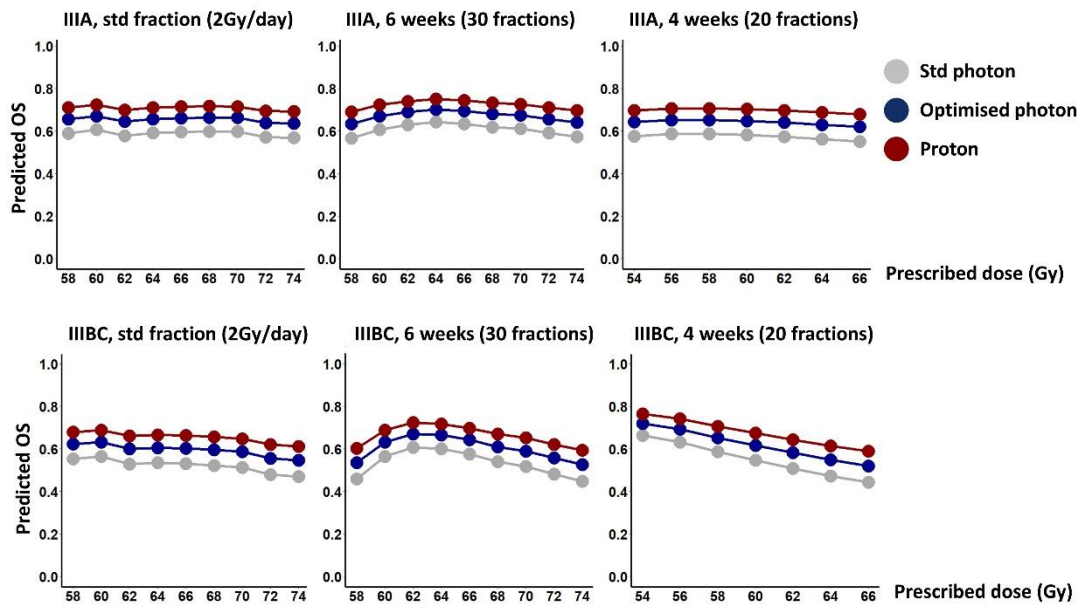


Figure 6.1. Modelled two-year OS rates for cCRT alone for all patients, treated with standard photon, optimised photon cardiac-sparing and proton. OS values are plotted for doses of 58 to 74Gy, for standard 2Gy-per-fraction and six-week schedules, and for 54 to 66Gy for the four-week schedule.

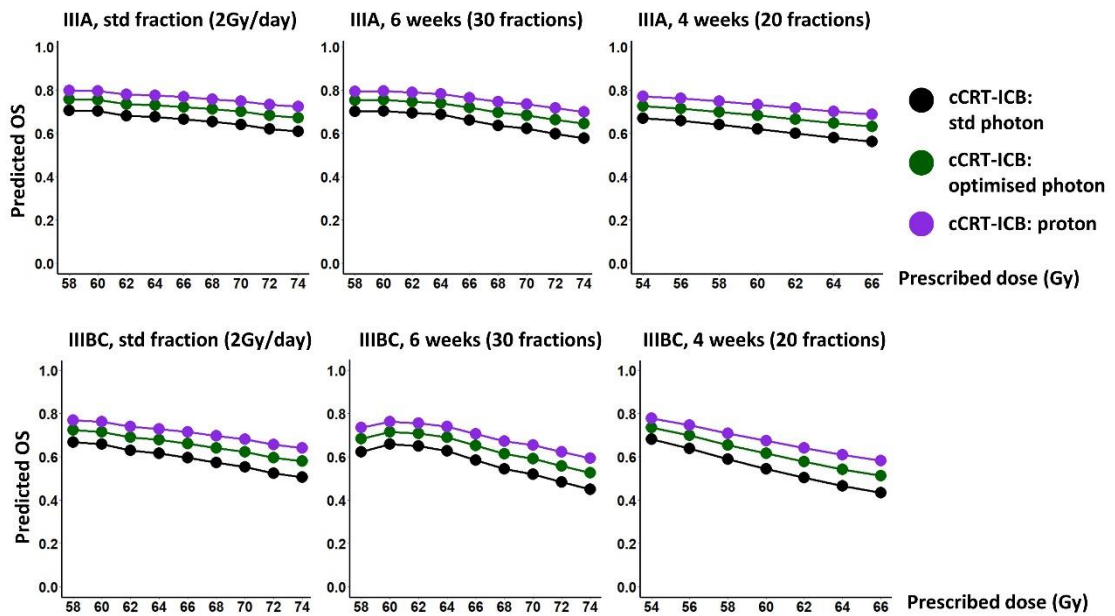


Figure 6.2. Modelled two-year OS rates for cCRT-ICB treatment for all patients.

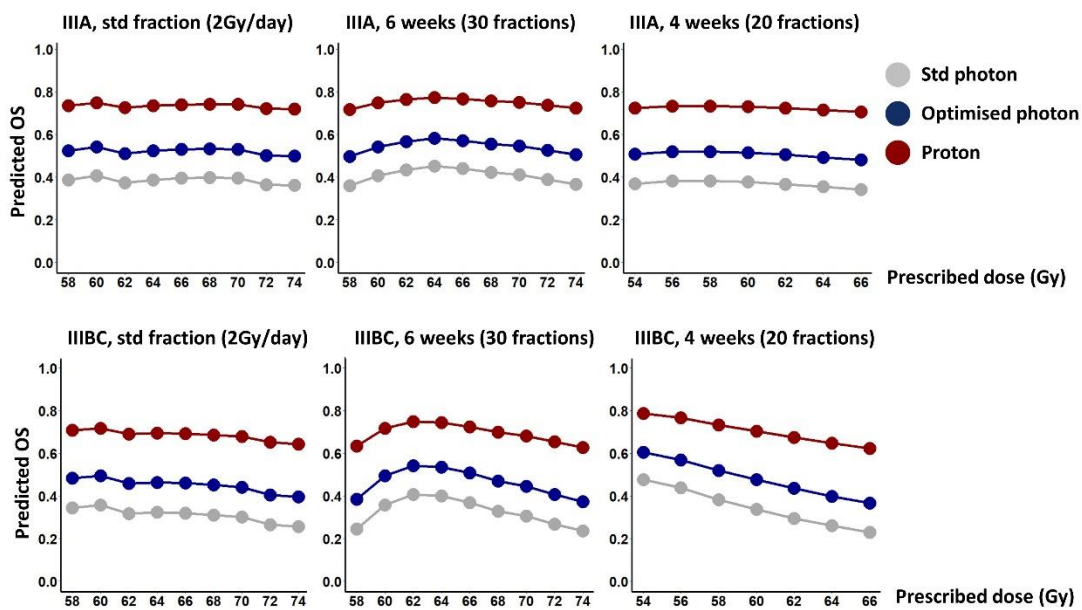


Figure 6.3. Modelled two-year OS rates for cCRT alone for patients with T7 tumours.

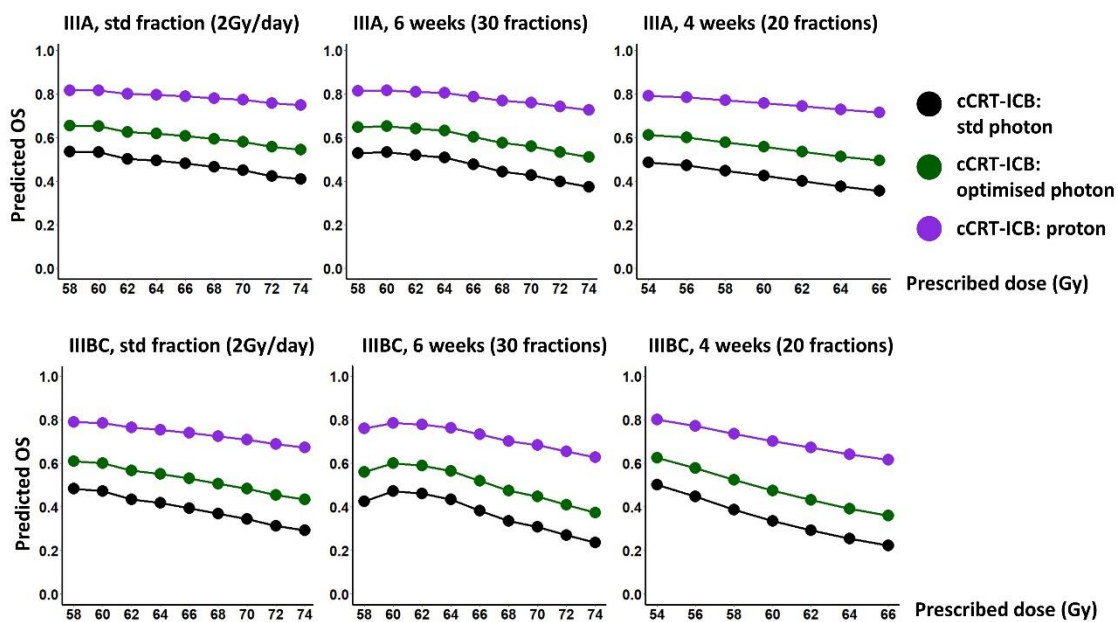


Figure 6.4. Modelled two-year OS rates for cCRT-ICB treatment for patients with T7 tumours.

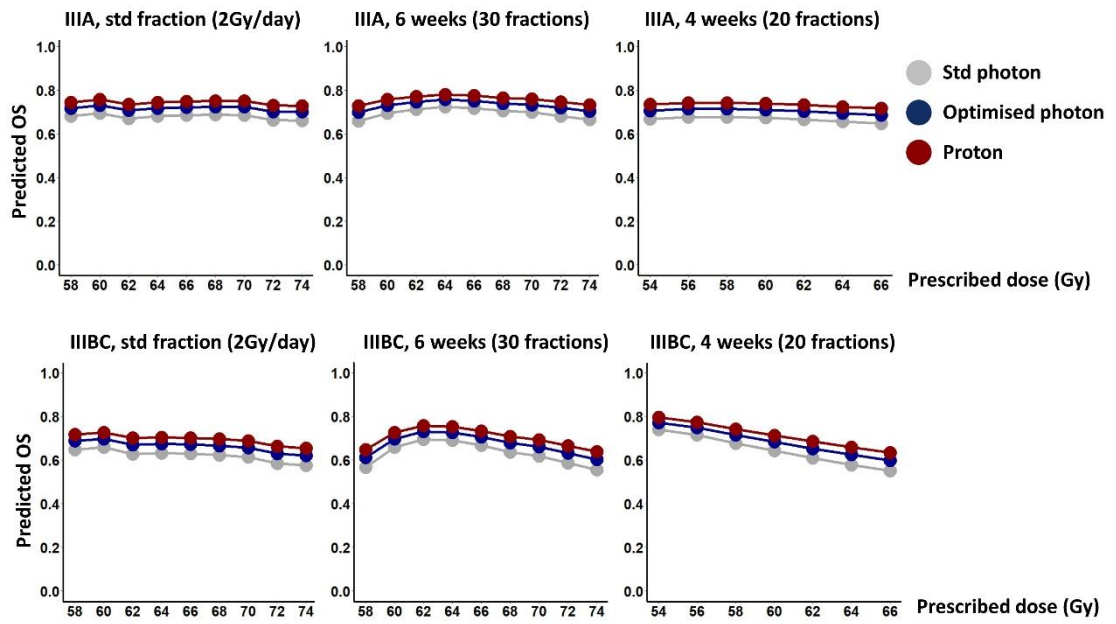


Figure 6.5. Modelled two-year OS rates for cCRT alone for patients with non-T7 tumours.

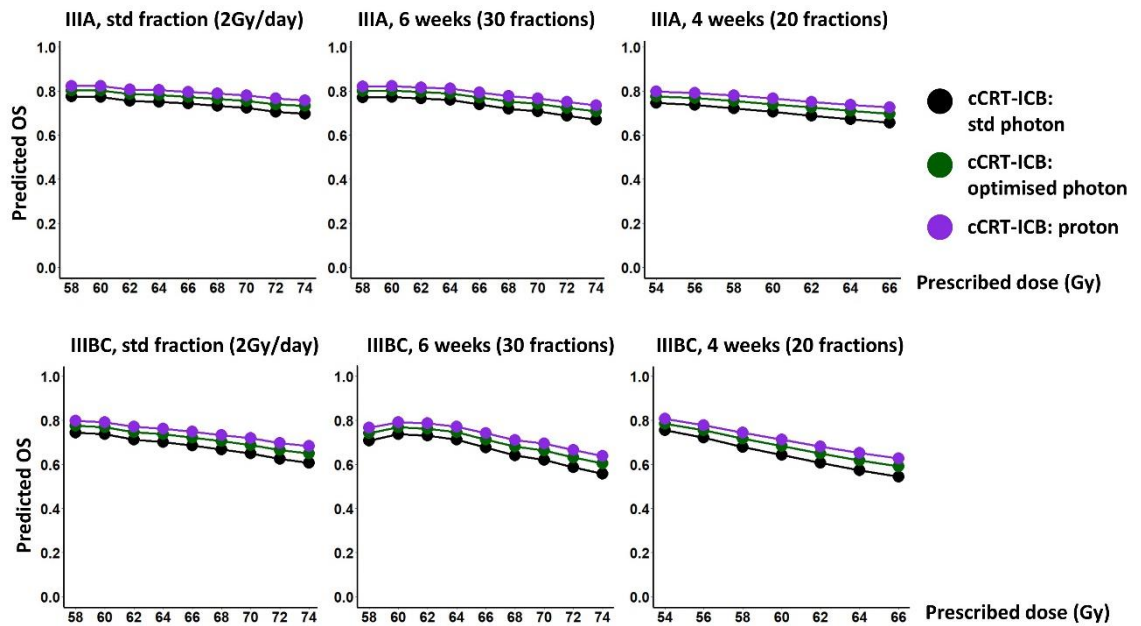


Figure 6.6. Modelled two-year OS rates for cCRT-ICB treatment for patients with non-T7 tumours.

It can be seen in Fig. 6.1 that across all patients receiving cCRT alone, regardless of dose fractionation schedules, a 5 to 10% increase in modelled 2-year OS was achieved by optimising photons to reduce MHDs compared to standard photons, with protons providing a further roughly 5 to 10% OS increase.

Fig. 6.2 shows modelled 2-year OS rates calculated for cCRT plus ICB. The same increases in modelled OS were achieved using cardiac dose-sparing as for cCRT alone, namely 5-10% for optimised photons and protons each.

Fig. 6.3 shows the effects of cardiac-sparing in patients with T7 tumours receiving cCRT alone. 10-15% increases in modelled OS could be achieved by reoptimising photon treatments to spare the heart (Fig. 6.3), with proton sparing roughly achieving a further 20%. Comparing Fig. 6.3 and 6.4, ICB contributed to another 5 to 10% of 2-year OS above cCRT alone for radiation given in 2Gy-per-fraction or six weeks, regardless of cardiac-sparing (Fig. 6.4).

Fig. 6.5 and 6.6 show modelled 2-year OS rates for patients with non-T7 tumours receiving cCRT alone and cCRT-ICB, respectively. In this group, standard photon delivery of cCRT alone was good enough to achieve OS levels of 60% or slightly higher, as cardiac doses were relatively low. Correspondingly, gains from cardiac-sparing were also lower for these patients, with $\leq 5\%$ for optimised photons and around 5% more for protons.

6.4 Discussion

Two scenarios of MHD changes and associated modelled OS changes have been studied: cardiac-sparing achieved using optimised photon or proton treatment plans versus standard photon plans. These changes were studied for all patients and for subgroups with T7 and non-T7 tumours. This is the first study applying the relative MHD risks to the radiation dose-response models, even exploratorily investigating with the ICB addition.

Key findings indicate that MHD photon cardiac-sparing provides 5-10% gains in modelled 2-year OS across all patients, rising to 10-20% for protons. For T7 tumours protons are particularly useful, potentially providing an additional OS gain of around 20% above optimised photons.

Uncertainties of cardiac-sparing modelling

The institutional cardiac indices were chosen as the HR definition, where MHD was 7.6Gy (range: 0.5, 32.2Gy) with HR_{OS} (Δ 1Gy) of 1.05 (95% CI: 1.01, 1.09) against OS²³⁰. Other studies have reported a range of HRs. In analyses against OS, Lee et al. found an HR of 1.03 (95% CI: 1.01, 1.05) with an average 12.6Gy MHD (range: 4.8, 19.5Gy)²³³; Dess et al. reported an HR of 1.01 (95% CI: 0.98, 1.03) with an average 11Gy MHD (range: 0.3, 46Gy)²³⁴; and Wang et al. reported an HR of 1.01 (95% CI: 1.00, 1.03) with 12.3Gy average MHD²³⁵. In a meta-analysis combining 1013 patients from three studies, the HR for developing late cardiac toxicity after (chemo-)radiotherapy was 1.06 (95% CI: 1.04, 1.08) per Gy MHD increase²³⁶. Thus, the 1.05 HR that I selected is close to other published results.

A negative association between OS and cardiac dose is a finding of data analysed and published, and I built this finding into OS dose-response models in a straightforward way. Therefore, the results for OS gains from cardiac-sparing for radiotherapy and cCRT are fairly data based. In contrast, the modelled OS for

cCRT-ICB reflects the results from CRT studies, together with an assumption in my modelling that the SLT term for CRT carries over directly to cCRT-ICB. No one has analysed the cardiac dose for cCRT-ICB studies to the best of my knowledge, and so empirically it is possible that future data might show no link between cardiac-sparing and OS for treatments that include ICB.

This research aimed to inform the comparisons of commonly used dose ranges instead of predicting many out-of-box effects with modelling randomisation. It might be arguable that both the Liverpool and Oxford studies which quantified MHD reductions used moderately escalated prescription doses (mean dose: 68.8Gy¹⁰⁸; 70Gy¹⁰⁹), resulting in possibly higher cardiac dose exposure as these doses are about 10% higher than standard ones. Therefore, if patients had been planned at regular tumour dose levels, changes in MHD might well have been 10% relatively lower. For example, the 9.7Gy difference between average MHDs for all patients obtained using proton and standard photon plans might have worked out around 8.7Gy instead, little different. Uncertainty on the HR used to convert dosimetric changes into modelled OS changes is a far greater source of possible errors in the results.

The CIs were not plotted in the results section, as the prediction combining HR and ICB uncertainties would have wider CIs than shown for cCRT-ICB in Chapter 5. Fig. 6.7 (i.e. Fig. 6.1 with CIs) shows CIs accounting for the uncertainty in HR alone. These CIs range from around 20% absolute (on modelled 2-year OS rates) for optimised photons to 30% for protons. This source of uncertainty will widen the bootstrap CIs shown in Chapter 5, leading to large overall uncertainties on modelled OS. Thus, caution is needed when interpreting these results, as some extrapolate beyond the data. For example, no prospective study has tested the OS of T7 tumours given proton cardiac-sparing, or investigated cardiac-sparing with cCRT-ICB.

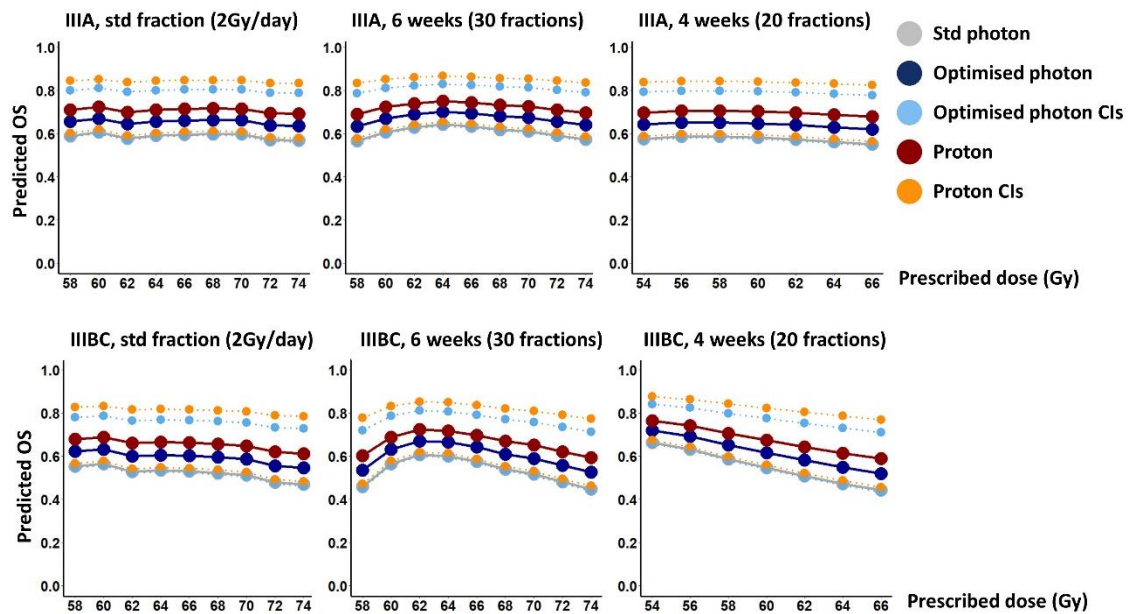


Figure 6.7. Modelled two-year OS rates for all patients with 95% CIs accounting for uncertainty on HR alone. Cohorts were treated with cCRT alone for all tumours. The 95% CIs were generated using best fits plus CIs of HR_{SLT} for cardiac-sparing effects.

Towards better cardiac toxicity optimisation

Several studies have reported significant associations between cardiac irradiation and OS for LA-NSCLC^{108,207,229}. Such phenomena might be cancer-type specific, as there was a 13% OS decrease in the high-dose arm of *RTOG-0617*⁵⁴. In comparison, there was only a 0.5% death risk increase related to ischaemic heart disease in breast cancer patients receiving additional 2Gy cardiac irradiation, similar to the increased doses reported in the high-dose arm of *RTOG-0617*^{54,108}. There is a limited understanding of toxicity for lung cancer compared to lymphoma or breast cancer, as the lung cancer toxicity model suffers heavy death-related censoring, which does not occur to nearly the same extent in breast or lymphoma where most patients are cured⁹⁹. In addition to the short OS, lung cancer is usually

seen in older patients²³⁷, increasing the difficulties of defining safe and consistent dose constraints due to worse performance status and comorbidities.

The causal relationships between cardiac irradiation and chronic cardiac symptoms have yet to be fully understood^{100,238}. An institutional study comparing photon- and proton- based cardiac-sparing (N=13 for each condition) generally supports my modelling assumptions, reporting that the average spared proton MHD (5.3Gy) was significantly lower than in photon plans (11.4Gy) ($p=0.032$)²³⁹. However, high 2-year OS rates for LA-NSCLC patients treated with protons have yet to be reported, perhaps due to the limited number of patients enrolled with T7 tumours.

For T7 patients, the gain from protons is much greater than optimised photons, whereas for non-T7 patients it is only a limited difference. Protons stop at specific depth whereas photons do not, causing the proton doses to be lower. Such characteristic benefits both T7 and non-T7 tumours. However, the penumbra of protons can be wider than those of photons²³⁸, which may cause the cardiac doses from protons to be higher than from photons, reducing the advantage of protons. In particular, the penumbra effects may be greater for parts of non-T7 tumours which finish just above the heart, as the heart lies in the inferior margin of the radiation beams. In contrast, the cardiac doses of non-T7 tumours which locate much higher than the heart are usually very low, regardless of penumbra effects.

The ongoing trial *RTOG-1308* compares the efficacies of photon and proton cCRT using a prescribed dose of 70Gy in 2Gy-perfraction⁴⁵. Therefore, I made an exploratory comparison according to its radiotherapy schedules (70Gy in standard 2Gy-per-fraction) and listed in Table 6.4. Protons provide >20% of additional OS over optimised photons for T7 tumours, whereas optimised photons seem good enough for non-T7 tumours. Such very large modelled benefits of protons would only require limited T7 patient numbers to test. It is worth noting that *RTOG-1308*

planned the photon treatments more like regular photons than optimised photons. Such predictions can be compared with published outcomes once data matures.

Table 6.4 Modelled 2-year OS with MHD sparing considering schedules given in *RTOG-1308* study: 70Gy in standard 2Gy-per-fraction. Cardiac-sparing values of all patients and patient subgroups with T7 and non-T7 tumours are listed in (A), (B), and (C), respectively.

(A)

| All tumours | IIIA (with 95% CIs) | IIIB/C (with 95% CIs) |
|------------------------|---------------------|-----------------------|
| cCRT, standard photon | 59% (45%, 73%) | 51% (36%, 62%) |
| cCRT, optimised photon | 66% (59%, 81%) | 59% (51%, 76%) |
| cCRT, proton | 72% (61%, 85%) | 65% (53%, 81%) |

(B)

| T7 tumours | IIIA (with 95% CIs) | IIIB/C (with 95% CIs) |
|------------------------|---------------------|-----------------------|
| cCRT, standard photon | 40% (21%, 56%) | 30% (13%, 47%) |
| cCRT, optimised photon | 53% (47%, 59%) | 44% (38%, 50%) |
| cCRT, proton | 74% (63%, 83%) | 68% (54%, 78%) |

(C)

| Non-T7 tumours | IIIA (with 95% CIs) | IIIB/C (with 95% CIs) |
|------------------------|---------------------|-----------------------|
| cCRT, standard photon | 68% (60%, 74%) | 61% (52%, 68%) |
| cCRT, optimised photon | 72% (60%, 87%) | 66% (52%, 87%) |
| cCRT, proton | 75% (61%, 92%) | 69% (53%, 92%) |

This study is hypothesis-generating, as cardiac toxicity might not be explicable via cardiac doses alone. The cardiac dose has been reported with possible immunosuppressive effects on LA-NSCLC radiotherapy. Heart V₅₀ (volume receiving ≥ 50 Gy) >25% shows a correlation with a higher neutrophil-to-

lymphocyte ratio at four months, with reduced OS (odds ratio: 2.0, $p=0.02$)²⁴⁰. Higher doses of irradiation to the immune system have been proved to link to the poor OS in LA-NSCLC^{241,242}; however, no research has tested whether such effects would change following the addition of ICB. Relatedly, higher c-reactive protein and higher neutrophil/lymphocyte ratio have been identified as prognostic factors for cCRT-ICB, indicating that systemic immune response (inflammation) might affect the treatment outcomes²⁴³. Additionally, it is worth noting that treatment planning should be done cautiously, as a study (N=15) suggested that CTV with proton sparing may be jeopardised by breathing pattern alteration, where 20% (N=3) of patients lacked CTV coverage using proton planning²⁴⁴.

Reducing irradiation to the heart benefits OS, although without caution in plan optimisation, it may reciprocally increase lung dose. Elevated lung dose can also lead to severe and unmanageable toxicity, such as breathlessness, radiation pneumonitis and lung fibrosis. How to prioritise cardiac-sparing over lung protection needs further investigation, although reductions in cardiac irradiation might be expected to have limited impact on integral lung doses, since the volume of the heart (~0.35 litres) is much smaller than the volume of the lung (~6 litres).

Radiation dose fractionation schedules

According to my analysis, modest dose de-escalation of 5Gy might be plausible for cCRT-ICB, matching my modelled results in Chapter 5 – with the addition of ICB, dose de-escalation seems to be appealing for patients with heavily irradiated OARs.

With cardiac-sparing, modelled 2-year OS rates for schedules giving 55 to 60Gy in four weeks (20 fractions) were as good as the best achieved using standard 60 to 66Gy in 2Gy-per-fraction given cardiac-sparing. Four-week schedules give a relatively high dose-per-fraction (i.e. ≥ 2.75 Gy); but the negative effects of the high dose-per-fraction on toxicity are reduced by cardiac-sparing, making the four-

week schedule competitive in terms of modelled OS. A four-week 20 fraction schedule would also be cheaper to deliver than schedules giving 30 or more fractions. Dose constraints for specific OARs should be carefully considered, since reducing treatment duration by 1/3 might change the tolerance of OARs.

6.5 Conclusion

Across all patients, photon-based cardiac dose sparing led to gains in modelled 2-year OS of 5 to 10%, while proton-based sparing led to increases of 10-20%. The degree of cardiac-sparing and associated modelled OS gain was particularly large for T7 tumours, with photon- and proton-based cardiac-sparing achieving modelled OS gains of around 10-15% and 30-35% respectively. However, gains from cardiac-sparing were more limited for non-T7 tumours, modelled OS gains being only $\leq 5\%$ for photon sparing, and around 5-10% for protons. For non-T7 patients, cardiac-sparing with photons seems a useful option, since it costs nothing and moderately improves modelled OS rates. For T7 patients, proton beam therapy seems a promising option despite its cost, since the large modelled increase in OS rates for these patients suggests that up to 2-years post-treatment it would prevent 1 death per 3 patients treated.

This analysis provides no indication that dose escalation might be useful for any of cCRT, cCRT-ICB, cCRT or cCRT-ICB with cardiac-sparing. It should, though, be borne in mind that results presented in this chapter have large statistical uncertainties and depend to some extent on the structure of the model fitted. They do, though, suggest it would be worthwhile testing four-week radiation schedules with cardiac-sparing, since these achieve as good or better modelled OS rates than do six-week and 2Gy-per-fraction schedules, and they are cost-effective in the clinic.

Chapter 7. Conclusion

7.0 Chapter overview

This chapter –

- Summarises the key findings of previous chapters.
- Highlights valuable findings described in this thesis which may contribute to future studies.

7.1 Summary of findings

Optimisation of radiotherapy fractionation schedules in combination treatments of inoperable locally-advanced non-small cell lung cancer (LA-NSCLC) is complicated with the effects of chemotherapy and immunotherapy. In this work I have developed novel survival models that incorporate radiotherapy and chemotherapy schedules, immunotherapy factors, and cardiac radiation toxicity indices. And I have fitted them to databases summarising results obtained for a wide range of treatments. Using the fitted models, options were explored for widening the therapeutic window for LA-NSCLC chemoradiotherapy (CRT) and immuno-CRT.

In **Chapter 3**, recently developed radiation dose-response survival models were extended by splitting parameters describing tumour repopulation, fractionation effects (α/β) and survival-limiting toxicity by treatment type (chemotherapy schedules: none vs sequential vs concurrent) and tumour stage. These efforts aimed to provide quantitative descriptions of reasons for the failure of radiation dose-escalation studies, and to reveal the underlying causes of the apparently inconsistent outcomes achieved using different radiation prescription

schedules. The best description of 2-year overall survival (OS) was achieved through a model that accounted for tumour accelerated repopulation progressing at a rate of 1.47Gy EQD2 (equivalent dose in 2Gy fractions) per day for concurrent CRT (cCRT), compared to 0.30Gy/day for sequential CRT (sCRT) and radiotherapy alone. These rates suggest that cCRT treatments should be administered in the shortest feasible time while maintaining prescribed doses, but that treatment acceleration offers less benefit for radiotherapy alone or sCRT. Hypofractionation can be used to accelerate cCRT, and the relatively low overall fitted tumour α/β ratio of 3.0Gy suggests this approach will be both effective and practical as long as the EQD2 for normal tissues is not increased in the process. These findings imply that moderate cCRT hypofractionation within normal tissue toxicity limits should be efficacious.

Chapter 4 quantified the survival benefits (OS gain) provided by adding immune checkpoint blockade (ICB) to cCRT for LA-NSCLC. Also, this research tried to identify factors which might affect the OS gain provided by ICB. A meta-analysis helped to understand outcomes from multiple trials of cCRT-ICB with heterogeneous study design. The estimated gain in 2-year OS from ICB was 9.9% overall and was significantly positively associated with patients with tumour PDL1 $\geq 1\%$, those with stage IIIB/C disease, and with duration of ICB greater than one year. The OS benefit from ICB was significantly negatively linked to patient age but showed no association with prescribed radiation dose, radiation duration or whether immune treatment began concurrently with or after completion of cCRT. This analysis suggests that OS following cCRT-ICB could be further enhanced by extending the delivery duration of ICB treatment beyond one year. Additionally, gains in survival due to ICB were more pronounced in younger patients and those with tumour PDL1 $\geq 1\%$ or tumours with advanced staging.

In **Chapter 5**, fitted dose-response models of 2-year OS following CRT and cCRT-ICB were used to study the OS rates predicted for ranges of prescribed doses

delivered using three different types of radiation schedule, aiming to find which doses and schedules achieved the best survival. As this chapter studied the effects of different dose-levels, including those higher than typically given, the structure of the immune component of the model used was changed from the purely empirical approach of Chapter 4, which represented ICB benefits as increases in OS (%) beyond those achieved by CRT, to a semi-mechanistic approach in which ICB was described as contributing to tumour cell killing via an additional effective total radiation dose (Gy). Specifically, the model fit described the impact of ICB on tumour control as an effective 13.5Gy increase in tumour radiation dose. In terms of radiation fractionation schedules, there was little benefit in either escalating or de-escalating doses from the standard cCRT-ICB schedule of 60Gy in 2Gy-per-fraction. However, modelled OS was only 2% lower at 55Gy than at 60Gy, suggesting that modest dose de-escalation might be an appealing option for patients with heavily irradiated organs at risk (OARs). Additionally, exploring the feasibility and outcomes of sCRT-ICB could be worthwhile.

Chapter 6 describes exploratory research, investigating the possible scale of OS benefits achieved at different prescribed doses using mean heart dose cardiac-sparing of cCRT and immuno-cCRT treatments. Sparing was achieved using optimised photons or protons, with both showing improvements in modelled OS. For patients with tumours anatomically overlapped the heart (T7 tumours), protons provided prominent OS advantages and should be considered as a treatment option.

In summary, this thesis comprises a sequence of studies investigating possible gains from modified radiotherapy, CRT and immuno-CRT treatments of inoperable LA-NSCLC. Chapter 3 was an analysis of cCRT treatments, the previous standard-of-care before the addition of ICB changed the landscape. It provided a thorough understanding of cCRT dose-responses, establishing a fitted model that was used in Chapter 4 as a foundation on which to construct a model of greater complexity describing outcomes from cCRT-ICB treatments. Using the extended model I

identified patient and treatment factors affecting OS following cCRT-ICB, the current standard-of-care (Chapter 4). Then I used a related model to study how modelled OS rates following cCRT/sCRT-ICB changed with radiation dose and schedule (Chapter 5). Finally, the modelling was extended further to account for changes in OS with the extent of heart irradiation, and with sparing of mean heart dose using different techniques and for different tumour locations (Chapter 6).

Together, these analyses provide information about likely effects on OS of changes in radiation dose and scheduling, cardiac avoidance, immune agent and patient factor, guiding the design of improved treatments and possible trials of these treatments. In particular, I found no indication that OS would be improved by changing the radiation dose given in cCRT-ICB treatments from 60Gy, though the use of 5Gy lower doses may be advantageous for patients with heavily irradiated OARs. But I found that gains may be made by administering ICB for 2 years rather than one. And I found strikingly large gains in modelled 2-year OS rates for proton-based cardiac-sparing for patients with T7 tumours.

7.2 Future directions

I have found several interesting and practically applicable findings in this thesis, allowing the clinic to test new LA-NSCLC treatment conditions. For examples, delivering ICB in 2-year versus 1-year and proton cardiac-sparing for patients with T7 tumours. Prospective clinical trials are needed to verify the modelled outcomes, evaluate cost-effectiveness, and update the clinical guidelines.

The treatment response of inoperable LA-NSCLC is complicated, especially in the tri-modality era of immuno-chemo-radiotherapy. More work is needed to analyse the clinical outcomes (e.g. OS, progression-free survival, toxicity) and related indices (e.g. dosimetry or genomics), to elucidate the associations and even causal relationships between observed results. *In-silico* models, such as the dose-response models that I used in this thesis, must keep updating with the newest datasets and proper hypotheses. Future models are needed to incorporate more biomarkers, imaging data, and longitudinal dynamic changes in tumour responses.

With a clearer understanding informed by future studies, further individualisation of dose prescriptions and toxicity tolerance might be achievable, leading the care of inoperable LA-NSCLC towards personalised treatment.

Chapter 8. Appendices

Appendix 1. Detail of CRT dataset. Authors, published year, study names and phases, randomisation, radiotherapy (RT) dose, fractions (Fx), dose-per-fraction, RT days, chemotherapy conditions, patient numbers with staging, and 2-year OS were listed.

| 1 | Author | Year | Study | Phase | Randomisation | Dose | Fx | Dose_per_Fx | RT_Days | Chemo | Concurrent | Pt | Stage_I | Stage_II | Stage_III/ | Stage_IIIE | OS |
|----|---------|------|-----------|-------|---------------|-------|------|-------------|---------|-------|------------|-----|---------|----------|------------|------------|-------|
| 2 | Landau | 2016 | IDEAL-CRT | I/II | N | 67.5 | 30 | 2.25 | 39 | Yes | YES | 84 | 0 | 6 | 57 | 21 | 0.68 |
| 3 | Bradley | 2015 | RTOG 0617 | III | Y | 63 | 30 | 2.1 | 42 | Yes | YES | 217 | 0 | 0 | 144 | 73 | 0.576 |
| 4 | | 2015 | | | | 77.7 | 37 | 2.1 | 52 | Yes | YES | 207 | 0 | 0 | 131 | 76 | 0.446 |
| 5 | Baumann | 2011 | CHARTWEL | III | Y | 60 | 40 | 1.5 | 17 | NONE | | 203 | 21 | 11 | 78 | 93 | 0.31 |
| 6 | | 2011 | | | | 66 | 33 | 2 | 46 | NONE | | 202 | 21 | 12 | 76 | 93 | 0.32 |
| 7 | Belani | 2005 | ECOG 2597 | III | Y | 60.48 | 36 | 1.68 | 16 | Yes | NO | 56 | 0 | 0 | 56 | 0 | 0.44 |
| 8 | | 2005 | | | | 67.2 | 32 | 2.1 | 46 | Yes | NO | 56 | 0 | 0 | 56 | 0 | 0.34 |
| 9 | Sause | 2000 | RTOG 8808 | III | Y | 63 | 30 | 2.1 | 40 | NONE | | 132 | 0 | 9 | 67 | 56 | 0.21 |
| 10 | | 2000 | | | | 63 | 30 | 2.1 | 42 | Yes | NO | 149 | 0 | 10 | 68 | 71 | 0.32 |
| 11 | | 2000 | | | | 73.08 | 58 | 1.26 | 40 | NONE | | 154 | 0 | 7 | 71 | 76 | 0.24 |
| 12 | Yu | 2014 | China | Local | Unknown | 65 | 25 | 2.6 | 21 | Yes | NO | 30 | 0 | 0 | 16 | 14 | 0.43 |
| 13 | | 2014 | | | | 60 | 30 | 2 | 35 | Yes | NO | 30 | 0 | 0 | 15 | 15 | 0.32 |
| 14 | Wu | 2003 | China | I/II | N | 73 | 31.7 | 2.303 | 43.5 | Yes | NO | 50 | 0 | 4 | 31 | 15 | 0.44 |
| 15 | Kong | 2005 | Michigan | I | Unknown | 67.2 | 32 | 2.1 | 44 | Yes | NO | 50 | 15 | 4 | 18 | 13 | 0.22 |
| 16 | | 2005 | | | | 79.8 | 38 | 2.1 | 52 | Yes | NO | 29 | 9 | 1 | 11 | 8 | 0.59 |
| 17 | Bradley | 2005 | RTOG 9311 | I/II | N | 74.5 | 33 | 2.258 | 45 | Yes | NO | 28 | 14 | 3 | 6 | 5 | 0.46 |
| 18 | | 2005 | | | | 81.27 | 36 | 2.257 | 50 | Yes | NO | 26 | 13 | 2 | 8 | 3 | 0.5 |
| 19 | | 2005 | | | | 88.04 | 39 | 2.258 | 53 | Yes | NO | 33 | 17 | 3 | 10 | 3 | 0.42 |
| 20 | | 2005 | | | | 94.81 | 42 | 2.257 | 58 | Yes | NO | 40 | 23 | 4 | 10 | 3 | 0.48 |
| 21 | Cox | 2011 | RTOG 9410 | III | Y | 66.15 | 34 | 1.946 | 49 | Yes | NO | 195 | 0 | 4 | 81 | 110 | 0.32 |
| 22 | | 2011 | | | | 66.15 | 34 | 1.946 | 49 | Yes | YES | 194 | 0 | 2 | 84 | 108 | 0.37 |
| 23 | | 2011 | | | | 73.08 | 58 | 1.26 | 42 | Yes | YES | 187 | 0 | 4 | 75 | 108 | 0.32 |

| | | | | | | | | | | | | | | | | | |
|----|-------------|------|-------------|-------|---------|-------|------|-------|------|----------|-----|-----|----|----|-----|-----|-------|
| 24 | Sim | 2001 | New York | Local | Unknown | 70 | 35 | 2 | 47 | NONE | NO | 70 | 0 | 0 | 34 | 36 | 0.22 |
| 25 | | 2001 | | | | 70 | 35 | 2 | 47 | Yes | NO | 82 | 0 | 0 | 25 | 57 | 0.31 |
| 26 | de Ruyscher | 2008 | HI-CHART | I/II | N | 63.18 | 35.1 | 1.8 | 23.5 | Yes | NO | 48 | 12 | 9 | 12 | 15 | 0.36 |
| 27 | Chen | 2013 | NKI | Local | Unknown | 66 | 24 | 2.75 | 31 | Yes | YES | 171 | 0 | 17 | 102 | 52 | 0.42 |
| 28 | Uyterlinde | 2013 | NKI | Local | Unknown | 66 | 24 | 2.75 | 31 | Yes | YES | 187 | 0 | 19 | 108 | 60 | 0.53 |
| 29 | Belderbos | 2006 | NKI | I/II | Unknown | 81 | 36 | 2.25 | 42 | NONE | | 88 | 34 | 12 | 27 | 15 | 0.34 |
| 30 | Cannon | 2013 | Madison WI | I | Unknown | 67.5 | 25 | 2.7 | 35 | Yes | NO | 73 | 0 | 7 | 21 | 45 | 0.44 |
| 31 | Bradley | 2010 | RTOG 0117 | II | Unknown | 77.7 | 37 | 2.1 | 52 | Yes | YES | 53 | 3 | 6 | 38 | 6 | 0.53 |
| 32 | Thirion | 2004 | Dublin | I/II | Unknown | 72 | 24 | 3 | 35 | NONE | | 25 | 0 | 9 | 16 | 0 | 0.46 |
| 33 | Rosenzweig | 2005 | New York | I | Unknown | 77.8 | 43.2 | 1.8 | 60 | Yes | NO | 98 | 0 | 30 | 34 | 34 | 0.42 |
| 34 | Rengan | 2004 | New York | Local | Unknown | 60.48 | 28.8 | 2.1 | 40 | Yes | NO | 37 | 0 | 0 | 11 | 26 | 0.18 |
| 35 | | 2004 | | | | 73.5 | 35 | 2.1 | 49 | Yes | NO | 35 | 0 | 0 | 9 | 26 | 0.4 |
| 36 | Hayman | 2001 | Michigan | I | Unknown | 84 | 40 | 2.1 | 56 | some NEO | NO | 97 | 24 | 4 | 43 | 26 | 0.4 |
| 37 | de Ruyscher | 2012 | MAASTRO | III | Unknown | 60 | 30 | 2 | 42 | Yes | NO | 177 | 0 | 0 | 55 | 122 | 0.28 |
| 38 | | 2012 | | | | 64.8 | 36 | 1.8 | 25 | Yes | NO | 143 | 0 | 0 | 44 | 99 | 0.44 |
| 39 | Angela | 2012 | MAASTRO | II | Unknown | 65 | 40 | 1.625 | 35 | Yes | YES | 137 | 0 | 1 | 50 | 86 | 0.524 |
| 40 | Wurstbauer | 2007 | Salzburg | I | Unknown | 80.9 | 44.9 | 1.8 | 33 | NONE | | 79 | 19 | 4 | 31 | 25 | 0.56 |
| 41 | Nakayama | 2009 | Japan | Local | Unknown | 60 | 30 | 2 | 42 | Yes | NO | 50 | 0 | 0 | 16 | 34 | 0.18 |
| 42 | | 2009 | | | | 69.4 | 35 | 1.983 | 49 | Yes | NO | 50 | 0 | 0 | 16 | 34 | 0.36 |
| 43 | Maguire | 2001 | Duke | II | Unknown | 76.8 | 48 | 1.6 | 34 | NONE | | 94 | 19 | 3 | 40 | 32 | 0.41 |
| 44 | Maguire | 2014 | SOCCAR | II | Y | 55 | 20 | 2.75 | 28 | Yes | YES | 70 | 0 | 0 | 31 | 39 | 0.5 |
| 45 | | 2014 | | | | 55 | 20 | 2.75 | 28 | Yes | NO | 60 | 0 | 0 | 26 | 34 | 0.46 |
| 46 | Adkison | 2008 | Madison WI | I | N | 75 | 25 | 3 | 35 | NONE | | 42 | 2 | 5 | 12 | 23 | 0.47 |
| 47 | Kepka | 2009 | Poland | Local | Unknown | 57.8 | 21 | 2.752 | 28 | NONE | | 173 | 0 | 0 | 96 | 77 | 0.32 |
| 48 | Harada | 2013 | Japan | II | Unknown | 74.6 | 37 | 2.016 | 51.8 | Yes | YES | 24 | 0 | 0 | 20 | 4 | 0.6 |
| 49 | Kaira | 2013 | Japan | II | Unknown | 60 | 30 | 2 | 42 | Yes | YES | 41 | 0 | 0 | 24 | 17 | 0.53 |
| 50 | Socinski | 2008 | CALGB 30105 | II | Y | 74 | 37 | 2 | 51.8 | Yes | YES | 42 | 0 | 0 | 26 | 16 | 0.5 |
| 51 | | 2008 | | | | 74 | 37 | 2 | 51.8 | Yes | YES | 26 | 0 | 0 | 10 | 16 | 0.39 |
| 52 | Movsas | 2005 | RTOG 9801 | III | Y | 73.08 | 58 | 1.26 | 40.6 | Yes | YES | 242 | 0 | 4 | 120 | 118 | 0.37 |

Appendix 2. Detail of cCRT-ICB dataset. Authors, published year, study names, RT dose, Fx, dose-per-Fx, RT days, chemotherapy conditions, patient numbers with staging, 2-year OS, and ICB information were listed.

| 1 | Author | Year | Study | Dose | Fx | Dose_perFx | RT_Days | Concurrent | Pt | Stage_I | Stage_II | Stage_IIIA | Stage_IIIBC | OS | ICB_drug | Drug_type | ICB_schedule |
|----|---------------|------|---------------------|------|----|------------|---------|----------------------|------|---------|----------|------------|-------------|-------|----------------------|-----------|--------------|
| 2 | Durm | 2019 | LUN-14-179 | 60 | 30 | 2 | 40 | YES | 92 | 0 | 0 | 55 | 37 | 0.62 | Pembrolizumab | PD1 | post_cCRT |
| 3 | Lin | 2020 | DETERRED | 66 | 33 | 2 | 45 | YES | 10 | 0 | 1 | 2 | 7 | 0.44 | Atezolizumab | PDL1 | post_cCRT |
| 4 | | 2020 | | 66 | 33 | 2 | 45 | YES | 30 | 0 | 5 | 12 | 13 | 0.8 | Atezolizumab | PDL1 | con_cCRT |
| 5 | Antonia | 2018 | PACIFIC | 60 | 30 | 2 | 40 | YES | 472 | 1 | 7 | 252 | 212 | 0.663 | Durvalumab | PDL1 | post_cCRT |
| 6 | Peters | 2021 | NICOLAS | 66 | 33 | 2 | 45 | YES | 78 | 0 | 0 | 28 | 50 | 0.637 | Nivolumab | PD1 | con_cCRT |
| 7 | Reck, Jabbour | 2022 | KEYNOTE-799 | 60 | 30 | 2 | 40 | YES | 112 | 0 | 0 | 41 | 71 | 0.643 | Pembrolizumab | PD1 | con_cCRT |
| 8 | | 2022 | | 60 | 30 | 2 | 40 | YES | 102 | 0 | 0 | 39 | 63 | 0.712 | Pembrolizumab | PD1 | con_cCRT |
| 9 | Bryant | 2022 | Institutional study | 60 | 30 | 2 | 40 | YES | 1006 | 0 | 0 | 574 | 432 | 0.619 | Durvalumab | PDL1 | post_cCRT |
| 10 | Landman | 2021 | Institutional study | 69.9 | 35 | 2 | 47 | YES | 39 | 0 | 0 | 27 | 12 | 0.68 | Durvalumab | PDL1 | post_cCRT |
| 11 | Zhou | 2022 | GEMSTONE-301 | 60 | 30 | 2 | 40 | YES (34% sequential) | 255 | 0 | 2 | 74 | 179 | 0.808 | Sugemalimab (CS1001) | PDL1 | post_cCRT |

Chapter 9. Bibliography

1. Hanahan, D. & Weinberg, R. A. The hallmarks of cancer. *Cell* **100**, 57–70 (2000).
2. Hanahan, D. & Weinberg, R. A. Hallmarks of cancer: the next generation. *Cell* **144**, 646–674 (2011).
3. Hanahan, D. Hallmarks of cancer: new dimensions. *Cancer Discov* **12**, 31–46 (2022).
4. Siegel, R. L., Miller, K. D. & Jemal, A. Cancer statistics, 2020. *CA Cancer J Clin* **70**, 7–30 (2020).
5. Bade, B. C. & Dela Cruz, C. S. Lung cancer 2020: epidemiology, etiology, and prevention. *Clin Chest Med* **41**, 1–24 (2020).
6. Ferlay, J. *et al.* Cancer incidence and mortality patterns in europe: estimates for 40 countries and 25 major cancers in 2018. *Eur J Cancer* **103**, 356–387 (2018).
7. Lung cancer statistics; <https://www.cancerresearchuk.org/health-professional/cancer-statistics/statistics-by-cancer-type/lung-cancer#heading-One>. *Cancer Research UK* (2023).
8. Schabath, M. B. & Cote, M. L. Cancer progress and priorities: lung cancer. *Cancer Epidemiology Biomarkers and Prevention* **28**, 1563–1579 (2019).
9. <https://www.who.int/news-room/fact-sheets/detail/cancer>. *World Health Organization* (2022).
10. Lung cancer mortality statistics; <https://www.cancerresearchuk.org/health-professional/cancer-statistics/statistics-by-cancer-type/lung-cancer/mortality#heading-Zero>. *Cancer Research UK* (2022).

11. Van Schil, P. E. *et al.* Metastatic non-small cell lung cancer: ESMO clinical practice guidelines for diagnosis, treatment and follow-up. *Annals of Oncology* **29**, iv192–iv237 (2018).
12. Zappa, C. & Mousa, S. A. Non-small cell lung cancer: current treatment and future advances. *Transl Lung Cancer Res* **5**, 288–300 (2016).
13. Goldstraw, P. *et al.* The IASLC lung cancer staging project: proposals for revision of the TNM stage groupings in the forthcoming (eighth) edition of the TNM Classification for lung cancer. *Journal of Thoracic Oncology* **11**, 39–51 (2016).
14. Amin, M. B. *et al.* The eighth edition AJCC cancer staging manual: continuing to build a bridge from a population-based to a more “personalized” approach to cancer staging. *CA Cancer J Clin* **67**, 93–99 (2017).
15. Ettinger, D. S. *et al.* NCCN Guidelines® insights: non-small cell lung cancer, version 2.2023. *J Natl Compr Canc Netw* **21**, 340–350 (2023).
16. Spyrtos, D. *et al.* Preoperative evaluation for lung cancer resection. *J Thorac Dis* **6**, S162–S166 (2014).
17. Brunelli, A. *et al.* Physiologic evaluation of the patient with lung cancer being considered for resectional surgery: diagnosis and management of lung cancer, 3rd ed: American college of chest physicians evidence-based clinical practice guidelines. *Chest* **143**, e166S–e190S (2013).
18. Lung cancer: early and locally-advanced non-small cell lung cancer. *NCCN Guidelines for Patients* (2019).
19. Al-Shahrabani, F. *et al.* Surgical strategies in the therapy of non-small cell lung cancer. *World J Clin Oncol* **5**, 595–603 (2014).

20. Howington, J. A. *et al.* Treatment of stage I and II non-small cell lung cancer: diagnosis and management of lung cancer, 3rd ed: American college of chest physicians evidence-based clinical practice guidelines. *Chest* **143**, e278S-e313S (2013).
21. Ramalingam, S. & Belani, C. Systemic chemotherapy for advanced non-small cell lung cancer: recent advances and future directions. *The Oncologist* vol. 13 5–13 Preprint at <https://doi.org/10.1634/theoncologist.13-s1-5> (2008).
22. Pisters, K. M. W. *et al.* Cancer Care Ontario and American Society of Clinical Oncology adjuvant chemotherapy and adjuvant radiation therapy for stages I-IIIa resectable non-small-cell lung cancer guideline. *Journal of Clinical Oncology* **25**, 5506–5518 (2007).
23. Ngwa, W. *et al.* Using immunotherapy to boost the abscopal effect. *Nat Rev Cancer* **18**, 313–322 (2018).
24. Liu, Y. *et al.* Abscopal effect of radiotherapy combined with immune checkpoint inhibitors. *J Hematol Oncol* **11**, 1–15 (2018).
25. Tray, N., Weber, J. S. & Adams, S. Predictive biomarkers for checkpoint immunotherapy: current status and challenges for clinical application. *Cancer Immunol Res* **6**, 1122–1128 (2018).
26. Teng, F. *et al.* Progress and challenges of predictive biomarkers of anti PD-1/PD-L1 immunotherapy: a systematic review. *Cancer Lett* **414**, 166–173 (2018).
27. Reck, M. & Rabe, K. F. Precision diagnosis and treatment for advanced non-small-cell lung cancer. *New England Journal of Medicine* **377**, 849–861 (2017).

28. Cooper, W. A. *et al.* PD-L1 expression is a favorable prognostic factor in early stage non-small cell carcinoma. *Lung Cancer* **89**, 181–188 (2015).
29. Califano, R. *et al.* Patient selection for anti-PD-1/PD-L1 therapy in advanced non-small-cell lung cancer: implications for clinical practice. *Future Oncology* **14**, 2415–2431 (2018).
30. Yu, H. *et al.* PD-L1 expression in lung cancer. *Journal of Thoracic Oncology* **11**, 964–975 (2016).
31. Cheng, M. *et al.* Modern radiation further improves survival in non-small cell lung cancer: an analysis of 288,670 patients. *J Cancer* **10**, 168–177 (2019).
32. Vansteenkiste, J. *et al.* Early and locally advanced non-small-cell lung cancer (NSCLC): ESMO clinical practice guidelines for diagnosis, treatment and follow-up. *Annals of Oncology* **24**, vi89–vi98 (2013).
33. The Royal College of Radiologists. *Radiotherapy dose fractionation, third edition.* (2019).
34. Baker, S. *et al.* A critical review of recent developments in radiotherapy for non-small cell lung cancer. *Radiation Oncology* **11**, (2016).
35. Robinson, C. G. *et al.* Patterns of failure after stereotactic body radiation therapy or lobar resection for clinical stage I non-small-cell lung cancer. *Journal of Thoracic Oncology* **8**, 192–201 (2013).
36. Senthil, S. *et al.* Outcomes of stereotactic ablative radiotherapy for central lung tumours: a systematic review. *Radiotherapy and Oncology* **106**, 276–282 (2013).
37. Tekatli, H. *et al.* Stereotactic ablative radiotherapy (SABR) for central lung tumors: plan quality and long-term clinical outcomes. *Radiotherapy and Oncology* **117**, 64–70 (2015).

38. Yan, M. *et al.* Stereotactic body radiotherapy for ultra-central lung tumors: a systematic review and meta-analysis and International Stereotactic Radiosurgery Society practice guidelines. *Lung Cancer* **182**, 107281 (2023).
39. Nix, M. G. *et al.* Chemoradiotherapy of locally-advanced non-small cell lung cancer: analysis of radiation dose-response, chemotherapy and survival-limiting toxicity effects indicates a low α/β ratio. *Radiotherapy and Oncology* **143**, 58–65 (2020).
40. Van Meerbeeck, J. P. *et al.* Randomized controlled trial of resection versus radiotherapy after induction chemotherapy in stage IIIA-N2 non-small-cell lung cancer. *J Natl Cancer Inst* **99**, 442–450 (2007).
41. Albain, K. S. *et al.* Radiotherapy plus chemotherapy with or without surgical resection for stage III non-small-cell lung cancer: a phase III randomised controlled trial. *The Lancet* **374**, 379–386 (2009).
42. Pless, M. *et al.* Induction chemoradiation in stage IIIA/N2 non-small-cell lung cancer: a phase 3 randomised trial. *The Lancet* **386**, 1049–1056 (2015).
43. Ettinger, D. S. *et al.* NCCN clinical guidelines in oncology: non-small cell lung cancer. *National Comprehensive Cancer Network* (2020).
44. Yan, M. *et al.* The radiation dose tolerance of the brachial plexus: a systematic review and meta-analysis. *Clin Transl Radiat Oncol* **18**, 23–31 (2019).
45. Giaddui, T. *et al.* Establishing the feasibility of the dosimetric compliance criteria of RTOG 1308: phase III randomized trial comparing overall survival after photon versus proton radiochemotherapy for inoperable stage II-IIIB NSCLC. *Radiation Oncology* **11**, 1–7 (2016).

46. Vyfhuis, M. A. L. *et al.* Advances in proton therapy in lung cancer. *Ther Adv Respir Dis* **12**, 1–16 (2018).
47. Liao, Z. *et al.* Bayesian adaptive randomization trial of passive scattering proton therapy and intensity-modulated photon radiotherapy for locally advanced non-small-cell lung cancer. *Journal of Clinical Oncology* **36**, 1813–1822 (2018).
48. Perez, C. A. *et al.* A prospective randomized study of various irradiation doses and fractionation schedules in the treatment of inoperable non-oat-cell carcinoma of the lung: preliminary report by the Radiation Therapy Oncology Group. *Cancer* **45**, 2744–2753 (1980).
49. Din, O. S. *et al.* Routine use of continuous, hyperfractionated, accelerated radiotherapy for non-small-cell lung cancer: a five-center experience. *Int J Radiat Oncol Biol Phys* **72**, 716–722 (2008).
50. Hatton, M. Q. F. *et al.* Accelerated, dose escalated, sequential chemoradiotherapy in non-small-cell lung cancer (ADSCaN): a protocol for a randomised phase II study. *BMJ Open* **9**, 1–7 (2019).
51. Kong, F. M. *et al.* High-dose radiation improved local tumor control and overall survival in patients with inoperable/unresectable non-small-cell lung cancer: long-term results of a radiation dose escalation study. *Int J Radiat Oncol Biol Phys* **63**, 324–333 (2005).
52. Machtay, M. *et al.* Higher biologically effective dose of radiotherapy is associated with improved outcomes for locally advanced non-small cell lung carcinoma treated with chemoradiation: an analysis of the radiation therapy oncology group. *Int J Radiat Oncol Biol Phys* **82**, 425–434 (2012).
53. Bradley, J. D. *et al.* A phase I/II radiation dose escalation study with concurrent chemotherapy for patients with inoperable stages I to III non-

small-cell lung cancer: phase I results of RTOG 0117. *Int J Radiat Oncol Biol Phys* **77**, 367–372 (2010).

54. Bradley, J. D. *et al.* Standard-dose versus high-dose conformal radiotherapy with concurrent and consolidation carboplatin plus paclitaxel with or without cetuximab for patients with stage IIIA or IIIB non-small-cell lung cancer (RTOG 0617): a randomised, two-by-two factorial phase 3 study. *Lancet Oncol* **16**, 187–199 (2015).
55. Movsas, B. *et al.* Quality of life analysis of a radiation dose-escalation study of patients with non-small-cell lung cancer a secondary analysis of the Radiation Therapy Oncology Group 0617 randomized clinical trial. *JAMA Oncol* **2**, 359–367 (2016).
56. Fenwick, J. D. *et al.* Long-term results from the IDEAL-CRT phase 1/2 trial of isotoxically dose-escalated radiation therapy and concurrent chemotherapy for stage II/III non-small cell lung cancer. *Int J Radiat Oncol Biol Phys* **106**, 733–742 (2020).
57. Bradley, J. D. *et al.* Long-term results of NRG oncology RTOG 0617: standard-versus high-dose chemoradiotherapy with or without cetuximab for unresectable stage III non-small-cell lung cancer. *Journal of Clinical Oncology* **38**, 706–714 (2020).
58. Ma, L. *et al.* A current review of dose-escalated radiotherapy in locally advanced non-small cell lung cancer. *Radiol Oncol* **53**, 6–14 (2019).
59. Van Diessen, J. *et al.* The acute and late toxicity results of a randomized phase II dose-escalation trial in non-small cell lung cancer (PET-boost trial). *Radiotherapy and Oncology* **131**, 166–173 (2019).

60. Zehentmayr, F. *et al.* Radiation dose escalation with modified fractionation schedules for locally advanced NSCLC: a systematic review. *Thoracic Cancer* **11**, 1375–1385 (2020).
61. Fenwick, J. D. *et al.* Escalation and intensification of radiotherapy for stage III non-small cell lung cancer: opportunities for treatment improvement. *Clin Oncol* **21**, 343–360 (2009).
62. Partridge, M. *et al.* Dose escalation for non-small cell lung cancer: analysis and modelling of published literature. *Radiotherapy and Oncology* **99**, 6–11 (2011).
63. Gotwals, P. *et al.* Prospects for combining targeted and conventional cancer therapy with immunotherapy. *Nat Rev Cancer* **17**, 286–301 (2017).
64. Fridman, W. H. *et al.* The immune contexture in cancer prognosis and treatment. *Nat Rev Clin Oncol* **14**, 717–734 (2017).
65. Patel, S. P. & Kurzrock, R. PD-L1 expression as a predictive biomarker in cancer immunotherapy. *Mol Cancer Ther* **14**, 847–856 (2015).
66. D’Incecco, A. *et al.* PD-1 and PD-L1 expression in molecularly selected non-small-cell lung cancer patients. *Br J Cancer* **112**, 95–102 (2015).
67. Althammer, S. *et al.* Automated image analysis of NSCLC biopsies to predict response to anti-PD-L1 therapy. *J Immunother Cancer* **7**, 1–12 (2019).
68. Stewart, R. *et al.* Identification and characterization of MEDI4736, an antagonistic anti-PD-L1 monoclonal antibody. *Cancer Immunol Res* **3**, 1052–1062 (2015).
69. Deng, L. *et al.* Irradiation and anti-PD-L1 treatment synergistically promote antitumor immunity in mice. *Journal of clinical investigation* **124**, 687–695 (2014).

70. Antonia, S. J. *et al.* Phase 1/2 study of the safety and clinical activity of durvalumab in patients with non-small cell lung cancer (NSCLC). *Annals of Oncology* **27**, vi421 (2016).
71. Antonia, S. J. *et al.* Durvalumab after chemoradiotherapy in stage III non-small-cell lung cancer. *New England Journal of Medicine* **377**, 1919–1929 (2017).
72. Antonia, S. J. *et al.* Overall survival with durvalumab after chemoradiotherapy in stage III NSCLC. *New England Journal of Medicine* **379**, 2342–2350 (2018).
73. Bang, A., Schoenfeld, J. D. & Sun, A. Y. Pacific: shifting tides in the treatment of locally advanced non-small cell lung cancer. *Transl Lung Cancer Res* **8**, S139–S146 (2019).
74. Peters, S. *et al.* Safety evaluation of nivolumab added concurrently to radiotherapy in a standard first line chemo-radiotherapy regimen in stage III non-small cell lung cancer - the ETOP NICOLAS trial. *Lung Cancer* **133**, 83–87 (2019).
75. Bradley, J. D. *et al.* PACIFIC-2: phase 3 study of concurrent durvalumab and platinum-based chemoradiotherapy in patients with unresectable, stage III NSCLC. *Journal of Clinical Oncology* **37**, TPS8573–TPS8573 (2019).
76. Tachihara, M. *et al.* Rationale and design for a multicenter, phase II study of durvalumab plus concurrent radiation therapy in locally advanced non-small cell lung cancer: the DOLPHIN study (WJOG11619L). *Cancer Manag Res* **13**, 9167–9173 (2021).
77. Chang, D. S. *et al.* *Basic radiotherapy physics and biology*. (Springer Cham, 2014).

78. Beyzadeoglu, M., Ozyigit, G. & Ebruli, C. *Basic radiation oncology*. (Springer Berlin Heidelberg, 2010).
79. Lally, B. E. *et al.* The risk of death from heart disease in patients with nonsmall cell lung cancer who receive postoperative radiotherapy: analysis of the surveillance, epidemiology, and end results database. *Cancer* **110**, 911–917 (2007).
80. Karakoyun-Celik, O. *et al.* Postoperative radiotherapy in the management of resected non-small-cell lung carcinoma: 10 years' experience in a single institute. *Int J Radiat Oncol Biol Phys* **76**, 433–439 (2010).
81. Hardy, D. *et al.* Cardiac toxicity in association with chemotherapy and radiation therapy in a large cohort of older patients with non-small-cell lung cancer. *Annals of Oncology* **21**, 1825–1833 (2010).
82. McWilliam, A. *et al.* Demystifying cardiac dose in RTOG-0617. *Int J Radiat Oncol Biol Phys* **111**, S125 (2021).
83. Landau, D. B. *et al.* IDEAL-CRT: a phase 1/2 trial of isotoxic dose-escalated radiation therapy and concurrent chemotherapy in patients with stage II/III non-small cell lung cancer. *Int J Radiat Oncol Biol Phys* **95**, 1367–1377 (2016).
84. Maguire, J. *et al.* SOCCAR: a randomised phase II trial comparing sequential versus concurrent chemotherapy and radical hypofractionated radiotherapy in patients with inoperable stage III non-small cell lung cancer and good performance status. *Eur J Cancer* **50**, 2939–2949 (2014).
85. Phernambucq, E. C. J. *et al.* Outcomes of concurrent chemoradiotherapy in patients with stage III non-small-cell lung cancer and significant comorbidity. *Annals of Oncology* **22**, 132–138 (2011).

86. Van Baardwijk, A. *et al.* Mature results of a phase II trial on individualised accelerated radiotherapy based on normal tissue constraints in concurrent chemo-radiation for stage III non-small cell lung cancer. *Eur J Cancer* **48**, 2339–2346 (2012).
87. Pöttgen, C. *et al.* Accelerated hyperfractionated radiotherapy within trimodality therapy concepts for stage IIIA/B non-small cell lung cancer: markedly higher rate of pathologic complete remissions than with conventional fractionation. *Eur J Cancer* **49**, 2107–2115 (2013).
88. Enami, B. Tolerance of normal tissue to therapeutic irradiation. *Reports of Radiotherapy and Oncology* **1**, 35–48 (2013).
89. Stam, B. *et al.* Dose to heart substructures is associated with non-cancer death after SBRT in stage I–II NSCLC patients. *Radiotherapy and Oncology* **123**, 370–375 (2017).
90. Loap, P., Fourquet, A. & Kirova, Y. Should we move beyond mean heart dose? *Int J Radiat Oncol Biol Phys* **107**, 386–387 (2020).
91. Common Terminology Criteria for Adverse Events (CTCAE) v.5.0. *National Cancer Institute* (2017).
92. Cox, J. D., Stetz, J. A. & Pajak, T. F. Toxicity criteria of the Radiation Therapy Oncology Group (RTOG) and the European organization for research and treatment of cancer (EORTC). *Int J Radiat Oncol Biol Phys* **31**, 1341–1346 (1995).
93. Baker, S. & Fairchild, A. Radiation-induced esophagitis in lung cancer. *Lung Cancer: Targets and Therapy* **7**, 119–127 (2016).
94. Werner-Wasik, M. *et al.* Normal-tissue toxicities of thoracic radiation therapy: esophagus, lung, and spinal cord as organs at risk. *Hematol Oncol Clin North Am* **18**, 131–160 (2004).

95. Trott, K. R., Herrmann, T. & Kasper, M. Target cells in radiation pneumopathy. *Int J Radiat Oncol Biol Phys* **58**, 463–469 (2004).
96. Ding, N.-H., Li, J. & Sun, L.-Q. Molecular mechanisms and treatment of radiation-induced lung fibrosis. *Curr Drug Targets* **14**, 1347–1356 (2013).
97. Giuranno, L. *et al.* Radiation-induced lung injury (RILI). *Front Oncol* **9**, 1–16 (2019).
98. Rancati, T. *et al.* Factors predicting radiation pneumonitis in lung cancer patients: a retrospective study. *Radiotherapy and Oncology* **67**, 275–283 (2003).
99. Bentzen, S. M. *et al.* Quantitative Analyses of Normal Tissue Effects in the Clinic (QUANTEC): an introduction to the scientific issues. *Int J Radiat Oncol Biol Phys* **76** (3), S3–S9 (2010).
100. Banfill, K. *et al.* Cardiac toxicity of thoracic radiotherapy: existing evidence and future directions. *Journal of Thoracic Oncology* **16**, 216–227 (2021).
101. Madan, R. *et al.* Radiation induced heart disease: pathogenesis, management and review literature. *J Egypt Natl Canc Inst* **27**, 187–193 (2015).
102. Thor, M. *et al.* Modeling the impact of cardiopulmonary irradiation on overall survival in NRG oncology trial RTOG 0617. *Clinical Cancer Research* **26**, 4643–4650 (2020).
103. Chun, S. G. *et al.* Impact of intensity-modulated radiation therapy technique for locally advanced non-small-cell lung cancer: a secondary analysis of the NRG oncology RTOG 0617 randomized clinical trial. *Journal of Clinical Oncology* **35**, 56–62 (2017).

104. Guberina, M. *et al.* Heart dose exposure as prognostic marker after radiotherapy for resectable stage IIIA/B non-small-cell lung cancer: secondary analysis of a randomized trial. *Ann Oncol* **28**, 1084–1089 (2017).
105. Faivre-Finn, C. Dose escalation in lung cancer: have we gone full circle? *Lancet Oncol* **16**, 125–127 (2015).
106. Papanikolaou, N. *et al.* AAPM report 85: tissue inhomogeneity corrections for megavoltage photon beams. *American Association of Physicists in Medicine* (2004).
107. Frank, S. J. *et al.* Treatment planning for lung cancer: traditional homogeneous point-dose prescription compared with heterogeneity-corrected dose-volume prescription. *Int J Radiat Oncol Biol Phys* **56**, 1308–1318 (2003).
108. Turtle, L. *et al.* Cardiac-sparing radiotherapy for locally advanced non-small cell lung cancer. *Radiation Oncology* **16**, 95 (2021).
109. Teoh, S. *et al.* Proton vs photon: a model-based approach to patient selection for reduction of cardiac toxicity in locally advanced lung cancer. *Radiotherapy and Oncology* **152**, 151–162 (2020).
110. Khan, F. M. & Gibbons, J. P. *The physics of radiation therapy, sixth edition.* (Wolters Kluwer, 2020).
111. Sureka, C. S. & Armpilia, C. *Radiation biology for medical physicists.* (Taylor & Francis, 2017).
112. Brand, D. H. & Yarnold, J. R. The linear-quadratic model and implications for fractionation. *Clin Oncol* **31**, 673–677 (2019).
113. McMahon, S. J. The linear quadratic model: usage, interpretation and challenges. *Phys Med Biol* **64**, 01TR01 (2019).

114. Zaider, M. *et al.* Tumour control probability: a formulation applicable to any temporal protocol of dose delivery. *Phys Med Biol* **45**, 279 (2000).
115. Jones, B. Modelling carcinogenesis after radiotherapy using Poisson statistics: implications for IMRT, protons and ions. *Journal of Radiological Protection* **29**, (2009).
116. Cho, G. A. *et al.* Radiation treatment dose optimisation using Poisson tumour control probability parameters. *J Phys Conf Ser* **489**, (2014).
117. Fenwick, J. D. Predicting the radiation control probability of heterogeneous tumour ensembles: data analysis and parameter estimation using a closed-form expression. *Phys Med Biol* **43**, 2159–2178 (1998).
118. Keall, P. J. & Webb, S. Optimum parameters in a model for tumour control probability, including interpatient heterogeneity: evaluation of the log-normal distribution. *Phys Med Biol* **52**, 291–302 (2007).
119. Buffa, F. M., Fenwick, J. D. & Nahum, A. E. An analysis of the relationship between radiosensitivity and volume effects in tumor control probability modeling. *Med Phys* **27**, 1258–1265 (2000).
120. Cella, L. *et al.* Complication probability models for radiation-induced heart valvular dysfunction: do heart-lung interactions play a role? *PLoS One* **9**, 1–11 (2014).
121. Cella, L. *et al.* Multivariate normal tissue complication probability modeling of gastrointestinal toxicity after external beam radiotherapy for localized prostate cancer. *Radiation Oncology* **8**, 221 (2013).
122. Katz, M. H. *Multivariable analysis*. (Cambridge University Press, 2011).
123. Kleinbaum, D. G. & Klein, M. *Logistic regression: a self-learning text (2nd ed.)*. (New York: Springer-Verlag, 2002).

124. Bewick, V., Cheek, L. & Ball, J. Statistics review 14: logistic regression. *Crit Care* **9**, 112–118 (2005).
125. Bradburn, M. J. *et al.* Survival analysis part II: multivariate data analysis - an introduction to concepts and methods. *Br J Cancer* **89**, 431–436 (2003).
126. Cox, D. R. Regression models and life-tables. *Journal of the Royal Statistical Society* **34**, 187–220 (1972).
127. Konishi, S. & Kitagawa, G. *Information criteria and statistical modeling*. (Springer New York, 2008).
128. Cui, S., *et al.* Introduction to machine and deep learning for medical physicists. *Med Phys* **47**, e127–e147 (2020).
129. Myung, I. J. Tutorial on maximum likelihood estimation. *J Math Psychol* **47**, 90–100 (2003).
130. Bolker, Ben. Maximum likelihood estimation and analysis with the bbmle package. <https://cran.r-project.org/package=bbmle> (2014).
131. Held, L. & Sabanés Bové, D. *Applied statistical inference: likelihood and bayes*. (Springer Berlin, Heidelberg, 2014).
132. Harel, O. & Zhou, X. H. Multiple imputation: review of theory, implementation and software. *Statistics in Medicine* (2007).
133. Sugden, R. A. & Rubin, D. B. Multiple imputation for nonresponse in surveys. *J R Stat Soc Ser A Stat Soc* (1988).
134. Evans, J. D. *Straightforward statistics for the behavioral sciences*. (Thomson Brooks/Cole Publishing Co, 1996).
135. O'Brien, R. M. A caution regarding rules of thumb for variance inflation factors. *Qual Quant* **41**, 673–690 (2007).

136. Pourhoseingholi, M. A., Baghestani, A. R. & Vahedi, M. How to control confounding effects by statistical analysis. *Gastroenterol Hepatol Bed Bench* **5**, 79–83 (2012).
137. Zhang, Z. Variable selection with stepwise and best subset approaches. *Ann Transl Med* **4**, 1–6 (2016).
138. Anderson, D. R., Burnham, K. P. & White, G. C. AIC model selection in overdispersed capture-recapture data. *Ecology* **75**, 1780–1793 (1994).
139. Akaike, H. A new look at the statistical model identification. *IEEE Trans Automat Contr* **19**, 716–723 (1974).
140. Heinze, G., Wallisch, C. & Dunkler, D. Variable selection - a review and recommendations for the practicing statistician. *Biometrical Journal* **60**, 431–449 (2018).
141. Roberts, S. A., Hendry, J. H. & Potten, C. S. Intestinal crypt clonogens: a new interpretation of radiation survival curve shape and clonogenic cell number. *Cell Prolif* **36**, 215–231 (2003).
142. Berrar, D. Cross-validation. *Encyclopedia of Bioinformatics and Computational Biology: ABC of Bioinformatics* **1**, 542–545 (2019).
143. Kreutz, C. *et al.* Profile likelihood in systems biology. *FEBS Journal* (2013).
144. Aitkin, M. Profile likelihood. *Wiley StatsRef: statistics reference online* (John Wiley & Sons, 2014).
145. Barbur, V. A., Montgomery, D. C. & Peck, E. A. *Introduction to linear regression analysis (6th edition)*. (Wiley, 2021).

146. Postmus, P. E. *et al.* Early and locally advanced non-small-cell lung cancer (NSCLC): ESMO clinical practice guidelines for diagnosis, treatment and follow-up. *Annals of Oncology* **28**, iv1–iv21 (2017).
147. Aupérin, A. *et al.* Meta-analysis of concomitant versus sequential radiochemotherapy in locally advanced non-small-cell lung cancer. *Journal of Clinical Oncology* **28**, 2181–2190 (2010).
148. Stewart, L. A. & Pignon, J. P. Chemotherapy in non-small cell lung cancer: a meta-analysis using updated data on individual patients from 52 randomised clinical trials. *Br Med J* **311**, 899–909 (1995).
149. Ramroth, J. *et al.* Dose and fractionation in radiation therapy of curative intent for non-small cell lung cancer: meta-analysis of randomized trials. *Int J Radiat Oncol Biol Phys* **96**, 736–747 (2016).
150. Majem, M. *et al.* Multidisciplinary consensus statement on the clinical management of patients with stage III non-small cell lung cancer. *Clinical and Translational Oncology* **22**, 21–36 (2020).
151. Kalemkerian, G. P. *et al.* Small cell lung cancer: clinical practice guidelines in oncology. *JNCCN Journal of the National Comprehensive Cancer Network* **11**, 78–98 (2013).
152. De Ruyscher, D. *et al.* Individualized accelerated isotoxic concurrent chemo-radiotherapy for stage III non-small cell lung cancer: 5-year results of a prospective study. *Radiotherapy and Oncology* **135**, 141–146 (2019).
153. Bucci, M. K., Bevan, A. & Roach, M. Advances in radiation therapy: conventional to 3D, to IMRT, to 4D, and beyond. *CA Cancer J Clin* **55**, 117–134 (2005).

154. Gianfaldoni, S. *et al.* An overview on radiotherapy: from its history to its current applications in dermatology. *Open Access Maced J Med Sci* **5**, 521–525 (2017).
155. Boyd, J. A. *et al.* Timing of local and distant failure in resected lung cancer: Implications for reported rates of local failure. *Journal of Thoracic Oncology* (2010).
156. Ginestet, C. ggplot2: elegant graphics for data analysis. *J R Stat Soc Ser A Stat Soc* **174**, 245–246 (2011).
157. Pawitan, Y. *In all likelihood: statistical modelling and inference using likelihood.* (Oxford University Press, 2001).
158. Wei, T. & Simko, V. R package ‘corrplot’: visualization of a correlation matrix (version 0.84). <https://cran.r-project.org/package=corrplot> (2017).
159. Richards, S. A. Dealing with overdispersed count data in applied ecology. *Journal of Applied Ecology* **45**, 218–227 (2008).
160. Okunieff, P. *et al.* Radiation dose-response of human tumors. *Int J Radiat Oncol Biol Phys* **32**, 1227–1237 (1995).
161. D’Alterio, C. *et al.* Paradoxical effects of chemotherapy on tumor relapse and metastasis promotion. *Semin Cancer Biol* **60**, 351–361 (2020).
162. Brenner, D. J. Accelerated repopulation during radiotherapy: quantitative evidence for delayed onset. *Radiat Oncol Investig* **1**, 167–172 (1993).
163. Ghosh-Laskar, S. *et al.* Conventional radiotherapy versus concurrent chemoradiotherapy versus accelerated radiotherapy in locoregionally advanced carcinoma of head and neck: results of a prospective randomized trial. *Head Neck* **38**, 202–207 (2016).

164. Nguyen-Tan, P. F. *et al.* Randomized phase III trial to test accelerated versus standard fractionation in combination with concurrent cisplatin for head and neck carcinomas in the radiation therapy oncology group 0129 trial: long-term report of efficacy and toxicity. *Journal of Clinical Oncology* **32**, 3858–3867 (2014).
165. Topkan, E. *et al.* Significance of overall concurrent chemoradiotherapy duration on survival outcomes of stage IIIB/C non-small-cell lung carcinoma patients: analysis of 956 patients. *PLoS One* **14**, 1–15 (2019).
166. Klement, R. J. *et al.* Estimation of the α/β ratio of non-small cell lung cancer treated with stereotactic body radiotherapy. *Radiotherapy and Oncology* **142**, 210–216 (2020).
167. Scott, J. G. *et al.* A genome-based model for adjusting radiotherapy dose (GARD): a retrospective, cohort-based study. *Lancet Oncol* **18**, 202–211 (2017).
168. Sun, Y. *et al.* Serum microRNA signature predicts response to high-dose radiation therapy in locally advanced non-small cell lung cancer. *Int J Radiat Oncol Biol Phys* **100**, 107–114 (2018).
169. Santiago, A. *et al.* Challenges in radiobiological modeling: can we decide between LQ and LQ-L models based on reviewed clinical NSCLC treatment outcome data? *Radiation Oncology* **11**, 67 (2016).
170. Jeong, J. *et al.* Modeling the cellular response of lung cancer to radiation therapy for a broad range of fractionation schedules. *Clinical Cancer Research* **23**, 5469–5479 (2017).
171. Van Leeuwen, C. M. *et al.* The alpha and beta of tumours: a review of parameters of the linear-quadratic model, derived from clinical radiotherapy studies. *Radiation Oncology* **13**, 1–11 (2018).

172. Tamponi, M. *et al.* Prostate cancer dose-response, fractionation sensitivity and repopulation parameters evaluation from 25 international radiotherapy outcome data sets. *British Journal of Radiology* **92**, 20180823 (2019).
173. Jin, J. Y. *et al.* Use a survival model to correlate single-nucleotide polymorphisms of DNA repair genes with radiation dose-response in patients with non-small cell lung cancer. *Radiotherapy and Oncology* **117**, 77–82 (2015).
174. Chen, X. *et al.* Plasma miRNAs in predicting radiosensitivity in non-small cell lung cancer. *Tumor Biology* **37**, 11927–11936 (2016).
175. Ma, W. *et al.* Up- regulation of miR-328-3p sensitizes non-small cell lung cancer to radiotherapy. *Sci Rep* **6**, 31651 (2016).
176. Cortez, M. A. *et al.* Therapeutic delivery of miR-200c enhances radiosensitivity in lung cancer. *Molecular Therapy* **22**, 1494–1503 (2014).
177. Li, J. *et al.* miRNA-200c inhibits invasion and metastasis of human non-small cell lung cancer by directly targeting ubiquitin specific peptidase 25. *Mol Cancer* **13**, 1–14 (2014).
178. Chen, D. *et al.* Interaction between lymphopenia, radiotherapy technique, dosimetry, and survival outcomes in lung cancer patients receiving combined immunotherapy and radiotherapy. *Radiotherapy and Oncology* **150**, 114–120 (2020).
179. Thor, M. *et al.* Toward personalized dose-prescription in locally advanced non-small cell lung cancer: validation of published normal tissue complication probability models. *Radiotherapy and Oncology* **138**, 45–51 (2019).

180. Robinson, A. G. *et al.* Causes of death and subsequent treatment after initial radical or palliative therapy of stage III non-small-cell lung cancer. *Current Oncology* **22**, 333–340 (2015).
181. De Ruyscher, D. *et al.* European Organization for Research and Treatment of Cancer (EORTC) recommendations for planning and delivery of high-dose, high precision radiotherapy for lung cancer. *Radiotherapy and Oncology* **124**, 1–10 (2017).
182. Martel, M. K. *et al.* Estimation of tumor control probability model parameters from 3-D dose distributions of non-small cell lung cancer patients. *Lung Cancer* **24**, 31–37 (1999).
183. Wedenberg, M. Assessing the uncertainty in QUANTEC’s dose-response relation of lung and spinal cord with a bootstrap analysis. *Int J Radiat Oncol Biol Phys* **87**, 795–801 (2013).
184. Werner-Wasik, M. *et al.* Radiation dose-volume effects in the esophagus. *Int J Radiat Oncol Biol Phys* **76**, S86–S93 (2010).
185. Boffa, D. J. The revised stage classification system for primary lung cancer. *Clin Chest Med* **32**, 741–748 (2011).
186. Valentinuzzi, D. & Jeraj, R. Computational modelling of modern cancer immunotherapy. *Phys Med Biol* **65**, (2020).
187. Huang, H. *et al.* Dose-response analysis describes particularly rapid repopulation of non-small cell lung cancer during concurrent chemoradiotherapy. *Cancers (Basel)* **14**, 4869 (2022).
188. Liu, N., Zhou, Y. & Lee, J. J. IPDfromKM: reconstruct individual patient data from published Kaplan-Meier survival curves. *BMC Med Res Methodol* **21**, 1–22 (2021).

189. DerSimonian, R. & Laird, N. Meta-analysis in clinical trials. *Control Clin Trials* **7**, 177–188 (1986).
190. Van Houwelingen, H. C., Arends, L. R. & Stijnen, T. Advanced methods in meta-analysis: multivariate approach and meta-regression. *Stat Med* **21**, 589–624 (2002).
191. Higgins, J. P. T. *et al.* *Cochrane handbook for systematic reviews of interventions, 2nd edition.* (The Cochrane and John Wiley & Sons, 2019).
192. Durm, G. A. *et al.* A phase 2 trial of consolidation pembrolizumab following concurrent chemoradiation for patients with unresectable stage III non-small cell lung cancer: hoosier cancer research network LUN 14-179. *Cancer* **126**, 4353–4361 (2020).
193. Lin, S. H. *et al.* Phase II trial of concurrent atezolizumab with chemoradiation for unresectable NSCLC. *Journal of Thoracic Oncology* **15**, 248–257 (2020).
194. Peters, S. *et al.* Progression-free and overall survival for concurrent nivolumab with standard concurrent chemoradiotherapy in locally advanced stage IIIA-B NSCLC: results from the European Thoracic Oncology platform NICOLAS phase II trial (ETOP 6-14). *Journal of Thoracic Oncology* **16**, 278–288 (2021).
195. Bryant, A. K., Sankar, K. & Zhao, L. De-escalating adjuvant durvalumab treatment duration in stage III non-small cell lung cancer. *Eur J Cancer* **171**, 55–63 (2022).
196. Reck, M. *et al.* Two-year update from KEYNOTE-799: pembrolizumab plus concurrent chemoradiation therapy (cCRT) for unresectable, locally advanced, stage III NSCLC. *Journal of Clinical Oncology* **40**, Poster 8508 (2022).

197. Zhou, Q. *et al.* Sugemalimab versus placebo after concurrent or sequential chemoradiotherapy in patients with locally advanced, unresectable, stage III non-small-cell lung cancer in China (GEMSTONE-301): interim results of a randomised, double-blind, multicentre, phase 3 trial. *Lancet Oncol* **23**, 209–219 (2022).
198. Landman, Y. *et al.* Durvalumab after concurrent chemotherapy and high-dose radiotherapy for locally advanced non-small cell lung cancer. *Oncoimmunology* **10**, e1959979 (2021).
199. Waterhouse, D. M. *et al.* Continuous versus 1-year fixed-duration nivolumab in previously treated advanced non-small-cell lung cancer: CheckMate 153. *Journal of Clinical Oncology* **38**, 3863–3873 (2020).
200. Paz-Ares, L. *et al.* Outcomes with durvalumab by tumour PD-L1 expression in unresectable, stage III non-small-cell lung cancer in the PACIFIC trial. *Annals of Oncology* **31**, 798–806 (2020).
201. Gong, X. *et al.* Combined radiotherapy and anti-PD-L1 antibody synergistically enhances antitumor effect in non-small cell lung cancer. *Journal of Thoracic Oncology* **12**, 1085–1097 (2017).
202. Tas, F. *et al.* Age is a prognostic factor affecting survival in lung cancer patients. *Oncol Lett* **6**, 1507–1513 (2013).
203. Lichtenstein, M. R. L. *et al.* Impact of age on outcomes with immunotherapy in patients with non-small cell lung cancer. *Journal of Thoracic Oncology* **14**, 547–552 (2019).
204. Foster, C. C. *et al.* Overall survival according to immunotherapy and radiation treatment for metastatic non-small-cell lung cancer: a national cancer database analysis. *Radiation Oncology* **14**, 18 (2019).

205. Weichselbaum, R. R. *et al.* Radiotherapy and immunotherapy: a beneficial liaison? *Nat Rev Clin Oncol* **14**, 365–379 (2017).
206. Gonzalez-Crespo, I. *et al.* A biomathematical model of tumor response to radioimmunotherapy with PDL1 and CTLA4. *IEEE/ACM Trans Comput Biol Bioinform* **20**, 808–821 (2022).
207. McWilliam, A. *et al.* Radiation dose to heart base linked with poorer survival in lung cancer patients. *Eur J Cancer* **85**, 106–113 (2017).
208. Huber, R. M. *et al.* Interdisciplinary multimodality management of stage III nonsmall cell lung cancer. *European Respiratory Review* **28**, 190024 (2019).
209. Soldera, S. V. & Leighl, N. B. Update on the treatment of metastatic squamous non-small cell lung cancer in new era of personalized medicine. *Front Oncol* **7**, 1–9 (2017).
210. Li, F. *et al.* Effect of histology on the efficacy of immune checkpoint inhibitors in advanced non-small cell lung cancer: a systematic review and meta-analysis. *Front Oncol* **12**, 1–13 (2022).
211. Spigel, D. R. *et al.* Five-year survival outcomes from the PACIFIC trial: durvalumab after chemoradiotherapy in stage III non-small-cell lung cancer. *Journal of Clinical Oncology* **40**, 1301–1311 (2022).
212. Syriopoulou, E. *et al.* Standardised survival probabilities: a useful and informative tool for reporting regression models for survival data. *Br J Cancer* **127**, 1808–1815 (2022).
213. Vandembroucke, J. P. *et al.* Strengthening the Reporting of Observational Studies in Epidemiology (STROBE): explanation and elaboration. *PLoS Med* **4**, 1628–1654 (2007).

214. Thor, M. *et al.* Pre-treatment immune status predicts disease control in NSCLCs treated with chemoradiation and durvalumab. *Radiotherapy and Oncology* **167**, 158–164 (2022).
215. Cho, Y. *et al.* Lymphocyte dynamics during and after chemo-radiation correlate to dose and outcome in stage III NSCLC patients undergoing maintenance immunotherapy. *Radiotherapy and Oncology* **168**, 1–7 (2022).
216. Serre, R. *et al.* Mathematical modeling of cancer immunotherapy and its synergy with radiotherapy. *Cancer Res* **76**, 4931–4940 (2016).
217. Kosinsky, Y. *et al.* Radiation and PD-(L)1 treatment combinations: immune response and dose optimization via a predictive systems model. *J Immunother Cancer* **6**, 1–15 (2018).
218. Elassaiss-Schaap, J. *et al.* Using model-based ‘learn and confirm’ to reveal the pharmacokinetics-pharmacodynamics relationship of pembrolizumab in the KEYNOTE-001 trial. *CPT Pharmacometrics Syst Pharmacol* **6**, 21–28 (2017).
219. Chatterjee, M. *et al.* Population pharmacokinetic/pharmacodynamic modeling of tumor size dynamics in pembrolizumab-treated advanced melanoma. *CPT Pharmacometrics Syst Pharmacol* **6**, 29–39 (2017).
220. Ahamadi, M. *et al.* Model-based characterization of the pharmacokinetics of pembrolizumab: a humanized anti-PD-1 monoclonal antibody in advanced solid tumors. *CPT Pharmacometrics Syst Pharmacol* **6**, 49–57 (2017).
221. Gray, J. E. *et al.* Three-year overall survival with durvalumab after chemoradiotherapy in stage III NSCLC - update from PACIFIC. *Journal of Thoracic Oncology* **15**, 288–293 (2020).

222. Abe, T. *et al.* Effect of durvalumab on local control after concurrent chemoradiotherapy for locally advanced non-small cell lung cancer in comparison with chemoradiotherapy alone. *Thoracic Cancer* **12**, 245–250 (2021).
223. Anscher, M. S. *et al.* Association of radiation therapy with risk of adverse events in patients receiving immunotherapy: a pooled analysis of trials in the US food and drug administration database. *JAMA Oncol* **20993**, 1–9 (2022).
224. Perez, C. A. *et al.* Long-term observations of the patterns of failure in patients with unresectable non-oat cell carcinoma of the lung treated with definitive radiotherapy: report by the Radiation Therapy Oncology Group. *Cancer* **59**, 1874–1881 (1987).
225. Conibear, J. Rationale for concurrent chemoradiotherapy for patients with stage III non-small-cell lung cancer. *Br J Cancer* **123**, 10–17 (2020).
226. Inoue, T. *et al.* Limited impact of setup and range uncertainties, breathing motion, and interplay effects in robustly optimized intensity modulated proton therapy for stage III non-small cell lung cancer. *Int J Radiat Oncol Biol Phys* **96**, 661–669 (2016).
227. Stuschke, M. *et al.* Potentials of robust intensity modulated scanning proton plans for locally advanced lung cancer in comparison to intensity modulated photon plans. *Radiotherapy and Oncology* **104**, 45–51 (2012).
228. Crosby, T. *et al.* Chemoradiotherapy with or without cetuximab in patients with oesophageal cancer (SCOPE1): a multicentre, phase 2/3 randomised trial. *Lancet Oncol* **14**, 627–637 (2013).

229. Vivekanandan, S. *et al.* The impact of cardiac radiation dosimetry on survival after radiation therapy for non-small cell lung cancer. *Int J Radiat Oncol Biol Phys* **99**, 51–60 (2017).
230. Vivekanandan, S. *et al.* Associations between cardiac irradiation and survival in patients with non-small cell lung cancer: validation and new discoveries in an independent dataset. *Radiotherapy and Oncology* **165**, 119–125 (2021).
231. Vuong, D. *et al.* Quantification of the spatial distribution of primary tumors in the lung to develop new prognostic biomarkers for locally advanced NSCLC. *Sci Rep* **11**, 1–10 (2021).
232. Xie, X. *et al.* Primary tumor location in lung cancer: the evaluation and administration. *Chin Med J (Engl)* **135**, 127–136 (2022).
233. Lee, C. C. *et al.* Association between radiation heart dosimetric parameters, myocardial infarct and overall survival in stage 3 non-small cell lung cancer treated with definitive thoracic radiotherapy. *Lung Cancer* **120**, 54–59 (2018).
234. Dess, R. T. *et al.* Cardiac events after radiation therapy: combined analysis of prospective multicenter trials for locally advanced non-small-cell lung cancer. *Journal of Clinical Oncology* **35**, 1395–1402 (2017).
235. Wang, K. *et al.* Heart dosimetric analysis of three types of cardiac toxicity in patients treated on dose-escalation trials for stage III non-small-cell lung cancer. *Radiotherapy and Oncology* **125**, 293–300 (2017).
236. Tohidinezhad, F. *et al.* Prediction models for treatment-induced cardiac toxicity in patients with non-small-cell lung cancer: a systematic review and meta-analysis. *Clin Transl Radiat Oncol* **33**, 134–144 (2022).

237. Aznar, M., Asteggiano, R. & Banfill, K. Radiotherapy and its consequences: what the cardiologist should know. *e-Journal of Cardiology Practice* **19**, 20.
238. Nestle, U. *et al.* ESTRO ACROP guidelines for target volume definition in the treatment of locally advanced non-small cell lung cancer. *Radiotherapy and Oncology* **127**, 1–5 (2018).
239. Natarajan, J. *et al.* Cardiovascular substructure dose and cardiac events following proton- and photon-based chemoradiotherapy for non-small cell lung cancer. *Adv Radiat Oncol* **8**, 101235 (2023).
240. Contreras, J. A. *et al.* Cardiac dose is associated with immunosuppression and poor survival in locally advanced non-small cell lung cancer. *Radiotherapy and Oncology* **128**, 498–504 (2018).
241. Ladbury, C. J. *et al.* Impact of radiation dose to the host immune system on tumor control and survival for stage III non-small cell lung cancer treated with definitive radiation therapy. *Int J Radiat Oncol Biol Phys* **105**, 346–355 (2019).
242. Jin, J. *et al.* Higher radiation dose to the immune cells correlates with worse tumor control and overall survival in patients with stage III NSCLC : a secondary analysis of RTOG0617. *Cancers (Basel)* **13**, 6193 (2021).
243. Öjlert, Å. K. *et al.* Immune checkpoint blockade in the treatment of advanced non-small cell lung cancer—predictors of response and impact of previous radiotherapy. *Acta Oncol (Madr)* **60**, 149–156 (2021).
244. Boer, C. G. *et al.* Substantial sparing of organs at risk with modern proton therapy in lung cancer, but altered breathing patterns can jeopardize target coverage. *Cancers (Basel)* **14**, 6 (2022).